SUBSURFACE DESCRIPTION AND MODELING OF GEOLOGIC HETEROGENEITY IN LARGE SUBSURFACE DATASETS: USING TEMPORAL AND SCALAR HIERARCHIES, POWDER RIVER BASIN, WY AND MT, U.S.A.

by

Jesse John Melick

A dissertation submitted in partial fulfillment
of the requirements for the degree

of

Doctor of Philosophy

in

Earth Sciences

MONTANA STATE UNIVERSITY
Bozeman, Montana

April 2013

©COPYRIGHT

by

Jesse John Melick

2013

All Rights Reserved

APPROVAL

of a dissertation submitted by

Jesse John Melick

This dissertation has been read by each member of the dissertation committee and has been found to be satisfactory regarding content, English usage, format, citation, bibliographic style, and consistency and is ready for submission to The Graduate School.

Michael H. Gardner

Approved for the Department of Earth Sciences

David Mogk

Approved for The Graduate School

Dr. Ronald W. Larsen

STATEMENT OF PERMISSION TO USE

In presenting this dissertation in partial fulfillment of the requirements for a doctoral degree at Montana State University, I agree that the Library shall make it available to borrowers under rules of the Library. I further agree that copying of this dissertation is allowable only for scholarly purposes, consistent with "fair use" as prescribed in the U.S. Copyright Law. Requests for extensive copying or reproduction of this dissertation should be referred to ProQuest Information and Learning, 300 North Zeeb Road, Ann Arbor, Michigan 48106, to whom I have granted "the right to reproduce and distribute my dissertation in and from microform along with the non-exclusive right to reproduce and distribute my abstract in any format in whole or in part."

Jesse John Melick

April 2013

DEDICATION

I dedicate this to my wife, Roberta Colombi-Melick.

ACKNOWLEDGEMENTS

Manuscript 1: The authors would like to thank Mark Sonnenfeld, Don Stone and Chris Zahm for their discussions on PRB and Wyoming geology. Ann Givan and Mike Beecher provided critical assistance in the data preparation. Jim Gilman reviewed the presentation draft and provided helpful comments. This project would not be possible if not for the permission by John Horne of El Paso Oil and Gas to use the RPI dataset donated by Dave Wheeler. This project is directed by Lee Spangler and funded by Z.E.R.T. (Zero Emissions Research Technology) at Montana State University – Bozeman and is also made possible by donations and discounts from MJ Systems (60,000 well log images), IHS (Petra license) and Schlumberger (Petrel software). TGS provided high quality digital logs at discounted rate.

Manuscript 2: As with any large project, there are many who contributed. Specifically, I would like to thank the following: Thesis advisors (Mike Gardner, Dave Bowen, Steve Custer and Mark Skidmore); Mike Uland and iReservoir.com (training/data prep); Alvin Lisenbee, Don Stone, Bob Weimer, Chris Zahm, Colin Shaw, Janok Bhattacharya, and Guy Plint for consultation and generous patience with teaching and critique of my interpretations; Mark Kirschbaum, Jeff May, and Sandra Mark for engaging discussions of Frontier core; RPI for large dataset; John Horne and Mike Wheeler for data access; TGS, MJ systems for well log data; Mike Beecher and John Porter for core description drafting and log digitizing and David Morrison for technical editing.

TABLE OF CONTENTS

1. GENERAL INTRODUCTION 1

Introduction 2
Study Area and Approach 3
Dataset and Subsurface Characterization 5
Basin-scale Modeling: Retaining Heterogeneity 6
Workflow 7
Geomodeling Methods 9
Characterizing Geologic Heterogeneity Based on Scale Dependent Processes 10
Physical/temporal Scales—The Stratigraphic Record 11
Frontier Formation Stratigraphy and Reservoir Architecture 12
Superimposed Geologic Controls and Foreland Basin Heterogeneity 14
Contributions 15
Impact of Stratigraphic Hierarchy and Sedimentation Regions 15
Modeling Workflow 16
Gross Pore Volume Calculation Methods 16
References Cited 23

2. GEOLOGIC HETEROGENEITY IN BASIN-SCALE GEOLOGIC CARBON STORAGE: EXAMPLES FROM THE POWDER RIVER BASIN, NE WYOMING AND SE MONTANA 26

Contribution of Authors 26
Manuscript Information Page 27
Abstract 28
Introduction 28
Meeting the Challenges of GCS 32
Modeling Approach 37
Study Area 39
Basin Geology and Model Overview 40
Data And Workflow 43
Methods for Basin Characterization and Developing Reservoir Portfolio 44
Reservoir Class Identification 45
Define Sedimentary Systems 45
Classify Basin's RC Portfolio 46
Subsurface Input Data and Calibration 50
Sedimentary Attribute Generation 52
Process Facies Attributes 53

TABLE OF CONTENTS - CONTINUED

Sedimentary Body Attributes....53
Sedimentary Attribute Distribution - Vertically....54
Defining Hierarchy of Stratigraphic Layers....54
Correlate Sequence Hierarchy to Modulate Reservoir Layers....55
RC4.1 and 4.2....56
RC4.3 and 4.4....57
RC.5....57
RC4.6....57
Sedimentary Attribute Distribution - Laterally....58
Sedimentation Region Analysis....58
Sequence Stacking Patterns....58
Workflow For GCS Geomodel Construction....61
Construct 3D Model Framework....62
Distribute Rock Properties in 3D Geomodel....62
Results....64
Heterogeneity Retention Increases with Rigorous Geologic Characterization....64
Static 3D Geomodel Ready for Upscale to Fluid Flow Simulation....66
Static GCS Geomodel Applications....67
Conclusions....68
References....98

3. ASSESSING PRESERVATION OF ANCIENT DEPOSITS AND APPLICABILITY OF MODERN DELTA MODELS: EXAMPLES FROM MID CRETACEOUS FRONTIER FM., POWDER RIVER BASIN, WYOMING AND MONTANA....105

Contribution of Authors....105
Manuscript Information....106
Abstract....107
Introduction....108
Data and Methods....110
Data....110
Facies Analysis....111
Stratigraphic Analysis....112
Sedimentation Region Analysis....114
Tectonic Analysis....116
Tectonic Setting: Tectonic Heterogeneity....117
Wyoming Platform Defined by Accreted Terrane and Aulacogens....118
Foreland Basin System of the Western Interior Cretaceous Basin....120
PRB Structural Basin Part of Larger Cretaceous Foreland Basin....121
Mid-Cretaceous Frontier Formation: Stratigraphic Framework....122

TABLE OF CONTENTS - CONTINUED

Greenhorn-Niobrara Second-order Frontier Cycle....123
Third-order Frontier Cycles....124
Belle Fourche Member: 124
Emigrant Gap Member: 125
Wall Creek-Turner Member: 126
Fourth-order Wall Creek-Turner Cycles 128
Discussion....130
Stratigraphic Remnants: Shoreface Rather Than Delta....131
Multiple Sediment Entry and Low Accommodation Strand Line....133
Wyoming Platform: Low Accommodation Depocenter 134
Conclusions....136
References....157

4. GENERAL CONCLUSIONS 169

Future Work....170

REFERENCES CITED....172

APPENDICES 190

APPENDIX A: Core Descriptions of the Frontier Formation....191
APPENDIX B: Sedimentary Bodies Descriptions of the Frontier Formation....208
APPENDIX C: Cross Sections of the Frontier Formation....213
APPENDIX D: Thickness, Facies and Sedimentation Region Maps of the Frontier Formation 216
APPENDIX E: Table of Log Facies Values....219
APPENDIX F: Contact Information for Obtaining Petrel Basin Model 221

LIST OF TABLES

Table Page

2.1 High-level screening of reservoir classes based on multivariate attributes at multiple scales. 70

2.2 Facies description and grouping strategies. 71

2.3 Tables showing calculation methods and summary of values used in calculation by reservoir class. 72

2.4 Summary of gross pore volume calculations by reservoir class and interpretation. 75

3.1 Literature review for the Frontier Formation of the PRB 138

3.2 Facies descriptions for the Frontier Formation of the PRB. 139

LIST OF FIGURES

Figure		Page
1.1	Powder River Basin (PRB) location and structural cross section	18
1.2	Block diagram illustrating gross pore volume calculation (GPV) methods.	19
1.3	Paleogeographic map showing sedimentary system for Middle Cretaceous Frontier Formation	20
1.4	Three scales of tectonic processes and composite map showing overprint	21
1.5	Chart showing GPV results highlighting three types of reservoir class	22
2.1	Sedimentary basins of U.S.A and Canada and PRB study map	76
2.2	Composite type well log of PRB fill, basement to top of Cretaceous	77
2.3	Structural west to east cross section across PRB	78
2.4	Multiple scales of investigation in a three-fold stratigraphic framework	79
2.5	Diagrams of specific scale-dependent responses to multiscale processes	80
2.6	Upscaling workflow determination of log facies	81
2.7	Core descriptions and grouping strategies	82
2.8	Sedimentation regions; attributes defining of the five regions	83
2.9	Workflow showing characterization of sedimentation regions	84
2.10	Definition of three-fold stratigraphic hierarchy	85
2.11A	Characterization reservoir class 1: Greenhouse carbonate ramp to platform, Madison Limestone	86

LIST OF FIGURES – CONTINUED

Figure		Page
2.11B	Characterization reservoir class 2: Icehouse mixed carbonate – clastic coastal system, Tensleep / Minnelusa Formation	87
2.11C	Characterization reservoir class 3: Clastic incised valley system, low accommodation, Muddy Sandstone	88
2.11D	Characterization reservoir class 4: Long-lived low accommodation clastic strand line, Frontier Formation	89
2.11E	Characterization reservoir class 5: Clastic shorelines, high accommodation, Shannon, Sussex and Parkman Sandstones	90
2.12	Model construction workflow indicating integration of engineering and geology based on well-defined goals	91
2.13	Structural model images from Petrel showing layering and high-level basin model configuration	92
2.14	Images from 3D model showing the greater control on porosity distribution when using fine-scale layering according to the hierarchical stratigraphic framework	93
2.15A	Block diagrams illustrating four methods of GPV for Type I RC (similar stratigraphy and similar sedimentation region arrangements)	94
2.15B	Block diagrams illustrating four methods of GPV for Type II RC (variable stratigraphy and similar sedimentation region arrangements)	95
2.15C	Block diagrams illustrating four methods of GPV for Type II RC (variable stratigraphy and variable sedimentation region arrangements)	96
2.16	Bar chart showing results of GPV calculations and impact of the four calculation methods on the three types of RC	97

LIST OF FIGURES – CONTINUED

Figure Page

3.1 Stratigraphic hierarchy, Powder River Basin (PRB) of eastern Wyoming.....140

3.2 Paleogeographic setting of the Western Interior Cretaceous Seaway during the Cenomanian and Turonian.....141

3.3 Map of PRB study area.....142

3.4 Multiple scales of investigation link porosity-permeability fields to sedimentary facies to sedimentation units and sediment bodies.....143

3.5 Core descriptions and grouping strategies.....144

3.6 Four-fold stratigraphic hierarchy, Middle Cretaceous Frontier Formation.....145

3.7 Sedimentation regions definition by well log, bodies, lithology and facies.....146

3.8A Stratigraphic cross section, Frontier Formation across the southern PRB.....147

3.8B Time stratigraphic cross section (Wheeler diagram) of Figure 3.8A.....148

3.9 Maps showing sediment regions, Frontier Formation.....149

3.10 Map of composite tectonic features along the Western Interior Cretaceous Seaway, including Precambrian crustal and Mesozoic foreland system.....150

3.11 Foreland system model.....151

3.12 Maps of sedimentation regions, second and third order sequences, Frontier.....152

3.13 Maps of sedimentation regions, fourth order sequences Wall Creek-Turner member of the Frontier Formation.....153

3.14 Sedimentation region maps of the Wall Creek-Turner member, Frontier.....154

3.15A-D Alternate models Wall Creek-Turner member of the Frontier Formation.....155

3.16 Block diagram, Wall Creek-Turner member sedimentary system as interpreted in this thesis.....156

NOMENCLATURE

PRB Powder River Basin

One Gigaton (Gt) equals one billion metric tons. One metric ton of gaseous CO_2 equals 505.5 cubic meters at 0° C and 1 atmosphere. One metric ton of supercritical CO_2, with density of 0.469 g/cm^3, will occupy 2.13 m^3 at 31.1° C and 72.8 atmospheres. One GT supercritical CO_2 therefore would occupy 2.13 km^3 of empty connected and accessible void space.

CCS – *carbon capture and storage*, refers to the entire process from capture at power plants etc., the transport, injection and monitoring of carbon (gas, liquid and supercritical phases).

GCS – *geologic carbon storage*, supercritical phase is required for injection and storage into the subsurface. This requires a suite of storage sites both areally and vertically within sedimentary basin fill. This may be a subset of the sedimentary basin if later tectonic overprint defines flow boundaries.

Process facies – facies that are defined by sedimentary processes that formed it, observed and described in core and/or outcrop.

Core facies – facies described in core that were grouped by similar process, high-graded process facies.

Log facies – well-log-derived facies that were calculated by if-then statements generating values based on core-calibrated intervals that defined cutoffs in up to four log well log suite.

Sedimentation regions are laterally restricted spatial domains within a small stratigraphic sequence that is characterized mainly by similar lithology, sedimentary facies, sedimentary body stacking patterns, sequence thickness and well-log motif. Sedimentation regions are restricted to ancient rock volumes, being distinguished from environments of deposition, which are restricted to the description of composite (laterally adjacent and contemporaneous) landscapes and seascapes sculpted by surficial geomorphic processes in modern depositional settings.

Reservoir class (RC) is a stratigraphic interval (typically correlating to a 2nd order cycle) characterized by high effective pore-volume that is composed of a dominant sedimentary system.

NTG Net pore containing thickness to Gross thickness assuming a 10% oil saturation lower cutoff

ABSTRACT

Three-dimensional fluid-flow simulation models provide attractive tools for understanding the potential behavior of the subsurface. Retention of high-resolution geologic heterogeneity in the characterization of large volumes presents significant challenges to this modeling.

A 2D dataset donated by Industry constrains a hierarchical stratigraphic framework based on 30,000 wells with log curves, 60 surfaces crossing the 70,000 cubic-kilometer Powder River Basin from Precambrian basement to top of the Cretaceous Lewis Shale. Five sedimentary systems subdivided into 25 stratigraphic intervals make up the 3D representation of 70 discrete modeling areas. These sedimentation regions group distinct sedimentary attributes (e.g., porosity, thickness, sedimentary architecture). These attributes relate to suites of rock properties, such as porosity, percentage of thickness with porosity and well log shape, which were compiled from 4000 wells with donated/purchased log ascii files, 15 cores, 300 wells with public core plug data, 115 published oil field reports, and basin rimming outcrops.

Sedimentary system analysis considered regional controls on the depositional setting from the craton-scale to the pore-scale and it employed techniques to group information and replicate the effect of fine-scale geologic heterogeneity in a static reservoir model. This process highlights the importance of understanding the role of tectonic anisotropy on the preservation of stratigraphic sequences when interpreting the depositional environment. Subdivision into the 70 sedimentation regions permitted calculation of the gross pore volume in each sedimentary system, using total porosity and a percentage of the vertical thickness for each modeling volume. The total volume calculated depended on the method; stratigraphic layering and sedimentation regions provided 600 cubic kilometers and equating to storage capability of over 250 gigatons of supercritical carbon dioxide, whereas using factors and no stratigraphy, the total volume was calculated at 460 cubic kilometers.

Pore volume distribution in the subsurface is more accurately characterized with high-resolution stratigraphic and sedimentation region analysis. Integrated tectonic analysis provides context that better constrains the application of outcrop analogs and depositional models, which guide sedimentation region analysis. This dissertation addresses the impact of geologic heterogeneity from crustal anisotropy to distributions of porosity and permeability and provides a tool to assess feasibility of gigaton-scale carbon dioxide sequestration.

CHAPTER 1

GENERAL INTRODUCTION

The larger goal within which this research fits is development of a predictive tool to assess feasibility issues associated with gigaton CO_2 sequestration projects. This predictive tool includes generation of a static 3-D geocellular model of the Powder River Basin (PRB, 70,000 km^2 by 3-5km deep; Fig. 1.1), characterizing five intervals with a range of wide-spread and also common reservoir-types (herein termed *reservoir classes, sensu* Geoscience Institute for Oil and Gas Recovery Research, 1990; and Ray et al., 1991), and then up-scaling that multi-million cell model to a tens-of-thousands-cell simulation model. At which point, dynamic injection scenarios would include a suite of injection targets and they could be interrogated with regard to challenges like injectivity, storage volume and migration of the supercritical CO_2. This research represents the initial steps of an integrated geologic characterization effort including input from, but not limited to disciplines such as stratigraphy, structural geology, hydrogeology, and reservoir engineering. Manuscript 1 describes the range of reservoir classes and outlines the integrated steps to building the large whole-basin model composed of a family of nested models. Manuscript 2 describes one of the reservoir classes and the methods involved with characterizing a reservoir class to capture the effects of fine-scale heterogeneity in the geocellular model.

One of the challenges with basin-scale modeling is retaining information about geologic heterogeneity during upscaling. Assessing storage and migration of CO_2

requires characterizing fine-scale geologic heterogeneity and capturing the effects on a geomodel cell (meter-thick, by tens-of-meters across; several feet thick, by hundreds of feet across). The workflow developed in this study deploys analytical methods developed at the scale of an oil field to the basin and retains multiscale heterogeneity in a family of geomodels that encompass multiple stratigraphic intervals, or reservoir classes. The workflow described is based upon outcrop modeling and is capable of retaining multiple scales of heterogeneity. This dissertation outlines an integrated method for estimating: 1) connected pore volume; 2) storage capacity; and 3) retention of supercritical CO_2 associated with geologic storage in subsurface reservoirs.

Introduction

The Powder River Basin (PRB) of eastern Wyoming and southeastern Montana was selected to develop this workflow example because it contains a unique and comprehensive basin-wide subsurface dataset. The PRB has a long history of fluid production and recently enhanced oil recovery programs using CO_2, and is representative of onshore Geologic Carbon Storage (GCS) sites. This research has developed a model-building workflow for screening storage sites, which retains geologic heterogeneity in basinwide geomodels for accurately characterizing the connected pore-volume in subsurface reservoirs across a structural basin.

The Middle Cretaceous Frontier Formation lends itself to a study of detailed geologic characterization. It has the most complete reservoir dataset in the PRB, best outcrop constraint for establishing the sedimentary hierarchy, and robust biostratigraphy.

Because the remaining intervals in the PRB have not been characterized in this detail, the basin geomodel is incomplete and inadequate for basin-scale simulation or use in policy decisions related to GCS. The approach, adapted from methods for building outcrop and oil field-scale reservoir models, includes three main steps: 1) define a hierarchy of sedimentary attributes spanning four orders of magnitude (based on core descriptions, high-resolution stratigraphic correlations and sedimentation region mapping); 2) erect a minimum threefold stratigraphic framework for controlling vertical variation in the lateral distribution of sedimentary attributes; and 3) characterize temporal and spatial distribution of reservoir attribute values based on stratigraphic and geomorphologic constraints (Appendices A-D). The Frontier Formation is best suited for demonstrating the level of detail suggested necessary and the upscaling steps required for development of a useful predictive basin-scale geomodel.

Study Area and Approach

The PRB was selected for study because many of the large onshore clastic deposits worldwide are contained within foreland basin fills. The main reservoir bearing intervals (reservoir classes) characterized in this study were chosen as representative of these common foreland basin successions (Fig. 1.1). Within the PRB, the five reservoir classes (RC1-5) characterized for GCS include:

- RC1 shallow-marine carbonate platform reservoirs (Madison Limestone),
- RC2 mixed carbonate, evaporite, and coastal clastic reservoirs (Minnelusa/ Tensleep Formation),
- RC3 coastal to piedmont clastic valley-fill reservoirs (Muddy Sandstone),

- RC4 fluvial-influenced clastic deltaic-turbidite reservoirs (Frontier Formation),
- RC5 wave-influenced clastic delta reservoirs (Mesaverde Group).

Detailed description and characterization of one reservoir class (RC4) provides an example 300-meter (1000 feet) thick, ancient, fluvial-influenced shoreface succession across the 20,000-km^2 (8000 mi^2) area, and is used to illustrate correlation strategies for characterizing complex sedimentary architecture in a hierarchical stratigraphic framework. Stratigraphic prediction requires analysis of the wide range of processes (sedimentary, stratigraphic and tectonic) that operate over geologic time, recognizing both the material (rock) and nonmaterial (surface) aspect of the sedimentary record. The range of Earth processes must also include tectonic processes operating at slower and lower rates than the surficial depositional environments they accommodate. This tectonic stress creates non-uniform crustal responses. That outcrop-scale attributes (e.g., site specific) cannot be reconciled with crustal-scale patterns (e.g., tectonic plates) does not preclude their use in prediction. Rather, the correlation between attributes and patterns (e.g., components of a depositional system) has been overprinted by longer lasting processes (e.g., low subsidence).

Forward models of Earth systems operating over, and affected by geologic time contain high uncertainty when using one data collection site (i.e., vertical well log core reference sections) commonly in climate and GCS modeling (DOE/NETL, 2010). Current methods used to characterize these complex systems oversimplify the analysis because they fail to account for all Earth processes and responses that operate over

different scales of geologic time (e.g., from deposition of a shoreface, to a stratigraphic sequence, to a clastic wedge, to construction of a continent). In short, current geologic characterization studies for GCS call for more comprehensive methods. Accurate geologic models will be needed if gigaton volumes of supercritical CO_2 are to be stored in Earth's subsurface. Developing methods and testing those using existing data sets to improve such characterization studies is the impetus for this study.

Dataset and Subsurface Characterization

Petrophysical measurements of rock properties calibrated to core and outcrop data define the pore-scale sedimentary attributes distributed within a reservoir class. Well logs were calibrated to core descriptions and petrophysical data, thus allowing sedimentary attributes (sedimentary facies and bodies) to be correlated to values and trends from the wells with 4000 log ascii files. Data from outcrop studies were used to constrain between-well correlations and define sedimentation regions.

The subsurface data (well locations, stratigraphic tops, well logs, cored intervals, etc.) were compiled in a 2-D well log database (Petra) for construction and correlation of 6 stratigraphic cross sections and 30 maps (each showing lithology, thickness, porosity; Appendices A-D). The stratigraphic cross section grids span the basin and constrain sequence and sedimentation region definition (e.g., depositional limits of shoreface sandstone). The 3-D geomodels for connected pore volume calculations were generated in reservoir modeling software (Petrel), using data generated and managed in Petra.

Basin-scale Modeling: Retaining Heterogeneity

The significant societal costs and industrial challenges to GCS demand more fidelity than the simplistic conclusions reached from modeling the subsurface as homogeneous media. Multiscale geologic heterogeneity is here proposed as necessary and sufficient for accurately predicting supercritical CO_2 capacity and flow in GCS modeling. Simplified models help isolate and understand uniform and steady flow in homogeneous media, but represent unrealistic natural conditions for assessment of important fluid movement and chemical reaction rates. As one example, homogeneous models of supercritical CO_2 displacing denser brine in a saline aquifer over-emphasize buoyancy and vertical well-bore leakage (Friedmann, 2007). Furthermore, non-uniform and unsteady variations in flow rate (well-documented behavior in subsurface fluid production) affects retention, which cannot be assessed using homogeneous models. Actual GCS reservoirs should not be isolated for study without consideration of dynamic basin aquifer systems, which requires that all GCS be imbedded into future power plant design and deployment be studied at the basin scale.

The PRB meets the site screening requirements established by the US DOE/NETL (NETL, 2010; Table 3.1, p. 12) for GCS projects (see Manuscript 1). Five RCs with high pore volumes are identified based on high resident fluid volumes recognized across a significant part of the PRB. The subsurface database (permitting cross section or map view examination) contains over 28,000 wells with digital raster-log images used to identify over 60 stratigraphic surfaces. Pre-existing fault and basin

tectonic studies are used to further constrain the structural framework. These data form the initial structural and stratigraphic framework utilized in the pore volume calculations.

Fluid types within the reservoirs range from potable water, brine, corrosive gas, oil, condensate, injected CO_2, and both biogenic and thermogenic gas. The suite of reservoir classes in this thesis represent approximately 40% of the 4 kilometers (2.5 miles) thickness of strata, which records over 300 million years of geologic time. This foreland basin fill contains a typical succession of geologic formations representing carbonate, mixed carbonate-siliciclastics, incised valley fills, low and high accommodation clastic shorelines. The PRB study therefore provides a GCS basin portfolio representative of continental structural basins worldwide.

Workflow

Modeling fluid movement through connected pore volume distributions at the basin scale requires adapting detailed sedimentary architecture to a finite number of uniform geometric cells, which in this model are 800 by 800 m area by one to three meters thick. Reservoir “upscaling” required for dynamic simulation reduces geologic complexity and heterogeneity. To minimize this affect, the explicit correlation of multiscale sedimentary attributes representing a wide range of geologic heterogeneity provides a technique to retain heterogeneity at different stages in upscaling.

A family of nested reservoir-specific and full basin geomodels represents an important starting point for GCS because it retains a hierarchy of detailed geologic characterization. The steps include:

1) classify subsurface geology by reservoir class and define basin portfolio of fluid storage sites and containment conditions,
2) calibrate rock-to-subsurface data to generate a hierarchy of sedimentary attributes consisting of process facies, sedimentation units, and sedimentary bodies for each reservoir class,
3) erect hierarchical stratigraphic framework based on sedimentary attributes and time-stratigraphic surfaces,
4) define and distribute sedimentation regions within stratigraphic framework based on sedimentary attributes,
5) utilize stratigraphic layering of sedimentation regions to modulate heterogeneity and property attributes.

These more realistic geomodels help address several GCS challenges: they represent assessment tools for evaluating implementation strategies; they provide more accurate estimates for storage, injectivity and migration (i.e., monitoring) in GCS at the basin scale; and they provide common datasets that encourage integration and input from the wide spectrum of expertise involved in interrogation of this problem, including but not limited to geologists, reservoir engineers, civil engineers, land planners, as well as government officials.

Manuscript 1 emphasizes techniques established in outcrop models, but is novel to subsurface modeling. The approach used here classifies spatial domains as specific *sedimentation regions* (Gardner et al., 2008). These are defined as mapable areas within a stratigraphically defined rock volume characterized by similar well log trends

(representing lithofacies and sedimentary body stacking patterns). Sedimentation regions differ from depositional environments and are restricted to ancient rock volumes. This is in contrast to depositional environments that describe composite (laterally adjacent and contemporaneous) landscapes and seascapes sculpted by surficial geomorphic processes in modern depositional settings. Sedimentation regions are here defined as a modeling area mapped at the finest stratigraphic layer possible, that is characterized by similar values and ranges of attributes, e.g., well log trend, thickness, sandstone percent, sedimentary facies. Representing discrete modeling domains, the sedimentation regions constrain averaging of rock properties in a hybrid deterministic/geostatistical manner that maintains heterogeneity based on data-rich areas, rather than averaging across the entire basin (e.g., Fig. 1.2).

Geomodeling Methods

Two deterministic methods are used to geostatistically populate the connected pore volume for a reservoir class. Primary porosity and permeability structure is controlled by the stacking pattern of sedimentation regions within and across the stratigraphic hierarchy. These spatial domains contain a broad range of attributes defined by a hierarchy of properties, process sedimentology facies, sedimentation units and sedimentary bodies. Vertical proportion curves by sedimentation region (when a representative number of samples are available) constrain the vertical distribution of these attributes based on the probability defined by the logs within a region, while areal proportion maps (including azimuth and degree of change laterally) guide attribute distributions. Because sedimentation regions represent remnants of preserved

depositional environments, they help define the sedimentary system. Sedimentation regions shift through time in accordance to Walther's Law (e.g., Middleton, 1973) in conformable succession of strata under high accommodation conditions. Low accommodation decreases preservation and increases uncertainty; the hierarchical stratigraphic framework used herein helps to mitigate.

Characterizing Geologic Heterogeneity Based on Scale Dependent Processes

A preserved ancient sedimentary succession is a composite record of responses to processes acting at all scales. Understanding the long-term processes can help explain poorly preserved stratigraphic patterns. Classifying a rock succession into a hierarchy of responses governed by scale-specific salient processes is a robust way to achieve this understanding. The level of incompleteness in the stratigraphic record varies from partial preservation of a sedimentary basin to the bypass of grains along the stoss side of a ripple. The processes responsible for such variability include allocyclic basinwide controls (e.g., tectonics, sea level) and autocyclic local controls governed by depositional/erosional patterns (e.g., compensational shifting of shoreface depocenters). These two end-member scales overlap and result in potentially confounding composite responses. Manuscript 2 examines the Mid-Cretaceous Frontier “shoreline bulge” and offers an alternative explanation to its deltaic interpretation (e.g., Cobban and Reeside, 1952; Barlow and Haun, 1966; Weimer, 1970; Fig. 1.3).

Physical/Temporal Scales—The Stratigraphic Record

The PRB represents a Mesozoic foreland basin overprinted by Cenozoic thrusting (Fig. 1.4). The portion of sedimentary basin that is preserved in the PRB is a small remnant representing the inner foreland in the simplified foreland basin system of Horton and DeCelles (1997). In the part of the Western Interior Cretaceous Seaway, coinciding with present-day Wyoming, the shoreline is reported to have bulged almost 100 miles to the east coinciding with a mappable sandstone wedge reaching 160 kilometers (100 miles) across the southern PRB (Cobban and Reeside, 1952; Barlow and Haun, 1966; Weimer, 1970; Fig. 1.3). However, coeval nonmarine rocks are not found east of Cody or the Rock Springs Uplift in Wyoming, leaving 300 kilometers (225 miles) distance to the enigmatic shoaling upward sandstone sequences reaching across Wyoming and into South Dakota.

Manuscript 2 addresses the fundamental distinction between spatial and temporal processes contributing to deltaic sedimentary architecture. A suite of areally limited and relatively short-term surficial processes defines modern geomorphic environments that compose the sedimentary system (e.g., channels, bays, crevasse splays, shoreface composing a delta). The challenge with the direct application of the principle of uniformity to the interpretation of ancient sedimentary architecture is identifying the dominant processes responsible for the differences between ancient and modern sedimentary systems. This is reflected in the contribution of stratigraphic preservation over geologic time relative to, for example, the distinction between wave, tide and river-dominated deltas, which can develop synchronously. Geologic time is recorded as both

material (rock) and nonmaterial (stratigraphic surfaces of nondeposition and erosion) components. Directly correlating the ancient sedimentary pattern in continental strata to modern depositional environments can therefore over-emphasize the material record of time in deposition at the expense of the surfaces recording nondeposition or erosion (Barrell, 1917).

Equally as significant is the effect of deep time on expanding the range of Earth processes that operate over longer durations (billions to millions of years, i.e., tectonics) but nonetheless contribute to preserved sedimentary architecture. Tectonic subsidence governs the regional preservation potential of sedimentary sequences, which in turn dictates the degree to which sea-level change impacts preservation. This study emphasizes the importance of considering the tectonic history and its impact on continental stratigraphy (Fig. 1.4). Variations in the strength and rheology of composite continental crust influence the expression of these longer-term tectonic processes (Fig. 1.4A; Tonnsen, 1986).

Manuscript 2 focuses on the temporal contribution from tectonic processes in a foreland basin on the interpretation of the deltaic sedimentary architecture of the Frontier Formation in the PRB. It hypothesizes that these architectural patterns may reflect temporal tectonic rather than site-specific deltaic geomorphic processes.

Frontier Formation Stratigraphy and Reservoir Architecture

Basin-scale geomodeling is constrained vertically by modeling layers. These coincide with stratigraphic surfaces and the sedimentary sequences they bound. A

hierarchy of stratigraphic framework (of surfaces bounding sequences) captures the range of cyclicity that is expressed in a hierarchy of stratigraphic cycles of deposition. The Frontier Formation of the PRB contains three 3rd-order stratigraphic cycles, which in turn contain up to four 4th-order cycles composed of two to four 5th order cycles (sensu Van Wagoner et al., 1990). This hierarchy frames the sedimentary architecture describing basinward to landward stepping cycle stacking patterns, blurred facies distributions (bioturbated and reworked shoreface successions) and bimodal proximal and distal sediment volume partitioning. The sand-rich Wall Creek (southwestern PRB) and its coeval Turner Member (southeast PRB) represent the uppermost 3rd-order cycle (representing approximately 2 million years). This Wall Creek-Turner member is correlated across the southern PRB crossing into South Dakota (Fig. 1.3) based on a basal unconformity and C. *woollgari* ammonite biozonation and a terminal flooding surface with a dated volcanic ash bed (Merewether et al., 1979; Cobban et al., 2006). The four 4th-order sequences within the Wall Creek-Turner member are defined by three bivalve biozones are also sand-rich and contain several 5th-order sequences. The four-fold stratigraphic framework used in this study documents a hierarchy of thin but laterally extensive sand-rich shoreface sequences correlated 100 of kilometers/miles across the southern PRB.

Beginning in the 1960s, workers have noticed the presence of a Mid-Cretaceous sandstone rich interval stretching from the Sevier Orogeny at the Wyoming – Idaho border to just east of the Bighorn and Laramie mountain ranges in the southern PRB and subsequently have proposed that it is a shoreline bulge (Barlow and Haun, 1966; Weimer,

1970). There is little consensus on interpretations of the sandstone members of Wall Creek – Turner member; being classified as representing deltas, offshore bars, shelf sand sheets, and incised valley fills (Asquith, 1970; Tillman and Almond, 1979; Weimer and Flexer, 1985; Gani and Bhattacharya, 2007). Observations that may be responsible for these variations include: 1) distance between observed shoreline deposits is hundreds of kilometers/miles away from the sandstones in the PRB; 2) pebble aligned surfaces present in distal eastern PRB deposits; 3) the general "shallow" nature of the sandstones, showing bioturbation and wave reworking structures being common in most of the wells and outcrops across the PRB. These observations can be better explained by expanding the extent of model investigation to include tectonic processes including terranes and aulacogens bounding the Wyoming Craton.

Superimposed Geologic Controls and Foreland Basin Heterogeneity

Analysis and interpretation of ancient sedimentary architecture here considers the role of geologic time on the suite of earth processes that contributed to the preserved sedimentary response, including tectonic drivers for sediment supply and accommodation distribution. For these reasons, and unlike deltas in high accommodation settings (e.g., Ferron Sandstone; Gardner, 1995), it is here hypothesized that the Frontier Formation is a poorly preserved clastic strand line rather than an ancient delta explained by an incomplete suite of short-term surficial processes. Supporting this hypothesis, the southern PRB is here interpreted as an area of low subsidence during the Mid Cretaceous controlled by variations in continental crust rheology that is responsible for the time-

averaged sediment bulge constructed by multiple sediment sources (Fig. 1.4B and blue in Fig. 1.4D). Non-uniform along-strike changes in sediment supply and accommodation along multiple foreland basin thrust segments formed discrete depocenters within the Western Interior Cretaceous Seaway (Fig. 1.4B and Fig. 3.10). Recognizing this composite tectonic/eustatic signature better accounts for the anomalous size and paleogeography of the upper Frontier Formation sediment bulge.

Contributions

This study provides three main contributions: 1) emphasis on multiple scales of stratigraphic cyclicity correlated to dominant formative processes; 2) illustration of a detailed geologic characterization workflow for one reservoir class; 3) implication of technique used to calculate gross pore volume in five reservoir classes representative of GCS in onshore structural basins worldwide.

Impact of Stratigraphic Hierarchy and Sedimentation Regions

This thesis emphasizes multi-scalar reservoir characterization recognizing that scale-dependent processes produce a remnant stratigraphic record. Although many datasets may have sparse detailed geologic analysis, full description of core and outcrop analog data can improve subsurface characterization and modeling. Furthermore, when application of a depositional model becomes difficult to establish, as in the case with the Frontier Formation of Wyoming, it may be likely that the scale of investigation should be

expanded and consider the role of preservation. Remnant patterns amplify tectonic subsidence and obscuring a clear link with shorter-term site-specific processes.

Modeling Workflow

Capturing multiple scales of geologic detail is fundamental to increasing the heterogeneity in 3-D basin-scale static reservoir models as well as their upscaled fluid simulation models. The workflow presented here outlines novel techniques at multiple scales whereby fine-scale geologic information can be retained in each stage of upscaling during the model-building process. Capturing spatial trends of attribute variation is well established in the petroleum industry but is typically at the reservoir scale. Representative prediction of CO_2 storage at the basin scale will benefit significantly by modeling using the workflow presented in this thesis.

Gross Pore Volume Calculation Methods

Four methods were investigated to illustrate the importance of stratigraphic sequence analysis and sedimentation regions. These methods highlight three types of reservoir class: 1) similar stratigraphy and sedimentation region arrangement; 2) variable stratigraphy, similar sedimentation region arrangements; and 3) variable stratigraphy and sedimentation region arrangement (Fig. 1.5). It is clear that a stratigraphic hierarchy of sequences has a large impact – increasing gross pore volume by up to half. This happens when the high net reservoir to gross thickness (NTG) with high porosity is isolated and represents a significant portion of the RC in type 2 and 3 RCs. Conversely, when stratigraphic sequences contain similar amounts of high NTG volume, their gross pore

volume is decreased by increasing resolution, as is generally the case with reservoir models in type 1 RCs. Type 3 RC is most complex as it contains high and low sandstone percent (NTG) and porosity sequences.

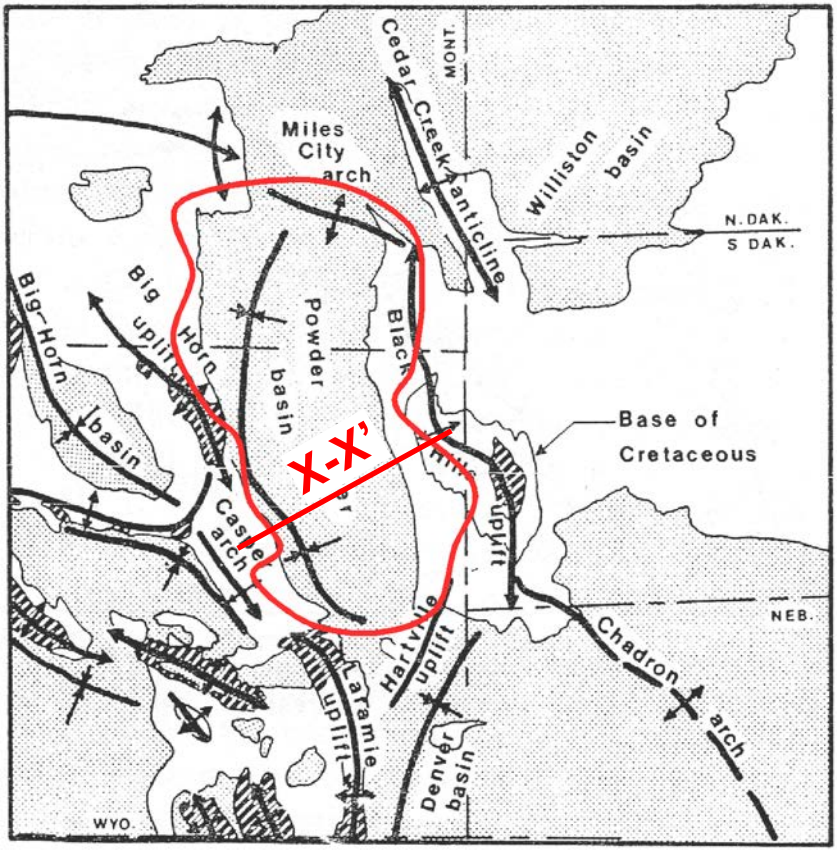

After Lisenbee, 1988

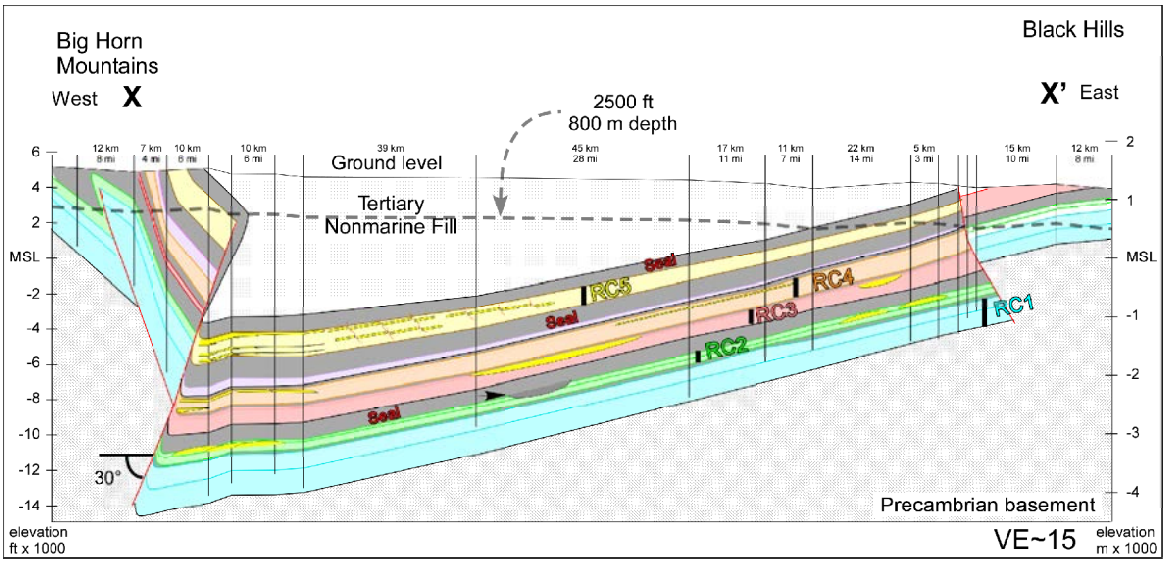

Figure 1.1. Powder River Basin location and structural cross section.

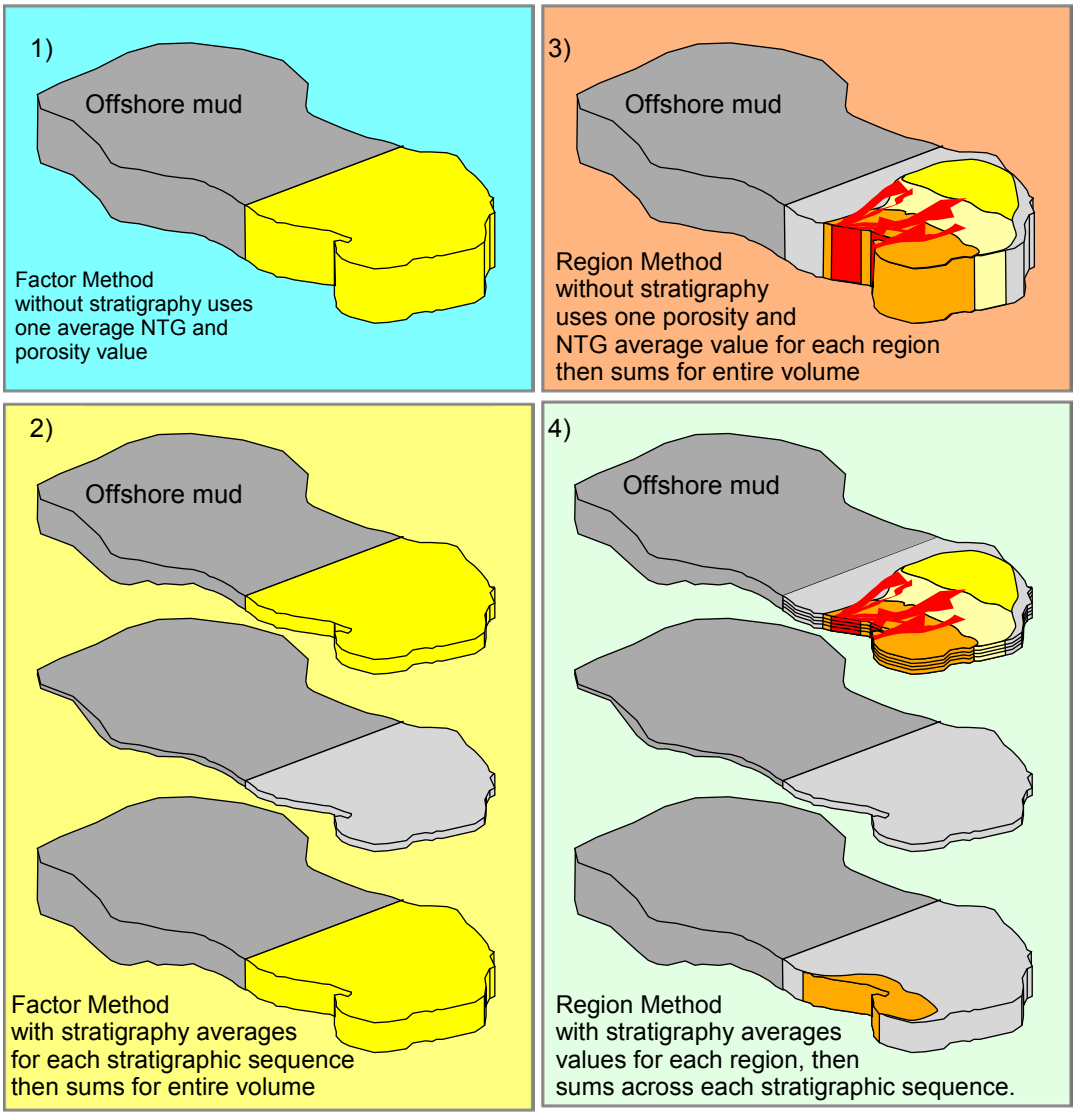

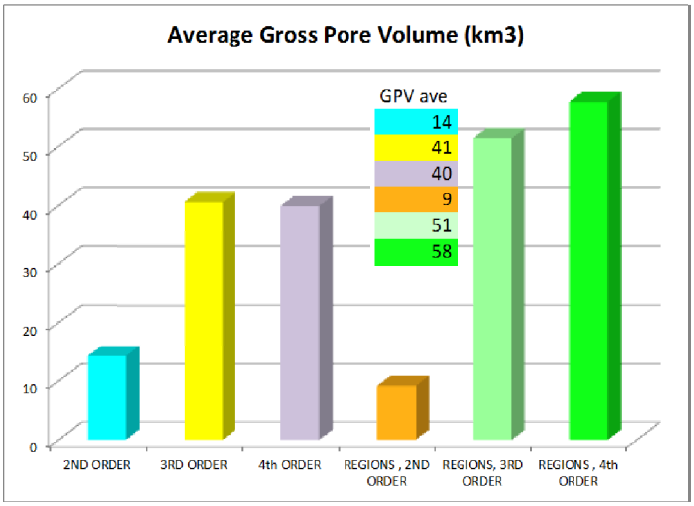

Figure 1.2. Block diagram and bar chart illustrating impact of four gross pore volume calculation methods (1-4) for RC4. Note, this RC4 was characterized in the southern PRB only and across a three-fold stratigraphic framework; the fourth-order stratigraphy is not included in block diagrams.

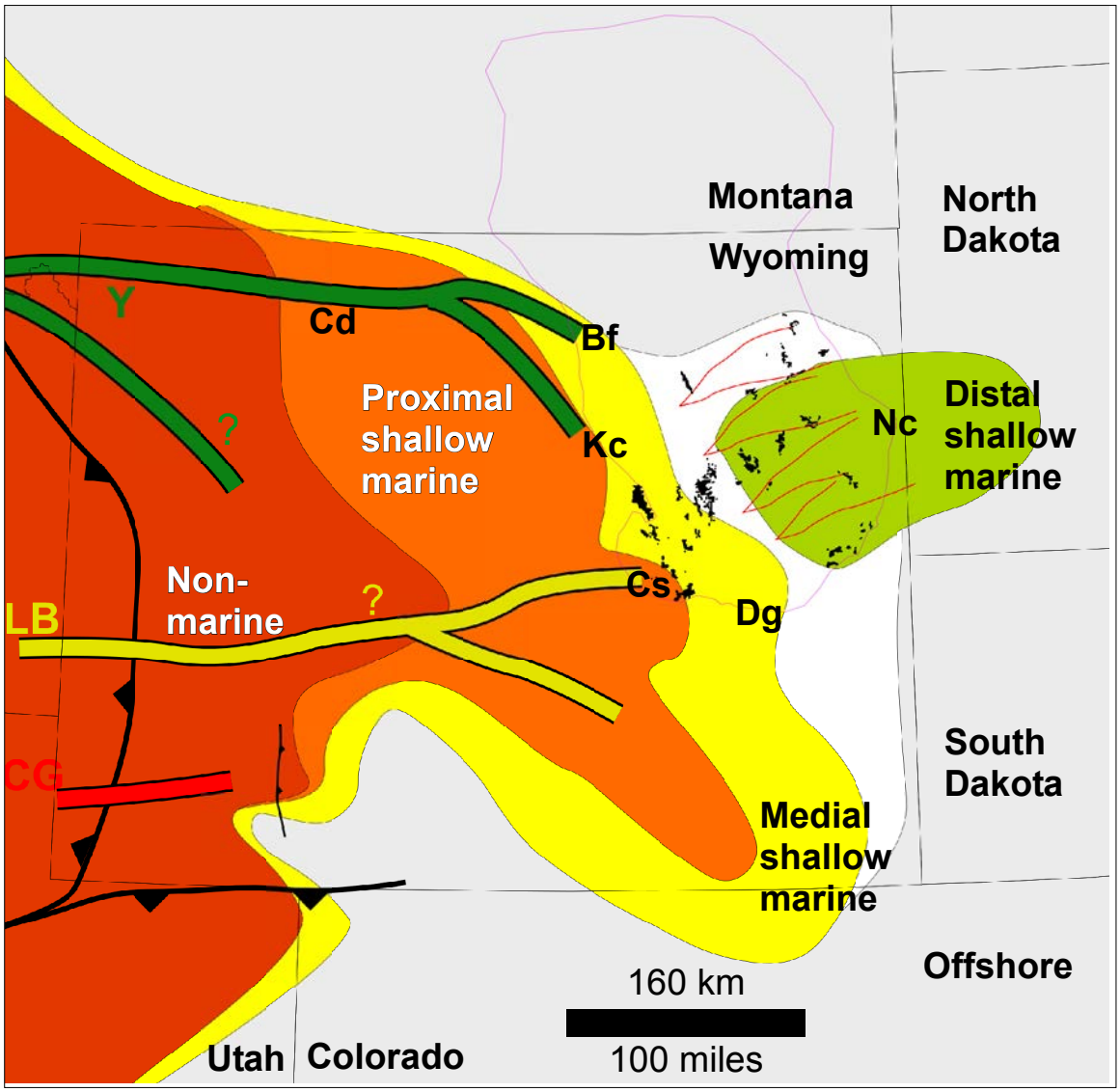

Figure 1.3. Paleogeographic map showing sedimentary system for Middle Cretaceous Frontier Formation (McGookey et al., 1972; Myers, 1977; Merewether et al., 1979; Merewether et al., 1984; Weimer & Flexer 1985; Hamlin, 1996; Bhattacharya & Willis 2001). LB - Labarge, CG - Cumberlin Gap, Y - Yellowstone sediment delivery systems. Wyoming towns: Cd - Cody, Bf - , Kc - Kaycee, Cs - Casper, Dg - Douglas, Nc - Newcastle are shown. Principle oil fields are indicated in black polygons

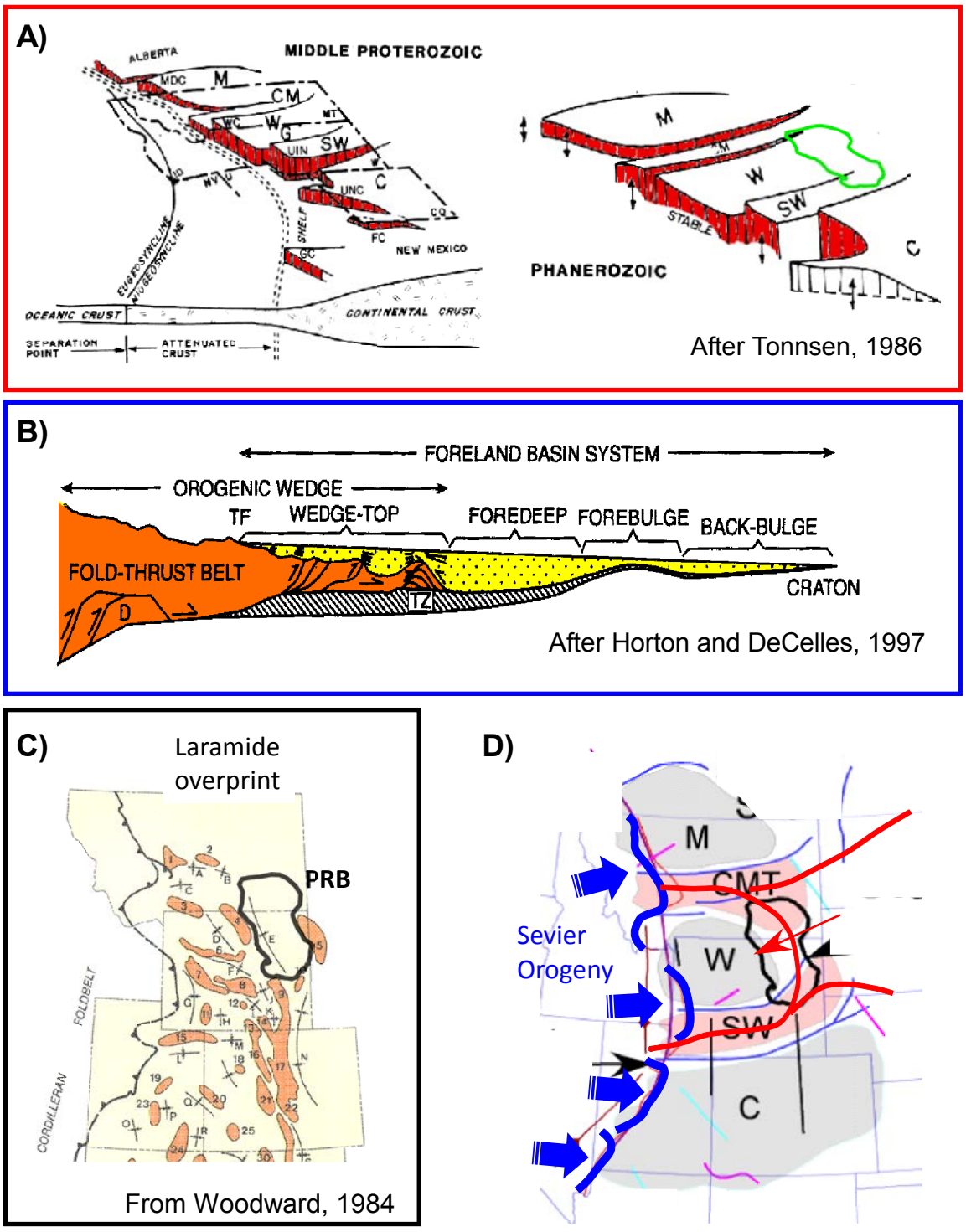

Figure 1.4. Three scales of tectonic process: A) Middle Proterozoic tectonic terranes and aulacogens; B) Foreland basin model used in this study; and C) Laramide overprint contribute to the formation of the crustal heterogeneities surrounding the Wyoming Craton (D).

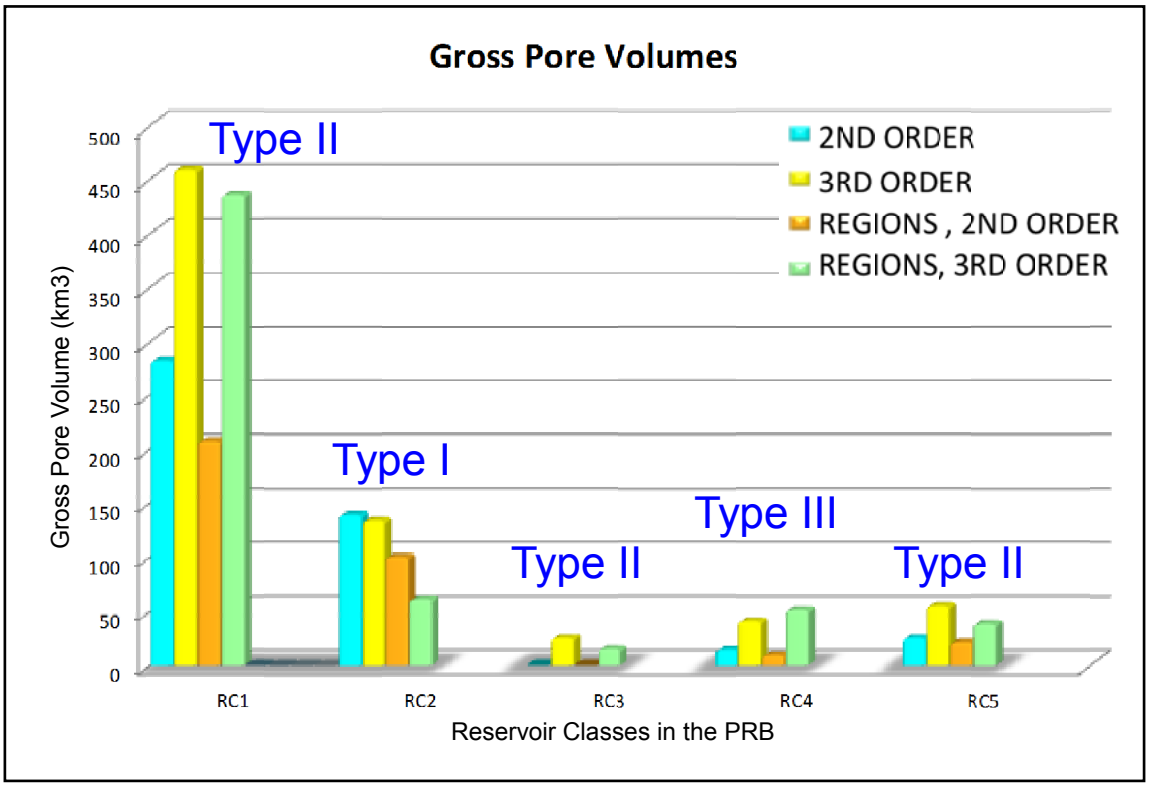

Figure 1.5. Chart showing Gross Pore Volume (GPV) results for the five reservoir classes (RC) highlighting three types of reservoir class. Type I RCs have similar stratigraphy and similar arrangement of sedimentation regions. Type II RCs have stratigraphic sequences without reservoirs, but similar arrangement of sedimentation regions. Type III RCs are most complex, having both variable stratigraphy and variable sedimentation region arrangements.

1) Factor method averaged across stratigraphy (blue)
2) factor method summed across stratigraphy then averaged (yellow)
3) region method averaged within region and across stratigraphy (orange)
4) region method averaged within region, summed across stratigraphy (mint green), see Figure 12 for calculation method.

References Cited

Asquith, D.O., 1970, Depositional topography and major marine environments, Late Cretaceous, Wyoming, AAPG Bulletin, 54/7: 1184-1224.

Barlow, J.A., Jr., and J.D. Haun, 1966, Regional stratigraphy of Frontier Formation and relation to Salt Creek field, Wyoming: AAPG Bull., 50/10: 2185–2196.

Barrell, J., 1917, Rhythms and the measurements of geologic time, Bulletin of the Geological Society of America 28: 745-904.

Bhattacharya, J.P., and B.J. Willis, 2001, Lowstand deltas in the Frontier Formation, Powder River Basin, Wyoming—Implications for sequence stratigraphic models: AAPG Bull, 85: 261–294.

Cobban, W.A., 1958, Late Cretaceous fossil zones of the Powder River Basin, Wyoming and Montana, In Wyoming Geological Association Guidebook, 13th Annual Field Conference, Powder River Basin: 114-119.

Cobban, W.A., Obradovich, J.D., Walaszcyk, I., and McKinney, K.C., 2006, A USGS Zonal Table for the Upper Cretaceous Middle Cenomanian−Maastrichtian of the Western Interior of the United States Based on Ammonites, Inoceramids, and Radiometric Ages, USGS Open-File Report 2006-1250, 47 p.

Friedmann, S.J., 2007, Geological Carbon Dioxide Sequestration, Elements, 3/3: 179-184.

Gani, M.R., and J.P. Bhattacharya, 2007, Basic Building Blocks and Process Variability of a Cretaceous Delta: Internal Facies Architecture Reveals a More Dynamic Interaction of River, Wave and Tidal Processes Than Is Indicated By External Shape, Journal of Sedimentary Research, 77/4: 284-302.

Gardner, M.H., 1995, Tectonic and Eustatic Controls on the Stratal Architecture of Mid-Cretaceous Stratigraphic Sequences, Central Western Interior Foreland Basin of North America, in S. Dorobek, and J. Ross (eds.), Stratigraphic Evolution of Foreland Basins, Society of Sedimentary Geology (SEPM) Special Publication 52, p. 283-303.

Gardner, M.H., Borer, J.M., Romans, B.W., Baptista, N., Kling, E.K., Hanggoro, D., Melick, J.J., Wagerle, R.N., Dechesne, M., Carr, M.M., Amerman, R., and Atan, S., 2008, Stratigraphic models for deepwater sedimentary systems. GCSSEPM Special Publication, Answering the Challenges of Production from Deepwater Reservoirs: Analogues and Case Histories to Aid a New Generation, p. 77-175.

Geoscience Institute for Oil and Gas Recovery Research, 1990, *Reservoir Heterogeneity Classification System for Characterization and Analysis of Oil Resource Base in Known Reservoirs,* prepared for U.S. Department of Energy, Office of Fossil Energy, Bartlesville Project Office.

Hamlin, H.S., 1996, Frontier Formation stratigraphy on the Moxa Arch, Green River Basin, Wyoming, Then Mountain Geologist 33/2: 35-44.

Horton, B.K. and DeCelles, P.G., 1997, The Modern foreland basin system adjacent to the Central Andes, Geology 25/10: 895-898.

Lisenbee, A.L., 1988, Tectonic history of the Black Hills uplift, Guidebook - Wyoming Geological Association, 39: 45-52.

McGookey, D.P., J.D. Haun, L.A. Hale, H.G. Goodell, D.G. McCubbin, R.J. Weimer, and G.R. Wulf, 1972, Cretaceous system, in Mallory, W.W., ed., Geologic atlas of the Rocky Mountain Region: Denver, Rocky Mountain Association of Geologists, p. 189–228.

Merewether, E.A., Blackmon, P.D. and Webb, J.C., 1984, The Mid-Cretaceous Frontier Formation near the Moxa Arch, Southwestern Wyooming, USGS Professional Paper 1290, 29 p.

Merewether, E.A., W.A. Cobban, and E.T. Cavanaugh, 1979, Frontier Formation and equivalent rocks in eastern Wyoming: The Mountain Geologist, v. 6, no. 3, p. 67–102.w

Middleton, G. W., 1973, Johannes Walther's Law of the Correlation of Facies: Geological Society of America Bulletin, v. 84, p. 979-988.

Myers, R.C., 1977, Stratigraphy of the Frontier Formation (Upper Cretaceous), Kemmerer area, Lincoln County Wyoming, Twenty-Ninth Annual Field conference – 1977 Wyoming Geological Association Guidebook: 271- 311.

N.E.T.L., 2010, Best practices for: Site screening, site selection, and initial characterization for storage of CO2 in deep geologic formations, http://www.netl.doe.gov/technologies/carbon_seq/refshelf/BPM_PublicOutreach.pdf.

Ray, M.R., J.P. Brashear, and J. Biglarbigi, 1991, Classification system targets unrecovered U.S. oil reserves, *Oil and Gas Journal,* 89/39, p. 89.

Tillman, R.W., and W.R. Almond, 1979, Diagenesis of Frontier Formation offshore bar sandstones, Spearhead Ranch Field, Wyoming, in Scholle, P.A., and P.R. Schluger, eds., Aspects of diagenesis: SEPM Special Publication 26: 337–378.

Tonnsen, J.J., 1986, Influence of tectonic terranes adjacent to the Precambrian Wyoming Province on Phanerozoic stratigraphy in the Rocky Mountain Region, AAPG Memoir 41: 21-39.

Van Wagoner, J.C., R.M. Mitchum, K.M. Campion, and V.D. Rahmanian, 1990, Siliciclastic sequence stratigraphy in well logs, cores, and outcrops: AAPG Methods in Exploration Series, no. 7, 55 p.

Weimer, R.J, 1970, Rates of deltaic sedimentation and intrabasin deformation, Upper Cretaceous of Rocky Mountain region, in JP Morgan, ed., Deltaic sedimentation, modern and ancient: SEPM Special Publication 15: 270-292.

Weimer, R.J., and A. Flexer, 1985, Depositional patterns and unconformities, Upper Cretaceous, eastern Powder River Basin, Wyoming, in Nelson, G.E., ed., The Cretaceous geology of Wyoming: Wyoming Geological Association 36th Annual Field Conference Guidebook: 131–147.

Woodward, L. A., 1988, Tectonic map of the Rocky Mountain region of the United States, in Sloss, L. L., ed., Sedimentary cover — North American craton: U.S.: Boulder, Colorado, Geological Society of America, Geology of North America, v. D-2, Plate 2.

CHAPTER 2

GEOLOGIC HETEROGENEITY IN BASIN-SCALE GEOLOGIC CARBON STORAGE: EXAMPLES FROM THE POWDER RIVER BASIN, NE WYOMING AND SE MONTANA

Contribution of Authors and Co-Authors

Manuscript in Chapter 2

Author: Jesse J. Melick

Contributions: Primary author (Jesse J. Melick) acquired and compiled all data in 2D database, performed all sedimentologic and stratigraphic interpretations on core, well logs and cross sections. Jesse J. Melick drafted all figures and tables presented and wrote the corresponding text.

Co-Author: Michael H. Gardner

Contributions: Secondary author (Michael H. Gardner) provided oversight and input for this project, including: (1) acquisition of dataset from RPI of Colorado and required permissions from El Paso Inc.; and (2) editing of text, figures and tables for this contribution. Funding was provided through ZERT of Montana State University.

Co-Author: Michael J. Uland

Contributions: Secondary author (Michael J. Uland) provided oversight and input for this project, including in-house training for geocellular model preparation and construction at iReservoir.com.

Manuscript Information Page

Jesse J. Melick, Michael H. Gardner and Michael J. Uland

Name of Journal: *Society of Petroleum Engineers*

Status of Manuscript:
____ Prepared for submission to a peer-reviewed journal
_X__Officially submitted to a peer-review journal
____ Accepted by a peer-reviewed journal
____ Published in a peer-reviewed journal

Publisher: Society of Petroleum engineers, PAPER NUMBER 126443

Abstract

Geologic carbon storage (GCS) requires consideration of storage capacity, injectivity and migration of gigatons of supercritical fluids in sedimentary basins. However, the size of basin-scale GCS models requires simplification that limits retention of geologic heterogeneity. Homogeneous GCS models (uniform and average properties in large cells) facilitate initial basin storage evaluation useful in screening, but cannot account for the actual reservoir architecture affecting both reaction and flow rates in heterogeneous media. The generation and integration of geological and petrophysical models (multi-field, regional aquifers) presented here highlight the uncertainty and risk created by using simplified GCS models to direct research and make policy decisions. This paper emphasizes a workflow that utilizes the natural hierarchy within sedimentary architecture to geologically upscale a family of static geomodels that retain multiple scales and types of heterogeneity. More importantly, geologic controls on heterogeneity can be explicitly manipulated to manage heterogeneity distributions known to change through the life of petroleum reservoirs. There is no reason GCS will not follow a similar path.

Introduction

Geologic storage of carbon (GCS) in subsurface reservoirs is an important component of research funding and policy decisions related to energy and the environment. This is because among the various methods to reduce the environmental impact of CO_2 emissions from energy generation, GCS presents the possibility to

accommodate a significant portion. The economic cost and societal impact of industrial-scale GCS, however, remains poorly understood and constrained. The challenges are significant and the solutions resource intensive. For example, GCS in the United States will require ~1 Gigaton per year (billion metric tonnes, Gt/yr) of CO_2 injection and storage by 2020 (U.S. D.O.E. N.E.T.L., 2008); this requires basin-scale storage solutions, since CO_2 use for EOR from existing oil fields will be insufficient in meeting the 2050 storage targets (Pacala and Socolow, 2004). The numerous single-to multi-well studies to date, (e.g., Celia, 2008; Nicot et al., 2008; Yamamoto et al., 2009; Zhou et al., 2010) simply cannot address questions related to the conflicting objectives of building complex, high-resolution models at the scale of the sedimentary basin.

This paper emphasizes the importance of static geocellular models, which are on the order of 100,000 km^2 by several km deep or more (*geomodel* hereafter). These multiscale heterogeneous geomodels are necessary for accurate forecasting and assessment of the long-term fate of industrial-scale volumes of supercritical fluids proposed for storage in sedimentary basins. The significant societal costs and industrial challenges to GCS are too great to use simple homogeneous models to assess complex reservoirs. Multiscale geologic heterogeneity is necessary and sufficient for modeling supercritical flow in GCS. The geomodels presented here incorporate many "plume scales" in multiple reservoir classes that span entire sedimentary basins (e.g., Zhou et al., 2010). This approach enables the retention of geologic heterogeneity at the multiple scales that affect subsurface fluid flow.

This contribution presents a novel workflow describing methods for constructing a family of basin-scale geomodels. This methodology preserves multiple scales of geological heterogeneity and retains flow unit connectivity in a large tectonic-sedimentary basin (70,000 km^2 by 5 km thick). This addresses the following GCS challenges, which include:

1) optimizing a diverse portfolio of CO_2 storage sites;
2) ensuring long-term safe storage and of multi-Gt volumes that meet proposed carbon emission limits;
3) assessing multiple orders of magnitude variation in heterogeneity on supercritical flow;
4) retaining multiscale heterogeneity at the basin scale;
5) integrating multiple and different facets of GCS research ranging from chemical reactions to long-term storage;
6) understanding the needs of a new GCS industry (economics, infrastructure, workforce).

The geomodel building workflow explicitly exploits different scale geological process-response relationships to establish pore to reservoir-class heterogeneity. Sedimentary responses to different scale formative processes help explain the four orders-of-magnitude variation in core porosity and permeability. This enables these sedimentary attributes to be correlated to reservoir heterogeneity and better retained in model upscaling and simulation. Because heterogeneity is related to sedimentary attributes, critical reproducibility is retained for managing long-term changes in flow and

reaction rates (e.g., 20%, 50% and 80% pore volume injected). This also helps in the quantification of effective permeability heterogeneity on acceptable retention time (100 to 10,000 yrs) for safe storage. Hierarchical treatment of geological heterogeneity better constrains flow migration pathways, regional seal integrity, and interrogation of dynamic models and flow simulation algorithms. The workflow utilizes a family of static geomodels for optimization at the basin scale and involves the following steps:

1) Classify subsurface geology by reservoir class and define basin portfolio of fluid storage sites and containment conditions.
2) Calibrate rock-to-subsurface data to generate a hierarchy of sedimentary attributes consisting of process facies, sedimentation units, and sedimentary bodies for each reservoir class.
3) Erect hierarchical stratigraphic framework based on sedimentary attributes and time-stratigraphic surfaces.
4) Define and distribute sedimentation regions within stratigraphic framework based on sedimentary attributes.
5) Utilize stratigraphic layering of sedimentation regions to modulate heterogeneity and property attributes.

The geomodels in this example incorporate 28,000 wells penetrating Paleozoic to Mesozoic strata (5-km thick by 70,000 km^2 of a structural basin) in a cratonic setting representative of current and proposed North American GCS sites. The Powder River Basin (PRB) of Wyoming and Montana is one of the largest in the United States (Fig. 2.1) and satisfies all four elements required for initial screening, *injection formations,*

adequate depth, confining systems and prospective storage resources (N.E.T.L. 2010) – this paper emphasizes the last two. The PRB represents a realistic candidate for GCS for five reasons: 1) sufficient basin size and stratigraphic diversity, there are five major reservoir classes for storage (Figs. 2.2 and 2.3); 2) robust data set compiled for geomodel generation; 3) necessary infrastructure, with CO_2 sources and pipelines in place for active EOR projects in a mature petroleum province; 4) nine nearby coal-fired power plants represent significant point sources for efficient CO_2 capture and storage (Fig. 2.1b); and the PRB is the single most important coal producing basin in the United States (Scott et al., 2011).

Meeting the Challenges of GCS

In order to cap the CO_2 concentration at 550 ppm, Pacala and Socolow (2004) outline steps required to reach this goal, of which one is GCS. They suggest that sequestration of 3 Gt / year is needed to significantly reduce global green house gas production. This is equivalent to about one-eighth of the current global CO_2 production and the same mass as the total annual global oil production (http://www.eia.doe.gov/neic/infosheets/crudeproduction.html), which will require the development of significant new infrastructure. Plume-scale pilot projects (e.g., Zhou et al., 2010, < 100 km^2) account for several million tonnes (Mt) CO_2/yr, and therefore must be increased up by a factor of 1000 for effective mitigation.

Current homogeneous GCS models use simple layering, few wells and averaged rock properties to interrogate uniform and steady fluid-flow phenomena. Flow in homogeneous media is modeled as uniform and steady fluid behavior to isolate and

understand rock-fluid reactions. Fluid displacement models in homogeneous media over emphasize the buoyancy of supercritical CO_2 displacing denser brine in a saline aquifer, which increases the duration of rock-fluid interactions in the overlying seal rock and the vertical movement of fluids along existing well bores. This produces generalized and symmetric fluid-flow simulations, where far reaching propagation of pressure build up does not reflect multiscale sedimentary architecture such as, stratigraphic pinchout (e.g., converging impermeable layers), lateral facies changes (e.g., interfingering of sandstones and mudstones), discontinuous seals, nor thief zones (high permeability, high flow zones, which may be potentially most important). These high permeability pathways, which typically follow facies-dictated or fracture-induced zones, can transmit pressure very efficiently and may pose the most significant risk to leakage in GCS projects. Most models also assume horizontal targets and seals that are laterally unchanging. This means spatial variations in flow rates are not constrained nor linked to geologic heterogeneity. Nor can a reservoir be isolated for study without consideration of dynamic basin aquifer systems. This complicates onsite GCS in future power plant design and deployment. Therefore, great effort should be applied to most accurately characterize and model geologic heterogeneity.

Until GCS geomodels contain layer heterogeneity (rather than simple geometries with simple property distributions) fluid flow simulations will retain large uncertainty. There are few 3D geomodels available to assess GCS (e.g., Nicot et al., 2008; Yamamoto et al., 2009; Zhou et al, 2010). However, due to the many millions of cells required to model CO_2 fluid flow, these models treat the geology as homogeneous, horizontal

formations with no leakage in caprock formations (Celia, 2008; Nicot et al., 2008; Yamamoto et al., 2009; Zhou et al, 2010). When compared to the geologic detail documented from outcrops, layer-averaged modeling of the effective pore volume structure in a sedimentary basin yields an overly simplistic depiction of sedimentary architecture (*e.g.,* Fischer et al., 2005).

Proper upscaling that retains geological detail is still a major challenge in flow simulation. However, hydrocarbon reservoir management experience suggests that geologic heterogeneity plays a major role in recovery uncertainty. Thus it is important that geologic models provide a sufficient level of detail such that future flow models can assess of impact of geologic heterogeneity on GCS. Current models incorporate some level of stratification, or vertical heterogeneity, typically as a vertical to horizontal permeability ratio (e.g., Hayek, et al., 2009 and references therein). Some authors are emphasizing porosity variability (e.g., *double porosity* = fracture + matrix, Carneiro, 2009) and some even multiscale heterogeneity associated with facies (e.g., Ambrose, et al., 2008). Fortunately, the multiple scales of heterogeneity in sedimentary rocks correlate to different geological processes over a wide range of temporal scales (e.g., Fig. 2.4). Explicit correlation of multiscale heterogeneity to geologic processes provides a method for capturing different scales of heterogeneity in a static basin-scale petrophysical model. Porosity and permeability, represented in Figure 4a as core-derived measurements can vary dramatically in a small distance, even within the same facies. The architecture of the effective pore volume accessible by fluids is therefore fundamental in mapping how porosity and permeability change at different physical scales, both sedimentary and

stratigraphic, through the 3D subsurface volume. Multiscale geologic heterogeneity correlates to sedimentary processes that record sedimentation spanning multiple scales (Fig. 2.5) from (1) individual sedimentary facies recording site-specific process (2) the facies assemblage (*sedimentation unit*) generated during a single event, to (3) the composite record of facies associations in 3D *sedimentary bodies*, to (4) the modulation of these attributes in hierarchical *stratigraphic framework*. The latter records larger-scale changes in the evolution of sedimentary systems occurring across the sedimentary basin. In the modeling workflow, different scale geologic processes, which define the components of a sedimentary system, are used to combine and group smaller scale attributes into larger elements. Though geologic detail is simplified through this process, the resulting grouping, at each step in the process, remains genetically linked to a common set of formative processes responsible for their origin.

In order for GCS to have a significant effect, current technology must scale up by a factor of 1000 (Snieder and Young, 2009). To accommodate this dramatic increase, GCS modeling takes advantage of the many types of geologic units, here termed *reservoir classes* (*RC* hereafter) representing different high effective pore-volume sedimentary systems bounded by competent confining systems, composing the basin fill, in addition to considering targets promising secondary recovery of oil (thus fulfilling two of the three obstacles presented by Snieder and Young, 2009). The distinction must be made between the sedimentary basins (any depression filled with sedimentary rocks) and tectonic basins (structures formed by compression of the crust), as hundreds of millions of years may be recorded in some basin fills. Sedimentary systems reflect their

sedimentary basin, but not necessarily the potentially later formed tectonic basin in which they presently reside. Because tectonic basins like the PRB can contain multiple sedimentary systems (which extended beyond the present basin boundary), and because sedimentary systems control pore volume distributions, characterizing a basin requires describing the portfolio of sedimentary systems present within and near the tectonic basin. Well productivity from zones within the basin is a first-order proxy for injectivity and storage and correlates to different reservoir classes in petroleum system analysis. This approach is used to characterize five reservoir classes (Figs. 1 and 2). Characterizing a portfolio of reservoir classes within a sedimentary basin permits assessment of the degree to which different geologic factors influence CCS, and enhances the portability of reservoir class characterization to other basin storage sites.

When added to the significant computational resources required for modeling dynamic multi-phase fluids (volumes, rates and phase changes) with fluid-rock interactions, it is not surprising that 1) static reservoir and 2) dynamic fluid flow modeling are being treated as separate problems. The inability to separate the impact of upscaling and oversimplification of the reservoir geology, from the behavior of the reservoir during fluid flow has even led to the suggestion that there is a poor correlation between depositional environment and fluid flow (*e.g.,* Larue and Yue, 2003). Despite the overlap between these two variables, the management of petroleum reservoirs has been aided by geologic characterization and the correlation of subsurface reservoir heterogeneity to analogous outcrops since the 1950s.

Applying the results of this study to multiple basins considered for CCS can help quantify the effective GT storage available and the potential implications of such requirements. Because this goal is so resource intensive, all may benefit from focusing efforts on a common dataset, such as the GCS geomodel for the PRB.

Modeling Approach

Stratigraphic heterogeneity can enhance sequestration capacity (Doughty et al., 2008; Havorka et al., 2004); CO_2 in homogeneous media may bypass most of rock volume, whereas flow paths in heterogeneous media are more dispersed, thus increasing wetted volume. However, highly laterally discontinuous effective permeability structure can decrease capacity, effectiveness and injectivity by decreasing sweep efficiency (where fingers of fluid move, leaving much unmoved). Models using layers with heterogeneous effective permeability and porosity structure will likely result in non-uniform pressure build-ups, more localized and focused far field effects and better predict impact of thief zones.

GCS modeling requires analysis of the entire sedimentary fill of the multiple overlapping sedimentary basins, which are confined with the present day tectonic basin (bound by tectonic structures, faults and folds). Although younger structural features bound these stratigraphic units, it is necessary to understand sedimentary patterns up to and beyond the model boundaries. The well logs (28,000 wells with raster images, 5000 of those with up to six log log ascii files), stratigraphic tops (from Precambrian basement to top of Cretaceous), basin bounding structure and the sedimentation regions reside in a subsurface database and permit constructing cross sections and maps. This GCS

geomodel is built with 35 stratigraphic tops (defining the model layers) on the order of 10-30 m thick within the RCs and up to 200m thick between RCs.

In order to better characterize and maintain heterogeneity across multiple scales in a GCS geomodel, two petroleum industry standard principles, typically applied to reservoirs, are employed in 3-D at the basin scale. The first is that multiscale geologic processes are the primary control on effective pore volume character and distribution (Fig. 2.4). Correlating geologic heterogeneity to processes responsible for its origin provides a method for characterizing under-sampled areas as well as upscaling rock properties by averaging them across regions recording a common set of formative processes. The second principle is that grouping at these pore to outcrop scales and using geology to guide upscaling (e.g., Fig. 2.5), structure modeling and rock property distribution will produce more realistic CO_2 fluid flow predictions.

This paper emphasizes techniques established in outcrop models, but is novel to subsurface modeling, e.g., where spatial domains are classified as specific *sedimentation regions* (Gardner et al., 2008). These are defined as laterally restricted areas within a stratigraphically defined rock volume characterized by similar lithofacies and sedimentary body stacking patterns. Sedimentation regions are distinguished from environments of deposition and are restricted to ancient rock volumes; whereas depositional environments are restricted to the description of composite (laterally adjacent and contemporaneous) landscapes and seascapes sculpted by surficial geomorphic processes in modern depositional settings. Using sedimentation regions helps

distribute rock properties to data-poor areas in a hybrid deterministic/geostatistical manner that maintains heterogeneity observed in more data-rich areas.

Although the main focus of this study is to develop the workflow for building a GCS geomodel, it is also important to link this static model to dynamic flow simulations in order to demonstrate the impact of heterogeneity. There exists over a century of production data from hundreds of oil and gas fields in PRB. The integration of derived information such as high-permeability channels from production history needs to be conducted intensively, and quick simulation studies (Finite Difference or Streamline simulations) on some sector models might be necessary in order to validate the geomodel.

Study Area

The 5.5 km thick PRB extends 400 km north from the Laramie Mountains to the Miles City Arch and 250 km east from the Bighorn Mountains to the Black Hills (Fig. 2.1). The sedimentary fill of the PRB represent over 500 million year evolution from Paleozoic carbonates, mixed carbonates and clastics, to Early Mesozoic marine shale and evaporites, to Cretaceous incised valley sandstones, marine clastics to Cenozoic fluvial and lacustrine systems (Figs. 2.2 and 2.3). From these, five intervals were selected for modeling, which correlate to five different types of sedimentary system (Fig. 2.3) and represent the principal *reservoir classes* (defined as a unit of rock characterized by like reservoir types and representing the high pore-volume units in a basin). Characterization of the five reservoir classes (RC), being more detailed than the intervening intervals, is based on published literature, unpublished theses and private consultation with local experts (Table 2.1). The stratigraphic architecture for the entire part of the basin fill used

in the model (basement to top of Cretaceous, approximately 2500-3000 m) is documented in an exceptional subsurface dataset from the PRB that builds upon previous works (unpublished data from RPI of Denver, Colorado and published literature). The dataset includes over 60 stratigraphic surfaces picked in over 28,000 wells tied to dozens of outcrop studies (Fig. 2.1).

Many oil and gas fields in the PRB are currently employing secondary recovery (EOR) techniques including CO_2 injection (Fig. 2.1b). The CO_2 projects require installation of approximately 500 kilometers of pipeline, with 330 more in the near future (O&G Journal, July 29; Aug 10, 2009). Nine coal-fired plants rim the basin provide over 37% of the coal to the U.S. (Luppens et al., 2008), producing approximately 0.05 GT/yr CO_2 (Bailie et al., 2007). These point sources of CO_2 emissions represent logical local providers of CO_2 for storage in the PRB. Two CCS partnerships share the PRB (Big Sky and PCO_2R) and several major enhanced oil recovery (EOR) projects are located in the PRB (Salt Creek 4 Mt/yr and proposed Bell Creek 1MT/yr) (Peterson, 2009).

Basin Geology and Model Overview

The PRB is the easternmost sub-basin of the broken Wyoming foreland flanking the Cordilleran Fold-and-thrust belt and forms a north-trending asymmetric syncline (Figs. 2.1b and 2.3). Basin formation is attributed to Late Cretaceous to Early Tertiary folding and high-angle reverse-faults correlated to the Laramide Orogeny (Blackstone, 1983; Stone 2003). The 7600 m offset in Precambrian rocks exposed in the crest of the Bighorn Mountains to the basin floor along the Piney Creek thrust (Stone, 2003) generated significant fault overhang, which forms a vertical fluid-flow barrier (Huntoon,

1976) for water recharging from the Bighorn Mountains. The gentle monoclines on the east side of the basin, associated with the Black Hills uplift serve as the recharge zone for westward flowing subsurface fluids. Lineament analysis correlated to resource production has identified eight lineaments that are linked to basement blocks that were periodically reactivated during basin filling and identify an important intrabasinal high (the Belle Fourche Arch) during much of the Cretaceous (Slack, 1981). These lineament features and production trends document fluid movement in the PRB. This geomodel focuses on documenting the static sedimentary architecture of five reservoir classes, with post-depositional structural deformation representing a basin-specific overprint not incorporated in the model. Lineament, fault and fracture flow was not addressed in this study, but needs to be incorporated into this geomodel for actual fluid flow modeling of the PRB.

The sedimentary fill of the PRB contains five stratigraphic intervals that host potential GCS targets, here termed RCs, and they correlate to five model types (Table 2.1). These RCs are characterized by the highest subsurface fluid volumes estimated from production (petroleum, water and gas) (Wyoming Geological Association, 2000). The five reservoir classes modeled here include: RC1 representing widespread shallow-water ramp/platform karsted carbonates (Madison Limestone); RC2 representing mixed coastal eolian siliciclastics and shelfal sabkah evaporites and carbonates (Upper Minnelusa); RC3 representing fluvial to estuarine incised valley fill (IVF) siliciclastics (Muddy Sandstone) (Muddy Sandstone); RC4 containing deltaic sandstones (Frontier Fm.); and RC5 composed of shoreface – shelf siliciclastics (Shannon, Sussex, and Parkman

Members). Core data from 300 wells incorporated with log data demonstrate that an RC can show six orders of sedimentary architecture, up to four orders of magnitude variation in permeability and one order variation in porosity (Fig. 2.4). To capture this range in the geomodel, petrophysical (rock property) data from 300 cores (porosity, permeability, grain density oil and water saturation) were correlated to sedimentological descriptions from 5 outcrops and 15 cores to help calibrate the subsurface digital data. Sedimentological descriptions of core and outcrop provide 1) lithofacies, 2) sedimentary bodies, which help define sedimentation regions, and 3) stratigraphic cycle data. When combined with detailed outcrop data, a hierarchy of lithofacies (Table 2.2, Fig. 2.6) and sedimentary bodies (Fig. 2.7) define sedimentation regions (Table 2.3 and Fig. 2.8) comprising sedimentary systems that are framed within a four-fold stratigraphic hierarchy (Fig. 2.9). Establishing a hierarchy of stratigraphic cycles links different scale processes to architectural patterns, one of the main sources of heterogeneity (Fig. 2.10).

The basal RC1 is a primary target for saline aquifer CO_2 storage given its total volume, thickness, and vertical/lateral connectivity; however limited well logs and a general lack of core data make it difficult to characterize the petrophysical properties and their distribution. Specifically, in carbonate formations the high-speed transportation through fractures and high storage capacity in/through vugs need to be characterized in more detail in addition to porosity and permeability trend constrained by analogs nearby. This can be achieved in the hierarchical geologic grouping of data and implementation of the sedimentation region as a sum of these characteristics.

Data And Workflow

This paper utilizes a robust dataset to emphasize a novel workflow that incorporates multiscale basin-wide geological heterogeneity, typically found in field-sized reservoir geomodels. These methods build upon CO_2 basin screening and characterization techniques, combining petroleum industry-standard practices of individual field reservoir modeling into a high-resolution large-volume 3D cube. Rock properties (both measured from core plugs and well logs) must be upscaled in a way that best retains the sub-meter scale resolution in cells that may be multiple meters thick by hundreds wide (Fig. 2.4). At each scale, steps are taken to group the well data that characterize and constrain them by geologic criteria (Fig. 2.5). The region-scale grouping is the sedimentation region (Fig. 2.8), which permits 3-D distribution of the critical properties (effective porosity, permeability, connectivity and seals) in honoring the heterogeneous nature of available data, thus reducing geologic uncertainty (Fig. 2.9). Sedimentation regions are most effective when characterized at the highest resolution stratigraphic sequence (Fig. 2.10). This workflow explicitly exploits the different scale geological processes responsible for generating the multiple physical and temporal scales, from localized facies to basin-wide stratigraphic cycle-scale sedimentary architecture, and more importantly the four order-of-magnitude variation in observed core porosity and permeability.

This workflow comprises two modeling phases, (1) homogeneous - site screening and selection involving geologic characterization of the sedimentary fill of the basin; and (2) heterogeneous geomodel construction. The basin selection process begins with a

continent-scale map of sedimentary basins and successions with sufficient thickness and aerial extent to host CCS projects (Fig. 2.1A) (e.g., Burruss et al., 2009). As candidate basins pass initial screening and are selected for CCS resource analysis, geologic characterization, as described in this paper, includes five steps prior to model construction; the first two relate to the screening and selection, whereas the last three describe building heterogeneous GCS models. These steps include: 1) classification of basin geology and ranking of basin's reservoir portfolio (Table 2.1); 2) definition of sedimentary systems and stratigraphic hierarchy (Figs. 2.5 and 2.10); 3) calibration of rock to subsurface digital data (Fig. 2.6); 4) correlation of sequence hierarchy to reservoir layers (Fig. 2.10); and 5) definition of sedimentation regions and documentation of their stacking patterns (Fig. 2.11A-E). Each of these steps involves some level of geologic coarsening. The steps below describe methods to retain geologic detail as information is grouped and "upscaled".

Methods for Basin Characterization and Developing Reservoir Portfolio

This section describes the steps necessary to characterize the effective pore volume of a structural basin. As described earlier, cratonic sedimentary systems typically show some younger tectonic overprint. For this reason it is important to characterize the *sedimentary* basin separately from the *tectonic* basin. Regions of prolonged subsidence will accumulate sediment, and in the case of foreland basins, these sediments get recycled as the thrust front propagates. During this process, lithified units get buckled and form mountain ranges and tectonic basins, which may represent a smaller area than that of the

previous sedimentary basins. In order to characterize these stratigraphic units in the subsurface, it is necessary to calibrate the data to the rocks they are measuring, which is the first step after basin selection.

Reservoir Class Identification: The majority of producing reservoirs in U.S. sedimentary basins have been discovered and to some extent characterized. Considering the distribution of producing reservoirs (past and present) helps define high pore volume intervals that need to be incorporated and characterized in detail in the GCS geomodel, here called reservoir classes. However, considering only producing reservoirs will underestimate storage, when deep saline aquifers also need to be considered. For this reason all known subsurface reservoirs are considered irrespective of the fluid type. The outcome is identification of RC and non-RC intervals throughout the basin fill. Between RCs, fewer data are required to characterize, as they are not being targeted for primary fluid storage. To best model these large volumes of the subsurface, multiple scales of investigation, each having an imbedded hierarchy, are integral to this workflow.

Define Sedimentary Systems: Because each of the five reservoir classes represents one or more sedimentary systems defined by many sedimentation regions, there is a high probability that truncation, local erosion and reworking can modify the depositional record (Table 2.1). In cases where sedimentation regions may be amalgamated or remnant, or data is too sparse to rigorously define sedimentation regions, it may be necessary to employ a more pragmatic approach and identify regions of similar

range of values. These may define domains in the subsurface dataset that override the sedimentation region *sensu stricto*.

The definition and arrangement of sedimentation regions within the highest frequency cycles is a critical step for controlling the distribution of rock properties in the geocellular model (Figs. 2.11A-E). When each of the sedimentary attributes described previously is assigned to a sedimentation region, one can distribute properties using geostatistical methods correlated to, and constrained by, geologic process e.g., geological upscaling. The correlation of response to process generates a level of reproducibility for the geologic scenario being modeled and justifies the selection and ranking of multiple geostatistical realizations of log facies distributions (Table 2.2).

Because there are multiple scales of stratigraphic cyclicity recorded by each reservoir class, mapping at the RC scale (approximately equivalent to 2^{nd}-order) fails to capture lateral variations in sedimentation that occur in the higher frequency cycles. To capture the high-resolution geologic heterogeneity, the small sequences (50 m) must be mapped, even if they will not be retained within the model. Therefore, to capture changes in sedimentation region through time requires sedimentation region maps for the total number of small sequences in each reservoir class. For example, a vertical boundary through the model would intersect multiple layers in which the region boundaries are laterally offset.

Classify Basin's RC Portfolio

Five reservoir classes were identified based on production (water, oil and gas), lithologic proportions (limestones, dolomites and sandstones vs. shales and evaporites),

EODs with high effective pore volumes (carbonate platforms, eolian dunes, incised valley fills, deltaic and strandline coastal sandstones), and depth below aquifers; these are summarized in Table 2.1. Each reservoir class is composed of one or more sedimentary systems and is bounded by surfaces correlated across the basin (Fig. 2.11A-E). The character of the rock volume varies considerably within this large volume and represents significant geologic heterogeneity at many scales recording over 250 million years of sedimentation processes.

The basal RC1 (Madison Limestone) is one of the primary targets for brine aquifer CO_2 storage (Fig. 2.11A). It has large total volume, ranging from 50 – 500 meters thickening northward and is composed of interbedded dolomites (representing oolites and peloidal packstones), limestones, and evaporites (Sonnenfeld, 1996). Five intermediate-scale stratigraphic sequences help correlate the limestone intervals and frame the dolomite architecture. While type I (primary) porosity is limited to small regions, type II (secondary) porosity (e.g., dolomitic and dissolution features) is concentrated in the lower portion; these provide the largest amount of effective porosity and permeability (Smith et al., 2004). Facies-selective type III (fractured) pore networks are concentrated in the upper Madison along lagoonal mudstones and brecciated intervals (Lorenz et al., 1997). Type II porosity involves dolomitized subtidal and lagoonal settings, with porosity averaging 16% and ranging from 10-35%. Zones that are not dolomitized have very low porosity and permeability. Permeability is highest in fracture zones, which are concentrated in specific facies, which promote detachment and brecciation during folding. Type II porosity mimics depositional patterns to produce a banded fabric with

breccia zones overprinted. The effective pore volume of RC1 is governed primarily by dissolution and solution related to the recharge in the east and pooling of brines in the deepest part in the west.

RC2 (Minnelusa Formation) contains three packages of unconformity-bounded intermediate-scale units composed of eolian and shallow marine sandstones, sabkah evaporites and shallow water carbonates (Fig. 2.11B) (Kerr et al., 1986). The reservoirs in this unit are high quality (type I pores) but localized, being formed by the draping of individual sand dunes by either dolomite or shale (Frederick et al., 1995). Type I and II porosity are depositional and permeability is limited to eolian sandstones, averaging 11% and ranging 10-22%. Permeabilities average 68 mD (milliDarcies) and range between 1-500 mD. Ergs are much more homogeneous and widespread than coastal dunes, between which variation in porosity and permeability is negligible. Complex interfingering of a thick eolian erg with transitional coastal dunes and sabkahs separates the erg sands from peritidal to subtidal clastics and dolomites. Although this is a smaller volume interval, RC2 is capped by a 300+ m-thick succession of shales, evaporites and limestones that represents a significant barrier to CO_2. These two RCs may effectively act as one combined flow unit. Additionally, the rich oil reserves in RC2 represent economic EOR potential.

RC3 consists of stacked incised valley fill (IVF) successions (e.g., the Lakota, Fall River and Muddy Sandstones) composed of fluvial, lagoonal, beach and deltaic sandstones and mudstones (Fig. 2.11C) (Wheeler, 1986; Gardner et al., 1995). Each of these porous and permeable fluvio-deltaic sandstones (type I pores) forms long narrow

compartmentalized permeability pathways along unconformities eroded into and capped by thin sealing shales, except above the uppermost unit (Muddy Sandstone) (Gardner, 2001). The upper IVF, RC3 will be modeled in this project; the lower two will remain for future work. The RC3 sandstones average 11% primary porosity and range 6-17%. Permeabilities average 35 mD with a range of 0.1 to 150. This system represents a corridor 10s of km long by several km wide and less than 20 m-thick geometry filled with a complex architecture, which creates the variety of depositional features that cause this three-order-of-magnitude range of permeability. This interval is rich in production, however being highly permeable; this RC may be in direct communication with outcrops (evidenced by oil staining in the outcrops and a hand-dug oil well) and therefore represent a potential leakage unit.

The deltaic and offshore sandstones in RC4 (Frontier Fm.) represent a 300 m-thick wedge of sandstone pinching eastward into shale (Fig. 2.11D). Sandstones in the lower long-term sequence are restricted to the southwestern portion of the PRB, while the upper crosses the study area. This upper large-scale sequence contains two intermediate-scale sequences that records seaward (eastward) progradation of the deltaic system and is generally encased in shales (Merewether et al., 1979; Weimer and Flexer, 1985; Bhattacharya and Willis, 2001). The migration of shallow-marine environments (e.g., delta front, shelf and offshore) results in highly variable pore types and networks (Winn et al., 1983). Sandstones have 21% primary porosity on average with a range of 10-32%. Average permeability is 270 mD, ranging from 85-500. These deposits are generally fan

shaped 5-10 km wide by 20-30 m thick. The greatest porosity is in the more channelized regions and the delta front region.

The uppermost RC5 represents strandline deposits associated with a series of disconnected offshore bars encased in mudstone (e.g., Shannon, Sussex and Parkman Members) that produce localized but high quality, high volume reservoirs when in fluid communication with each other (Fig. 2.11E) (Weimer, 1960; Tillman and Martinsen, 1987; Tillman, 1997). As a result of wave and current energy reworking and effectively "cleaning" these sands, the resulting large reservoirs can have voluminous pore networks (Tillman, 1997). Primary porosity averages 13% and ranges between 6-20%. Permeability averages 30 mD with a range of 1 to 100. Being encased in shales, these represent long linear sealed containers (up to 10 km long by 1 km wide and 20 m thick) that progressively thin and pinch out eastward into marine mudstone. The paleomarine wave-base across a wave and storm dominated clastic shoreface determined sedimentation regions that change from sand-rich shoreface, eastward to interbedded sand and mud shelf, to mudstone toward the axis of the Cretaceous seaway. This RC is the shallowest of the five and may contain a suite of moderate volume, high quality storage sites.

Subsurface Input Data and Calibration

The PRB has a rich dataset for constructing a GCS geomodel integrating both geology and engineering. The 2D subsurface database (permitting cross section or map view examination) contains over 28,000 wells with over 60 stratigraphic tops (some are shown on Fig. 2.1B) that were used as initial geologic control to calibrate the structural

and stratigraphic framework used in the 3D geomodel. Only vertical wells were used in this geomodel construction and are shown in Figure 2 with color-coding for the five RCs used in the geomodel. The 2D database includes 28,000 wells with digital raster-log images that were used in the initial basin-scale reservoir characterization and data quality control. The laboratory core analyses for 300 wells were digitized for use in porosity log calibration and for permeability prediction in the 3D geomodel. For the 5260 wells with digital log ascii data, 4000 wells with higher quality porosity log suites (density + neutron + sonic + resistivity) were used for estimating log facies, effective-porosity, and matrix permeability for use in the geomodel property distributions. The higher quality logs included 1540 high-quality, normalized bulk density (RHOB) plus neutron porosity (NPHI) combination log suites, 1290 good-quality density + resistivity log suites and 1170 moderate-quality suites, just sonic + resistivity logs. The core-to-log facies were calibrated using 15 cores (510 m) with descriptions tied to log petrophysical responses (Fig. 2.6). Pre-existing basin outcrop studies (e.g., Bhattacharya and Willis, 2001, and many others) were used to calibrate architecture in the subsurface correlations. Pre-existing fault and basin tectonic studies (e.g., Blackstone, 1983; Stone, 2003) were used to constrain the geomodel structural framework. Lack of core data coverage in RC1 (Madison Limestone) was compensated by incorporating subsurface analogs of nearby basins (Sonnenfeld, 1996; Sonnenfeld pers. comm. 2009/2010) and large-scale recharge analysis of the PRB to constrain porosity and predict permeability trends across the basin.

In order to take full advantage of petrophysical data measured in labs, the sedimentary information contained in core and outcrop is upscaled by the geologist as

opposed to the engineer or model builder. This includes the steps described above in facies and architectural element analysis (Figs. 2.5 and 2.6). The 22 core facies defined in this study preserve depositional fabric and are related to hydrodynamic conditions during their formation. During the process of well log clean up and normalization, these core facies provide a way to calibrate the log-derived log facies established from log cutoffs and algorithms (e.g., if-then statements [Appendix E], fuzzy logic, etc.). Two calculated logs are derived from this calibration step (total porosity and shale volume) to calculate effective porosity. When core porosity and log porosity are calibrated, log permeability can be correlated and estimated from core permeability, providing relationships for permeability distribution.

Sedimentary Attribute Generation

Process Facies Attributes: The depositional fabric of sedimentary rocks records a spectrum of sedimentation processes that occurred during their deposition and preservation. The formative depositional processes are characterized during facies analysis, which bins potentially similar, and often overlapping, but distinct fabrics into a discrete and finite number of lithofacies (e.g., ripple laminated fine sandstone, trough cross bedded coarse sandstone, finely interlaminated siltstone and very fine sandstone). Because these lithofacies can number in the dozens and have overlapping petrophysical properties, they must be group into facies assemblages (representing sedimentation units) based on a common set of rock properties (Table 2.2 and Fig. 2.6). It is common to see up to four orders of magnitude range in these petrophysical properties from the poorest to

highest quality reservoir rock (Fig. 2.4A). Using lab measured porosity and permeability cross plots, it is possible to correlate these broad property distributions of lithofacies to define a narrower range of facies assemblages (Fig. 2.4B). It is this set of genetically derived facies that are used to calibrate and condition log-derived log facies (Fig. 2.6 and Appendix A).

Sedimentary Body Attributes: The compound and time-averaged record of multiple geologic lithofacies is reflected in three-dimensional sedimentary bodies bounded by surfaces, commonly referred to as a facies association (Fig. 2.7) (e.g., Van Wagoner, 1985). These 3D bodies represent discrete sedimentary volumes (e.g., linear channelform or accretion wedges) that contain diagnostic lithofacies associations. Linking the subsurface modeling volume to lithofacies associations of sedimentary bodies helps constrain property distribution. Sedimentary bodies are defined by lithology, thickness and log facies trends to describe mesoscale sedimentary architecture. This is typically underemphasized in many studies, but acts to tie facies to stratigraphy.

Sedimentary Attribute Distribution - Vertically

Defining Hierarchy of Stratigraphic Layers: Sedimentary process facies, sedimentary bodies, and sedimentation regions change through time and therefore need to be placed within a hierarchical stratigraphic framework (Fig. 2.10). The smallest-scale sequences within the framework record the conformable migration of laterally adjacent sedimentation regions. These compose a series of larger-scale sequences defined by the stacking patterns of the smaller sequences. This produces a sedimentary architecture that

documents spatial trends in lithofacies, bodies and regions and groups them into a hierarchy of stratigraphic sequences. Furthermore, this identifies sequence stacking patterns, which record lateral migration of the depositional profile and permit prediction in data poor sections of the model.

A hierarchy of stratigraphic sequences provides the context for analyzing changes in sedimentary architecture. These sequences are bound by mappable stratal surfaces, which represent widespread erosion and/or nondeposition and that change to conformable rock volumes elsewhere. These changes complicate stratigraphic correlation. The high well density in this dataset facilitates recognition of surface-to-rock correlations that occur across the sedimentary systems. This stratal-surfaces classification scheme is applicable to all sedimentary systems and is used to consistently classify surface types and calibrate results to the other systems and sedimentary basins; the stratal surface classification scheme includes these four types:

1) Time significant unconformable surfaces caused by erosion, karsting, or dissolution (sequence boundaries).
2) Lithologic contacts (based on changes in rock type).
3) Time significant marine flooding surfaces and condensed sections (typically deeper water rocks over shallow/terrestrial water rocks).
4) Geologically instantaneous event beds or “timelines” (in this case defined by volcanic ash fall deposits forming claystone).

Establishing a stratigraphic framework based on a hierarchy of stratigraphic cycle for the PRB enables the partitioning of sedimentation regions and the correlation of

reservoir layers to the stratigraphic framework. In the case of RC4, regional paleogeography maps were created to capture stratigraphic changes in region architecture. These maps document local uplift and subsidence, lateral sedimentation and shoreline trends and the longitudinal profile consisting of the delta-front/shoreface, marine shelf and offshore marine regions. They are correlated to isochore and facies proportion maps and vertical proportion curves to capture sedimentation patterns in each region. The four-fold hierarchy of stratigraphic cycles (2^{nd}- to 5^{th}-order) for the PRB 1^{st} order fill includes, in order of decreasing duration and thickness:

1) One 1^{st}-order cycle (420 m.y. Paleozoic and Mesozoic) entire PRB fill (up to 15,000 ft/ 4500 m)Five 2^{nd}-order cycles (8-12 m.y.) roughly coinciding with reservoir classes (800-1500 ft/ 250-450 m
2) Four to six 3^{rd}-order cycles (2 m.y.) in each 2^{nd} order, (150-700 ft/ 50-200 m thick)
3) Three to eight 4^{th}-order cycles (ca. 400 k.y.), in each 3^{rd} order (100-300 ft/ 30-100m thick)
4) Up to four 5^{th}-order cycles (ca. 100 k.y.), in each 4^{th} order, (less than 15 ft/ 50 m thick). They represent the fundamental reservoir pore-volume units within the reservoir class.

Correlate Sequence Hierarchy
to Modulate Reservoir Layers: Stratigraphic cross sections, oriented parallel and perpendicular to direction of sediment transport, were constructed and a subset of wells were correlated (using baselevel fall and rise hemicycles) at less than 15 meter resolution

(as a pilot in RC4) to assess the architecture at the sub 5th-order cycle scale (Fig. 3.11D and focus of Manuscript 2). Mapping at this scale, being below the resolution of the 50-meter model layer, allows characterizing the depositional trends and the fine-scale architecture that comprises them. This was done within a high-resolution framework containing ten basin-wide marker beds (bentonites representing altered volcanic ash). Ten thickness (isopach) and lithology (isolith) maps were constructed to guide interpretation of the sedimentary architecture. Thickness maps were compared to isolith maps to understand the distribution of pore volumes, such as distinguishing sand-rich thicks from sand-poor ones.

Basin-wide marker beds permit modeling at 60-200 m thick 3rd-order sequences. The fundamental pore-volume compartments, sandstone bodies 10-40 km wide by up to 30 m thick, can be offset by up to 50 km or more within the 5th-order stratigraphic sequence (denoted as RC4.1, 4.2 etc.). This produces multiple isolated pore-volume compartments in one modeling layer. If these are not identified at the sub-modeling scale, they will be averaged and over-represent the effective pore volume distribution.

RC4.1 and 4.2: The basal model layers have high pore volume in the SW part of model area. The area consists of lobate or pod-shaped wave-dominated accretionary wedge complexes 30 km wide and less than 70 km long and up to 30 m thick (Fig. 2.11D). They form local sediment thicks in the topset and represent the upper part of upward coarsening and sandstone bed thickening successions. More channelization is inferred when these sediment thicks are highly elongate, 5 km wide by 30 km long and over 35 m thick and fine-upward. A basin-wide bentonite marker associated with a shale

interval separates RC4.2 from RC4.3; this interval represents a significant vertical flow boundary and confining layer.

RC4.3 and 4.4: The middle layer consists of mostly mudrocks with generally little pore volume. Two isolated RC4.3 elongate sandstone bodies along the western margin of the model area have similar dimensions to the fluvial valley fill in RC4.1. A basin-wide erosional surface separates

RC4.5 strata from RC4.4 strata with local remnant valley fill sandbodies (the RC4.5, Emigrant Gap Member of the Frontier Formation) preserved in the SW and eastern parts of the basin, where they overlie the RC4.3 sandbodies and RC4.3 carbonaceous shales, respectively.

RC4.6: The uppermost layer (Wall Creek/Turner Sandy Member) unconformably overlies RC4.5 and has the highest pore volume in this RCl. Lithology maps helped identify sand-prone areas within the shoreface, shelf and offshore sedimentation regions. Vertical proportion curves capture vertical trends within these sedimentation regions, such as the upward increase in sandstone content common in shallowing-up sequences. The basinward-stepping sequences in this interval stack to form a broad sandy shoreface region consisting of prograding clinothems that thin and change to shelf/slope mudstones basinward. The SW portion of the study area consists of amalgamated accretion wedge complexes up to 50 m thick and 40 km wide and long. The inclined slope is dominated by mudstones that separate shoreface and proximal shelf regions. The proximal shelf passes basinward into the distal shelf containing thin-bedded sandstone turbidite lobes and

channels detached and isolated from the more sandstone-rich source area to the SW. The distal shelf region is more layered and contains smaller and more vertically isolated sandstone lobe bodies 3-6 m thick by 5-10 km wide separated by up to 5 m thick mudstones (Fig. 2.8 and 2.11d).

Sedimentary Attribute Distribution – Laterally

Sedimentation Region Analysis: A sedimentation region is defined by a suite of properties (e.g., lithofacies and sedimentary bodies) and it records environments of deposition (and erosion) governed by site-specific, geomorphic scale processes that generate recognizable sedimentation patterns (e.g., shoreface, channel and lobe) (Table 2.3 and Fig. 2.8). These can be quantified by the following sedimentary attributes: lithology, grain size and process facies, sedimentary body (shapes), azimuth (lateral trend and spread), vertical trend (vertical proportion curves) and thickness.

Sequence Stacking Patterns: This step uses the two previous deterministic methods to geostatistically populate a subset modeling volume. Porosity and permeability structure is controlled by the stacking pattern of lithofacies in bodies and sedimentation regions within and across the stratigraphic hierarchy. These larger rock volumes contain a broader range of properties and trends reflecting the more diverse suite of bodies and facies that comprise these geomorphic domains. This variability is captured through vertical proportion curves (a technique used to help constrain the vertical distribution of facies based on the probability defined by a subset of logs) and areal proportion maps (including azimuth and degree of change laterally) to guide distribution of the range of

properties. Because sedimentation regions correlate to environments of deposition they also help define the sedimentary system. Sedimentation regions migrate in accordance to Walther's Law (e.g., Middleton, 1973) in conformable succession of strata under high accommodation conditions, but can be more complex under low accommodation and therefore require a stratigraphic framework for definition (Fig. 2.10).

To demonstrate the workflow, the sedimentation regions of the upper part of RC4 are here examined (see also Chapter 3 for detailed sedimentological description). This reservoir class houses the majority of its oil production in the upper sequence (RC4-5 and 4-6, Emigrant Gap and Wall Creek/Turner Sandy members, respectively), which represents shoreface and reworked proximal shelf and associated enigmatic shelf/slope sheet sandstone system characterized as follows (see Fig. 2.7 and Manuscript 2, Figs. 3.12-14).

The *shoreface region* (restricted to the southwestern PRB, the Wall Creek Member) consists of amalgamated sandstones that coarsen and thicken upward (decreasing gamma ray) and have good porosity (12-20%) and permeability 0.5 – 100 mD. Focused sedimentation at the river mouth can form large reworked swash bar and beach barrier ridge wedge sedimentary bodies that stack to form 30-50 and long, 5-20 km wide, by up to 50 m thick composite wedge bodies.

The *proximal shelf region* consists of reworked shoreface sandstones amalgamated across regional sequence boundaries, commonly intensely bioturbated and showing a bimodal to blocky (>10 m-thick) shoaling up log motif. This may be the result of localized forced regression and erosion during transgression.

The *distal shelf region* (restricted to southeastern PRB in RC4-6, Turner Sandy Member) consists of thinly interbedded and/or bioturbated sandstones and mudstones, with sandstones showing good porosity (8-13%), but low permeability (less than five mD). The thin sandstones beds are isolated vertically and laterally but can form relatively sandstone-rich successions. Three northward-stepping depocenters were identified in isochore and sandstone percent maps and record compensation to higher-accommodation sites, still undergoing significant reworking of deltaic derived sediment (transported eastward) by southward-directed long-shore currents.

Localized linear *channel regions* dissect all three previously described regions. These have higher sandstone percent, blocky (< 10-m thick) to fining up The *topset valley fill region* (restricted to RC4-5) consists of amalgamated sandstones that thin and fine upward (increasing gamma ray) and show good porosity (12-20%) and fair permeability (0.5-10 mD). They form narrow and elongated sand bodies 5km wide, up to 70 km long and up to 70 m thick.

It is at this level of detail that the fundamental porosity and permeability architecture can be grouped into geocellular models retaining important heterogeneity that governs the subsurface target and seal characteristics for GCS projects. This geological characterization provides the modeling inputs identified on the bottom right of Figure 2.12. In this study, fluids, pressure and dynamic data are not included. These will be fundamental in the reservoir simulation phase not discussed here.

Workflow For GCS Geomodel Construction

One of the challenges with this subsurface study is utilizing established modeling methods that retain multiple scales of heterogeneity in a petrophysical model designed for simulation at the basin scale. This requires expansion of the geologic upscaling methods derived from the outcrop modeling studies and an increased reliance on depositional environments defined from more general descriptions of the sedimentary systems that define the five reservoir classes in the PRB. The modeling workflow deployed in this study builds on methods established in geologic modeling of outcrop analogs for deep-water reservoirs (Atan et al., 2001; Borer, 2005). Unlike subsurface models where the geology can never be verified, outcrop modeling can establish methods that reproduce the target sedimentary architecture of the outcrop being modeled.

The GCS geomodel construction employs outcrop modeling techniques as well as reservoir characterization methods. These geomodels were constructed in phases, first the RC4 (Frontier) as a southern 1/3 basin sector model to test stratigraphic layering strategies and data distribution cases. Then the larger whole basin geomodel was constructed incorporating all five RCs with 30 surfaces and 20 zones (Fig. 2.13). The workflow for the initial RC 4 GCS sector model is similar to the other RC GCS geomodels, but with different internal stratigraphic layering constraints. The complete basinwide CGS geomodel required larger geo-cell sizes, but with the use of upscaled geologic constraints still retained sufficient heterogeneity used in flow simulation testing.

Construct 3D Model Framework

The whole basin geomodel was constructed using a thrust-faulted framework containing all five RC units. However, the five individual basin sector models did not incorporate faults, and were simply terminated near the basin edge. All thrust faults were approximated as piecewise linear planes to simplify the geomodel construction in complex basin edges, and yet retain the overall structural configuration (Stone, 2009 pers. com.). The master structural surfaces for each of the five RC's and basement were mapped, hand edited in sparse data areas, and tied to stratigraphic picks in wells. Internal stratigraphic surfaces within each RC unit were mapped as isochores, hand edited, and then added to the controlling structural surface to create new 3D internal structural constraining surfaces that were also tied to stratigraphic picks. The present day surficial elevation grid was used as the top of geomodels and upper bounding unconformity.

For the five individual RC basin sector models the fine stratigraphic layering was set to approximately one to three meter range depending on the flow unit geologic detail required. The five individual RC basin sector models used an areal xy grid cell size of 400 x 400 meters, which is approximately 40 acres. For the whole basin geomodel, the fine stratigraphic layering ranged from two to 15 m-thick depending on the flow unit geologic detail required. The whole basin geomodel used an area xy grid cell size of 800 x 800 meter, which is approximately 160 acres.

Distribute Rock Properties in 3D Geomodel

To distribute the rock property data in the geomodels, the wells (n=3000) with usable digital data for log facies, shale volume, effective porosity and estimated

permeability were imported into the 3D modeling package. The 0.15 meter-scale log ascii data was then blocked (upscaled) to the local vertical grid size (e.g. one to three m averages) in the individual RC basin sector models. Two cases for porosity and permeability were distributed. One case distributed log facies using vertical proportion curves and regions and then added porosity and permeability within log facies. The other case relied only on the internal stratigraphic geo-grid details to distributed porosity using co-kriging (based on well logs and geo-templated maps), then permeability using a permeability/porosity transform (Fig. 2.14). All cases used RC and sedimentation region specific variograms. Vertical variograms were generated from log data. The areal azimuthal variograms were based on depositional analogs, since even within developed fields there is usually insufficient close-spaced well data to reliably estimate areal variograms.

At each step of geomodel construction, quality control cross section and 2D average maps were made throughout the 3D geomodel volume to check for realistic geologic data distributions away from well log hard data controls. Both whole basin model (100 million geocells) and the single RC basin sector models (50 to 80 million geocells each) will be available as a deliverable for flow-simulation upscaling and testing of GCS strategies. These static geomodels are a work in progress and are a starting point for further geo-constraint additions including additional structural and stratigraphic detail, and fracture descriptions for characterizing natural fracture permeabilities. Geomodels of this size require significant computational resources, including 64 bit operating systems that can access a minimum of 12 gigabytes of memory.

Results

This study provides three main contributions to test the feasibility of GCS: 1) implication of gross pore volume calculations in five reservoir classes, representative of GCS in onshore structural basins; 2) illustration of detailed geologic characterization workflow for one reservoir class; and 3) impact of geologic considerations on the portrayal of connected pore volume distributions at the basin scale. Outcomes from this study represent a compilation of data and workflow that results in a large high-resolution 3D model at a scale required for CCS screening and feasibility assessment. To impact emissions, GCS deployment scenarios must build upon assumptions that retain maximum geologic detail in order to minimize uncertainty and reduce risk.

The full basin geomodel for all the RCs is constrained by 30 surfaces and 20 regions (Fig. 2.13). These calculations demonstrate that increased heterogeneity reduces the connected pore volume and highlights the problem with homogeneous models for assessment of GCS. The complete GCS geomodel required 100 million geocells, but with the use of upscaled geologic constraints and the single RC basin sector models (50 to 80 million geocells each) it still retained sufficient heterogeneity.

Heterogeneity Retention Increases With Rigorous Geologic Characterization

A simple test was conducted to assess the impact of geologic characterization (stratigraphic hierarchy and sedimentation regions) on gross pore volume (GPV as an estimate of potential total pore volume in the static geology only, no account for faults or fractures, fluid presence or quality, static or dynamic pressure, nor production history).

Publicly available oil field data (Wyoming Geological Society, 2000; WOGCC, 2008-2009) were used to calculate GPV by using two methods: a *factor* (one average value across entire study area) vs. *region* method (constraining average values to discrete modeling layers and domains characterized by similar properties; Appendix B). Bulk rock volumes (n=38) were computed using stratigraphic surfaces gridded in 2-D database software for the hierarchy of sequences that comprise each RC. Polygons (n=103) were created outlining sedimentation regions in each of the small sequences and volumes were computed.

Reservoir properties from oil field data, *porosity* and *net to gross thickness* (percent of gross thickness containing porosity used, NTG) based on 137 data points, were averaged differently for the two methods (factor vs. regions) and with and without stratigraphy (four total values). For the factor method, porosity was calibrated to and averaged across the net pay and sequence thicknesses, which allowed computing a NTG. NTG values for this method therefore reflect GPV averaged across entire basin for whole RC and each sequence in stratigraphic hierarchy, permitting evaluation of impact of stratigraphic hierarchy without sedimentation region constraint (box 1 and 2 in Figs. 2.15A-C). The region method used sedimentation region polygons to group values to average both without stratigraphy and then averaged by each sequence and summed, this compares the impact of stratigraphy alone (box 3 and 4 in Figs. 2.15A-C). These region-specific values were then summed to provide a total GPV for each sequence (Table 2.4). The impact of sedimentation regions on the total GPV for a large sequence is based on sedimentation regions characterized at that scale.

The result is that a 2nd-order GPV for an RC generated by regions and hierarchy of sequences may vary from GPV generated by regions without hierarchy of sequences (Fig. 2.16). Because the RCs represent different sedimentary systems, they were analyzed individually in Table 2.3 and summarized in Table 2.4. This allowed identification of three types of reservoir classes: 1) similar stratigraphy and sedimentation region arrangements; 2) dissimilar stratigraphy but similar sedimentation region arrangements; and 3) dissimilar stratigraphy and sedimentation region arrangements (Fig. 2.16). This illustrates the importance of sedimentation region analysis at the highest resolution sequence scale.

Static 3D Geomodel Ready for
Upscale to Fluid Flow Simulation

Construction of this GCS geomodel has provided a detailed workflow outlining the importance of geological grouping techniques and emphasizing the impacts of retaining multiscale geological heterogeneity. Because this study was designed for analyzing GCS potential, the workflow methods can be applied to basin studies in any onshore basin targeted for CCS or in areas with inherently high uncertainty.

The outcomes of this research include a family of GCS geomodels (Table 2.1 and Fig. 2.13). A whole basin model was constructed from 30 surfaces from Precambrian basement to present day topography and contain 20 zones. 3000 wells were used to distribute the four properties (log facies, Vshale, effective porosity, matrix permeability) in this 170,000 km^3 volume containing 50 million cells, each measuring up to 800 by 800 meters on a side and 3 meters thick. There are six faults bounding the whole basin

geomodel, four severing and two partially puncturing the strata. Basin-wide sector models characterize each of the reservoir classes using 50-80 million cells and 3000 wells, constructed of up to ten surfaces and nine zones with cells 400 by 400 meters on a side and up to one meter thick. These RC-specific sector models can be exported to other data-poor basins where they can be calibrated with sparse data.

Static GCS Geomodel Applications

Flow-simulation ready GCS geomodels provide geological input to predict long-term migration path risks during the life of the injection simulation (e.g., 20%, 50% and 80% geomodel pore volume injected) and permit quantification of effective permeability heterogeneity on CO_2 sequestering retention time (100, to 10,000 yrs). Many of the questions being discussed at national and international CCS conferences can be addressed by assessing some key geological attributes such as, geo-connectivity for CO_2 flow paths and seals, geo-input for testing upscaling options as well as for flow simulations to test sequestering options like lithology for storage and seal integrity and matrix for retention.

Accurate forecasting and assessment of uncertainty and risk for industrial-scale storage of CO_2 in basins require multiscale heterogeneous geomodels incorporating multiple disciplines. The geological characterization and geomodel construction provide many platforms for this multiscale study to bring together many different but integrated areas of research to provide potential solutions to industrial scale CCS. Further model applications include: basin-scale CO_2 storage volume estimates, site screening, identifying high-risk flow migration pathways, characterizing regional seal integrity, testing alternate upscaling methods and flow simulation algorithms.

Conclusions

The Powder River Basin represents an exceptional laboratory for characterizing geology, generating input for 3D geomodels and examining industrial scale CCS issues. The robust high quality data set permits characterizing a portfolio of five different reservoir classes that are common to most onshore cratonic basins and documenting their multiscale heterogeneity at a resolution previously reserved for field-scale reservoir geomodels. This permits interrogating a 3D geomodel based on actual geology with questions regarding the many different facets of CCS deployment strategies. Impacts of alternative methods for upscaling than those used in this study can be assessed. The PRB is essentially GCS ready; it contains large CO_2 resources, is near ample point sources of CO_2, and it has in place and proposed CO_2 pipeline. Collaboration of a diverse range of scientists and policy makers could influence actual CCS deployment. Industrial-scale CCS includes both government regulators and industry partners that together enable CCS in the PRB and effectively immediately impact emissions.

The PRB geomodel represents a valuable dataset because of the realistic geologic characterization. The PRB workflow emphasizes steps used in the construction of a family of geomodels required to retain multiscale heterogeneity in a portfolio of reservoirs at the basin scale. The geologic characterization workflow created a portfolio of GCS resources within an entire basin and identified three types of reservoir classes. Impacts of gross pore volume calculations are significantly impacted (up to a factor of 2) by the degree of detail included in the computation. Workflows presented (defined) for retaining geodetails are linked to upscaling and assessing gridding strategies and stress

the importance of a hierarchical stratigraphic framework embedded with sedimentation region analysis at the highest resolution possible. More realistic geomodels represent platforms to assess implementation strategies; they provide gross volumetric estimates for storage, injectivity and migration (i.e., monitoring); and they represent common datasets that encourages more integration of all members in this new industry.

RC # and Sedimentary Attriubutes	1: Carbonate Ramp to Platforms (Permian Madison Limestone)	2: Mixed Carbonate - Clastic Coastal Systems (Pennsylvanian -Permian Tensleep/Minnelusa)	3: Incised Valley Fill Systems (L. Cretaceous Lakota, Fall River, Muddy SS)	4: Low Accommodation Strand Line-shelf systems (Middle Cretaceous Frontier Fm)	5: Clastic Shorelines (Upper Cretaceous U. Steele and L. Mesaverde)
Basin Type	cratonic	foreland	cratonic	Early foreland	Late foreland
Lithologies Porosity ( ) Permeability (K)	Limestone: : 0-5%; K: low Dolomite: : 15-35%; K: high Evaporite: : <3%; K: low Karst breccia: : 0-50%; K: variable	Limestone : <5%; K: V. low Dolomite : 10-15%; K: V. low Evaporite: : <3%; K: v. low Sandstone: : 15-20%; K: very high Mudstone	Fluvial SS: 11%; K: very high Estuarine SS: 4%; K: mod Shoreface (valley fill): 12%; K very high Mudstone	Shoreface SS: 10-12%, moderte Reworked Shoreface SS: 2-8% Hyperpycnite SS: 1-11% Mudstone Carbonaceous Mudstone	Strandline shoreface: 10-14%; K high Offshore bar SS: 8-10%; K high Muddy slope: <4% Mudstone
Total and net thickness Sediment Accumulation Rate	0-425 meters (m); 0-1400 feet (ft) 60-120 m; 200-400 ft < 35 meters/million years (my) < 120 feet/million years (ft/my)	0-200 m; 0-600 ft 60-90 m; 200-300 ft 45 m/my; 150 ft/my	15-45 m; 50-150 ft 12-22 m; 40-75 ft 22 m/my; 75 ft/my	Compensatory lobate strand line clastic wedge	250-300 m; 800-1000 ft <30 m; <100 ft 75 m/my; 250 ft/my
Well log data quantity and quality	100 wells 18% density/neutron porosity well log suite	800 wells 80% density/neutron porosity well log suite	1300 wells 90 % density/neutron porosity well log suite	1100 wells 60% density/neutron porosity well log suite	1300 wells 50% density/neutron porosity well log suite
Age Cycle forcing Duration Hierarchy	Mississippian (large continental seas) Greenhouse 11 million years 3 orders (2-4th)	Lower Permian Icehouse - more hi frequency, hi mag SL changes 4-6 million years 3 orders (2-4th)	Lower Cretaceous (Boreal/Tethian cratonic seas) Greenhouse 2 million years 3 orders (2-4th)	Mid Cretaceous (Iniation of Western Cretaceous Seaway) Greenhouse 10 million years 3 orders (2-6th)	Upper Cretaceous (Culmination of Western Cretaceous Seaway) Greenhouse 5 million years 4 orders (2-5th)
Surface Types Seal Type	Karst Dissolution vugs Subaerial erosion Seal irregular and discontinuous	Mud-filled incised valley fill unconformity at top; Flooding surface Evarporite caps; Shale drape	Incised valley fill, unconformity at base; Flooding surface Shale drape	Mud-draped transgressive surfaces of erosion. Forced regression unconformities.	Transgressive surface of erosion Shale drape
Sedimentation regions Shape Strataregions	laterally continuous cratonic carbonate platform with large shelf and many isolated buildups	coastal eolian shoreface, sabkha, wadi, shallow water carbonates	Flood-based back-filling valley fill encased in mudrocks long linear high perm bodies	Compensatory lobate shorefaces (laterally discontinuous)-hyperpycnite (laterally continuous) clastic wedge	Linear, fault-controlled clastic Strandplain wedge partitioned by mudrocks
Connectivity Vertical Horizontal Lateral	Widespread high connected pore volume layers bound by no flow limestones	clastic wedge segregated by widespread dolomites, high horizontal permeability, low vertical permeability	Long linear channel belts with high horizontal and vertical permeability	Isolated flow units, moderate horzontal permeability, variable vertical permeability	Thin high horizontal permeability zones, very vertically partitioned
Connected Pore Volume	Largest pore volume resource	Variable high volume	Moderately low	Moderately hi	Moderately high
CO2 migration Rate	low to very low	Locally high	High leakage pathway	Moderate	High leakage pathway Connected to faults

Table 2.1. Reservoir classes are defined by multivariate attributes at multiple scales.

Explanation to colors

Favorable (e.g., low risk + high volume)	**Moderately Favorable**
Moderately Unfavorable	**Unfavorable (e.g., high risk ± low vol)**

#	Facies	Grain size	Sorting	Primary structures	Bed (thickness)	Bedset (cm)	SS%	Perm (mD) min	Perm (mD) max	Porosity (%) min	Porosity (%) max	Process interpretation
1	Coarse lag	med SS - granule	poor	aligned grains, planar laminae	<10	NA	100	0.1	100	12	20	erosional and/or reworked surface,
2	Clast-rich to conglom SS	Med - coarse SS	poor	Structureless, planar laminae	20-50	NA	100	0.1	0.3	4	6	freezing of debris flow to high concentration flow
3	Amalgamated cross-bedded SS	UF - coarse SS	mod well - well	Trough cross stratification	30-50	100+	100	0.01	20	2	14	repeated deposition from mostly unidirectional low concentration high velocity flow
4	PT Cross bedded SS	UF - coarse SS	mod well - well	planar tabular cross stratification	20-50	<100	100	0.1	150	4	23	deposition from uni/bidirectional low concentration mod velocity flow
5	Muddy cross beds	F-Med SS	mod - mod poor	Trough cross stratification, mud clasts or drapes	20-30	<80	100	0.05	0.1	4	6	unidirectional low concentration mod to high velocity flow
6	Soft sed deformed SS	F-Med SS	mod - mod poor	dewatering/load structures	20-50	100+	95	0.02	0.05	2	4	rapid deposition from high-concentration flow
7	Structureless SS	Uf - med SS	mod - mod poor	structureless	20-30	100+	100	0.01	50	2	17	freezing or rapid deposition from high-concentration flow
8	Plane parallel SS A	Uf - med SS	mod well - well	planar laminae	10-20	<50	100	0.01	150	2	15	deposition from moderate concentration, moderate velocity flow (traction carpets)
9	Swaley SS	Fine SS	mod well - well	plane parallel to low angle strat with reactivation surfaces	20-40	80-120	100	0.1	0.1	3	12	deposition or reworking from uni/bidirectional flow, above FWWB
10	Hummocky SS	Fine SS	mod well - well	plane parallel to low angle stratification	10-30	60-80	100	0.01	150	4	18	deposition or reworking from uni/bidirectional flow, at or below FWWB
11	Plane parallel SS B	VF SS	mod - well	plane parallel, structureless	5-20	<50	100	0.01	40	1	11	deposition from low concentration mod to low velocity flow
12	Faintly stratified amalgamated SS	F SS	mod - mod poor	Faint plane parallel, wispy discontinuous mud drapes	100+	100+	95	0.01	2	1	14	repeated rapid deposition from high-concentration flow, locally dewatered
13	Interbedded deformed/bioturbated SS	VF - Fine SS	mod poor - poor	Burrows, loads, rip up clasts	2-10	100+	85	0.01	1	2	12	intermittant rapid deposition from high-concentration flow, locally dewatered and/or burrowed
14	Amalgamated bioturbated SS	VF - Fine SS	mod poor - poor	Diverse and abundant burrows	5-15	200+	95	0.01	2	5	12	low frequency deposition from flows, poss reworked by waves, above FWWB
15	Ripple laminated SS	VF - Fine SS	well	Ripple cross laminae	1-8	1-20	100	0.6	50	1	23	unidirectional low concentration low velocity flow
16	Interbedded thinly laminated SS with mud drapes	VF - Fine SS	mod well - well	Planar laminae, mud drapes	1-3	100+	70-90	0.01	100	2	20	low frequency deposition from flows, poss reworked by waves, between FWWB and SWB
17	Bioturbated SS and mud	VF - Fine SS	mod poor - poor	Diverse and abundant burrows	1-3	100+	30-50	0.1	0.1	13.5	13.5	low frequency deposition from flows, poss reworked by waves, at or below SWB
18	Interlaminated mud and SS	Silt - VF SS		fine parallel laminae	<3	100+	50-70					low frequency deposition from low concentration low velocity flows,
19	Bioturbated mud and SS	Shale - silt			1-3	200+	60-80	0.01	15	8	17	low frequency deposition from very low concentration very low velocity flows,
20	Shale with thin SS beds	Shale - silt			<1	10-00+	<50	0.08	2	2	2	very low frequency deposition from very low concentration very low velocity flows,
21	Dark marine shale	Shale			<1	10-100+	<10					suspension deposition
	Claystone	clay	NA	none			none					weathered volcanic ash deposit
23	cemented	variable	na									

Core Facies Grouping

- Coarse grain to pebble lag
- Cross-bedded upper fine - coarse SS, thick & medium bed, or muddy fine-medium SS
- Fine-medium SS, plane parallel stratification lined with pebbles
- Deformed SS, mud clasts
- Swaley, hummocky fine SS; or bioturbated SS with no discernible structure
- Faintly laminated +/- wispy mud laminations, may be structureless thick to thin bedded
- Parallel - ripple laminated very fine to fine SS
- Thinly interlaminated fine SS siltstone, bioturbated
- Thinly interlaminated siltstone and mudstone bioturbated
- Shale and bentonite
- Calcite cement

Log Facies Grouping

- Higher energy facies
- Stratified or thick bedded SS
- Lower energy facies
- Interbedded or bioturbated SS/mud
- Lowest energy facies
- Mudrock
- Cemented SS

Facies	GR	DT	RHOB	REST	NPHI
1 MAX	60	70	3	299	0.11
1 MIN	0	0	2.45	1	0
2 MAX	85	75	2.7	200	0.165
2 MIN	30	60	2.4	3	0.1
3 MAX	100	120	2.7	100	0.18
3 MIN	60	70	2.4	1	0.12
4 MAX	400	120	2.625	50	1
4 MIN	85	70	0	0	0.16

Table 2.2. Facies descriptions and interpretations help define grouping strategies. Right, well log values defining analog facies: Gamma Ray, (GR in API), Bulk Density (RHOB in grams per cubic centimeter), Neutron Porosity (NPHI - % porosity), Sonic (DT - microseconds per foot) and Resistivity (REST - Ohms). It is necessary to group based on the scale that the logs permit recognition. For example, all the facies 1-13 were indistinguishable in well logs, so were lumped into "higher energy facies". See Appendix E for statistical analysis of well-log generated log facies.

1) : Ave_{strat} (Vol*NTG*POR)

2) : Ave_{strat} [Σ_{strat} (Vol*NTG*POR)]

3) : Ave_{strat} [Ave_{reg} (Vol*NTG*POR)]

4) : $\Sigma_{strat, region}$ (Vol*NTG*POR)

Cycle	poros	perm	Thick3rdO	NTG3rdO	SedReg3rd
					3rd order
2-3 minn B	0.13	34	18	28%	1
2-3 minn b	0.13	46	118.9	114%	1
2-2 tensleep	0.141	136.7	94.3	82%	1
2-2 minn C	0.127	46	75.5	20%	1
2-2 minn C	0.115	350	72.6	19%	1
2-2 minn c	0.088	14.4	118.9	32%	1
2-2 minn B	0.12	137	74	28%	1
2-1 minn D dc	0.126		81.5	10%	1
2-4? minn	0.161	60	65	31%	2
2-4 minn a	0.175		69	29%	2
2-4 minn a	0.18	300	83	20%	2
2-4 Minn A	0.188	205	65	49%	2
2-4 minn a	0.14	50	16	94%	2
2-3 minn B	0.18	9.6	40	35%	2
2-3 minn B	0.173	93	38	47%	2
2-3 minn b	0.15	40	72.4	26%	2
2-3 minn a	0.16	3.3	52	17%	2
2-2? min A	0.17	68 to 8	86	19%	2
2-2 minn C	0.19	224	93	43%	2
2-1? minn C	0.2	500	94	28%	2
2-1? Minn	0.126	100	128	8%	2
2-4 minn a	0.14	21	30	47%	3
2-4 minn a	0.172	112	101	10%	3
2-3 minn b?	0.0193	0.03	199	3%	3
2-3 minn b	0.12	40.2	99	7%	3
2-3 minn b	0.2		147	23%	3
2-3 minn b	0.09	10	83	0%	3
2-4 minn a	0.015	0.05	78	3%	4
2-2 Uminn c	0.09	42	83	17%	4
2-2 Uminn c	0.0792	1.92	41	46%	4
2-2 Uminn c	0.111	45.5	56	50%	4
2-2 tensleep?	0.12		89.6	56%	4
2-1 Uminn d	0.0873	9.46	121	68%	4
2-4 minn a	not reported		77.4	8%	5
2-2 minn c	0.01	0.02	83	0%	5
2-2 minn c	0.01	0.05	141	0%	5

region	interval	total km3	% NTG ave	Φ ave	GPV ave
no regions	RC2	3495	31%	13%	139
3459	RC2-4	360	35%	15%	19
	RC2-3	650	30%	14%	26
	RC2-2	1074	32%	11%	36
	RC2-1	1375	28%	13%	53
1) north	RC2	1045	40%	12%	51
396	RC2-4	Eroded			
	RC2-3	4	71%	13%	0.37
	RC2-2	61	38%	12%	2.75
	RC2-1	331	10%	13%	4.09
2) E central	RC2	396	31%	17%	20.84
528	RC2-4	0.000126	45%	17%	0.00
	RC2-3	113	31%	17%	5.88
	RC2-2	181	31%	18%	10
	RC2-1	234	18%	16%	6.85
3) central	RC2	166	18%	12%	3.75
545	RC2-4	11	28%	16%	0.49
	RC2-3	33	8%	11%	0.30
	RC2-2	186			
	RC2-1	314			
4) S central	RC2	777	38%	8%	24.42
888	RC2-4	112	3%	2%	0.04
	RC2-3	186			
	RC2-2	278	42%	10%	12
	RC2-1	312	68%	9%	18
5) S east	RC2	1112	4%	1%	0.4
1240	RC2-4	2.97	8%	nd	
	RC2-3	314			
	RC2-2	495	0%	1%	
	RC2-1	428			

Homogeneous *(factors)*

Ave_{strat} [Vol NTG $\Phi_{ave, max, min}$] = GPV

- NTG is similar to h_n/h_g factor used in Probability and Monte Carlo method:*

E_{saline} =

(A_n/A_t) (h_n/h_g) (ϕ_e/ϕ_{tot}) x E_A E_I E_g E_d

area *ntg* *poro* *efficiency*

This technique uses published tables to estimate values immediately surrounding single well injectors (after US DOE, NETL, 2008, W.G.A., 2000)

Heterogeneous *(sedimentation regions)*

Σ_{strat} [Vol Σ_{sr}NTG Σ_{sr} $\Phi_{(ave, max, min)}$] = GPV

- At highest resolution stratigraphy, this retains stratification of pore volume in sedimentation regions' distribution
- Permits "smart" use of cells in model, locally refining grid in good reservoir zones, and relaxing in non-reservoir zones

Table 2.3. Example of gross pore volume (GPV) calculation methods including four methods: 1) Factor method averaged across stratigraphy (each orange porosity and NTG is averaged in the blue row); 2) factor method summed across stratigraphy then averaged (each row in yellow is average of that stratigraphy in each region, then summed); 3) region method averaged within region and across stratigraphy (each orange color averages the porosity and NTG, and is then summed) and 4) region method averaged within region, summed across stratigraphy (sum of all mint green colors).

RC1

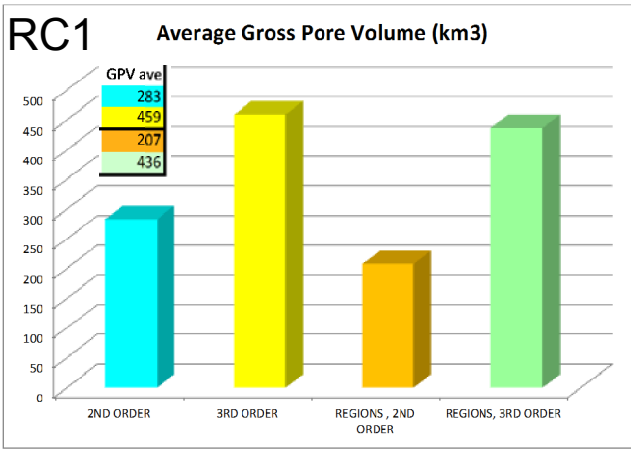

	cycle	V km3	% NTG ave	Φ ave	GPV ave
No Regions	**RC1**	16331	26%	7%	283
	RC1-4to6	2174	0%	0%	
	RC1-3	3642	66%	14%	330
	RC1-2	4806	19%	7%	59
	RC1-1	5709	19%	7%	70
S east	**RC1**	2871	29%	9%	70
	RC1-4to6	465	0%	0%	
	RC1-3	822	61%	15%	75
	RC1-2	854	27%	10%	22
	RC1-1	729	27%	10%	18
west	**RC1**	2554	31%	8%	61
	RC1-4to6	335	0%	0%	
	RC1-3	851	*63%*	*11%*	59
	RC1-2	815	*30%*	*10%*	24
	RC1-1	553	*30%*	*10%*	17
north	**RC1**	10906	19%	4%	77
	RC1-4to6	1374	0%	0%	
	RC1-3	1968	*75%*	*15%*	221
	RC1-2	3137	*0%*	*0%*	
	RC1-1	4427	*0%*	*0%*	

RC2

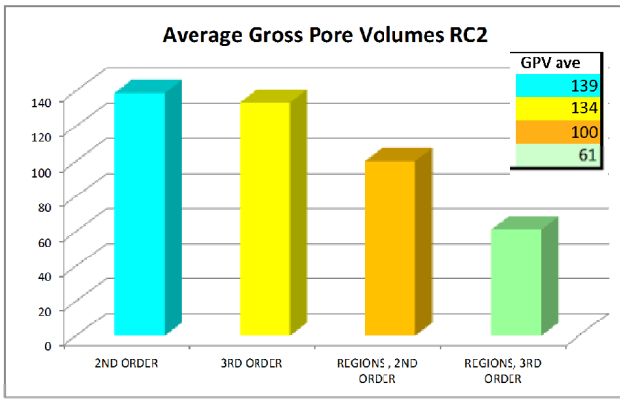

region	interval	total km3	% NTG ave	Φ ave	GPV ave
no regions	**RC2**	3495	31%	13%	139
3459	RC2-4	360	35%	15%	19
	RC2-3	650	30%	14%	26
	RC2-2	1074	32%	11%	36
	RC2-1	1375	28%	13%	53
1) north	**RC2**	1045	40%	12%	51
396	RC2-4	Eroded			
	RC2-3	4	71%	13%	0.37
	RC2-2	61	38%	12%	2.75
	RC2-1	331	10%	13%	4.09
2) E central	**RC2**	396	31%	17%	20.84
528	RC2-4	0.000126	45%	17%	0.00
	RC2-3	113	31%	17%	5.88
	RC2-2	181	31%	18%	10
	RC2-1	234	18%	16%	6.85
3) central	**RC2**	166	18%	12%	3.75
545	RC2-4	11	28%	16%	0.49
	RC2-3	33	8%	11%	0.30
	RC2-2	186			
	RC2-1	314			
4) S central	**RC2**	777	38%	8%	24.42
888	RC2-4	112	3%	2%	0.04
	RC2-3	186			
	RC2-2	278	42%	10%	12
	RC2-1	312	68%	9%	18
5) S east	**RC2**	1112	4%	1%	0.4
1240	RC2-4	2.97	8%	nd	
	RC2-3	314			
	RC2-2	495	0%	1%	
	RC2-1	428			

RC3

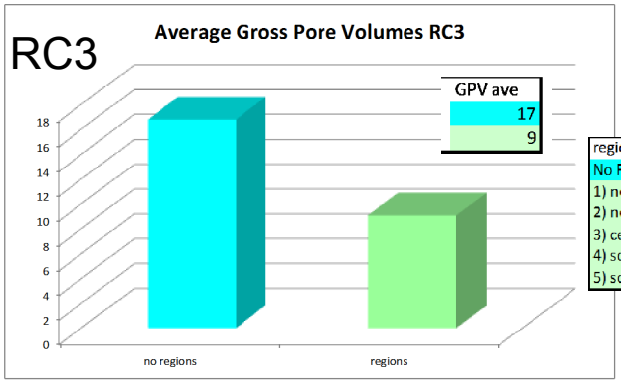

region	area km2	total km3	% NTG ave	Φ ave	GPV ave
No Regions	72478	2642	7%	9%	17
1) north	32817	1691	2%	2%	0.67
2) north vlley	4645	191	14%	18%	4.81
3) central	21690	516	2%	8%	0.86
4) south valley	6225	143	13%	14%	2.59
5) south	7101	101	4%	3%	0.14

Table 2.3 continued. Table for each reservoir class (RC) showing results of calculation by four methods.

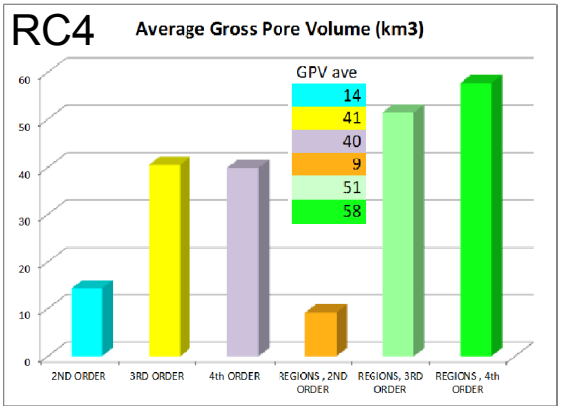

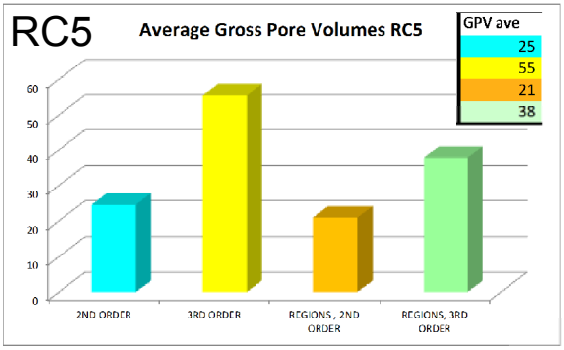

region	interval	total km3	% NTG ave	Φ ave	GPV ave
data	**RC5**	24710	0.8%	13.0%	24.6
	RC5-4	5598	2.5%	14.0%	19.9
	RC5-3	8229	0.0%		0.0
	RC5-2	3699	3.9%	11.7%	17.0
	RC5-1	4043	3.5%	13.3%	18.6
west	**RC5**	8925	0.6%	12.8%	7.3
	RC5-4	2665	2.4%	12.7%	8.1
	RC5-3	2923			
	RC5-2	1723	2.8%	11.4%	5.6
	RC5-1	1446	3.5%	13.3%	6.7
central	**RC5**	9613	1.1%	13.4%	13.6
	RC5-4	2152	2.7%	15.3%	8.8
	RC5-3	3051			
	RC5-2	1526	4.7%	12.0%	8.6
	RC5-1	1713	-	-	-
east	**RC5**	6172			

Frontier

	interval	area km2	total km3	NTG ave	Φ ave	GPV ave
stratigraphy	RC4	42200	13275	5%	2%	14.2
	RC4-7	42200	1826	0%	0%	0.0
	RC4-6	42200	2471	20%	7%	35.8
	RC4-6-5	42200	358	0%	0%	0.0
	RC4-6-4	42200	649	16%	7%	6.9
	RC4-6-3	42200	662	12%	5%	4.1
	RC4-6-2	42200	536	31%	9%	15.5
	RC4-6-1	42200	539	23%	7%	8.4
	RC4-5	42200	401	0%	0%	0.0
	RC4-4	42200	2840	0%	0%	0.0
	RC4-1to3	42200	5738	3%	3%	4.8
	RC4-3	42200	1095	7%	4%	2.7
	RC4-2	42200	2041	3%	4%	2.2
	RC4-1	42200	2624	0%	0%	0.0

region	interval	area km2	total km3	NTG ave	Φ ave	GPV ave
1 chan	RC4		421	4%	2%	0.26
	RC4-7	0	0	0%	0%	0
	RC4-6	5721	390	12%	5%	2.2
	revised		0			
	RC4-6-5	0	0			
	RC4-6-4	1301	21	30%	6%	0.4
	RC4-6-3	1232	29	10%	5%	0.1
	RC4-6-2	2796	34	14%	4%	0.2
	RC4-6-1	1798	18	0%	0%	0.0
	RC4-5	3414	31	0%	0%	0
	RC4-4	0	0			
	RC4-1to3	0	0			
	RC4-3	0	0			
	RC4-2	0	0			
	RC4-1	0	0			
2 shfce	RC4	6521	1648	10%	5%	8.14
	RC4-7	0	0	0%	0%	0
	RC4-6	7113	506	36%	9%	16
	revised		807	13.5%	9.0%	10
	RC4-6-5	0	0	0%	0%	0.0
	RC4-6-4	9957	155	26%	13%	5.3
	RC4-6-3	8041	158	41%	10%	6.3
	RC4-6-2	6631	83	43%	8%	2.8
	RC4-6-1	8502	121	36%	5%	2.2
	RC4-5	2900	48	0%	0%	0
	RC4-4	0	0	0%	0%	0
	RC4-1to3	9193	1094	13%	11%	14.5
	RC4-3	4165	162	28%	14%	6.4
	RC4-2	6888	417	10%	17%	7.3
	RC4-1	6521	514	0	0	0
3 prx shlf	RC4		356	7%	2%	0.46
	RC4-7	0	0	0%	0%	0
	RC4-6	9127	356	34%	10%	12
			555			18
	RC4-6-5	0	0			
	RC4-6-4	9127	135	23%	9%	2.7
	RC4-6-3	5596	87	11%	4%	0.4
	RC4-6-2	6138	71	78%	15%	8.3
	RC4-6-1	5390	63	24%	10%	1.5
	RC4-5	0	0	0%	0%	0
	RC4-4	0	0	0%	0%	0
	RC4-1to3	0	0	0%	0%	0
	RC4-3	0	0	0%	0%	0
	RC4-2	0	0	0%	0%	0
	RC4-1	0	0	0%	0%	0
4 dist shlf	RC4		288	4%	3%	0.27
	RC4-7	0	0	0%	0%	0
	RC4-6	6272	288	18%	13%	7
	revised		507			12
	RC4-6-5	0	0	0%	0%	
	RC4-6-4	3176	50	0%	6%	0.0
	RC4-6-3	4225	51	0%	6%	0.0
	RC4-6-2	6905	82	20%	20%	3.3
	RC4-6-1	7946	104	54%	19%	10.6
	RC4-5	0	0	0%	0%	0
	RC4-4	0	0	0%	0%	0
	RC4-1to3	0	0	0%	0%	0
	RC4-3	0	0	0%	0%	0
	RC4-2	0	0	0%	0%	0
	RC4-1	0	0	0%	0%	0

Table 2.3 continued. Table for each reservoir class (RC) showing calculation four methods. Equations summarize technique. The impact of these two methods is discussed in the text.

Reservoir Class	Data source	Stratigraphy	Regions	Impact
RC1: Carbonate ramp to platform – highly variable stratigraphy and predictable distribution of high porosity facies	Porosity, NTG, estimates from Sonnenfeld pers. Comm.	2nd- and 3rd-orders; stratigraphy eroded in the southern PRB, upper 3 sequences 0% NTG	Based on zones of anhydrite (west) and depositional facies (north, south)	3rd-order stratigraphy almost doubles GPV, while regions reduce it by 10-30%, more so without stratigraphy
RC2: Cyclic sequences of dolomite capped shoreface to eolian sandstones, separated by areas of sabkah and lower shoreface mud	Porosity and NTG data based on oil field data*	2nd- and 3rd-orders; stratigraphy eroded in northern PRB, stratigraphic variation low; high-continuity (H) but very low-connectivity (V)	5 regions based on complex setting from eolian dune fields, coastal dunes/sabkah, shoreface and marine mud	Regions remove low porosity areas further reducing GPV, more effective when constrained by 3rd order stratigraphy
RC3: 3rd-order Incised valley fill – isolates reservoir sand to dendritic valley regions	Porosity and NTG data based on oil field data	3rd-order only; 4th-order sequences can be added to isolate fluvial from deltaic and shallow marine sequences	Two valley systems; southern capped by mud, northern one capped by deltaic/ shallow marine	Regions critical in isolating GPV to valley regions
RC4: Low-accommodation clastic shoreline; restricted to southern PRB; significant lacunas truncate lower sequences in SW PRB; upward increase in lateral continuity	Porosity and NTG data based on oil field data	2nd-4th-orders; highly variable stratigraphy, lower sequences truncated in SW but conformable in SE PRB, high-resolution sequences defined in upper part (4-3)	Lower part restricted to western PRB, middle constrained to valleys and upper part thin but continuous shoreface, shelf and offshore regions correlate across southern PRB	2nd-order over-emphasizes GPV by averaging over large volume; 3rd-order with regions emphasizes high GPV zones, but removes 0% NTG zones, otherwise under-estimated
RC5: Low accommodation strand lines bound by thick mud sequences	Porosity and NTG data based on oil field data	2nd- and 3rd-orders; Reservoir intervals very stratified, thin sandstones at top of thick mudstone section composing sequence, one mud-prone sequence	High NTG regions restricted to western PRB, muddy shelf over much of the area/	Stratigraphy without regions leads to over-estimate GPV at the 3rd order, extrapolating high porosity and NTG values over thick mud interval (5-3)

Table 2.4. . Summary of Gross Pore Volume (GPV) calculations. Regions that are similar in each stratigraphic sequence will reduce GPV, but if they vary drastically with stratigraphy they may increase GPV.

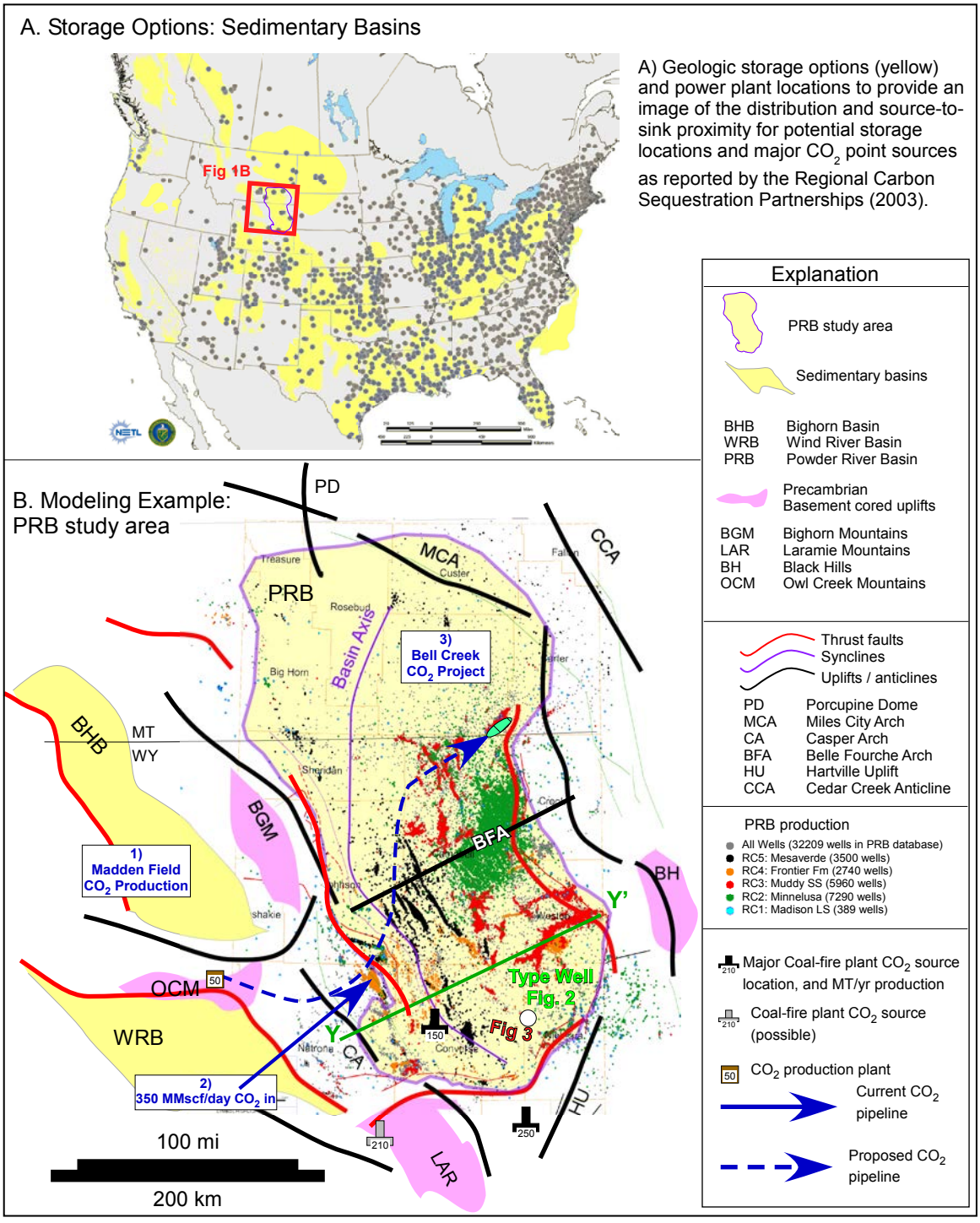

Figure 2.1. Maps of study area. A) Study area location in context with other basins (yellow) and CO_2 point sources. B) Map of PRB study area showing structural setting, well data coverage and GCS infrastructure. Coal-fired power plants, with present and proposed CO_2 pipelines are indicated. Note type well in Figure 2.2 and structural cross section X-X' in Figure 2.3 shown. CO_2 entering basin reported in MMscf/day - million standard cubic feet per day.

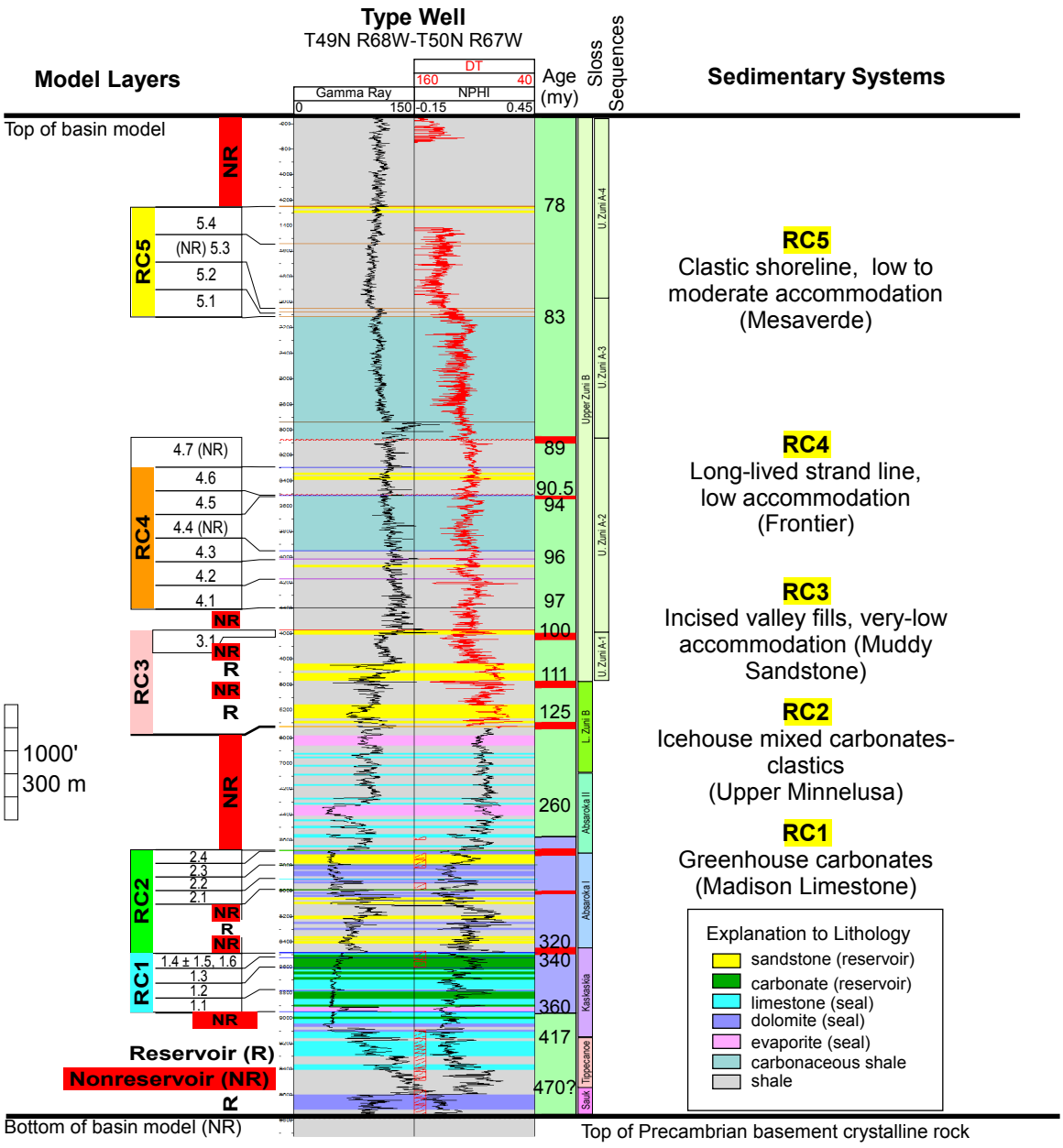

Figure 2.2. Composite type well showing how modeling structure relates to stratigraphy and the vertical distribution of RCs (RC1-5). Note, RC4, is example interval for high-resolution methods. RCs have different sedimentary systems in each; the example used in this model for each is indicated in parenthesis. these RCs represent approximately 40% of Paleozoic and Mesozoic fill.

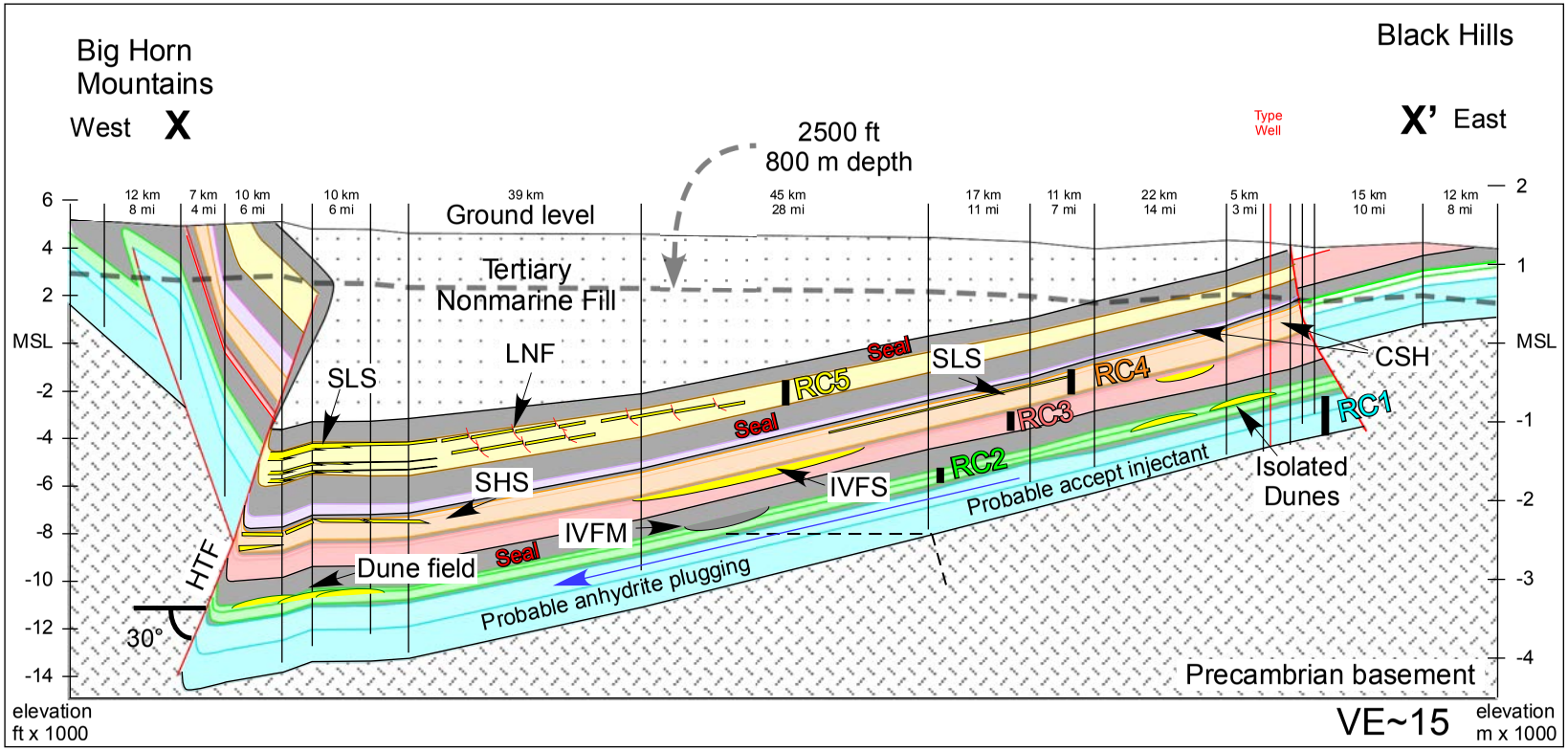

Sedimentary Elements

SLS	Sheet-like shelf sandstone
SHS	Shingled shelf sandstone
CSH	Calcareous shale
IVFS	Incised valley fill sandstone
IVFM	Incised valley fill mudstone

Structural Elements

LNF	Listric normal faults
HTF	High angle thrust fault

Position of wells used to construct cross section, type well in red

Figure 2.3. Structural cross section showing modeling structure and stratigraphic distribution of RCs (RC1-5) and basin bounding faults. Note, schematic heterogeneity produced by the architecture of each RC. Big Horn Mountain thrust based on seismic interpretation (Stone, 1993).

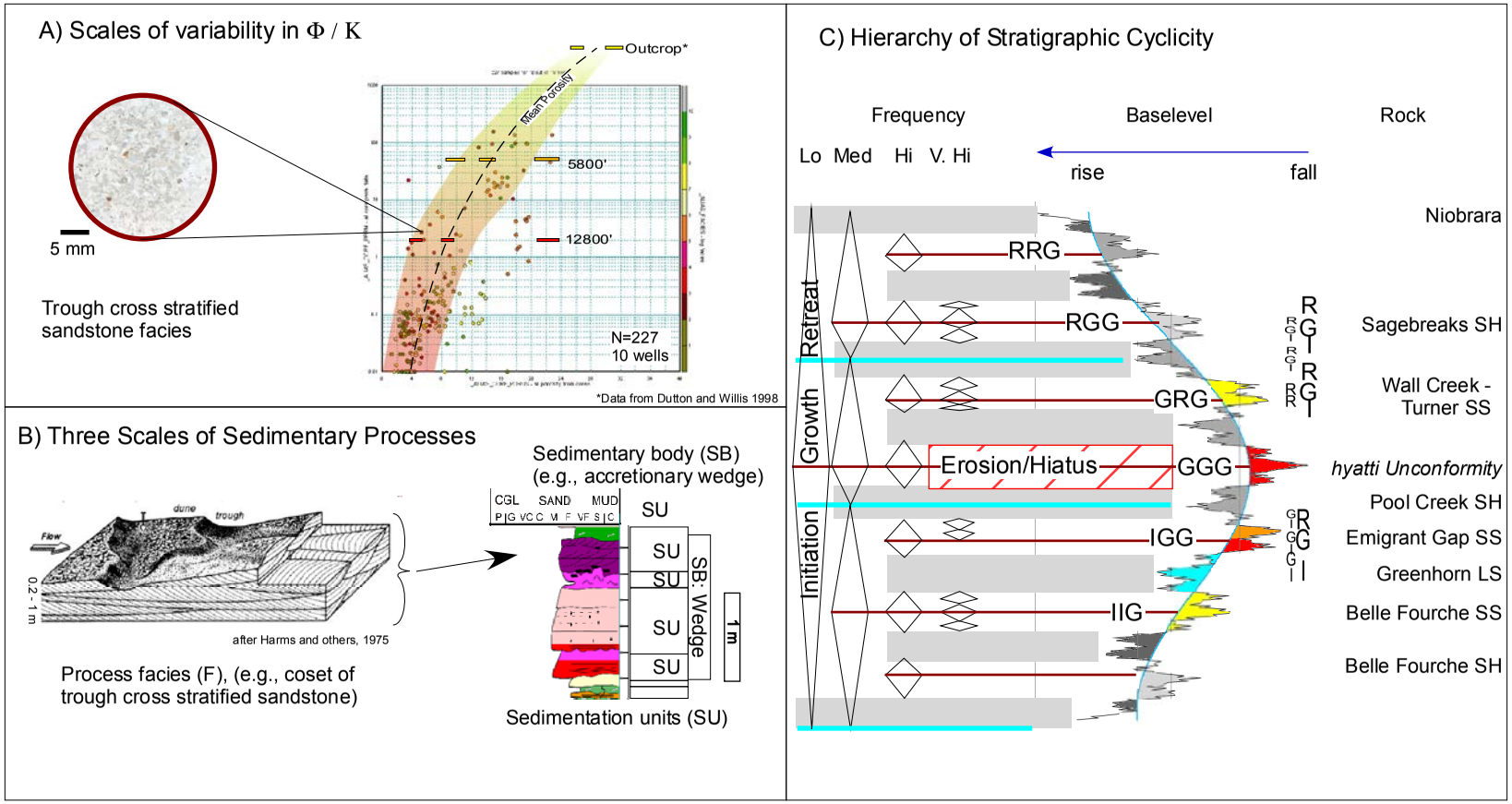

Figure 2.4. Multi-scale geologic heterogeneity varies at each order, from pore to basin scale. A) Porosity logs calibrated to core permeability incorporates up to four orders of magnitude variation in values in the well log data. B) Multiscale geologic heterogeneity correlates to sedimentary processes that record sedimentation spanning multiple scales. C) At least 3 orders of stratigraphic cyclicity are required in order to to document modulation of these attributes in hierarchical stratigraphic framework.

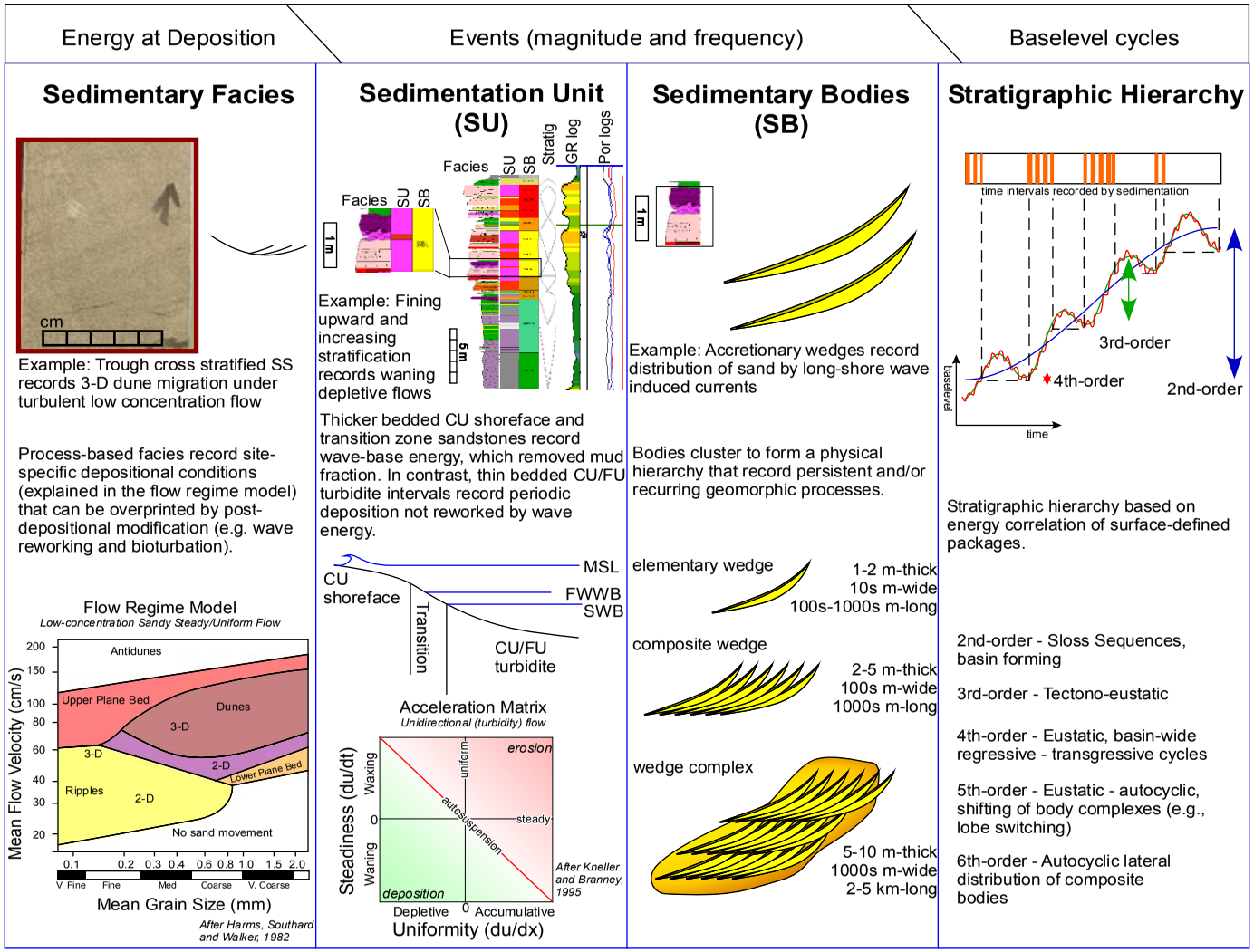

Figure 2.5. Four scales of investigation each involve hierarchies. These include grain-scale, facies that record the energy at the moment of deposition, to sedimentation units and bodies that record the magnitude and frequency of events, to stratigraphic cyclicity that provides a temporal hierarchy of scales to document changes rock attributes.

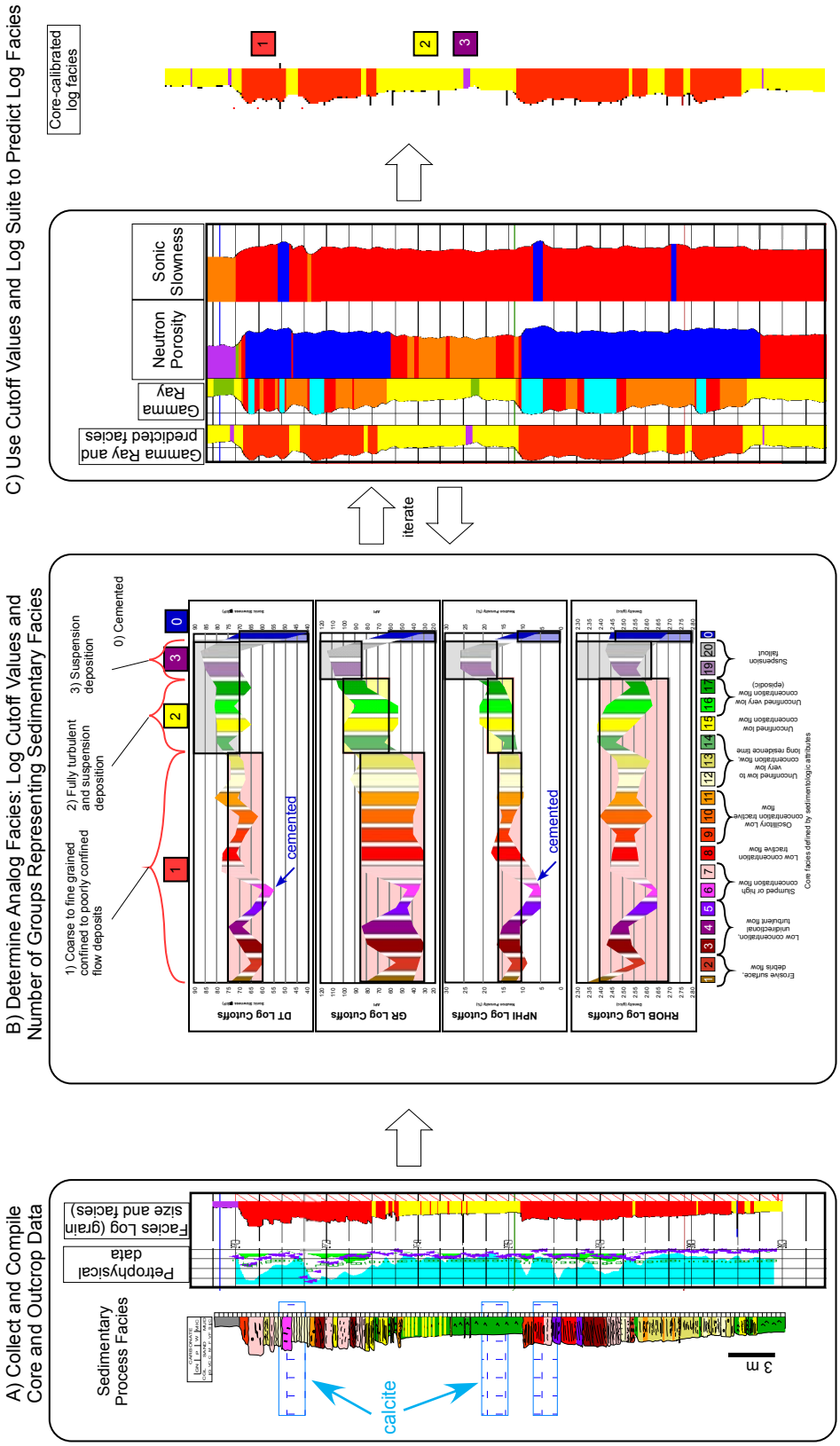

Figure 2.6. Workflow describing process used to group 20 sedimentary facies into 4 log facies to be distributed throughout geomodel. A) Compiled facies data observed in core and outcrop produce core facies. B) Plots comparing log values by core facies (see table 2); this identified four facies that can be distinguished with the well log data. C) Plot of well log suite with the cutoffs (used in Figure 11) are compared to sedimentary facies. A script in the software used IF-THEN statements (appendix 1) incorporated log values at each 0.5 ft from up to 5 well logs in each well to predict the log facies. The final result is the core-calibrated log facies curve, which was used to populate the remaining 1250 wells for the Frontier (RC4).

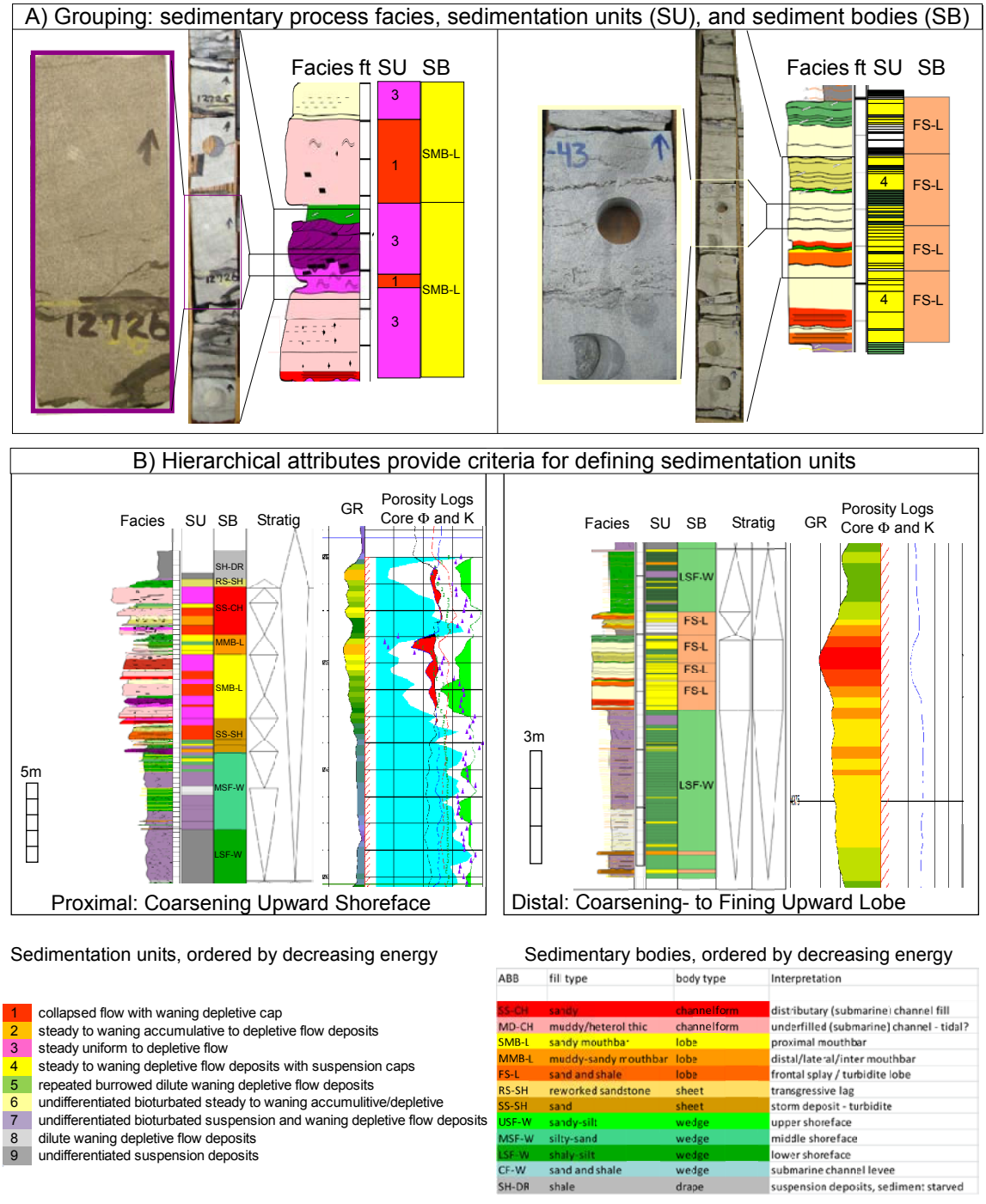

Figure 2.7. Steps taken for upscaling core facies: (A) into sedimentation units and then sedimentary bodies; and (B) 3D Sedimentary bodies defined by facies and sedimentation units form characteristic log shapes represent sedimentation regions. See Tables 2.2 for facies.

Region	log shape	bodies	lithology (%SS)	facies
1. Submarine Channel	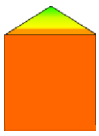	Multi-story channels	60-100%	5+m amalgamated planar to cross stratified fine to medium sandstone
		Single-story channels	30-60%	<5 m interval of .5-1 m beds of fine to medium cross stratified sandstone with pebble lag at base
2. Shoreface	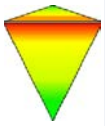	Middle-upper shoreface	75-100%	5-10m CU succession, bioturbated to cross bedded fine to medium SS
	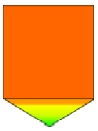	Amalgamated Shoreface	90-100%	5-10m CU to predominantly constant GS succession, bioturbated to cross bedded fine to medium SS, 0.5 to 1.5 m beds
3. Proximal Shelf	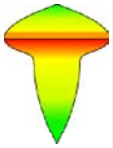	Amalgamated bioturbated Shoreface	30-100%	3-15 m of bioturbated fine sandstone, no clear bedding and vague grain size variation, typically mottled and oil stained
4. Distal Shelf		Bioturbated thin bedded lobes	50-80%	2-5 m thick successions of CU to FU packages of thin bedded ripple-laminated fine to very fine cm bedded sandstone, bedding plane burrows common
	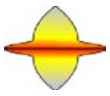	Bioturbated/ reworked thin bedded lobes	20-60%	2-5 m thick successions of CU to FU packages of moderately to intensely bioturbated ripple-laminated fine to very fine cm bedded sandstone,
5. Off-shore		Sheets	<20%	Mudstone and claystone

Figure 2.8. Sedimentation regions as map domains are defined by thickness, sandstone percent, facies, bodies, and well log shape. CU - coarsening upward, FU - fining upwards. Log shape cartoon represents gamma ray/resistivity profile and colors in indicate facies in that part of the cycle (Table 2.2). 1 meter = 3.3 feet; 1 centimeter = 0.4 inches.

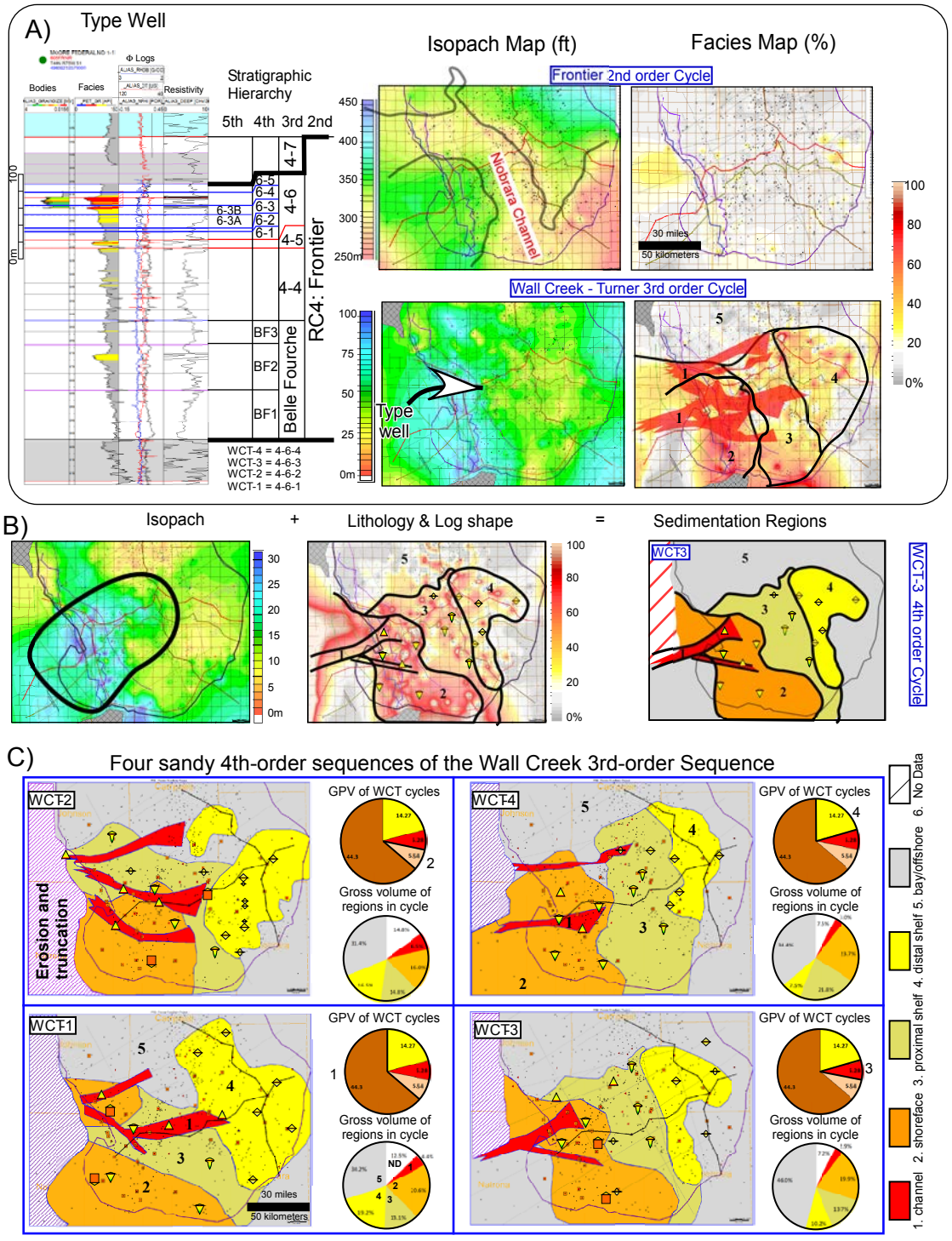

Figure 2.9. Maps of southern PRB showing sediment region characterization (example in RC4). Low stratigraphic resolution results in composite map (A). Sedimentation regions are defined at the highest stratigraphic resolution, typically at the 4th or when possible 5th-order (B). 1000 wells with high-quality logs, core reports and sedimentary profiles were used in all maps (C). Note variability between volume of cycles vs. regions in pie charts (brown-WCT1, peach-WCT2, red-WCT3 and yellow-WCT4).

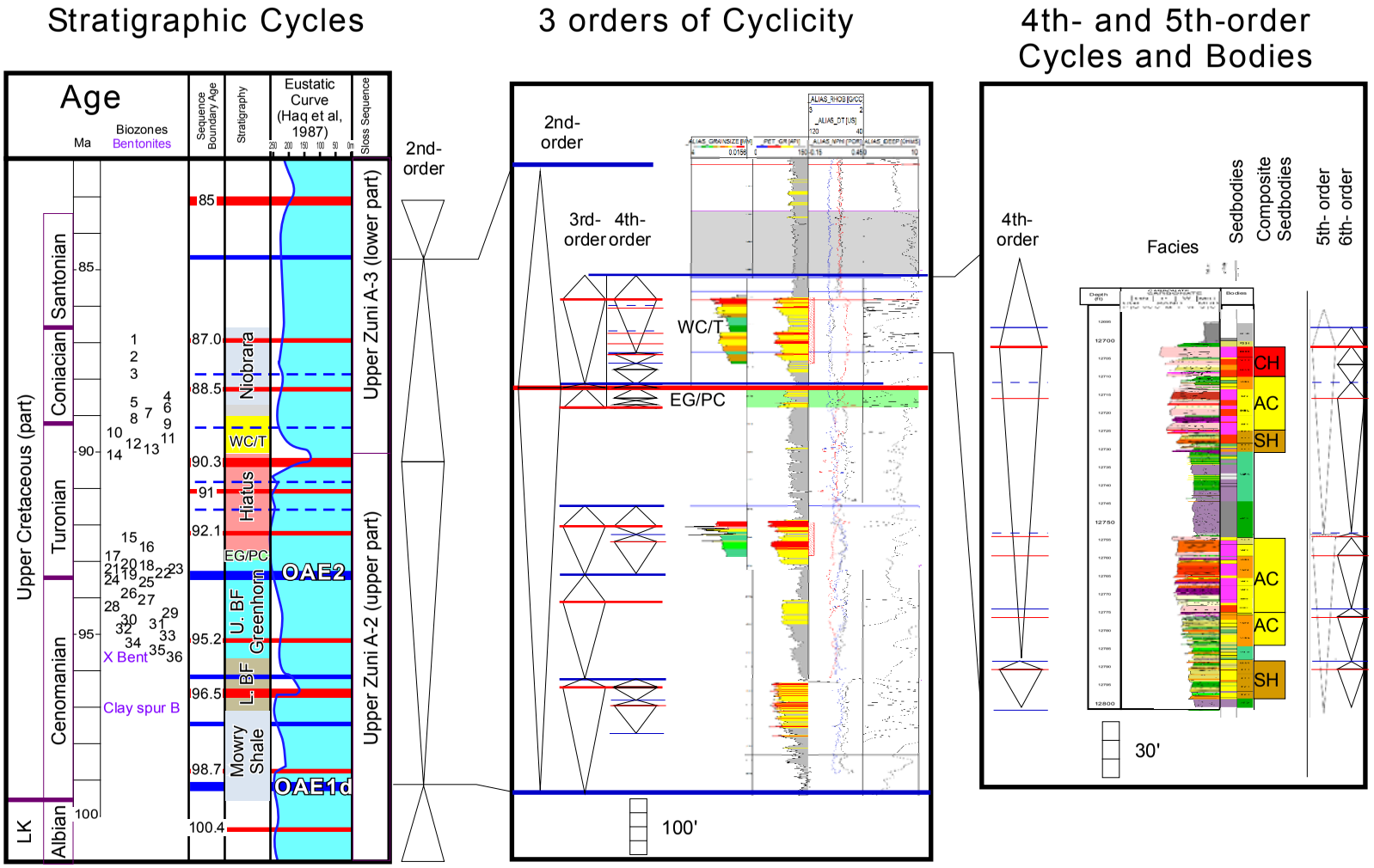

Figure 2.10. A three-fold stratigraphic hierarchy is the minimum requirement for modeling large subsurface volumes. Time scale from Gradstein, 2004 and biozone data from Merewether et al., 2007; refer to Figure 2.1 for biozone numbers. OAE = global anoxic event (OAE1D - Erbacher, Thurow and Littke, 1996; OAE2 - Sageman, 2004). WC/T = Wall Creek-Turner member, EG/PC = Emigrant Gap / Pool Creek, BF = Belle Fourche. See Figure 2.7 for sedimentary bodies explanation.

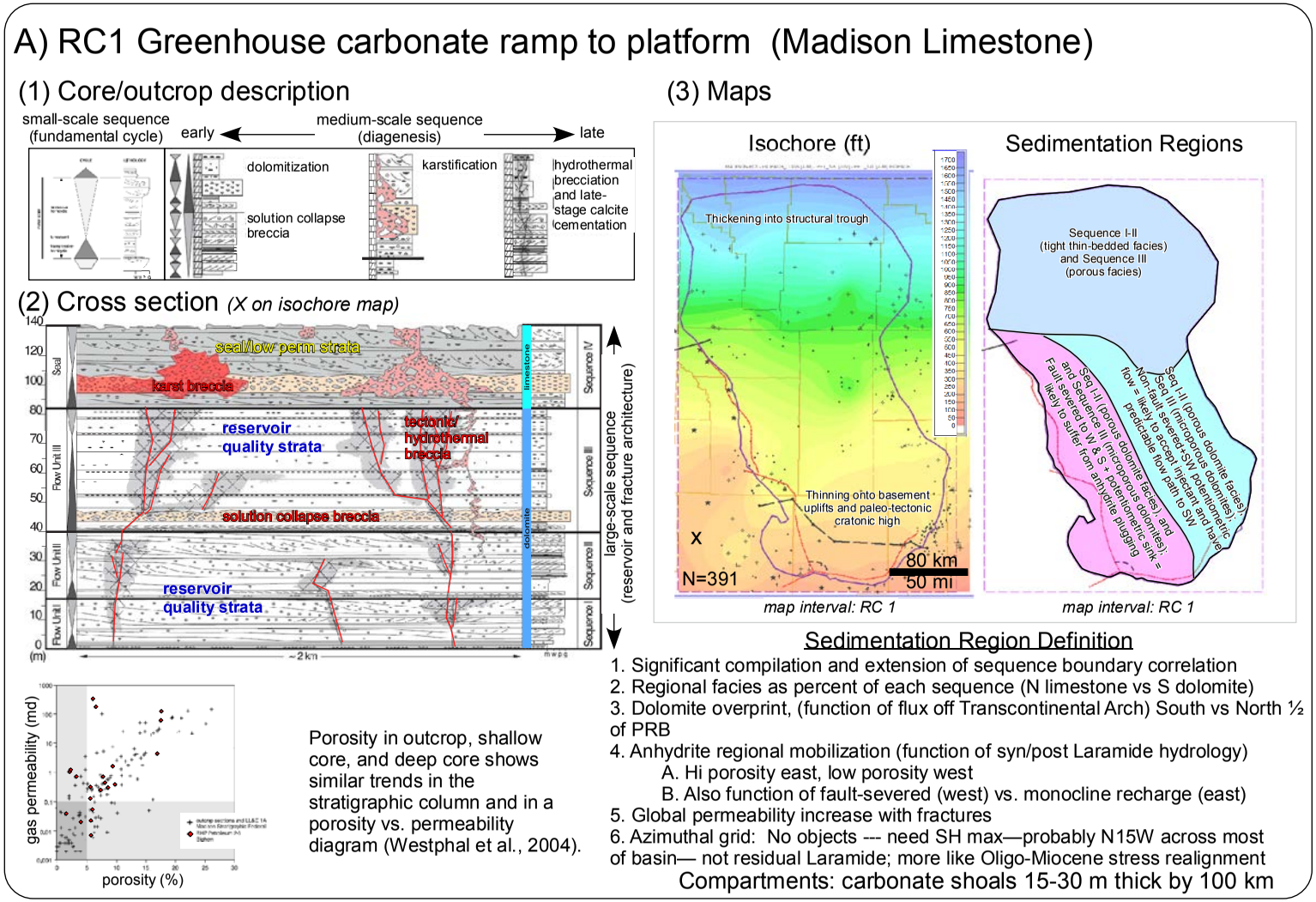

Figure 2.11A. Sedimentary processes and post-depositional modification create reservoir heterogeneity at multiple scales in carbonate platform RCs. (1) Hierarchy of stratigraphic sequences show complexity of initial heterogeneity. (2) Schematic distribution of reservoir heterogeneity (example from Mississippian Madison Formation). (3) Northward thickening at each scale and facies partitioning reflecting increasing water depth, result in greater amalgamation to the south and intensity of brecciation.

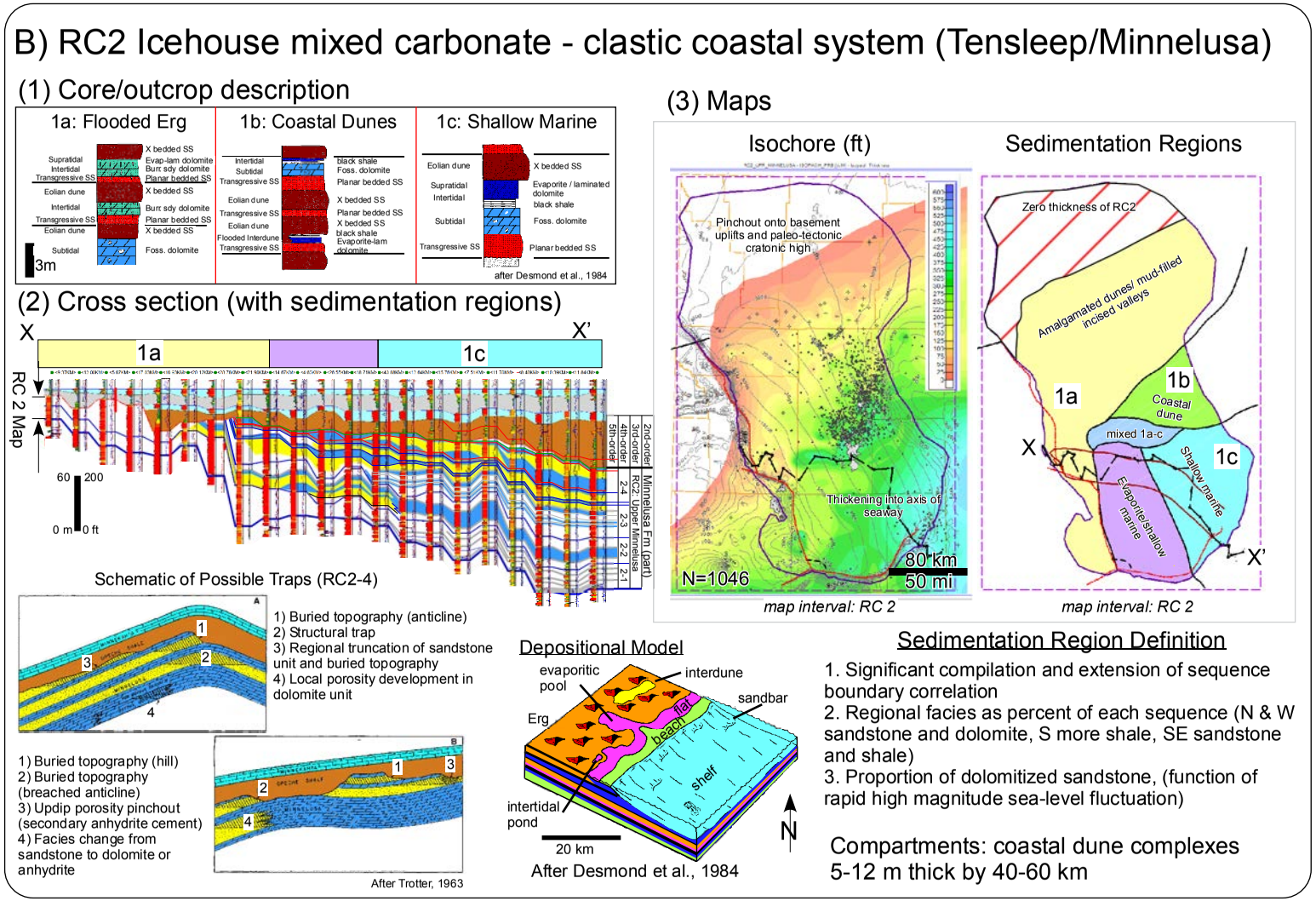

Figure 2.11B. Sedimentary processes across a hierarchy of scales permits defining fundamental cycles, their facies (see Table 2 for facies colors) and their larger stacking patterns. Tabular eolian and shallow marine sandstone bodies capped by dolomitized low permeability zone, create high lateral connectivity and rapid pressure communication. This RC has localized communication with under lying RC1.

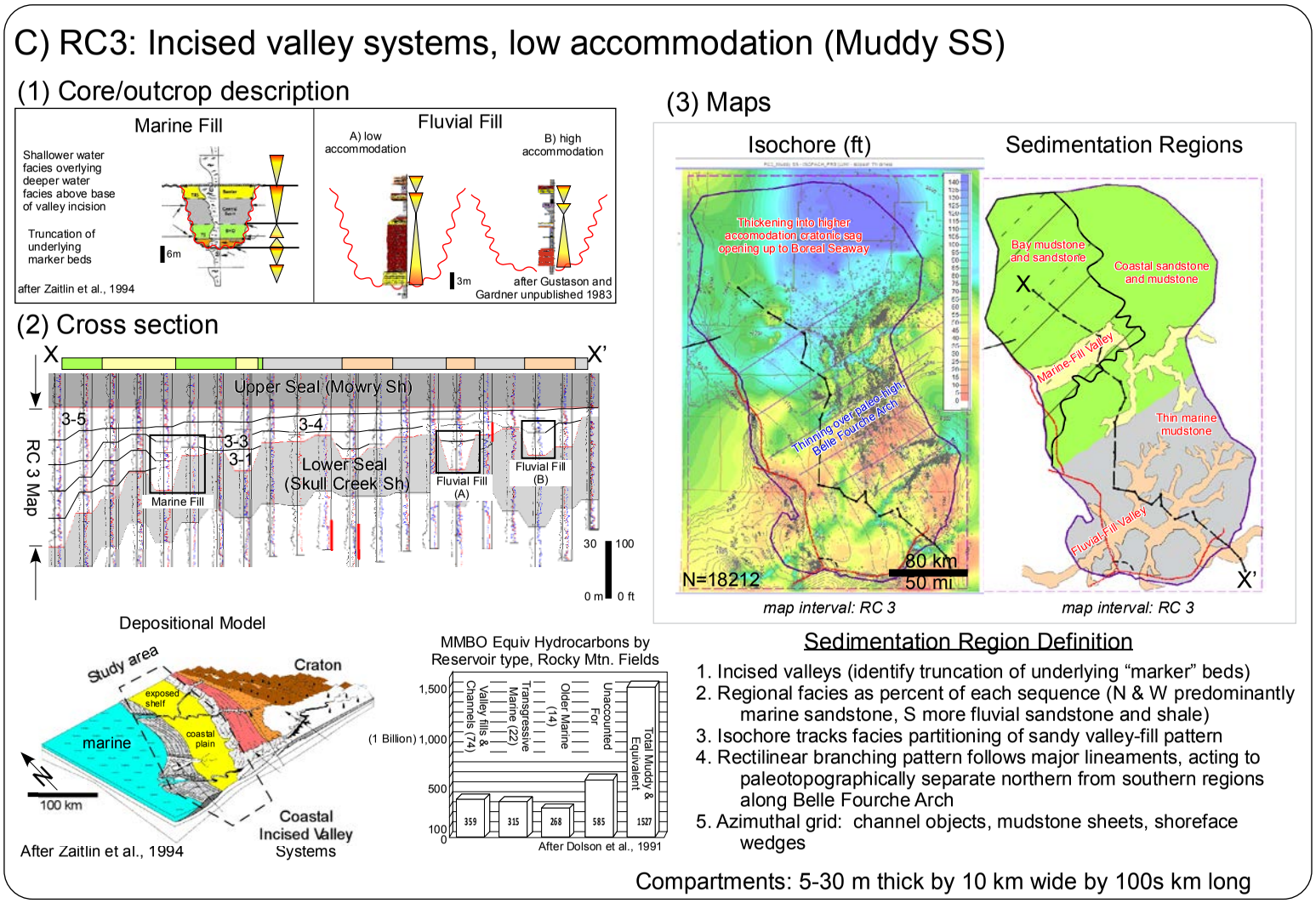

Figure 2.11C. Sedimentary processes partitioned across the study area record the effect of fluvial incision and a hierarchy of stratigraphic cycles permits identifying regions of dominant environments. These long linear highly connected and permeable pathways result in relatively constant pressure regimes across the sedimentation regions and represent hazards to leakage of CO_2.

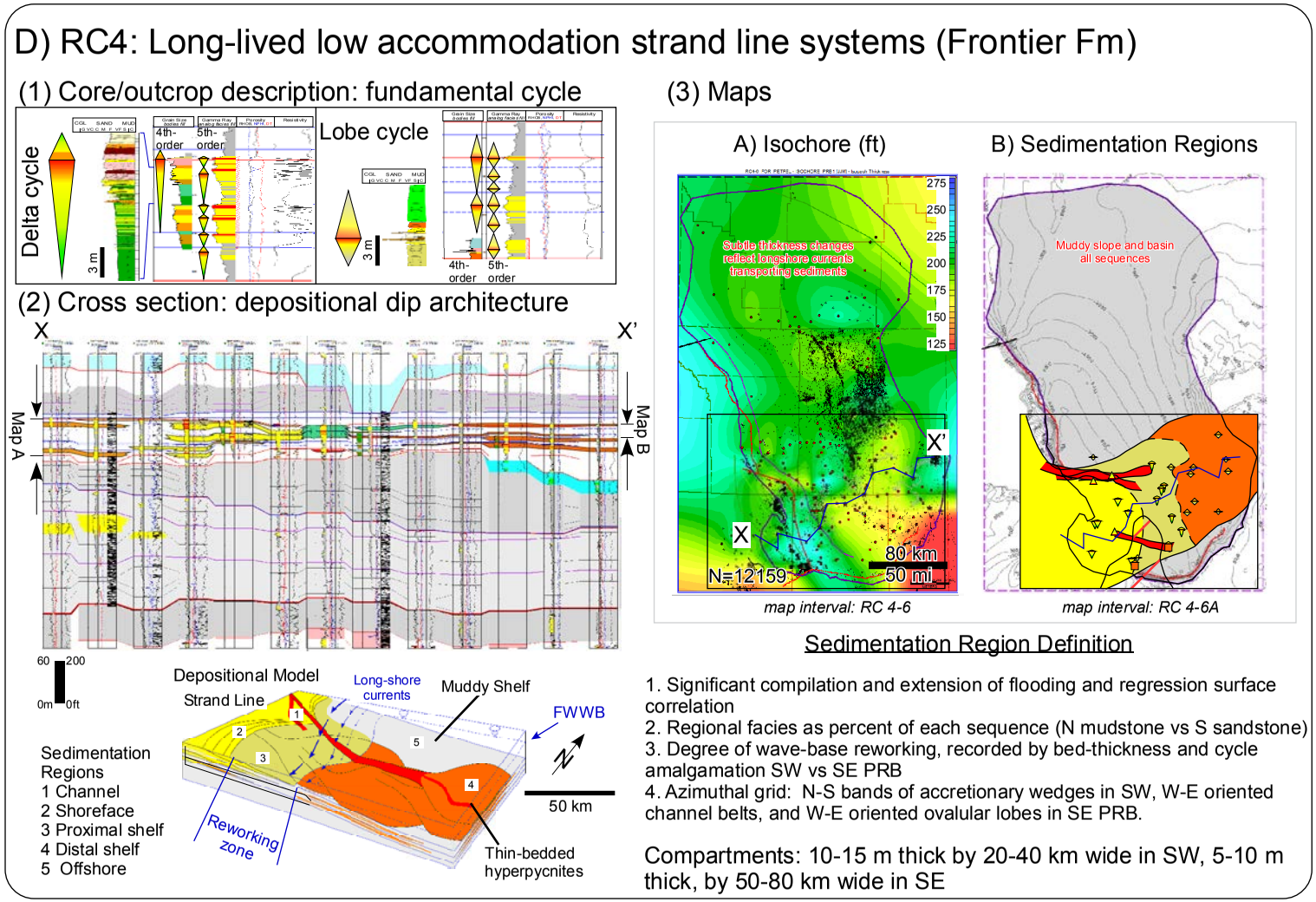

Figure 2.11D. Primary sedimentation by strand line processes, which reworked and remobilized sandbodies resulting in a remnant architecture of amaglamated and truncated sequences. Reservoir quality variations result from compensating cycle stacking patterns, distance from source (deltaic vs. hyperpycnite deposition) and localized facies specific cementation. Maps are at two scales; map A is whole Wall Creek - Turner sequence, while map B is one of the Wall Creek Turner sequences.

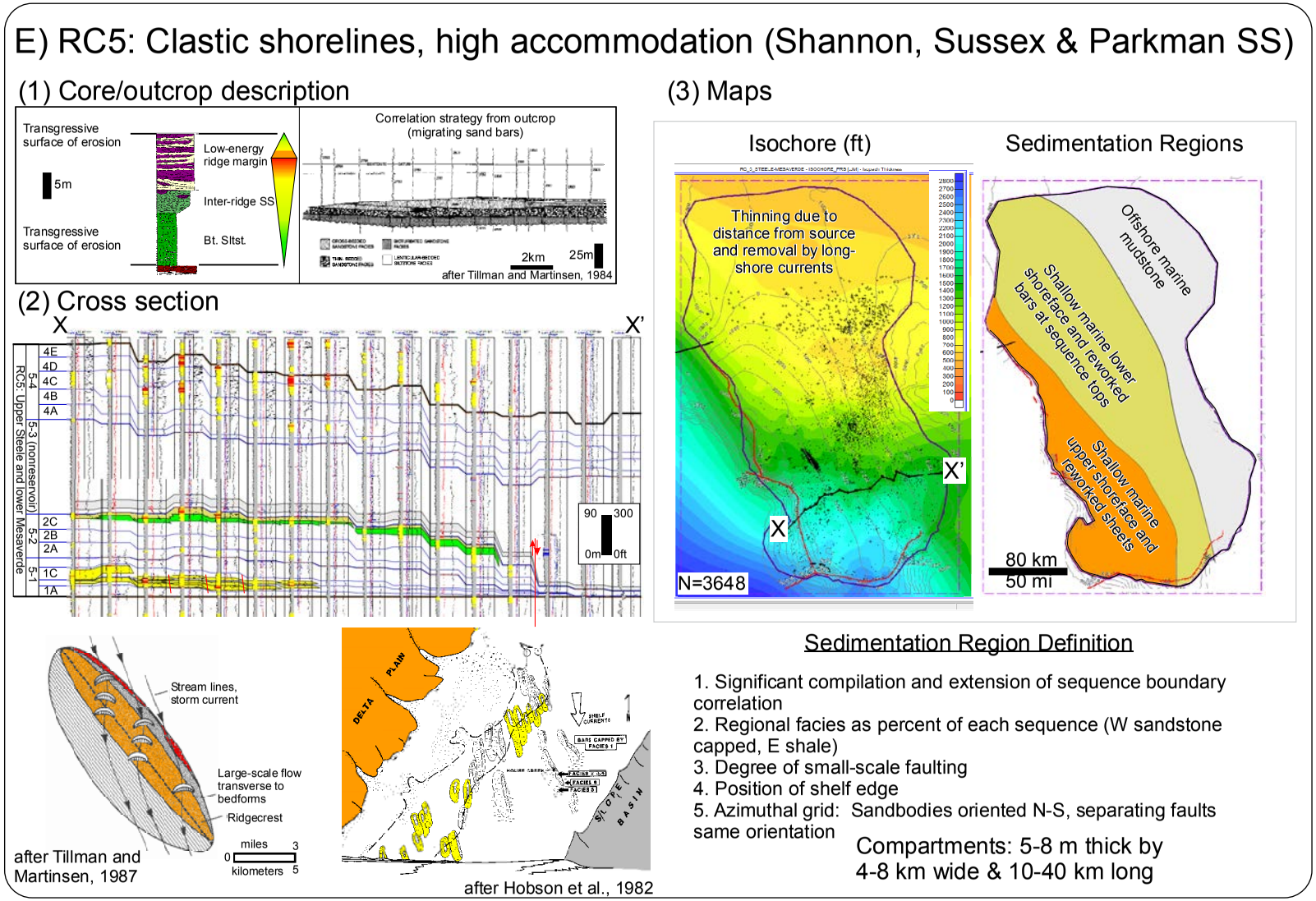

Figure 2.11E. High accommodation is recorded in the thick mudstone intervals, whereas the sheet-like sandstone packages suggest rapid regression and reworking upon subsequent transgression by predominantly long-shore currents acting on a broad very low angle shelf. This closely spaced several meter offset fault pattern forms smaller isolated effective pore volumes, with potentially transmissive fractures presenting risk to upward migration of CO_2.

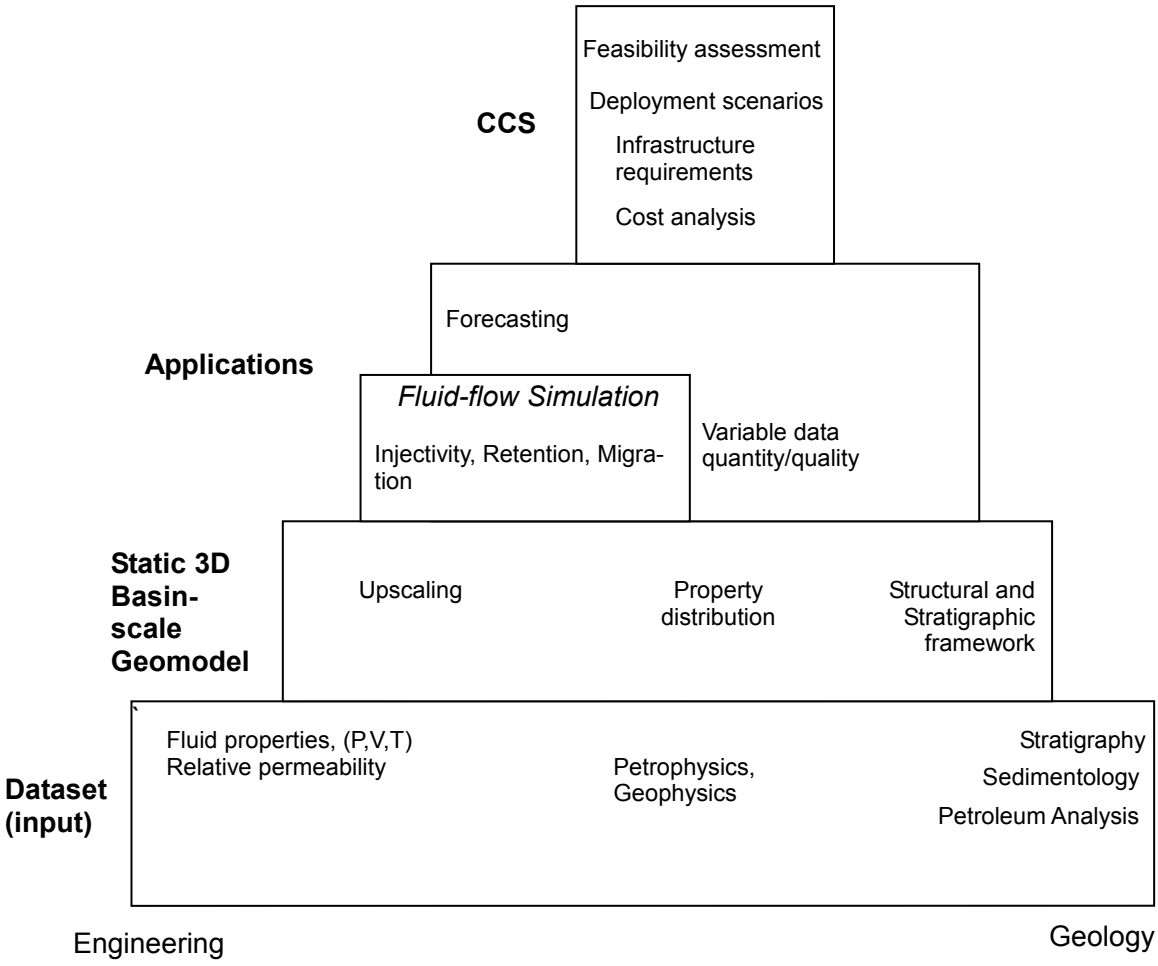

Figure 2.12. Simplified schematic of workflow showing integration of engineering and geology based on well defined goals for model building.

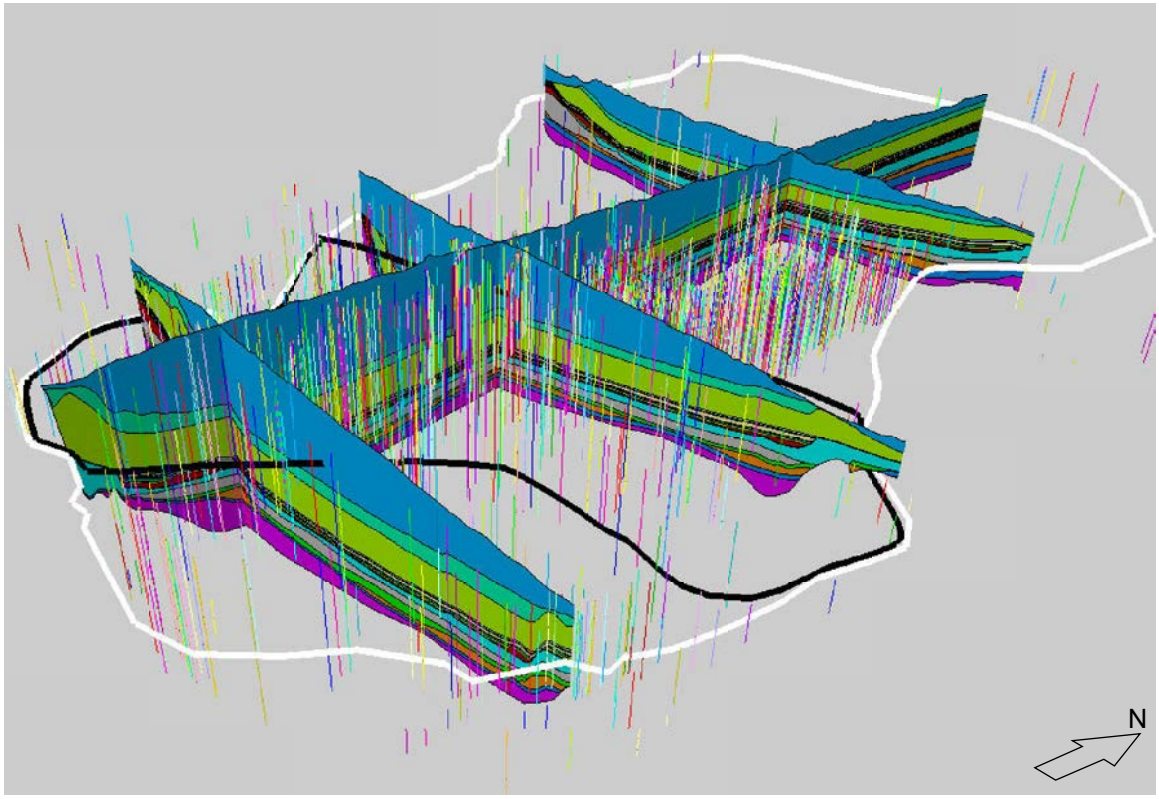

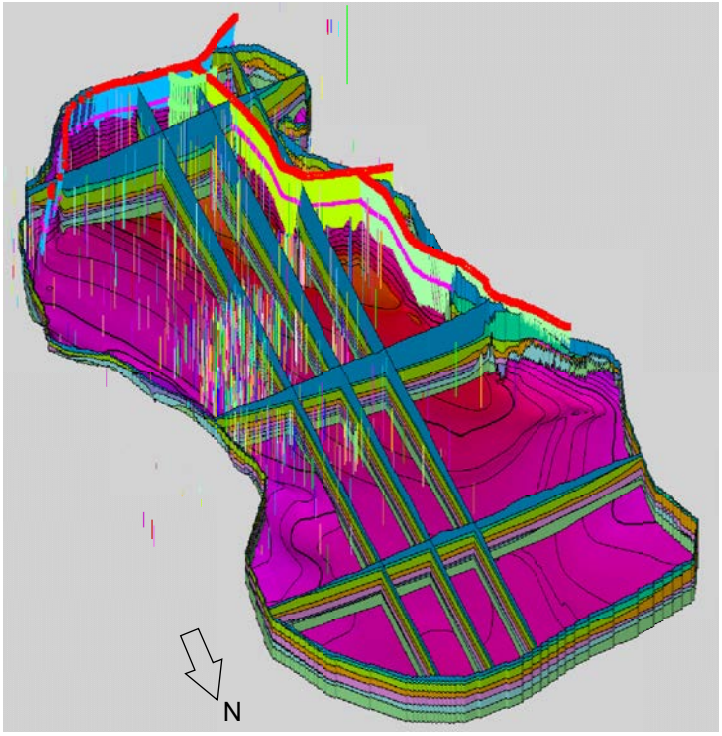

Figure 2.13. Images from 3D modeling package for the entire PRB. Above, 3000 wells are shown as sticks and fence shows how RCs are distributed. Right, PRB model shows basement surface with faults intersecting western side. Modeling layers are highlighted on the basin rim. White outline is model boundary. Cross sections show coarse layering (colors indicate separate modeling zone), overlain on 3D Petrel image colored by depth.

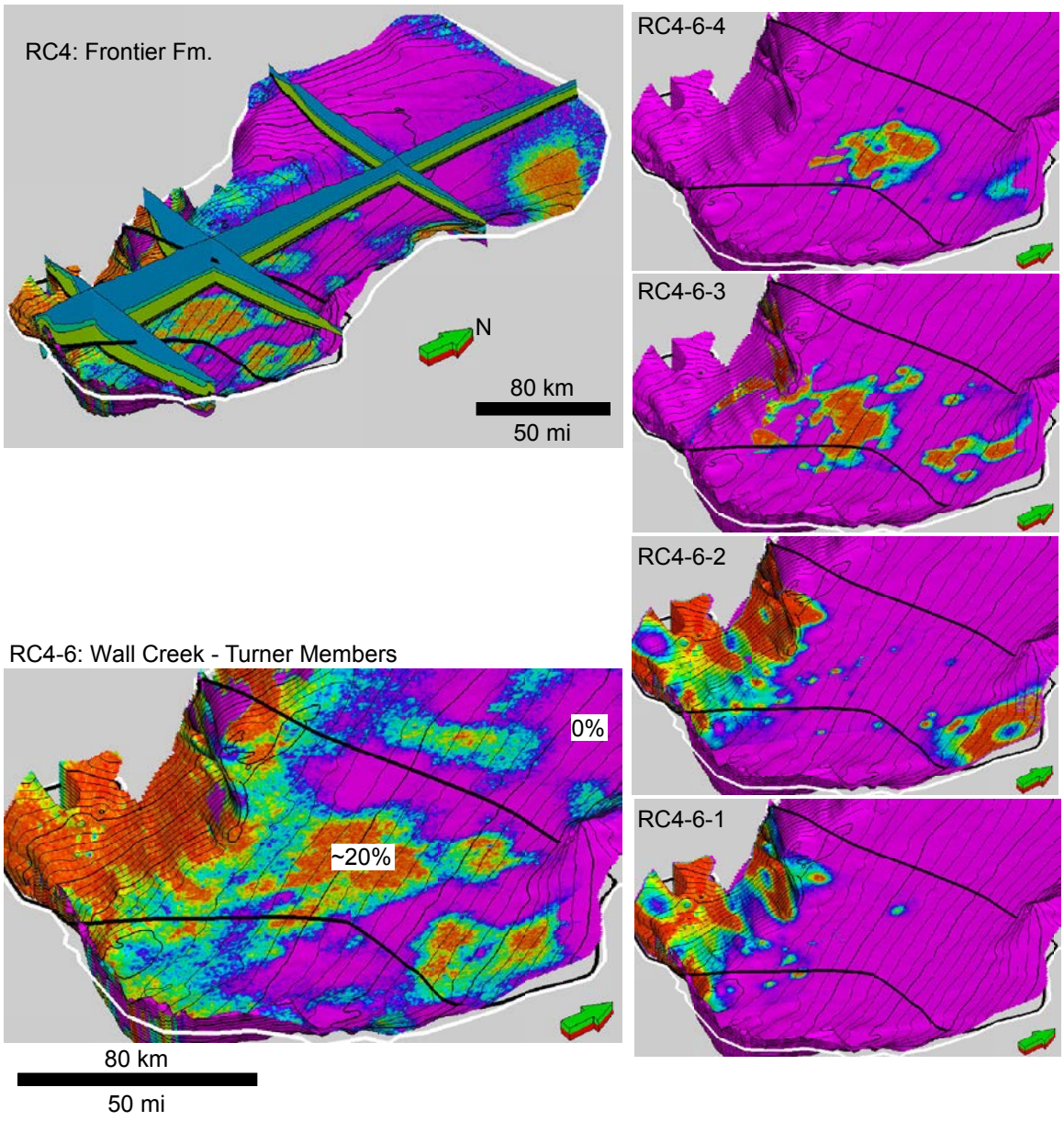

Figure 2.14. Images from 3D modeling package. Upper left shows porosity (red is high, pink is zero percent) distribution in RC4 with fence diagram (200-300 m thick). Lower left shows sector model boundaries and general porosity distribution based on averaging the entire RC4-6 (50-60 m thick interval). Right, from bottom to top, the four small-scale sequences (10-20 m thick) better document the migration of porosity distribution upward through the medium-scale sequence of RC4-6. The black polygon is approximate area of detailed study area.

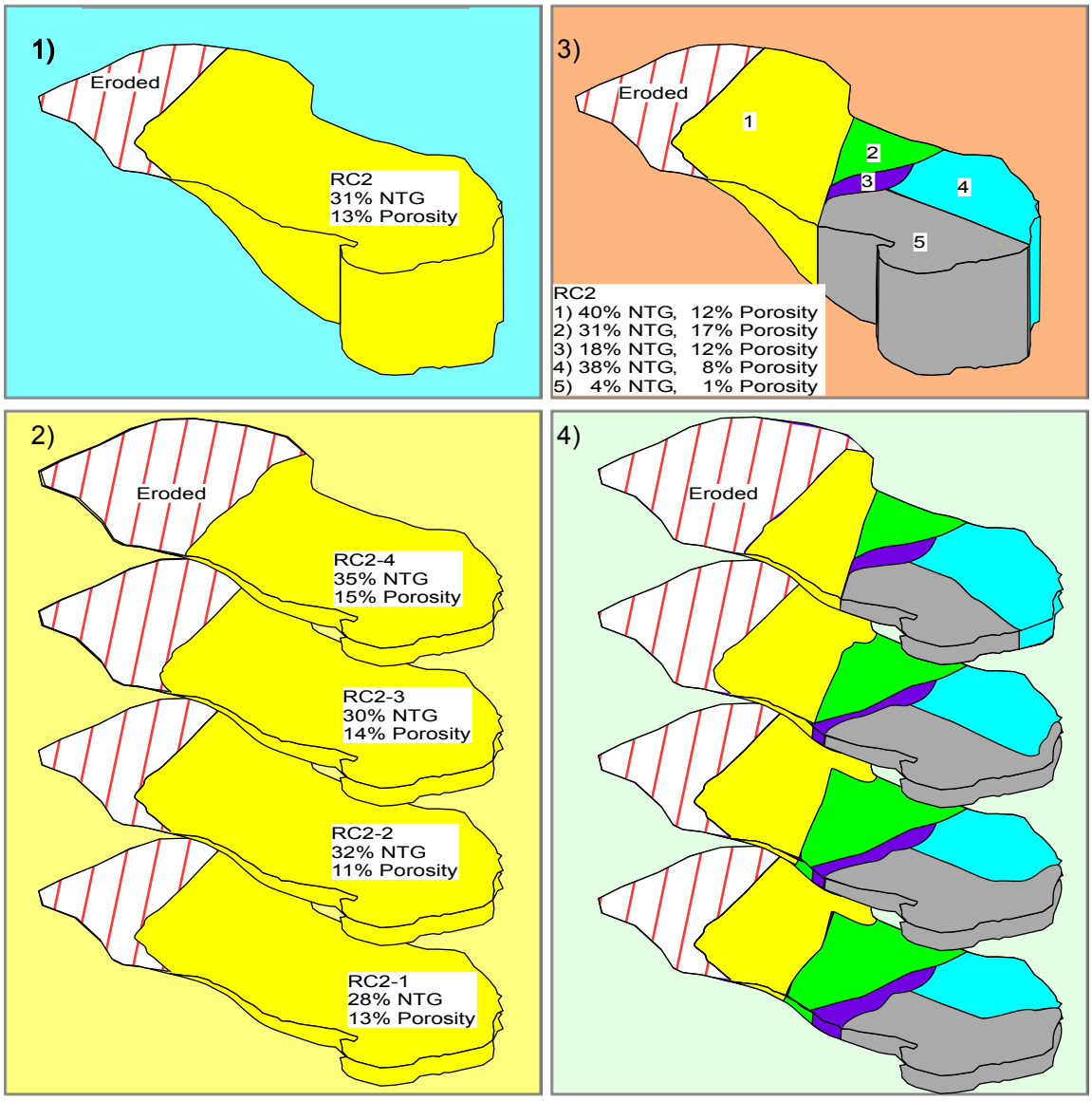

Figure 2.15A. Block diagram illustrating four methods (1-4) used to calculated gross pore volume (GPV) for RC2.
1) Factors (porosity and NTG) averaged across entire volume
2) Factors averaged across stratigraphy then summed across entire volume
3) Regions method averaged within region and across stratigraphy (each orange color averages the porosity and NTG, and is then summed) and
4) region method averaged within region, summed across stratigraphy (sum of all mint green colors).

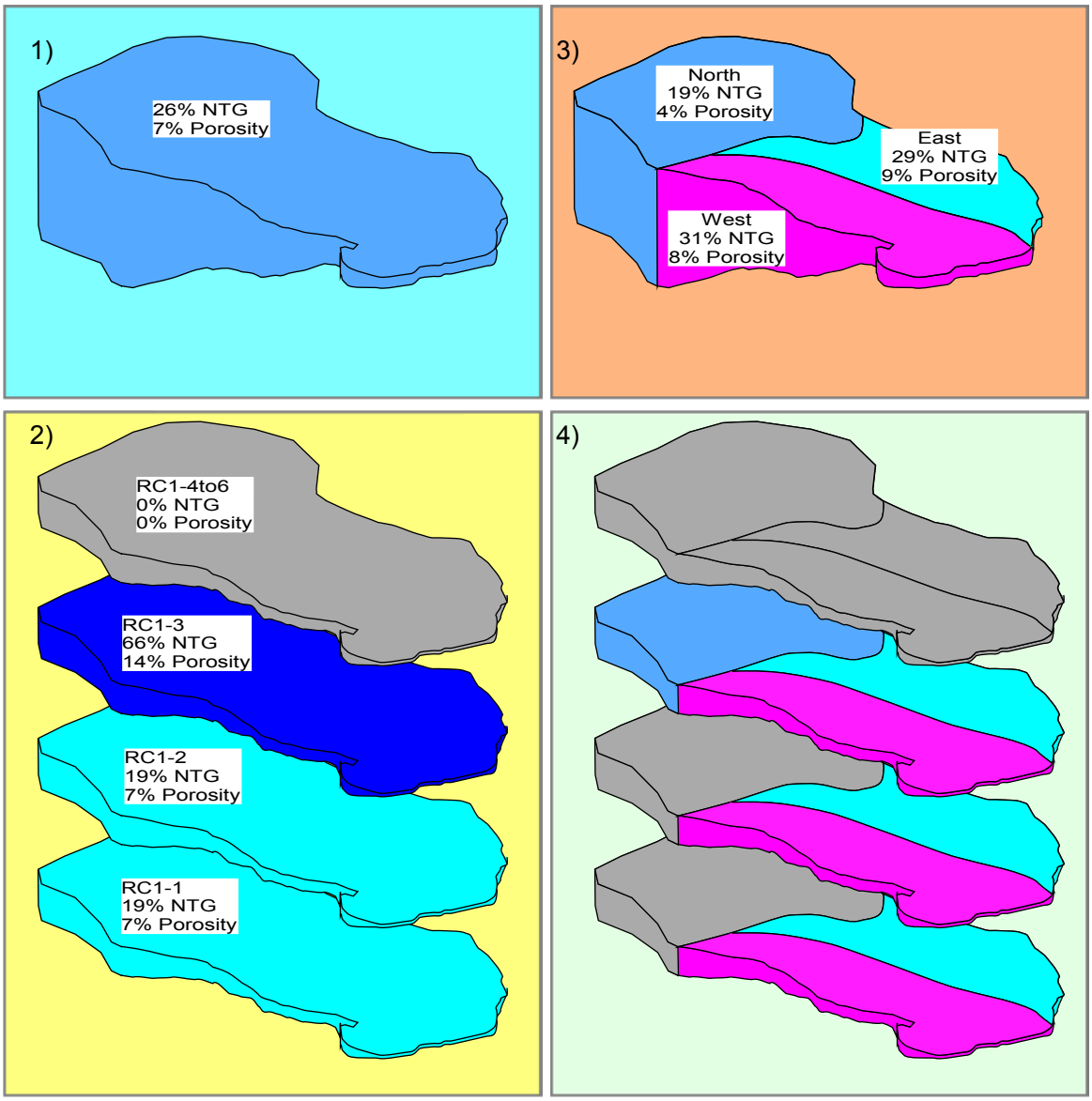

Figure 2.15B. Block diagram illustrating four methods (1-4) used to calculated gross pore volume (GPV) for RC1.
1) Factors (porosity and NTG) averaged across entire volume
2) Factors averaged across stratigraphy then summed across entire volume
3) Regions method averaged within region and across stratigraphy (each orange color averages the porosity and NTG, and is then summed) and
4) region method averaged within region, summed across stratigraphy (sum of all mint green colors).

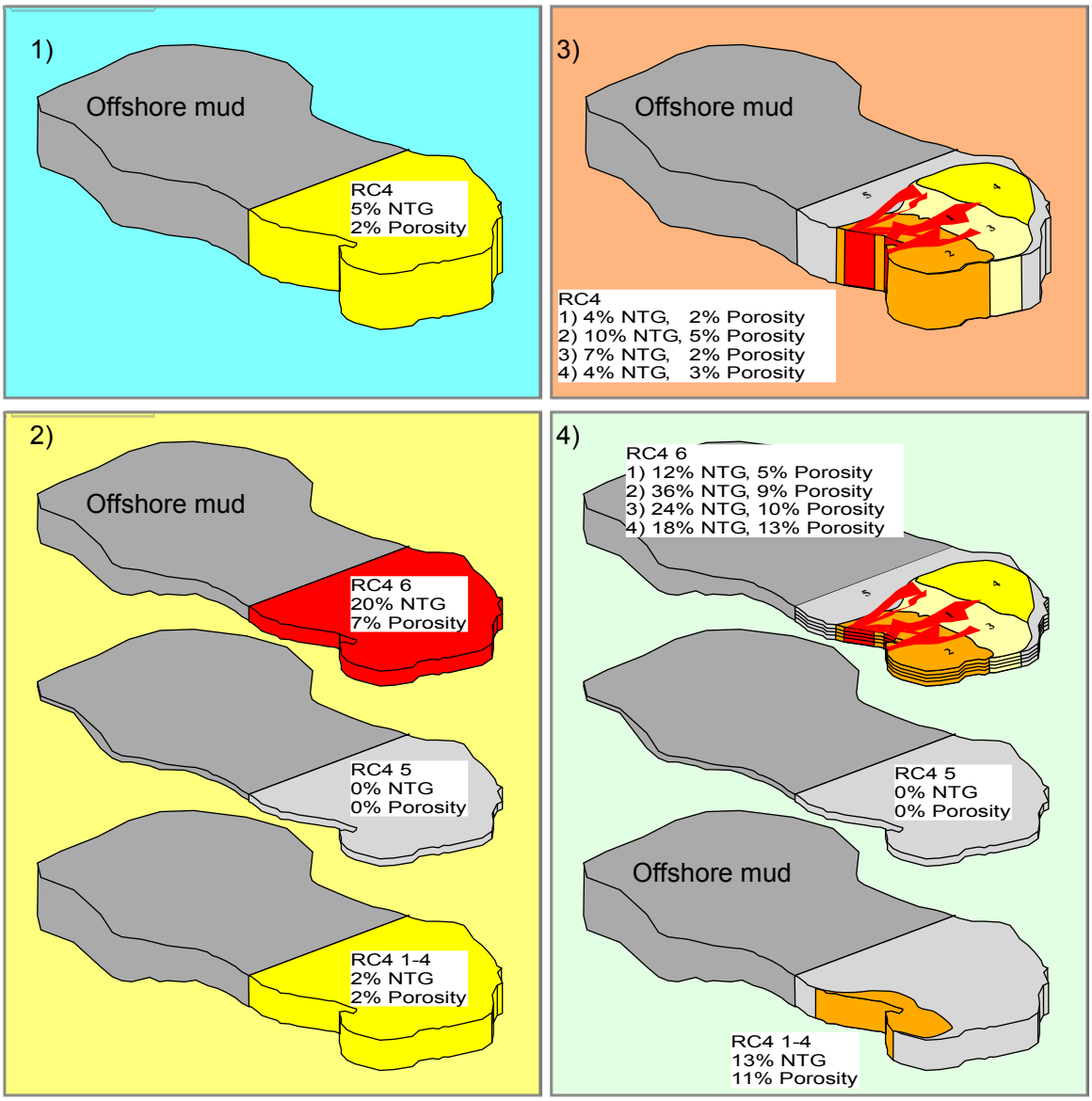

Figure 2.15C. Block diagram illustrating four methods (1-4) used to calculated gross pore volume (GPV) for RC4.
1) Factors (porosity and NTG) averaged across entire volume
2) Factors averaged across stratigraphy then summed across entire volume
3) Regions method averaged within region and across stratigraphy (each orange color averages the porosity and NTG, and is then summed) and
4) region method averaged within region, summed across stratigraphy (sum of all mint green colors).

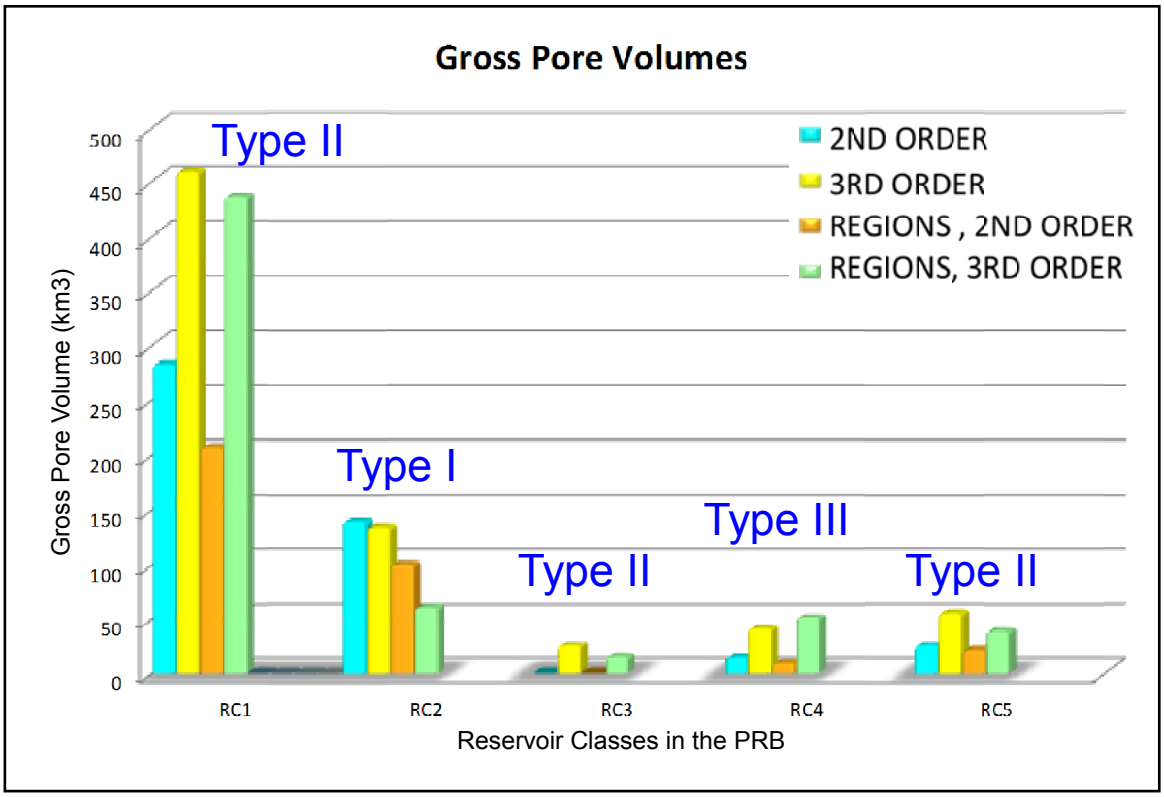

Figure 2.16. Chart showing Gross Pore Volume (GPV) results for the five reservoir classes (RC) highlighting three types of reservoir class. Type I RCs have similar stratigraphy and similar arrangement of sedimentation regions. Type II RCs have stratigraphic sequences without reservoirs, but similar arrangement of sedimentation regions. Type III RCs are most complex, having both variable stratigraphy and variable sedimentation region arrangements.

1) Factor method averaged across stratigraphy (blue)
2) factor method summed across stratigraphy then averaged (yellow)
3) region method averaged within region and across stratigraphy (orange)
4) region method averaged within region, summed across stratigraphy (mint green), see Figure 2.12 for calculation method.

References Cited

Ambrose, W.A., Lakshminarasimhan, S., Holtz, M.H., Nunez-Lopez, V., Hovorka, S.D. and Duncan, I., 2008, Geologic factors controlling CO_2 storage capacity and permanence: case studies based on experience with heterogeneity in oil and gas reservoirs applied to CO_2 storage, Environmental Geology 54:1619–1633.

Atan, S., Gardner, M.H., Borer, J.M., and Wagerle, R.N., 2001, Implications of Upscaling Submarine Channel Reservoir Models, American Association of Petroleum Geologists National Convention, Abstracts with Program, Denver.

Bailie, A., Strait, R., Roe, S., Jamison, A. and Lindquist, H., 2007, Wyoming Greenhouse Gas Inventory and Reference Case Projections 1990-2020, downloaded from The Center for Climate Strategies, www.climatestrategies.us/library/library/download/411.

Bhattacharya, J.P. and Willis, B.J., 2001, Lowstand deltas in the Frontier Formation, Powder River basin, Wyoming: Implications for sequence stratigraphic models, AAPG Bull., 85/2: 261–294.

Blackstone, D. L., Jr., 1983, Laramide compressional tectonics, southeastern Wyoming: Contributions to Geology, University of Wyoming, Rocky Mountain Geology, v. 22, p. 1–38.

Borer, J. M., 2005, Outcrop Analysis and Geologic Modeling of Submarine Channel and Related Strata, Permian Middle Brushy Canyon Formation, West Texas, USA: unpublished Ph.D. thesis, Colorado School of Mines, Golden, Co, 269p.

Burruss, R.C., and 13 others, 2009, Development of a probabilistic assessment methodology for evaluation of carbon dioxide storage, U.S.G.S. Open-file report 2009-1035: 81p.

Carneiro, J. F., 2009, Numerical simulations on the influence of matrix diffusion to carbon sequestration in double porosity fissured aquifers, *International Journal of Greenhouse Gas Control* 3: 431-443.

Celia, M.A., 2008, Geological storage as a carbon mitigation option, The 2008 Darcy Lecture (Final Version), http://www.princeton.edu/cee/people/data/c/celia/profile/the-darcy-lecture-outline/the-darcy-lecture/Darcy-Lecture-NGWA-3Dec08.pdf Accessed July 2, 2010.

Desmond, R.J, Steidtmann, J.R. and Cardinal D.F., 1984, Stratigraphy and depositional environments of the middle member of the Minnelusa Formation, Central Powder River Basin, Wyoming, 35th Annual Field Conference, Wyoming Geological Association Guidebook: 213-239.

DOE/NETL-401/090808, 2010, Site Screening, Selection, and Initial Characterization for Storage of CO2 in Deep Geologic Formations, http://www.netl.doe.gov/technologies/carbon_seq/refshelf/project%20portfolio/2010/BP-Manuals/BPM-SiteScreening.pdf.

Dolson, J., Muller, D., Evetts, MlJ., and Stein, J.A., 1991, Regional Paleotopographic Trends and Production, Muddy Sandstone (Lower Cretaceous), Central and Northern Rocky Mountains, *American Association of Petroleum Geologists Bulletin* 75/3: 409-435.

Doughty, C., B.M. Freifeld, and R.C. Trautz. 2008. Site characterization for CO_2 geologic storage and vice versa: The Frio brine pilot, Texas, USA as a case study. *Environmental Geology* 54, no. 8: 1635–1656.

Dutton, S.P. and Willis, B.J., 1998, Comparison of outcrop and subsurface sandstone permeability distribution, Lower Cretaceous Fall River Formation, South Dakota and Wyoming, *Journal of Sedimentary Research*, 68/5: 890-900.

Elrick, M., 1990, Development of cyclic ramp-to-basin carbonate deposits, Lower Mississippian, Wyoming and Montana: [unpublished Ph.D., dissertation]: Virginia Polytechnic Institute, 170 p.

Fischer, D.W., Smith, S.A., Peck, W.D., LeFever, J.A., LeFever, R.D., Helms, L.D., Sorensen, J.A., Steadman, E.N., and Harju, J.A., 2005, Sequestration Potential of the Madison of the Northern Great Plains Aquifer System (Madison Geological Sequestration Unit), Plains CO2 Reduction (PCOR) Partnership Report: 19 pp.

Frederick, J.B., Dean, K.T., Fryberger, S.G., and Wilcox, T.D., 1995, Donkey Creek North Minnelusa 3-D: Challenging conventional wisdom, in: Ray, R.R. ed., High-definition seismic guidebook, Rocky Mountain Association of Geologists: 135-141.

Gardner, M. H., Borer, J. M., Romans, B. W., Baptista, N., Kling, E., K., Melick, J. J., Wagerle, R., and Carr, M. M., 2008, Stratigraphic Models for Deepwater Sedimentary Systems, 28th Annual GCSSEPM, December 7-9, 2008, Houston, Texas.

Gardner, M.H., Barton, M.D., Tyler, N., and Fisher, R.S., 1992, Architecture and permeability structure of fluvial-deltaic sandstones, Ferron Sandstone, east-central Utah, in Flores, R.M., ed., Mesozoic of the Western Interior: Society of Economic Paleontologists and Mineralogists, Theme Meeting Field Guidebook, p. 5-21.

Gardner, M.H., Willis, B.J., and Dharmasamadhi, I.N.W., 1995, Outcrop-based reservoir characterization of low accommodation/sediment supply fluvial deltaic sandbodies, *in* Japan National Oil Company, Technology Research Center, Special Publication 5, Reservoir Characterization: Integration of Geology, Geophysics, and Reservoir Engineering, p. 17–54.

Gradstein, F., J. Ogg and A. Smith, eds., 2004, A Geologic Time Scale, Cambridge, London.

Harms, J.C., Southard, J.B., Spearing, D.R., and Walker, R.G., 1975, Depositional environments as interpreted from primary sedimentary structures and stratification sequences, SEPM Short Course, no.2, 161pp.

Heyek, M., Mouche, E. and Mugler, C., 2009. Modeling vertical stratification of CO2 injected into a deep layered aquifer. *Advances in Water Resources* 32: 450–462.

Hobson, J.P., Fowler, M.L., and Beaumont, E.A., 1982, Depositional and statistical exploration models, Upper Cretaceous off shore sandstone complex, Sussex Member, House Creek Field, Wyoming, *AAPG*, 66/6: 689-707.

Hovorka, S.D., Doughty, C., Benson, S.M., Puress, K. and Knox, P.R., 2004, The impact of geological heterogeneity on CO2 storage in brine formations: a case study from the Texas Gulf Coast, IN: Baines, S.J. and Worden, R.H. (eds) Geological Storage of Carbon Dioxide. Geological Society, London, Special Publications, 233: 147-163.

Huntoon, P.W., 1976, Permeability and ground water circulation in the Madison Aquifer along the eastern flank of the Bighorn Mountains of Wyoming, 28th annual Field Conference, Wyoming Geological Association Guidebook: 283-290.

Kerr, D.R., Wheeler, D.M., Rittersbacher, D.J. and Horne, J.C., 1986, Stratigraphy and sedimentology of the Tensleep Sandstone (Pennsylvanian and Permian), Bighorn Mountains, Wyoming, *Earth Science Bull*., 19/1-2: 61-78.

Kneller, B.C. and Branney, M.J., 1995, Sustained high density turbidity currents and the deposition of thick massive sands. *Sedimentology*, 42: 607-616.

Larue, D.K. and Yue, Y., 2003, How stratigraphy influences oil recovery: a comparative reservoir database study concentrating on deepwater reservoirs, *The Leading Edge*, April: 332-339.

Lisenbee, A L. 1978, Laramide structure of the Black Hills Uplift, South Dakota-Wyoming-Montana, Memoir - Geological Society of America, 151: 165-196.

Lisenbee, A.L., 1988, Tectonic history of the Black Hills uplift, Guidebook - Wyoming Geological Association, vol. 39: 45-52.

Lisenbee, A.L., 1993, Laramide evolution of the Black Hills Uplift, Memoir - Geological Survey of Wyoming, volume 5: 374-412.

Lorenz, J.C., Rizer, W.D., Farrell, H.E., Sonnenfeld, M.D., and Hanks, C.L., 1997, Characteristics of natural fractures in carbonate strata, Carbonate Seismology, Geophysical Development Series 6: 179-201.

Luppens, J.A., Scott, D.C., Haacke, J.E., Osmonson, L.M., Rohrbacher, T.J., and Ellis, M.S., 2008, Assessment of coal geology, resources, and reserves in in the Gillette Coalfield, Powder River Basin, Wyoming, U.S. Geological Survey Open-File Report 2008-1202.

Merewether, E.A., Cobban, W.A., and Cavanaugh, E.T., 1979, Frontier Formation and equivalent rocks in Eastern Wyoming, *The Mountain Geologist*, 16/3: 67-101.

Middleton, G. W., 1973, Johannes Walther's Law of the Correlation of Facies: *Geological Society of America Bulletin*, 84: 979-988.

N.E.T.L., 2010, Best practices for: Site screening, site selection, and initial characterization for storage of CO2 in deep geologic formations, http://www.netl.doe.gov/technologies/carbon_seq/refshelf/BPM_PublicOutreach.pdf .

Nicot, J.P. 2008. Evaluation of large-scale CO_2 storage on freshwater sections of aquifers: An example from the Texas Gulf Coast Basin. *International Journal of Greenhouse Gas Control* 2, no. 4: 582–593.

Pacala, S., and Socolow, R., 2004, Stabilization wedges: Solving the climate problem for the next 50 years with current technologies: *Science*, v. 305, p. 968–972.

Peterson, C., 2009, The Beaver Creek Field, Madison CO2 Project – Spring 2009 update, Wyoming EORI, 3rd Annual Wyoming CO2 Conference.

Regional Carbon Sequestration Partnerships, 2003, http://www.netl.doe.gov/technologies/carbon_seq/infrastructure/rcsp.html.

Slack, P.B., 1981, Paleotectonics and hydrocarbon accumulation, Powder River Basin, Wyoming, *AAPG*, 65/6: 730-743.

Smith, L. B. Jr., G. P. Eberli, and M. D. Sonnenfeld, 2004, Sequence-stratigraphic and paleogeographic distribution of reservoir-quality dolomite, Madison Formation, Wyoming and Montana, in G. M. Grammer, G. P. Eberli, and P. M. Harris, eds., Integration of outcrop and modern analogs in reservoir modeling: AAPG Memoir 80, p. 94–118.

Sneider, R.; Young, T., 2009, Facing major challenges in carbon capture and sequestration, *GSA Today*, 19/11: 36-37.

Sonnenfeld, M.D., 1996, An integrated sequence stratigraphic approach to reservoir characterization of the Lower Mississippian Madison Limestone, emphasizing Elk Basin field, Bighorn Basin, Wyoming: Unpublished Ph.D. dissertation, Colorado School of Mines, Golden Colorado 437 p.

Stone, D.S., 1993, Basement-involved thrust-generated folds as seismically imaged in the subsurface of the central Rocky Mountain foreland, Special Paper - *Geological Society of America*, vol. 280: 271-318,

Stone, D.S., 2002, Morphology of the Casper Mountain uplift and related, subsidiary structures, central Wyoming; implications for Laramide kinematics, dynamics, and crustal inheritance, *AAPG Bulletin*, 86/8: 1417-1440.

Stone, D.S., 2003, New Interpretations of the Piney Creek thrust and associated Granite Ridge tear fault, northeastern Bighorn Mountains, Wyoming, *Rocky Mountain Geology*, 38/2: 205-235.

Tillman, R.W., 1997, Shannon Sandstone, Salt Creek Area, Wyoming, Prospect to Pipeline, 48th Annual WGA Field Conference, Guidebook: 29-68.

Tillman, R.W., and Martinsen, R.S., 1987, Sedimentological model and production characteristics of Hartzog Draw field, Wyoming, A Shannon shelf-ridge sandstone, IN: Tillman, R.W., and Weber, K.J., eds., Reservoir sedimentology, Society of Economic Paleontologists and Mineralogists Special Publication No. 40: 15-67.

Trotter, J.F., 1963, The Minnelusa play of the Northern Powder River, Wyoming and adjacent areas, 18th Annual WGA Field Conference, Guidebook: 117-122.

U.S. Department of Energy, National Energy Technology Laboratory, 2008, Carbon sequestration atlas of the United States and Canada (2nd ed.; Atlas II): 142 p.

Van Wagoner, J.C., 1985, Reservoir facies distribution as controlled by sea-level change, abstract: Society of Economic Paleontologists and Mineralogists Mid-year Meeting, Golden, Colorado, August 11-14, p. 91-92.

Weimer, 1960, Upper Cretaceous stratigraphy, Rocky Mountain area, AAPG Bull. 44/1: 1-20.

Weimer, R.J., and Flexer, A., 1985, Depositional patterns and unconformities, Upper Cretaceous, Eastern Powder River Basin, Wyoming, IN: The Cretaceous Geology of Wyoming, 36th Annual WGA Field Conference Guidebook, 131-147.

Westphal, H., Eberli, G.P., Smith, L.B., Grammer, M. and Kislak, J., 2004, Reservoir characterization of the Mississippian Madison Formation, wind River basin, Wyoming, AAPG Bull., 88/4: 405-432.

Wheeler, 1986, Stratigraphy and sedimentology of the Tensleep Sandstone, Southeast Bighorn Basin, Wyoming, Unpublished Masters Thesis, Colorado School of Mines, 169 p.

Winn, R.D., Stonecipher, S.A., and Bishop, M.G., 1983, Depositional environments and diagenesis of offshore sand ridges, Frontier Fm, Spearhead Ranch field, Wyoming, The Mountain Geologist, 20/2: 41-58.

Wyoming Geological Association, 2000, Wyoming oil and gas fields symposium, Powder River Basin, 2 volume set, Mountain States Lithographing Company, Casper, Wyoming: 565 pp.

Wyoming Oil and Gas Conservation Commission (WOGCC) website, http://wogcc.state.wy.us/ , accessed between 2006 and 2011.

Yamamoto, H., K. Zhang, K. Karasaki, A. Marui, H. Uehara, and N. Nishikawa. 2009. Numerical investigation concerning the impact of CO2 geologic storage on regional groundwater flow. *International Journal of Greenhouse Gas Control* 3, no. 5: 586–599.

Zaitlin, B.A., Dalrymple, R.W. and Boyd, R., 1994, The stratigraphic organisation of incised-valley systems associated with relative sea-level changes. In: Incised-valley systems: Origin and sedimentary sequences, Ed. by R. W. Dalrymple, R. Boyd and B. A. Zaitlin, Spec. Publication Society of Economic Paleontologists and Mineralogists, 51, 45–62.

Zhou, Q., Birkholzer, J.T., Mehnert, E., Lin, Y. and Zhang, K., 2010, Modeling basin- and plume-scale processes of CO_2 storage for full-scale deployment, *Ground Water* 48/4: 494–514.

CHAPTER 3

ASSESSING PRESERVATION OF ANCIENT DEPOSITS AND APPLICABILITY OF MODERN DELTA MODELS: EXAMPLES FROM MID CRETACEOUS FRONTIER FM., POWDER RIVER BASIN, WYOMING AND MONTANA

Contribution of Authors and Co-Authors

Manuscript in Chapter 3

Author: Jesse J. Melick

Contributions: Primary author (Jesse J. Melick) acquired and compiled all data in 2D database, performed all sedimentologic and stratigraphic interpretations on core, well logs and cross sections. Jesse J. Melick drafted all figures and tables presented and wrote the corresponding text.

Co-Author: Michael H. Gardner

Contributions: Secondary author (Michael H. Gardner) provided oversight and input for this project, including: (1) acquisition of dataset from RPI of Colorado and required permissions from El Paso Inc.; and (2) editing of text, figures and tables for this contribution. Funding was provided through ZERT of Montana State University.

Manuscript Information Page

Jesse J. Melick and Michael H. Gardner

Name of Journal: *American Association of Petroleum Geology*

Status of Manuscript:
__X_Prepared for submission to a peer-reviewed journal
____ Officially submitted to a peer-review journal
____ Accepted by a peer-reviewed journal
____ Published in a peer-reviewed journal

Publisher: American Association of Petroleum Geology

Abstract

Linking modern sedimentary environments to sedimentary architecture requires robust calibration of their temporal and spatial equivalence. A direct application of the principle of uniformity uses sedimentary attributes and stratal relationships to link depositional process to architectural response. Surficial processes, emphasized in delta models, often cannot explain the variance in modern response and the poor correlation between modern and ancient deltas. This contribution presents a solution to the challenges with the application of the delta model so well defined in depositional terms, to ancient stratigraphic sequences. Barrell (1917) used deltas to illustrate the material and nonmaterial nature of geologic time (*rock* vs. *diastem*-surfaces with time value, respectively). The physical expression of time and the role of preservation are emphasized in evaluating Middle Cretaceous "delta" of the Frontier Fm. in NE Wyoming. The following factors suggest that preservation is a primary control (in addition to deposition) on ancient sedimentary architecture: 1) the downward trajectory in parasequence stacking pattern; 2) thin, elongate, offset and isolated sandstone thicks; 3) regional correlation of multiple and closely spaced erosional surfaces; 4) thin interval (300 m) spanning a significant period of time (3 m.y.); and 5) the absence of delta-plain deposits. The poor correlation between the regional Frontier delta shape in the Powder River Basin and the suite of sedimentary components of modern deltaic environments is better explained by remnants of shoreline and shelf sediments incompletely preserved and spread across a broad stable tectonic platform. Foreland basin subsidence was lower on this tectonic terrane than the aulacogens bounding it. Movement of different thrust

segments along 10000-km (6000 mi) length of the North American Cordillera produced multiple depocenters where sand was distributed the farthest eastward on this discrete Wyoming Platform. This study provides an examination of current geologic characterization for evaluating feasibility of subsurface carbon capture and storage. That effort requires accurate geologic models that can predict the long-term fate of subsurface storage of gigaton volumes of supercritical CO_2.

Introduction

This paper addresses the fundamental distinction between spatial and temporal processes contributing to a suite of areally limited and relatively short-term surficial processes that defines the geomorphology of modern deltas. The challenge with applying the principle of uniformity to the interpretation of sedimentary architecture is identifying differences created by deposition and preservation. For example, the preservation of sedimentary architectural elements produced by wave, tide, and river-dominated deltas or depositional differences between deltas and strand line shorefaces. Stratigraphy records geologic time both as material rock and nonmaterial surfaces and directly correlating an ancient sedimentary pattern to a modern depositional environment can focusing more on deposition, under-emphasizing the role preservation. This conclusion impacts geologic characterization studies requiring high-resolution geologic models used for evaluating subsurface carbon capture and storage. Such an effort requires large heterogeneous geologic models that accurately predict the long-term fate of subsurface storage of gigaton volumes of supercritical CO_2.

Ancient deltaic systems are commonly identified using models of modern deltaic processes (Gilbert, 1885; Barell, 1912; Fisk and McFarlan, 1955; Grabau, 1960; Coleman and Wright, 1975; and Galloway, 1975). These include: 1) long-lived, commonly tectonically-controlled fluvial sediment input to the shoreline protrusion distributed by channels separated by marshes, lagoons, and bays; 2) repeated seaward outbuilding of clastic shoreline, whose position is governed by relative sea-level fluctuations; and 3) sediment accumulated more rapidly than it can be redistributed by basinal processes (1000 to 10,000+ feet thick), thereby generating a deposition-subsidence feedback loop, by which deposition induces subsidence which in turn accommodates more sediment. The outbuilding shoreline and high subsidence rates promote the development of marsh environments and coal deposits. An important difference between ancient and modern deltas is preservation. The geomorphology of a modern delta can be severely modified by future wave ravinement upon the regional transgressions before it is buried in the rock record (e.g., Dunvegan of Western Canada Cretaceous foreland basin, Plint and Kreitner, 2007).

The effect of deep geologic time (e.g., pre-existing crustal continent assembly formed billions of years ago) is imprinted in the sedimentation of ancient deltas. Considering deep time in a study requires considering the full range of events that contribute to basin fill on continental crust, in particular differences in crustal rheology. Tectonic subsidence often governs the regional-scale preservation potential of sedimentary sequences. Variations in the strength and rheology of a Proterozoic assemblage of continental crustal fragments influence the expression of the subsequent

Mesozoic foreland basin. This paper examines an 8 million year stratigraphic succession from the Western Interior Cretaceous Seaway framed in the 80 million year 1st-order basin fill (Figs. 3.1 and 3.2). This permits assessing the role of crustal heterogeneities on the interpretation of the easternmost sandstone wedge formed during the Turonian (Fig. 3.2D).

This work examines the temporal contribution of tectonic heterogeneity on a foreland basin and the deltaic interpretation of the mid Cretaceous Frontier Formation in the Powder River Basin of east-central Wyoming. The hypothesis to be tested here is that these poorly preserved sedimentary patterns record variations in tectonic subsidence from crustal heterogeneity and crustal anisotropy, rather than depositional deltaic processes.

Data And Methods

Data

This study builds upon previous work (Table 3.1) and a dataset including over 30,000 wells and stratigraphic tops and incorporates rock property measurements from over 300 core plugs, two-dozen core descriptions and outcrop analogs from the Powder River Basin (PRB), Wyoming and Montana (purple outline in Fig. 3.3). Uplifts (black lines) and basement cored anticlines (black lines) rimming the basin margins expose outcrops that controlled the subsurface core and well-log correlations across the 200 by 575 kilometer (125 by 360 mile) PRB. Core descriptions (orange stars) permit the facies classification and documentation of systematic proximal to distal transition from shoreface dominated to remnant storm-reworked shoreface (Appendix A and B). Over

12,000 wells with raster log images (small black dots in Fig. 3.3) were correlated to establish the structural and stratigraphic framework (containing up to 20 stratigraphic sequences; Appendix C). The core plug data were digitized for interpretation and log calibration.

To calibrate the subsurface digital data, core plug data (porosity, permeability, grain density, oil and water saturation) were correlated to sedimentological descriptions from 5 outcrops and 15 cores (Table 3.2; Appendix A). 1200 wells with high quality porosity log suites were used (e.g., neutron, density and sonic porosity plus resistivity) to estimate log facies, effective-porosity, and matrix permeability, including 1540 high-quality, normalized neutron-density combination logs, 1290 good-quality log suites (two porosity logs and resistivity) and 1170 moderate-quality log suites (one porosity log and resistivity) (big black dots in Fig. 3.1). The core-to-log facies were calibrated to 23 cores (510 meters, 1700 feet,) with core descriptions tied to petrophysical log responses (Manuscript 1, Fig. 2.6).

Facies Analysis

The formative sedimentary processes are characterized by facies analysis, which divides potentially similar but distinct fabrics into a discrete and finite number of lithofacies (Table 3.2; e.g., ripple laminated fine sandstone, trough cross bedded coarse sandstone, finely interlaminated siltstone and very fine sandstone). These lithofacies can number in the dozens and have overlapping petrophysical properties; therefore they are grouped into log facies (representing similar porosity and permeability relationships) based on a common set of rock properties (Table 3.2). Six orders of sedimentary

architecture were documented with wireline well-log data, up to four orders of magnitude variation in permeability, and one order variation in porosity (Fig. 3.4*).* Using lab measured porosity and permeability cross plots, it is possible to correlate these broad property distributions of lithofacies to define a narrower range of log facies that can be correlated to wireline logs (Table 3.2). Genetically derived facies are used to calibrate and generate log facies (Fig. 3.5 and Appendix A). They also compose a hierarchy of sedimentary bodies, defined by log shape, thickness, lithofacies and log facies attributes.

Stratigraphic Analysis

Stratigraphic sequences were correlated around the basin using more than 20 bentonite ash beds (which form gamma ray spikes in well log) to frame sandy intervals (Appendix B). These were correlated to ammonite biozones to confirm ages from west to east. Biozone bounded sandstone units were first documented by Merewether and others (1979), where they divided the Frontier into eight units (Fig. 3.1 and 3.6). Bhattacharya and Willis (1991) grouped these eight into three members (Belle Fourche, Emigrant Gap and the Wall Creek) and Weimer and Flexer (1985) recognized a lower and upper Turner Sandy member. This study uses these divisions combined with the three biozones of Cobban (2006) to erect a four-fold hierarchy of stratigraphic cycles (Fig. 3.6). This allows construction of thickness maps and vertical constraints to examine attribute distribution to assess stacking patterns, facies distributions, and typical log shape necessary to designate sedimentation regions (Fig. 3.7).

Based on detailed correlation, isopach, net sandstone and sedimentation region maps were constructed across the four-fold stratigraphic hierarchy (Fig. 3.8). These were

based on 1200 wells in the southern PRB (15,500 square kilometers, 6000 square miles) where log density varied from several per section to one per township (Fig. 3.3). The gridding for the maps was set at 60-meter (200-foot) on a side and gridded in Petra software, which was then hand edited and recontoured to represent geologic features more clearly (Fig. 3.9).

The stratigraphic hierarchy in this study builds sedimentary facies into sedimentation units (defining depositional events) that build facies associations (also called sedimentary bodies; Table 3.2, Figs. 3.4A and B). These sedimentary attributes are used to define stratigraphic cycles and their stacking patterns (Fig. 3.4C). This approach defines a hierarchy of stratigraphic cycles (initiation, growth and retreat phases, after Gardner et. al., 2008).

Surfaces and/or strata that record minimum depositional energy conditions define stratigraphic cycles at all scales in this study, except in the middle of the 2nd-order cycle where removed by million-year hiatuses (Fig. 3.4C; Merewether and Cobban, 1986; Gardner, 1995). This approach employs methods and concepts associated with stratigraphic base-level analysis (Wheeler, 1964; Cross, 1988; Cross and Lessenger, 1998, Gardner et al., 2004). This method is based on the stratigraphic correlation of relative sedimentary energy conditions and sediment volume partitioning within and across a hierarchy of stratigraphic cycles. This technique is preferred over other stratigraphic methods because of its emphasis on diachronous rock to surface correlation suitable to settings dominated by depositional remnants (sensu Martinsen, 2003A and B).

Diachronous stratigraphy emphasizes preservation and deposition in the generation of sedimentary architecture.

The energy signal of a marginal marine clastic system (governed by a combination of tectonics, sediment supply and sea level) is commonly characterized by multiple scales of cyclicity (short, intermediate and long-term), where the long-term maximum energy is placed at the overlap of the maximum at all three scales (Figs. 3.4 and 3.6; Gardner et al., 2008). The terms *initiation, growth and retreat* are energy phases independent of place or forcing function as implied by the terms highstand, lowstand and transgressive systems tracts.

In the Frontier Fm., the Belle Fourche Member represents the initiation phase, the Emigrant Gap the growth and the Wall Creek-Turner the retreat phase (Fig. 3.4). In the Belle Fourche *initiation*, clastic sedimentation is restricted to a small area in a proximal portion of the basin. In contrast, the Emigrant Gap growth phase, coinciding with a global eustatic sea level fall, records regional deglaciation represented by an erosional surface recording two million years and a very thin interval suggesting limited sedimentation localized to erosional depressions. The Wall Creek-Turner Member was deposited during the subsequent transgression and records outbuilding of the strand line in successively back-stepping cycles.

Sedimentation Region Analysis

Sedimentation regions are spatial domains within a stratigraphic sequence defined by a hierarchy of sedimentary attributes representing responses to surface processes of a different scale (Fig. 3.7). *S*edimentary attributes include lithology, grain size and process

facies, sedimentation units, sedimentary body (shapes), azimuth (lateral trend and spread), vertical trend and thickness. A hierarchy of stratigraphic cycles can be correlated to sedimentation regions at multiple scales. Regional paleogeography maps document region distribution, which is based on similar groups of the sedimentary attributes. Shoreface, proximal, and distal marine shelf regions are defined by longitudinal gradient and dispersal patterns reflecting the interaction between focused (channelized) flow associated with fluvial input, combined flow (sensu Myrow and Southard, 1991), and semi-focused oscillatory long-shore current flow.

The *shoreface region* consists of amalgamated sandstones that coarsen and thicken upward. Focused sedimentation in the southwestern PRB area formed large reworked coarse to fine-grained shoreface sedimentary bodies that stack to form 30-50 km long, 5-20 km wide, by up to 50 m thick composite strand-plain successions associated with deposition above fair weather wave base.

The *proximal shelf region* consists of reworked shoreface sandstones amalgamated across discordant erosional surfaces; it is commonly intensely bioturbated and can show a bimodal to blocky (>10 m-thick) shoaling up well-log motif. These are composed of fine to very-fine sandstones with discontinuous mudstone interbeds and are associated with deposition between fair weather and storm weather wave base.

The *distal shelf* consists of thinly interbedded fine to very-fine sandstone and mudstone, where very-fine sandstones are bioturbated. The thin sandstones beds are isolated vertically and laterally but form four 4^{th}-order northeastward-stepping depocenters containing up to 60% sandstone.

Localized linear *channel regions* dissect shoreface and shelf regions, with higher sandstone percent, blocky (< 10-m thick) to fining up grain-size trend. These sand-rich features are oriented at a high angle to the north-south shoreline.

The *muddy shelf* region lies beyond the distal shelf and in the Wall Creek-Turner only, separates the proximal and distal shelf in a narrow band (less than 8-km, 5-mi wide).

Tectonic Analysis

Boundary conditions imposed by superposed interactions between different temporal and spatial orders of tectonic deformation preclude the application of a simple foreland basin model to explain tectonic controls on sedimentation for this study. Crustal anisotropy generated during Proterozoic craton assembly influenced Mesozoic foreland tectonics (Gardner, 1995). In attempt to assign controls to temporal phases of deformation, this paper employs the following tectonic scales: *Long-term*: Plate boundary conditions for orogenic event (i.e. respective plate boundary, plate boundary configuration and plate accretion and craton growth), which include features such as aulacogens, craton boundaries, collisional zones. *Intermediate-term*: Crustal shortening, subsidence and rebound generally control foreland basin system. *Short-term*: Components of foreland basin system include salients, re-entrants, lateral ramps, and localized sedimentary depocenters linked to discrete thrust salients (Fig. 3.10).

Tectonic Setting: Tectonic Heterogeneity

The present plate boundary configuration is a static snapshot of exceedingly slow but continuous plate motion, continental accretion and basin formation. This present view limits plate tectonics to conditions from which the evolution of the system cannot be established. An incomplete system description hinders the ability to predict.

Thrust movement of discrete sheets loading variable crustal rheology most likely created non-uniform subsidence and sediment sources. Cretaceous biozones, coupled with $^{40}Ar^{39}Ar$ dated ash beds, provide a robust biostratigraphic framework for the Western Interior Cretaceous Seaway (e.g., Cobban, 1956; 1961; Merewether and Cobban, 1972; Merewether et al., 1976; Merewether, 1980; Merewether and Cobban, 1986; Cobban, 1990). Gardner (1995) constructed maps showing regional distributions of facies and unconformities used to identify five main Mid-Cretaceous foreland sub-basins with eight associated deltas (Fig. 3.10). Each depocenter coincided with thrust salient and structural lineaments bounding them, therefore they were interpreted to record the discontinuous and non-contemporaneous advance of thrust sheets (Gardner, 1995). The southward younging trend observed in middle Cretaceous depocenters suggests lateral variations in thrust propagation, most likely related to discrete movement on thrust segments (Gardner, 1995).

More recently, Merewether and others (2007) produced a series of biozone maps that help distinguish lacunas from sites of continuous faunal record that were associated with the three clastic 3rd-order cycles of the Frontier Fm. They demonstrated significant erosion associated with an unconformity between the Belle Fourche and Emigrant Gap

members concentrated in central and western Wyoming (red hatchered areas in Fig. 3.10). This lacuna shifted eastward during the approximately 2 million year period between the Emigrant Gap and Wall Creek-Turner members. This early Turonian lacuna is greatest in southeast Wyoming (PRB) decreasing in duration to just beyond Cody, Buffalo and Newcastle, Wyoming (Fig. 3.2D). The Wall Creek-Turner biozones 13, 12 and 11 (in order of decreasing age) are shown to progressively westward onlap. Sandstone extent and lacunas in biozone markers indicate Wall Creek-Turner sedimentation was more complete in the southern PRB, east-central Wyoming. These lacunas correspond with zones of low tectonic subsidence and help emphasize the importance of local changes in tectonic subsidence. Merewether and others (1979) documented a shift in sediment delivery from the northern PRB during the Cenomanian Labarge Delta to the southern PRB during the Turonian Cumberland Delta (De Chadenes, 1975). Sandstone distribution is shown to expand from the southwest part of the PRB eastward past Newcastle in the upper three units, corresponding to the Wall Creek-Turner member.

Wyoming Platform Defined by Accreted Terrane and Aulacogens

The Wyoming Tectonic Platform is a relatively stable Archean craton bounded by crustal weaknesses, visible in magnetic and gravity data (Jachens et al., 1993) that were mobile during the Phanerozoic and coincide with failed aulacogens (Tonnsen, 1986). An accreted island arc younger than 1.8 billion years is found south of the Laramie Shear Zone and Trans-Hudson orogeny to the east (defining the position of the Black Hills

Uplift; Fig. 3.10) and these anisotropic crustal elements generate a non-uniform tectonic response in the foreland.

These two aulacogens form the northern and southern boundaries of the Wyoming Platform, while terranes bound the eastern and western margins of the platform. Middle Proterozoic aulacogens are important east-west oriented zones of weakness along the western margin of the Canadian Shield (Tonnsen, 1986; Anna, 1986). The two relevant to this study are the Central Montana Trough and southern Wyoming aulacogens. The northern aulacogen has over 600 meters (2000 feet) of Turonian sediments suggesting that was an area of higher accommodation (delta 1 in Fig. 3.10; Roberts and Kirchbaum, 1995). The Southern Wyoming aulacogen is defined by the Cheyenne Belt southwest to the Uinta Mountains (Tonnsen, 1986). These formed about 800 million years ago as part of east-west continent rifting through Idaho and Nevada (Stewart, 1976; Sears and Price, 1978).

These two zones of weakness (Central Montana and Southern Wyoming; CMT and SW in Fig. 3.10) were inherited from the Archean crustal assemblage and the breakup of the Kenorland super continent (circa two billion years; Hills and Armstrong, 1974; Cox et al., 2000; Bekker and Erikson, 2003; Dahl et al., 2006). The Wyoming Tectonic Province (herein after Wyoming Craton) is defined by its older cratonic crust greater than 2.5 billion years (WY in Fig. 3.10). It is bounded by the Cheyenne Belt, containing the Laramie Shear Zone to the southeast, and the Black Hills to the east, which define the western limit of the Trans-Hudson Province (Fig. 3.10; Shaw et al., 2003).

Lineaments in the PRB are well studied and are a composite response to over a billion years of processes (Fig. 3.3). Slack (1981) documents a series of NE trending lineaments that are tied to distinct basement blocks that have moved up and down throughout the Cretaceous. Marrs and Raines (1984) used satellite imagery, isopach, gravity and modern eolian dunes to document two predominant lineament sets (065-080° and 315-340°) that dissect much of the basin fill. These trends are oriented approximately parallel and perpendicular to the slightly arcuate (045-060°) Laramie Shear Zone, as well as the western north-south rift margin coinciding with the Idaho-Wyoming border (SW in Fig. 3.10; Tonnsen, 1986).

Foreland Basin System of the Western Interior Cretaceous Basin

The North American Western Interior Cretaceous basin was one of the broadest cratonic basins in the world, spanning 800-1650 kilometers (500 to 1000 miles) from the Sevier fold-and-thrust belt in the west to the outer foreland Canadian shield in the east, connecting the Boreal and Tethian seas after the middle Cretaceous (Fig. 3.2; Dickinson, 1976; Eicher and Diner, 1985; Kaufmann, 1985). The thrust loading on thick continental crust created a foreland basin that widened and deepened over time (Cross, 1986; Bird, 1995). This study uses the foreland basin system following DeCelles and Giles (1996) and Horton and DeCelles (1997), defined by the fold-and-thrust belt, wedge top, foredeep and foreland structural domains (Fig. 3.11a). Temporal variations in uplift and erosion result in under-filled and over-filled conditions, whereby the depocenter shifts across the foredeep (Figs. 3.11b and c).

PRB Structural Basin Part of
Larger Cretaceous Foreland Basin

The PRB is a north-trending westward dipping slab that resembles a syncline, and records three tectonic phases: 1) Proterozoic continental assemblage; 2) Mesozoic retro-arc foreland system; and 3) Laramide flat-slab compartmentalization of the foreland system (Figs. 3.3 and 3.11)., The Laramie shear zone and Black Hills remnant Wyoming Craton boundaries, define the southern and eastern edge of the PRB, respectively (Fig. 3.11). The Cretaceous foreland basin was compartmentalized and overprinted by late and post foreland basin tectonics. Late Cretaceous to early Tertiary folding and high-angle reverse faults rimming the PRB (red lines in Fig. 3.3) have been interpreted as caused by the low angle of slab subduction (Blackstone, 1983; Stone, 1993; 2003). These faults created 7600 m (25,000 ft) offset in Precambrian rocks along the western basin margin (Berg, 1962; Stone, 2002; 2003). Gentle monoclines along the Black Hills form the eastern margin of the PRB (Lisenbee, 1978; Jenkins 1985; King, 1990; Lisenbee, 1988; Mancarci, 1989; Hu, 1992; Lisenbee, 1993; and Naus, 2000). Lineaments in the PRB, which correlate to hydrocarbon production, are linked to periodic reactivation of the basement blocks (Slack, 1981) by shifting tectonic stress fields. These lineaments correlate to intrabasinal highs e.g., the Belle Fourche Arch and are documented in outcrop (Weimer, 1984).

Mid-Cretaceous Frontier Formation: Stratigraphic Framework

This approximately 100,000 square kilometers (45,000 square miles) study area of the Western Cretaceous Interior Seaway provides a data-rich laboratory to analyze the Mid-Cretaceous (Cenomanian – Coniacian) Frontier Formation (here after Frontier Fm.) forms a clastic wedge, conformably overlying the Mowry Shale and eroded unconformably by the Niobrara Formation of the Cody Shale (Fig. 3.1). The sand-rich portions of the Frontier Fm. are restricted to the western and southern PRB and thin from 370 to 100 meters (1200 to 300 feet) in thickness west to east. This clastic wedge records almost 10 million years of marine siliciclastic deposition punctuated by periods of long-lasting basin-wide hiatuses (Fig. 3.3). The Frontier Fm. forms an apparent "bulge" in the western shoreline of the Cretaceous seaway and has been interpreted as a delta in this area (Fig. 3.2; Cobban and Reeside, 1952; Barlow and Haun, 1966; Weimer, 1970). To explain the lack of delta plain deposits overlying delta front deposits in a succession obeying Walther's Law (e.g., Middleton, 1973), this feature is here re-interpreted as a strandline and shallow shelf setting dominated by regressions and strong long-shore currents and significant wave energy, especially during transgressions.

Chronostratigraphic frameworks correlate basinwide time equivalent markers such as biostratigraphic markers (using index Ammonite taxa from outcrop) and volcanic ash beds (which weather to bentonite clay recognizable on well logs) to bracket coeval sandstones and mudstone-dominated areas. Third-order sequence mapping allows distinction of general sediment thicks and lithology distributions, but facies and body

arrangements are still resolved (Fig. 3.12). For this reason, this study describes the arrangement of attributes within each third-order cycle, with detailed attention given to the 4th- and 5th- order Wall Creek-Turner Member cycles (Fig. 3.13).

Greenhorn-Niobrara Second-order Frontier Cycle

The Middle Cretaceous 2nd-order cycle of the Western Interior, containing the global oceanic anoxic event (recording periods of oxygen starvation in the basin; OAE2; e.g., Jenkyns, 2010), occurred in the late Cenomanian, culminated during early Turonian and marks the first time the Tethian and Boreal seas were connected to form the Western Interior Cretaceous Seaway (Fig. 3.1; McGookey, 1972; Sageman, Meyers and Aurther, 2006)). This marine deepening and continental flooding event was followed by the Mid-Turonian rapid global sea-level fall, which subaerially exposed much of the Western Interior Cretaceous Seaway and resulted in significant erosion (Sloss, 1963). Sea level rose through the end of the Middle Cretaceous, culminating in the Niobrara Limestone in the early Coniacian (Fig. 3.1; McGookey, 1972). The Wall Creek-Turner clastic wedge occurs during the beginning of this overall eustatic rise that continued through deposition of the overlying Sage Breaks shale and the Niobrara Limestone (Fig. 3.1, Table 3.1).

Sedimentation patterns in the Frontier Fm. fundamentally record tectonic pulses associated with the emplacement and evolution of a retro-arc foreland basin (Gardner, 1995; DeCelles, 2004). Relative sea-level change was amplified in the short-term cycles (Gardner, 1995), due to the maximum subsidence being to the west of western Wyoming structural basement culminations (sensu DeCelles, 2004) and the Wyoming Platform was likely stable,. This is supported by the laterally continuous but thin Wall Creek-Turner

member, which records widespread clastic shallow-marine sedimentation. Furthermore, coeval deltaic deposits in the Western Interior Cretaceous Seaway are mostly restricted to the west in the foredeep except the Wall Creek-Turner member (Merewether et al., 1979; Bhattacharya and Willis, 2001). This is likely due to low subsidence in an overfilled foreland with sediment distributed across a broad area by far-reaching regressions and transgressions (e.g., DeCelles 1997).

Third-order Frontier Cycles

The Frontier Fm. in the PRB contains three 3rd-order sandstone-rich stratigraphic cycles, the Belle Fourche, the Emigrant Gap and the Wall Creek-Turner member from oldest to youngest (Fig. 3.1). Each of these in turn contains up to four 4th-order cycles and two to four 5th-order cycles each (Figs. 3.4 and 3.6). This hierarchy of cycles describes cycle stacking pattern, blurred facies distribution (e.g., reworked and/or incomplete shoaling-up sequences) and sediment volume partitioning.

Belle Fourche Member: The Cenomanian and lower Turonian Belle Fourche member spans approximately 4.5 million years from the Clay Spur Bentonite to *Mammites nodosoides* and is bounded by Oceanic Anoxic Events 1D and 2 (Fig. 3.6A). The sandstones in this lower 3rd-order clastic wedge (the Frontier *initiation*) are restricted to the southwest edge of the PRB with no correlative sandy deposits eastward of Casper (Fig. 3.12; Bhattacharya and Willis, 2001). Stratigraphic correlations identify three to four 4th-order cycles that form upward-coarsening and sandstone bed-thickening successions, 30 kilometers wide and less than 70 kilometers long and up to 30 meters

thick (20 x 45 miles and 100 feet thick) (Bhattacharya and Willis, 2001). They contain basinward to landward stepping depocenters forming lobate or pod-shaped wave-dominated top-truncated shorefaces. Their north-south orientation and restriction to the western PRB, suggests sediment input originating from the Yellowstone National Park area and being delivered to a shoreline positioned somewhere near Sheridan (Dyman et al., 2008).

The lower two sequences form elongate sediment thicks, 5 km wide by 30 km long and over 35 m thick (3 x 20 miles by 115 feet thick) that fine-upward and correlate to channelized processes (Sandstone I-III of Merewether et al., 1979; Harlan, Willow and Frewens/Posey lowstand deltas of Bhattacharya and Willis, 2001). A basin-wide shale interval containing the distinctive "Soap Box" bentonite marker (sensu Bhattacharya and Willis, 2001) records a 4^{th}-order marine deepening event. The uppermost 4^{th}-order sequence contains two isolated north-south oriented elongate sandstone bodies restricted to the western margin of the PRB (Sandstone IV of Merewether et al., 1979; *Second Frontier* of Vakarelov and Bhattacharya, 2009). The Belle Fourche deposits show generally south-southeast paleoflow and are associated with the LaBarge sediment entry (De Chadenedes, 1975). Above this, a thick succession of mudrocks and carbonaceous shales, correlating to the Bridge Creek Limestone and Global Anoxic Event II (Sageman and Arthur, 1994), represents a widespread baselevel rise and 3^{rd}-order retreat.

Emigrant Gap Member: The Middle Turonian Emigrant Gap Member and bounding unconformities span over 2.5 million years from *C. woollgari* through *P. macombi,* while biostratigraphic zones indicate that it coincides with a regional-scale

lacuna and is the Mid-Turonian global sea level low stand (Cobban and Reeside, 1952; Merewether, 1983; Cobban et. al., 2006). The Emigrant Gap Member is predominantly restricted to topographic lows in the southwesternmost part of the PRB; in the eastern part it has been termed the Pool Creek member (Weimer and Flexer, 1985).

A basin-wide erosional surface underlies the Emigrant Gap Member after Cavanaugh (1976). This 3rd-order sequence contains local remnant tide-dominated to marine valley fills preserved in the southwestern and eastern parts of the basin, where they overlie the Belle Fourche sand bodies and Greenhorn carbonaceous shales, respectively (these correspond to Sandstone V of Merewether et al., 1979 and the *unnamed member* of Merewether, 1983, as well as the Pool Creek member (of Haun, 1958) in the Black Hills). These deposits consist of non-amalgamated thin-bedded sandstones that thin and fine upward (defined in well logs as increasing gamma ray) and form narrow and elongated west-east oriented sediment thicks up to 5-km wide, and 70 km long and 70 m thick (3 x 20 miles by 115 feet thick) (black lines in Fig. 3.12). The Emigrant Gap Member marks the maximum sea-level drop in the Middle Cretaceous seaway and is recognized as a worldwide eustatic sea-level fall (Fig. 3.6).

Wall Creek-Turner Member: The sand-rich Wall Creek-Turner Member represents the uppermost 3rd-order cycle and is correlated across the southern PRB crossing into South Dakota (Fig. 3.8; Merewether et al., 1973), spans approximately 1-2 million years (including *S. warren* through *P. germari*) and is an important hydrocarbon reservoir (Fig. 3.3). The four sand-rich 4th-order sequences, defined by a bivalve biozones (*S. warreni/ferronensis, S. whitfieldi* and *S. quadratus),* contain more than one 5th-order

sequence (Fig. 3.4), while the sand-poor uppermost 4th-order sequence contains a dated ash bed (Cobban, 2006). This framework documents a hierarchy of thin but laterally extensive sand-rich sequences bounded by bentonite and biozones correlated over 160 kilometers (100 miles), that contain no non-marine deposits (e.g., Plint and Kreitner, 2007). The overall back-stepping stacking from the Emigrant Gap to the Sage Breaks Shale is consistent with a 2nd-order marine deepening.

This unconformity-bounded 3rd-order sequence is underlain by the Mid-Turonian unconformity representing up to 2 million year lacuna (Merewether et al., 1976; 1979; Merewether, 1980). Unlike the underlying Emigrant Gap member, the Sage Breaks Shale of the Carlile Shale is locally incised by the unconformity at the base of the Niobrara Formation (here termed the "Niobrara channel" (Fig. 3.12; Larue, 1995). The Wall Creek-Turner Member represents the most areally significant sandstone tongue of the Frontier cycle, characterized by shoreface, proximal and distal shelf sedimentation regions (Fig. 3.5; Lindquist, 1986). These regions, defined for each of the four 4th-order sequences, show general basinward-stepping migration and increased connectivity between proximal and distal shelf regions (Fig. 3.14).

Sedimentary attributes documented in this unit have led workers to a variety of explanations for its origin. These observations include: 1) 500 kilometers (over 300 miles) distance between observed nonmarine deposits at Cody Wyoming and the sandstones in the PRB; 2) pebble-lined surfaces present in the most distal deposits in the eastern PRB; and 3) the general shallow-water nature of the sandstones, bioturbation and wave reworking structures common in most of the wells and outcrops. There is little

consensus in the interpretations of these sandstones. They have been classified as representing deltas, offshore bars, hyperpycnites, shelf sand sheets, and incised valley fills (Fig. 3.15) (Asquith, 1974; Tillman and Almond, 1979; Weimer and Flexer, 1985; Winn, 1991; Larue, 1995; Bhattacharya and Willis, 2001; Sadeque, 2006).

Fourth-order Wall Creek-Turner Cycles

The Wall Creek-Turner Member is composed of four sandy 4th-order cycles (WCT1-4 upward). Each ranges in thickness from 3-30 meters (10-100 feet) and show depocenters shifting up to 20 kilometers generally to the east and north (Figs. 13 and 14). The lower two show downward trajectory, suggesting possible forced regressions (Fig. 3.8; sensu Fitzsimmons and Johnson 2000) and are similar to sharp-based shoreface sequences of Plint (1988). In contrast, the upper two are backstepping.

WCT1 was deposited on a 2 m.y. unconformity that becomes to a conformable contact in the eastern PRB. It has two principle depocenters, one in the Newcastle area with 70% sandy facies, and the other in the Casper-Kaycee area with 100% sandy facies; both reach 25 meters (75 feet) thick. Branching distributary channels delivered sand to the eastern distal shelf, which shows increasing sandy facies southward, indicating redistribution of sandy hyperpycnal flows by the southerly geostrophic flow. Nearly equal proportions of shoreface and distal shelf regions represent 40% of the southern PRB, with 13% belonging to the proximal shelf and 4% to channels (Fig. 3.13).

WCT2 conformably overlies WCT1, and its depocenter (20 m, 60 feet) shows compensational stacking, above a WCT1 thin (Fig. 3.13). It shows similar sedimentation patterns, with reduced total area, but more equilibrated shoreface, proximal and distal

shelf regions and a 50% increase in channelized regions. The overlying shale markers of these two sequences are the most laterally continuous and coincide with bentonites over much of the area.

WCT3 represents a significant increase in sandy facies compared to WCT1 or 2 and shows a 50 km (35 miles) northeastward shift (backstep) in depocenter (which is over 30 m, 100 feet). Sand facies represent 50-70% of the thickness over almost half the area, which is dominated by the shoreface region (20% of entire area), and lesser amount of proximal and distal shelf regions (14% and 10% respectively). The shift of depocenter is associated with a more focused area of sandstone as the channels shifted northward away from the thicks associated with WCT1 and 2. This 20% increase in sandy regions and increase in shoreface area suggest a strong phase of outbuilding associated with the growth of the Wall Creek-Turner cycle.

WCT4 is the uppermost 4th-order cycle in the Wall Creek-Turner Member and records a nearly 100 km northeastward shift in depocenter, where it reaches 25 meters (75 feet) thick and shows similar distal shelf positioned sandy facies (60-70%). The southward decrease in sandy facies suggests a decrease in long-shore transport along the extensive shoreface (24% of the area). This results in a 20 meter- (60 foot) thick proximal shelf separated from its shoreface, which was likely modified upon subsequent transgression when southerly currents were remobilizing and "smearing" the deposits across 22% of the study area, nearly 60% greater than the other cycles.

Fourth-order isopach and facies maps of the Wall Creek-Turner Member sequences document the variability associated with shifting depocenters as well as areas

of nondeposition and erosion that point to a strand line-turbidite depositional setting (Fig. 3.16). The lowest unit (WCT-1) is thick near Casper and represents a prograding shoreface, while near Newcastle the depocenter represents a more distal shelf with more tabular bodies. WCT-2 marks a northward shift in depocenter and more shoreface to proximal shelf near Kaycee and similar distal shelf depocenter. These two units have channelized regions between Buffalo and Kaycee, suggesting sediment was delivered here, then reworked along shore southward, but periodically mobilized eastward potentially as hyperpycnal flows (sensu Plint et al., 2009). WCT-3 and WCT-4 are almost twice as thick in northward shifted depocenters and have the most shoreface area with a less extensive sandy distal shelf. The proximal shelf is quite sand-rich in these two units and is both extensively bioturbated and amalgamated to form 50+ feet homogeneous sand intervals. This change in architecture between the lower two and upper two units may reflect an increase in marine processes associated with the overlap of 2^{nd} and 3^{rd}-order transgressions.

Discussion

Two important contributions arise from this study: 1) the Frontier Fm. is better interpreted as a top-truncated strandline; and 2) the shoreline bulge of the Frontier was driven by low accommodation due to the relatively low subsidence of the Wyoming Shelf, coinciding with Archean crustal heterogeneities. Poor correlation of depositional sedimentary attributes to stratigraphic remnants by previous workers led them to conclude that pore to outcrop-scale attributes cannot be used to predict regional-scale

stratigraphic patterns. The data presented here point to another explanation for this apparent incongruity. Strict adherence to the principle of uniformity underpins the previous interpretation, when in fact both temporal and spatial processes contribute to ancient sedimentary architecture. This is amplified when crustal heterogeneity, not apparent in surficial process-responses, influences modern depositional through variable subsidence due to crustal anisotropy created by multiple orogenic events in the plate tectonic assemblage of a craton.

Stratigraphic Remnants: Shoreface Rather Than Delta

The poor preservation of the Wall Creek parasequences was first discussed by Ryer and Martinsen (2003), who called them *depositional remnants*. They were the first to recognize incomplete preservation of geomorphic patterns across Wyoming Western Interior Cretaceous Seaway. Using this approach, the sandstones reaching across the southern PRB can be viewed as severely truncated shoreface parasequences (Fig. 3.16). This contribution integrates the stratigraphic architecture documented in this study with past studies to conclude that the Frontier Fm. is best explained by longer-term tectonic processes, reflecting temporal control, rather than a geomorphic explanation of the shoreline bulge as delta.

The sedimentary facies of the Frontier indicate shallow-marine clastic sedimentation with several important characteristics that, taken in concert, represent a particular set of processes (Table 3.2). First, non-marine deposits are not documented east of Cody Wyoming and the Rock Springs Uplift (Myers, 1977; Merewether, et al., 1984;

Hamlin, 1996) suggesting that they were deposited, but then removed by wave erosion ravinement. This is supported by the top-truncation of the upper shoreface. Secondly, the sandstones in the south-central PRB show pervasive bioturbation – even mixing sand with mud to create thick muddy sandstone successions. The biologically mediated sediment mixing indicates significant residence time after sand deposition characterized by low to no wave reworking.

The most debated aspect of the Wall Creek-Turner Member is the genesis of its easternmost sandstones (i.e., the Turner Sandy member). These are thin to medium beds of rippled and swaley very fine to medium sandstone, locally conglomeratic and phosphatic, and containing abundant shark teeth at the base (Rubey, 1930) suggesting erosive and rapid transgressions. Biostratigraphic correlation ties them to the Wall Creek age (Cobban, 1958), but the following attributes are not similar: facies, bedding architecture, nearly 3-fold thickness variations across the Black Hills outcrops and their disconformable lower contact with the Pool Creek member (Knechtel and Patterson, 1962; Robinson et al., 1964). Weimer and Flexer (1985) report upward evolution from parallel to low angle cross-stratified or scour-and-fill bedding, to interbedded sandstone and siltstone, to mainly bioturbated generally structureless top. Rice and Keighin (1989) document fining upwards bedsets of hummocky cross stratified very fine sand with sharp erosional bases with sole marks, commonly capped by wave ripples with *Cruziana* ichnofacies. Three distinct interpretations exist to explain the coeval sand-rich east and western PRB, which is separated by a narrow north-south oriented sand-poor zone (up to 8 kilometer/5 mile wide): 1) fully exposed shelf and sand transport through incised valley

fills (Weimer and Flexer, 1985; Rice and Keighin, 1989); 2) reworked deltaic lobes (Merewether and Cobban, 1986); and 3) hyperpycnites delivered across a broad shallow shelf (Winn, 1991 and this study).

Multiple Sediment Entry and Low Accommodation Strand Line

The sediment bulge in the Western Interior Cretaceous Seaway shoreline across the PRB has been interpreted as a delta for over half a century. Building on past studies (e.g., Merewether et al., 1979; Weimer and Flexer, 1985; Bhattacharya and Willis, 2001), this study has established a high-resolution framework used to describe the remnants of variable and superimposed depositional environments similar to those documented in the Vernal "Delta" of Ryer and Lovekin (1986; Fig. 3.16).

Merewether and others (1979) first described the three-fold hierarchy of biostratigraphically constrained sandy units of the Frontier (I-VIII). The lower sands (I-IV) were redistributed in southerly migrating bodies that terminated between Kaycee and Douglas Wyoming. The Emigrant Gap Member (sand V) has been mapped as an east-trending incised valley system positioned just north of Casper. The Wall Creek-Turner Member (sands VI-VIII) contains the far-reaching sand-rich units extending northeastward from Kaycee to Gillette and eastward to Newcastle Wyoming. The 3rd-order maps fail to identify one main depocenter for Wall Creek-Turner. It is at the 4th-order that the five gross sedimentation regions can be mapped (channelized, shoreface, proximal shelf, distal shelf, muddy shelf; Fig. 3.16).

Wyoming Platform: Low
Accommodation Depocenter

Slack (1981) and shortly thereafter Weimer (1984) were the first to recognize the role of movement on paleotectonic structural elements on sedimentary patterns. These workers considered the underlying basement blocks, outlined by the lineaments observed on the present day surface, and how differential movement was likely playing a dominant role in defining higher and lower accommodation areas across the southern PRB. This was possible because of the relatively thin but laterally continuous sandstone intervals, which show marked thickness variation across the lineaments. The importance of the lineaments is further tied to the rheology of the Wyoming Craton that is dense cold cratonic rock older than 2.45 billion years when Wyoming Craton was part of Kenorland supercontinent (Williams et al. 1991, Roscoe and Card 1993, Harlan et al. 2003). The surrounding younger rocks (< ~1.8 billion years) to the north (Great Falls tectonic zone also called the Central Montana Trough), east (Black Hills), and south-southeast (Laramie Range) record later rifting and subsequent accretion of less dense and warmer rocks (Chamberlin, 1998; Bekker and Eriksson, 2003). These boundaries remained zones of weakness that would react to loading differently during mid Cretaceous thrusting.

There appears to be a poor correlation between the simple foreland basin model and Western Interior Cretaceous Seaway sedimentation patterns and lacuna distributions identified by Merewether and Cobban (1986), which was recognized by Gardner (1995) and Krystinik and DeJarnett (1995). Considering the north-south crustal heterogeneity that has been documented, it is not surprising that the Sevier Orogeny thrusting events generated laterally varying amounts of accommodation in the foredeep. This is supported

by the clastic deltaic deposits that are 6 times thicker just to the northwest and southwest of the Wyoming Shelf (McGookey et al., 1972, their fig. 22).

Gardner (1995; 2004) documented multiple depocenters that appear to have filled at slightly different times (generally younging to the south) through the Cenomanian and Turonian during the Greenhorn-Niobrara 2nd-order cycle. Deltas such as SW Montana and NW Wyoming and the Last Chance delta of the Ferron Sandstone of Utah are thick but not laterally extensive, recording high accommodation (1 and 3a in Fig. 3.10, respectively; Gardner et al, 2004). In contrast, the Wall Creek-Turner records low accommodation (2b in Fig. 3.10). Foreland basin models may not capture this variability in clastic deposition if they don't consider along-strike variations in thrust emplacement and the crustal provinces upon which the thrust belts impinge.

The sedimentary architecture of deposits in a foreland system is directly governed by sediment delivery and subsidence of the receiving basin. Comparing the deposits along a thrust belt to its underlying crustal composition can help to clarify sedimentary response. Figure 3.10 composite map compares crustal provinces and sedimentary the impact inherited structural features can have on sedimentary patterns.

The Mid-Cretaceous Wyoming Shelf was a large paleogeographic feature of the Western Interior Cretaceous Seaway. Did this feature impact southward-directed long-shore currents governing sediment dispersal as well as carbon accumulation and water chemistry (Fig. 3.2; Sageman and Arthur, 1994)? The sandstone tongue mapped south of the PRB that reaches nearly to Cheyenne (Merewether et al., 1979) suggests there was sediment a starved area just to the south of the Wyoming Shelf. Combined with low

clastic influx, upwelling of waters highly enriched in organics circulating into this area likely deposited significant accumulations of organic-rich mudstones (Sageman and Arthur, 1994).

The Wyoming Shelf, being associated with more stable crust, is interpreted to have undergone lower subsidence as supported by distributions of lacunas documented by Merewether and Cobban (1986). Sea-level low stands were more likely to expose this area and create progressive hiatuses and onlaps during subsequent transgression.

Conclusions

1) Analysis and interpretation of ancient sedimentary architecture must consider the role of geologic time on the suite of earth processes contributing to a preserved sedimentary response, which extends beyond those surficial processes observed to be operating in modern depositional environments.
2) For these reasons, the Frontier Fm is not an ancient delta that can be explained by an incomplete suite of short-term surficial processes that define the modern delta.
3) An area of low subsidence centered over east-central Wyoming is bounded by variations in continental crust rheology and is responsible for the time-averaged Middle Cretaceous clastic wall Creek-Turner wedge created by multiple foreland basin sediment sources.
4) Sediment delivery reflects non-uniform along-strike changes along multiple foreland basin thrust segments, which were much smaller than the length of

the Western Interior Cretaceous Seaway. It is here recognized that the composite tectonic/eustatic nature of the Western Interior Cretaceous Seaway better accounts for its anomalous size and paleogeography.

5) Stratigraphic prediction requires analysis of the full range of processes that operate over geologic time. This requires more than consideration of just time as a surface, but also tectonic processes operating at slower and lower rates than the surficial depositional environments they accommodate, characterized by non-uniform crustal response to tectonic stress. In order for temporal processes to be usable in prediction when pore to outcrop-scale attributes cannot be reconciled with regional-scale patterns, the scope of temporal processes considered must be expanded.

6) Attempts to predict Earth systems affected by long periods of geologic time for a given location based on little data results in high uncertainty. Climate and CO_2 modeling performed in the context of a foreland basin tectonic model based on isotropic and elastic crust could result in widely ranging outcomes. This is not to say that Earth systems cannot be predicted, only that the current methods oversimplify these complex processes because they don't account for Earth processes and responses over deep geologic time. This conclusion is central to the reason for this study - an examination of current geologic characterization studies for evaluating feasibility of subsurface carbon capture and storage. That effort requires accurate geologic models that can predict the long-term fate of subsurface storage of gigaton volumes of supercritical CO_2.

2nd order: Frontier	large scale	thickness	width (dip)	width (strike)	Stacking pattern	Bodies	Facies	reservoir properties
Merewether et al 1979 *Frontier: 8 SSbodies*	SSI-VIII	10 to 35m, SSVIII over 60 m	50 to 100km, (I-V) 250km-basinwide (VI-VIII)	70-100km (I-V) 100-105 km (VI-VIII)	two fore/ back stepping			
Curry 1986 (chronostrat) Belle Fourche Mbr (A-D) Wall Creek (upper-lower)	A-D, l/ UWall Creek	10 to 60m	basin wide	basin wide	fore to back stepping			
3rd order	large scale	thickness	width (dip)	width (strike)	Stacking pattern	Bodies	Facies	
Bhattacharya & Willis 2001 *lower Belle Fourche* *(SSI - SSII)*	Posey (several CU) Frewens (2 CU) Willow (2 CU) Harlan (3 CU)	37 m 35 m 35 m 55 m	100+ km 5 km 60 km 100 km	75 km 20 km 80 km 120 km	lateral shifting: south to north then middle, fixed seaward limit, all backstep except last	Sandbars: elongate NW/ SE, 5-10 km wide, few tens km long	F1: thin bedded SS/ mdst F2: isolated dm-thSS F3: beds het lith x strata F4: compound Xstrat F5: m-thk sets of Xstrat SS	
Merewether et al., 1979 *Emigrant Gap (SSV)* *Weimer & Flexer 1985* *Pool Creek*	no internal sequences	<30 m	30 km	>120 km	none implied	not mapped		
Winn et al., 1983 Wall Creek	none used, CU	15 m thick				ridges: 8-15m, 3 km wide, 10-15 km long ridge margin,		
Winn 1991 Wall Creek - Turner	SSVI- VIII of Mer79, uses 4 units - sand sheets	10 to 20 m	not mapped	not mapped	none implied	basinward dipping SSsheets	no scheme	
Sadeque 2006 *SSVI- VIII*	five units, with 8 paraseqeunces, 22 sandbodies	15 to 20m	35 km, PS4 - 65 km	20km, PS4 - 60 km	generally northward shifting, negtrajectory, sw step in youngest	22 sandbodies: 15-20 m thick, 60-80 km^2		
Weimer & Flexer 1985 Rice & Keighin 1989 *Turner Sandy Member* *(SSVI-VIII)*	Upper and Lower	20 m	basin-wide	basin-wide	none implied	channels: 4 m x <1.5 km wide, 10km long, E-W; lobes: 12m x <70km^2	CH: Tr/ Tab Xstrat, LB: thin-bedded bioturbated to interbedded planar to rippled VFS with HCS	poros-ch: <20% perm-ch: <100 md poros-lb: 15% perm-lb: <0.5 md
4th order	large scale	thickness	width (dip)	width (strike)	Stacking pattern	Bodies	Facies	
Vakarelov & Bhattacharya 2007 *2nd Frontier (SSIII and probably IV)* *facies based on environments*	Parasequences A-G	5 to 25 m	2 to 7 km	2 to 3 km	offlapping NW to SE nearly south		FAi: heterolithic siltst/ SS, mudst FAii: bioturb mdst, sltst, sandy mdst FB: amalgamated platar and HCSS FC: planar to Xstrat Ophio burrowed SS FD: Xstrat SS FE: peb-bear muddy-SS, sandy mud, mud FF: beach conglomerate	
5th order	large scale	thickness	width (dip)	width (strike)	Stacking pattern	Bodies	Facies	
Gani and Bhattacharya 2007	Upper 6th of 7 sandstones	10 m	30 km	60 km	sw stepping, negtrajectory (from 500m outcrop)	prodeltafines (F1/ F2) frontal splay (F3) channel (F4) storm sheet (F6) bar accretion (F5a) tidally modulated deposit (F5b)	F1: laminated sandy mudstones F2: heterolithics F3: massive to parall-lam SS F4: channelized SS F5a: Tr Xstrat SS F5b: bipolar Xstrat SS F6: HCS	

Table 3.1. Literature review for stratigraphic architecture for the Frontier Fm.

Table 2. Facies Description and Grouping Strategies

#	Facies	Grain size	Sorting	Primary structures	Bed (thickness)	Bedset cm)	SS %	Perm (mD)		Porosity (%) min	max	Process interpretation
1	Coarse lag	med SS - granule	poor	aligned grains, planar laminae	<10	NA	100	0.1	100	12	20	erosional and/or reworked surface,
2	Clast-rich to conglom SS	Med - coarse SS	poor	Structureless, planar laminae	20-50	NA	100	0.1	0.3	4	6	freezing of debris flow to high concentration flow
3	Amalgamated cross-bedded SS	UF - coarse SS	mod well - well	Trough cross stratification	30-50	100+	100	0.01	20	2	14	repeated deposition from mostly unidirectional low concentration high velocity flow
4	PT Cross bedded SS	UF - coarse SS	mod well - well	planar tabular cross stratification	20-50	<100	100	0.1	150	4	23	deposition from uni/bidirectional low concentration mod velocity flow
5	Muddy cross beds	F-Med SS	mod - mod poor	Trough cross stratification, mud clasts or drapes	20-30	<80	100	0.05	0.1	4	6	unidirectional low concentration mod to high velocity flow
6	Soft sed deformed SS	F-Med SS	mod - mod poor	dewatering/load structures	20-50	100+	95	0.02	0.05	2	4	rapid deposition from high-concentration flow
7	Structureless SS	Uf - med SS	mod - mod poor	structureless	20-30	100+	100	0.01	50	2	17	freezing or rapid deposition from high-concentration flow
8	Plane parallel SS A	Uf - med SS	mod well - well	planar laminae	10-20	<50	100	0.01	150	2	15	deposition from moderate concentration, moderate velocity flow (traction carpets)
9	Swaley SS	Fine SS	mod well - well	plane parallel to low angle strat with reactivation surfaces	20-40	80-120	100	0.1	0.1	3	12	deposition or reworking from uni/bidirectional flow, above FWWB
10	Hummocky SS	Fine SS	mod well - well	plane parallel to low angle stratification	10-30	60-80	100	0.01	150	4	18	deposition or reworking from uni/bidirectional flow, at or below FWWB
11	Plane parallel SS B	VF SS	mod - well	plane parallel, structureless	5-20	<50	100	0.01	40	1	11	deposition from low concentration mod to low velocity flow
12	Faintly stratified amalgamated SS	F SS	mod - mod poor	Faint plane parallel, wispy discontinuous mud drapes	100+	100+	95	0.01	2	1	14	repeated rapid deposition from high-concentration flow, locally dewatered
13	Interbedded deformed/bioturbated SS	VF - Fine SS	mod poor - poor	Burrows, loads, rip up clasts	2-10	100+	85	0.01	1	2	12	intermittant rapid deposition from high-concentration flow, locally dewatered and/or burrowed
14	Amalgamated bioturbated SS	VF - Fine SS	mod poor - poor	Diverse and abundant burrows	5-15	200+	95	0.01	2	5	12	low frequency deposition from flows, poss reworked by waves, above FWWB
15	Ripple laminated SS	VF - Fine SS	well	Ripple cross laminae	1-8	1-20	100	0.6	50	1	23	unidirectional low concentration low velocity flow
16	Interbedded thinly laminated SS with mud drapes	VF - Fine SS	mod well - well	Planar laminae, mud drapes	1-3	100+	70-90	0.01	100	2	20	low frequency deposition from flows, poss reworked by waves, between FWWB and SWB
17	Bioturbated SS and mud	VF - Fine SS	mod poor - poor	Diverse and abundant burrows	1-3	100+	30-50	0.1	0.1	13.5	13.5	low frequency deposition from flows, poss reworked by waves, at or below SWB
18	Interlaminated mud and SS	Silt - VF SS		fine parallel laminae	<3	100+	50-70					low frequency deposition from low concentration low velocity flows,
19	Bioturbated mud and SS	Shale - silt			1-3	200+	60-80	0.01	15	8	17	low frequency deposition from very low concentration very low velocity flows,
20	Shale with thin SS beds	Shale - silt			<1	10-00+	<50	0.08	2	2	2	very low frequency deposition from very low concentration very low velocity flows,
21	Dark marine shale	Shale			<1	10-100+	<10					suspension deposition
	Claystone	clay	NA	none			none					weathered volcanic ash deposit
23	cemented	variable	na									

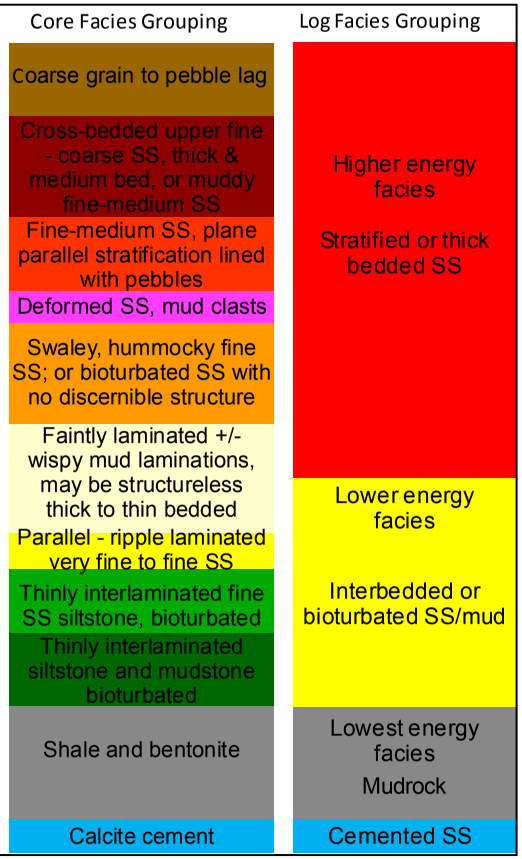

Table 3.2. Facies descriptions and interpretations help define grouping strategies. Right, well log values defining analog facies: Gamma Ray, (GR in API), Bulk Density (RHOB in grams per cubic centimeter), Neutron Porosity (NPHI - % porosity), Sonic (DT - microseconds per foot) and Resistivity (REST - Ohms). It is necessary to group based on the scale that the logs permit recognition. For example, all the facies 1-13 were indistinguishable in well logs, so were lumped into "higher energy facies". See appendix E for statistical analysis of well-log generated analog facies.

Facies	GR	DT	RHOB	REST	NPHI
1 MAX	60	70	3	299	0.11
1 MIN	0	0	2.45	1	0
2 MAX	85	75	2.7	200	0.165
2 MIN	30	60	2.4	3	0.1
3 MAX	100	120	2.7	100	0.18
3 MIN	60	70	2.4	1	0.12
4 MAX	400	120	2.625	50	1
4 MIN	85	70	0	0	0.16

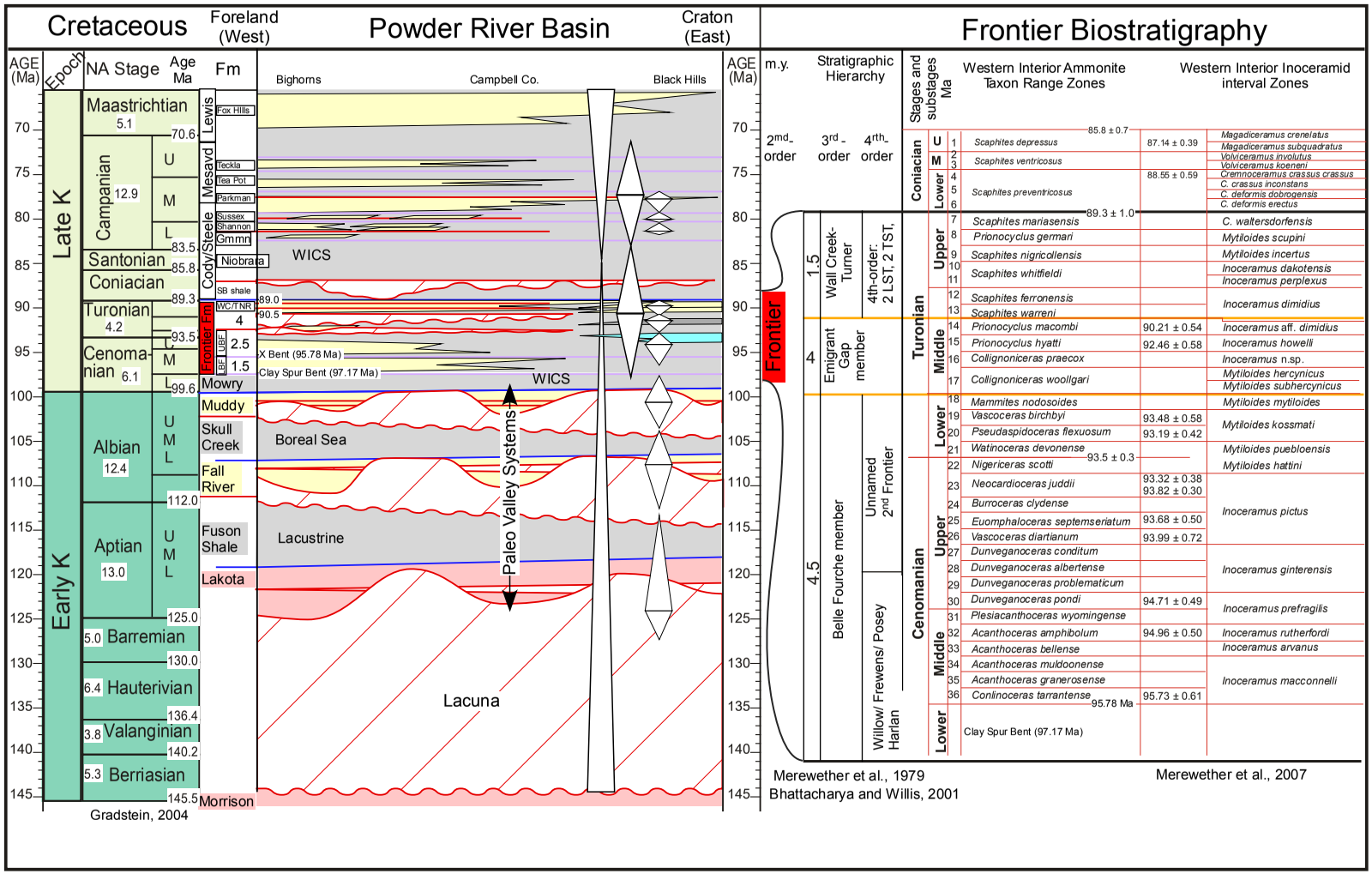

Figure 3.1. Stratigraphic hierarchy of Western Interior Cretaceous Seaway (WICS) in the Powder River Basin, eastern Wyoming and Montana. Biostratigraphy and volcanic ash beds provide robust time constraints on Mid-Cretaceous Frontier stratigraphy (triangles refer to hierarchy of baselevel cycles after Cross 1988). SB shale - Sage Breaks Shale, BF - Belle Fourche, WC/TNR - Wall Creek - Turner, m.y. - million years)

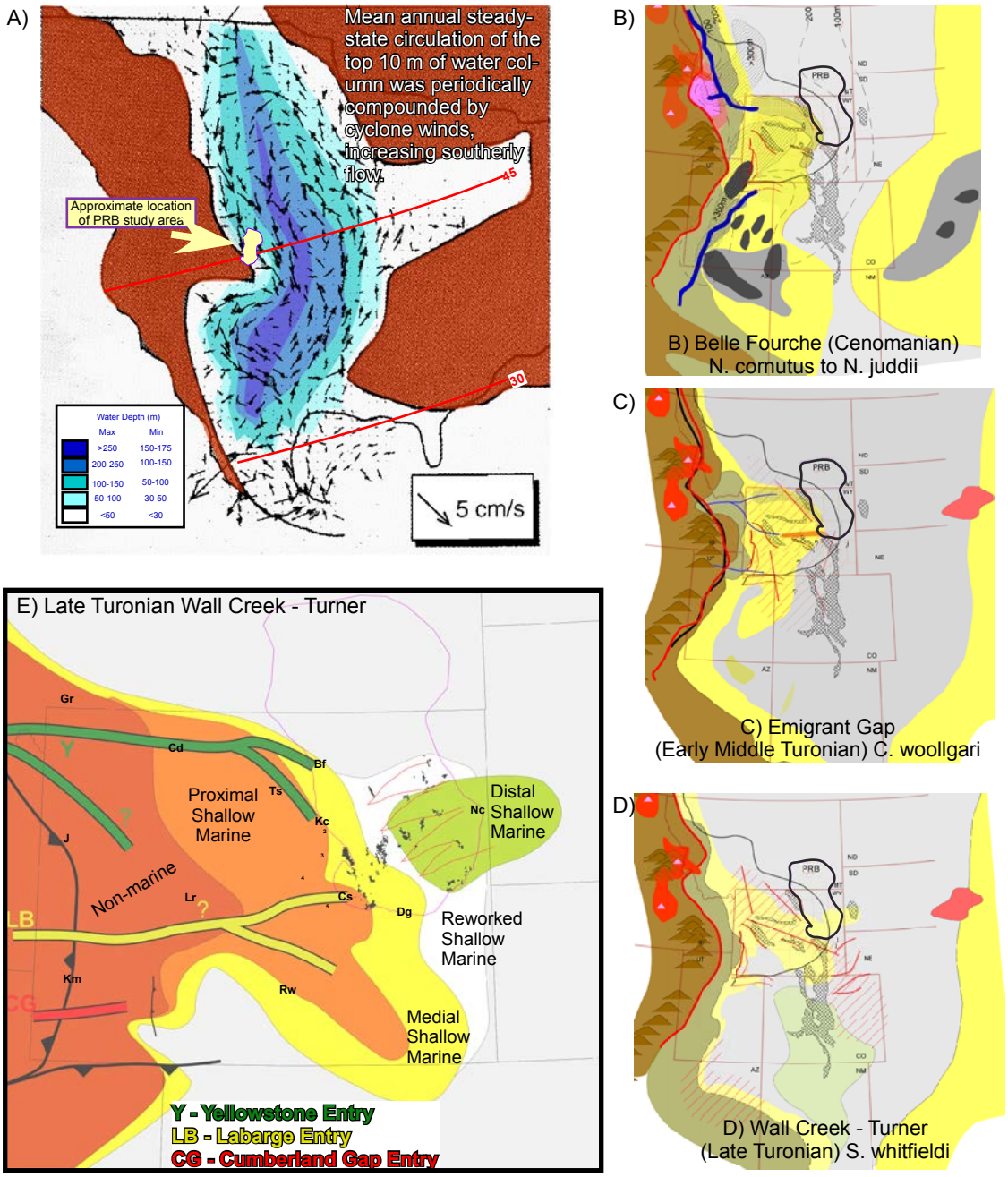

Figure 3.2. A) Paleobathymetric map during Early Turonian, (Sageman and Arthur, 1996) approximately fit to map showing paleoflow data modeled by Slingerland et al., (1996). B-D) Paleogeographic reconstruction maps highlighting lacunas (hatchered) and prominant shoreface sandstone (yellow) (after Roberts and Kirschbaum, 1995). E) Late Turonian composite depositional environments (after Myers 1977, Merewether et al., 1979, McGookey et al., 1972, Roberts and Kirschbaum, 1995, Hamlin 1996).

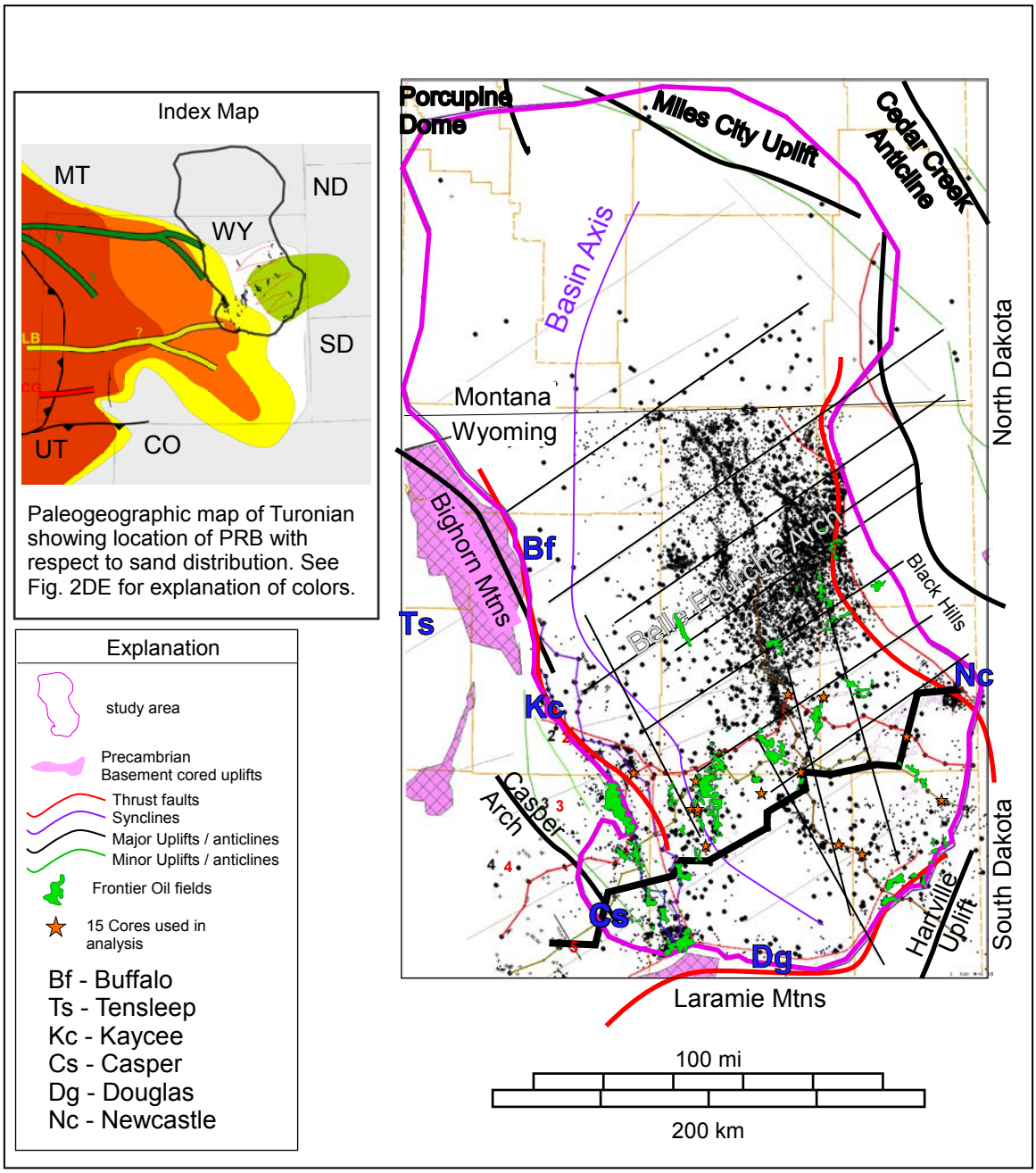

Figure 3.3. Map of Powder River Basin (PRB) study area. Dominant lineaments (black) and subordinate (gray) document basement block movement throughout the Phanerozoic (Slack, 1981; Marrs and Raines, 1984). Summary map shows structural setting, data coverage. Over 30,000 wells (small dots) were used, from the more than 100,000, in geologic analysis. 12250 wells with raster images were used for initial correlation, while 1000 wells with high quality log ascii images (large dots) were used for final and high resolution stratigraphic framework and log calculations. Cross sections in Appendix C are highlighted in thin colored lines. Orange indicates county boundaries.

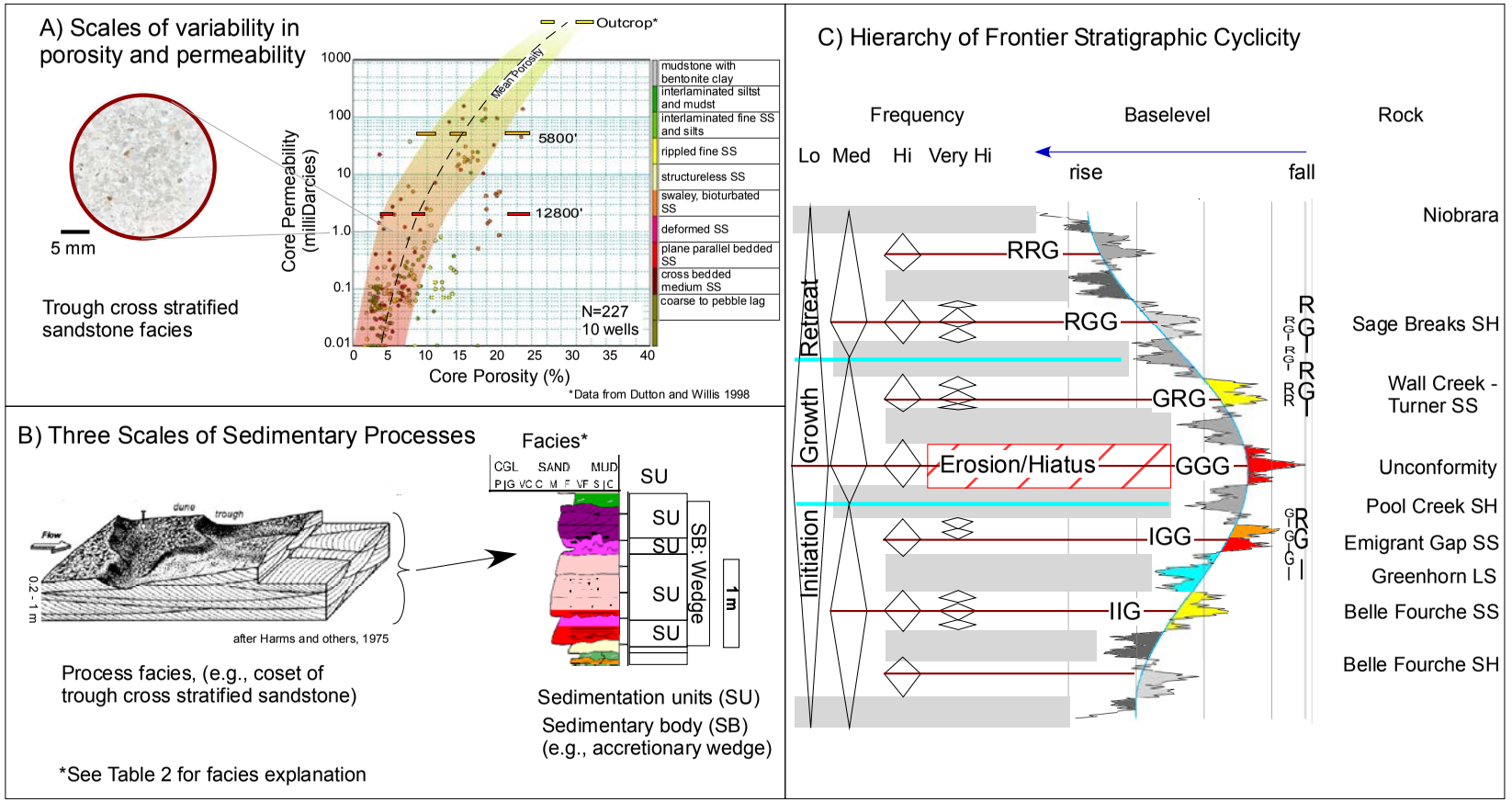

Figure 3.4. Multi-scale geologic heterogeneity varies at each order, from pore to basin scale. A) Porosity logs calibrated to core permeability incorporates up to four orders of magnitude variation in values in the well log data. B) Multiscale geologic heterogeneity correlates to sedimentary processes that record sedimentation spanning multiple scales. C) At least 3 orders of stratigraphic cyclicity are required in order to document modulation of these attributes in hierarchical stratigraphic framework (I-initiation, G-growth, R-retreat, after Gardner et al., 2008). Yellow indicates clastic wedges, orange - incised valley fills, red - erosion/hiatus, light gray - mudstone deposition, dark gray - highstand mudstone.

A) Grouping: sedimentary process facies, sedimentation units (SU), and sediment bodies (SB)

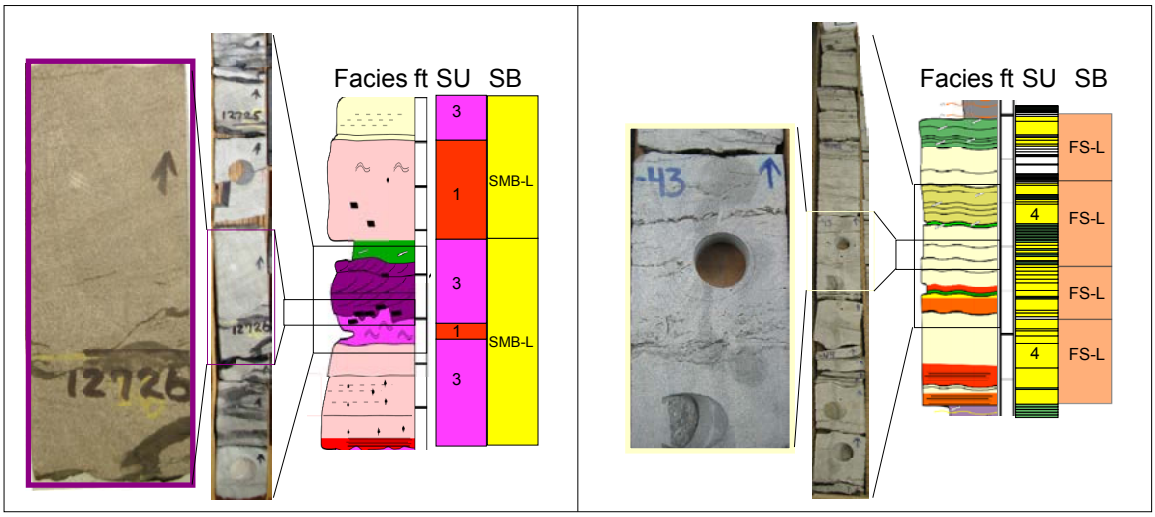

B) Hierarchical attributes provide criteria for defining sedimentation units

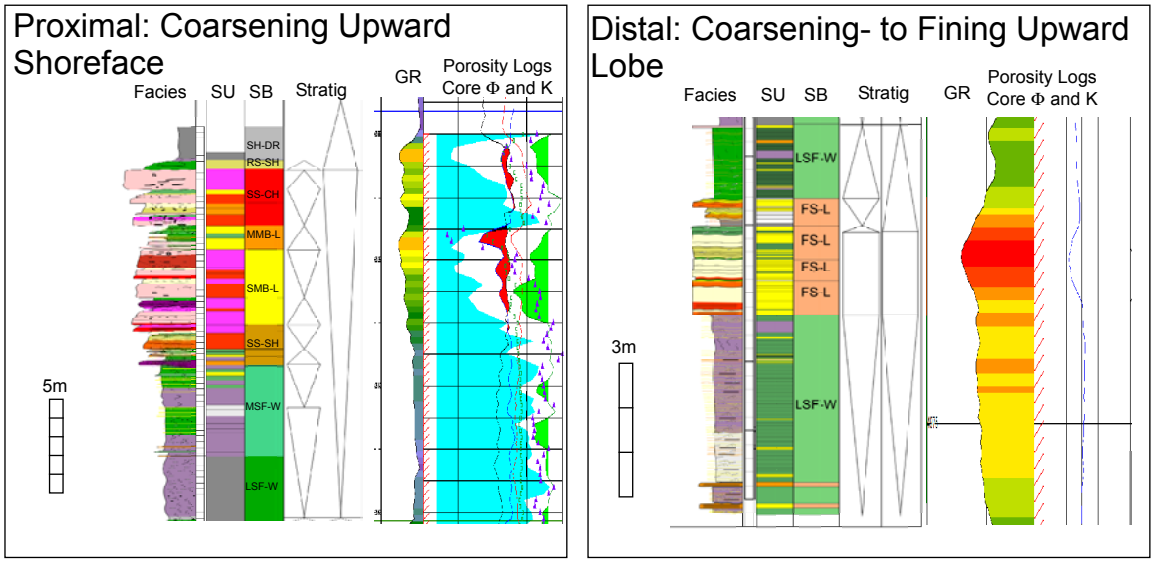

Sedimentation units, ordered by decreasing energy

1 collapsed flow with waning depletive cap
2 steady to waning accumulative to depletive flow deposits
3 steady uniform to depletive flow
4 steady to waning depletive flow deposits with suspension caps
5 repeated burrowed dilute waning depletive flow deposits
6 undifferentiated bioturbated steady to waning accumulitive/depletive
7 undifferentiated bioturbated suspension and waning depletive flow deposits
8 dilute waning depletive flow deposits
9 undifferentiated suspension deposits

Figure 3.5. Steps taken for upscaling core facies (A) into sedimentation units and then sedimentary bodies (B) 3D Sedimentary bodies defined by facies and sedimentation units form characteristic log shapes represent sedimentation regions (see Fig. 3.7). See Table 3.2 for facies explanation, and Plate 1 for bodies explanations. 1 foot (ft) = 0.305 meters.

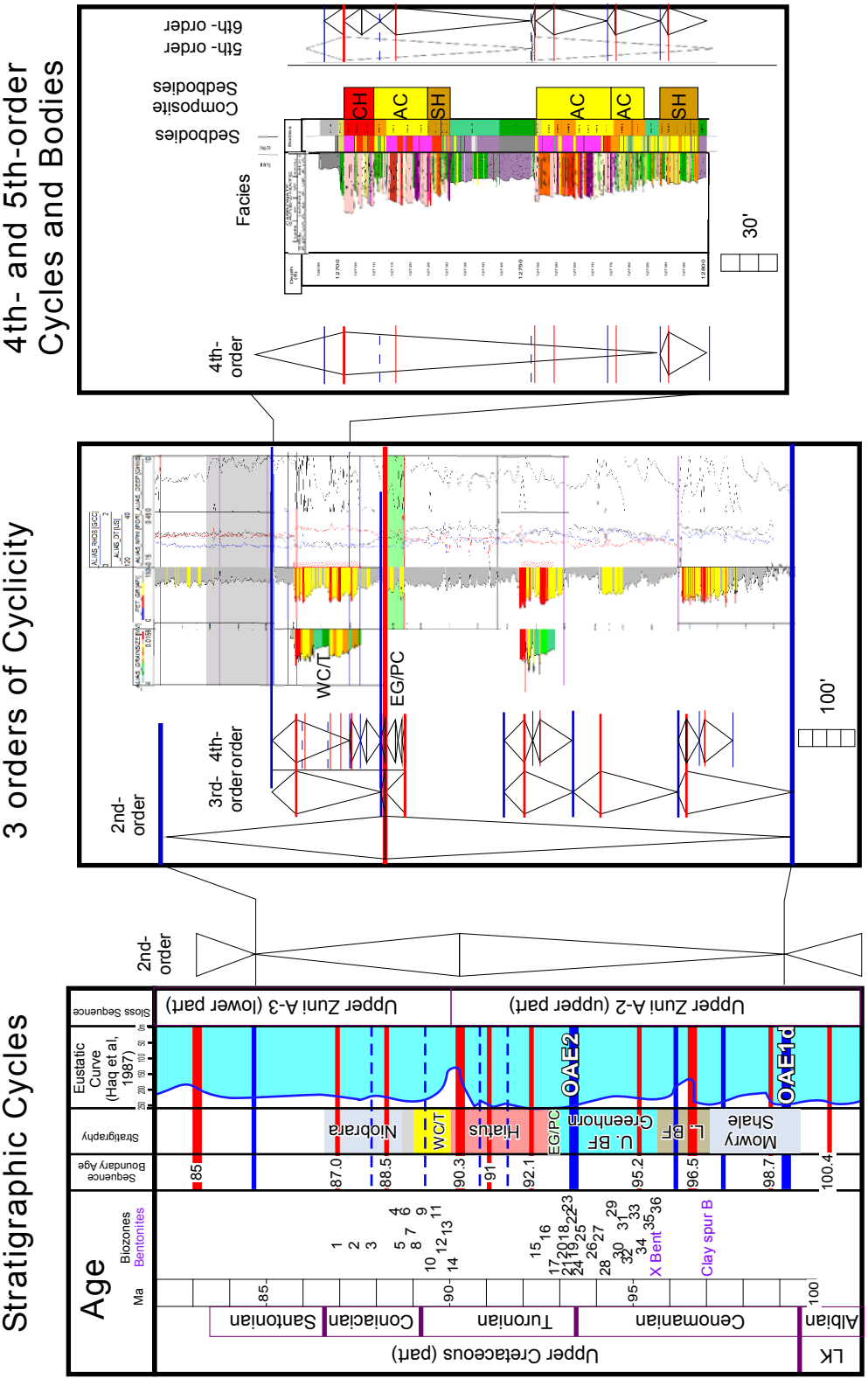

Figure 3.6. A three-fold stratigraphic hierarchy is the minimum requirement for modeling large subsurface volumes. Time scale from Gradstein, 2004 and biozone data from Merewether et al., 2007; refer to Figure 3.1 for biozone numbers. OAE = global anoxic event (OAE1D - Erbacher, Thurow and Littke, 1996; OAE2 - Sageman, 2004). WC/T = Wall Creek-Turner member, EG/PC = Emigrant Gap / Pool Creek, BF = Belle Fourche. See Appendix B for sedimentary bodies explanation.

Region	log shape	bodies	lithology (%SS)	facies
1. Submarine Channel	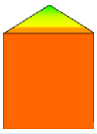	Multi-story channels	60-100%	5+m amalgamated planar to cross stratified fine to medium sandstone
		Single-story channels	30-60%	<5 m interval of .5-1 m beds of fine to medium cross stratified sandstone with pebble lag at base
2. Shoreface		Middle-upper shoreface	75-100%	5-10m CU succession, bioturbated to cross bedded fine to medium SS
	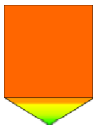	Amalgamated Shoreface	90-100%	5-10m CU to predominantly constant GS succession, bioturbated to cross bedded fine to medium SS, 0.5 to 1.5 m beds
3. Proximal Shelf		Amalg. bioturbated Shoreface	30-100%	3-15 m of bioturbated fine sandstone, no clear bedding and vague grain size variation, typically mottled and oil stained
4. Distal Shelf	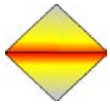	Bioturbated thin bedded lobes	50-80%	2-5 m thick successions of CU to FU packages of thin bedded ripple-laminated fine to very fine cm bedded sandstone, bedding plane burrows common
	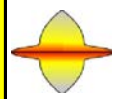	Bioturbated/ reworked thin bedded lobes	20-60%	2-5 m thick successions of CU to FU packages of moderately to intensely bioturbated ripple-laminated fine to very fine cm bedded sandstone,
5. Off-shore		Sheets	<20%	Mudstone and claystone

Figure 3.7. Sedimentation regions as map domains are defined by thickness, sandstone percent, facies, bodies, and well log shape. CU - coarsening upward, FU - fining upwards. Log shape cartoon represents gamma ray/resistivity profile and colors in indicate expected facies in that part of the cycle (Table 3.2). 1 meter = 3.3 feet; 1 centimeter = 0.4 inches.

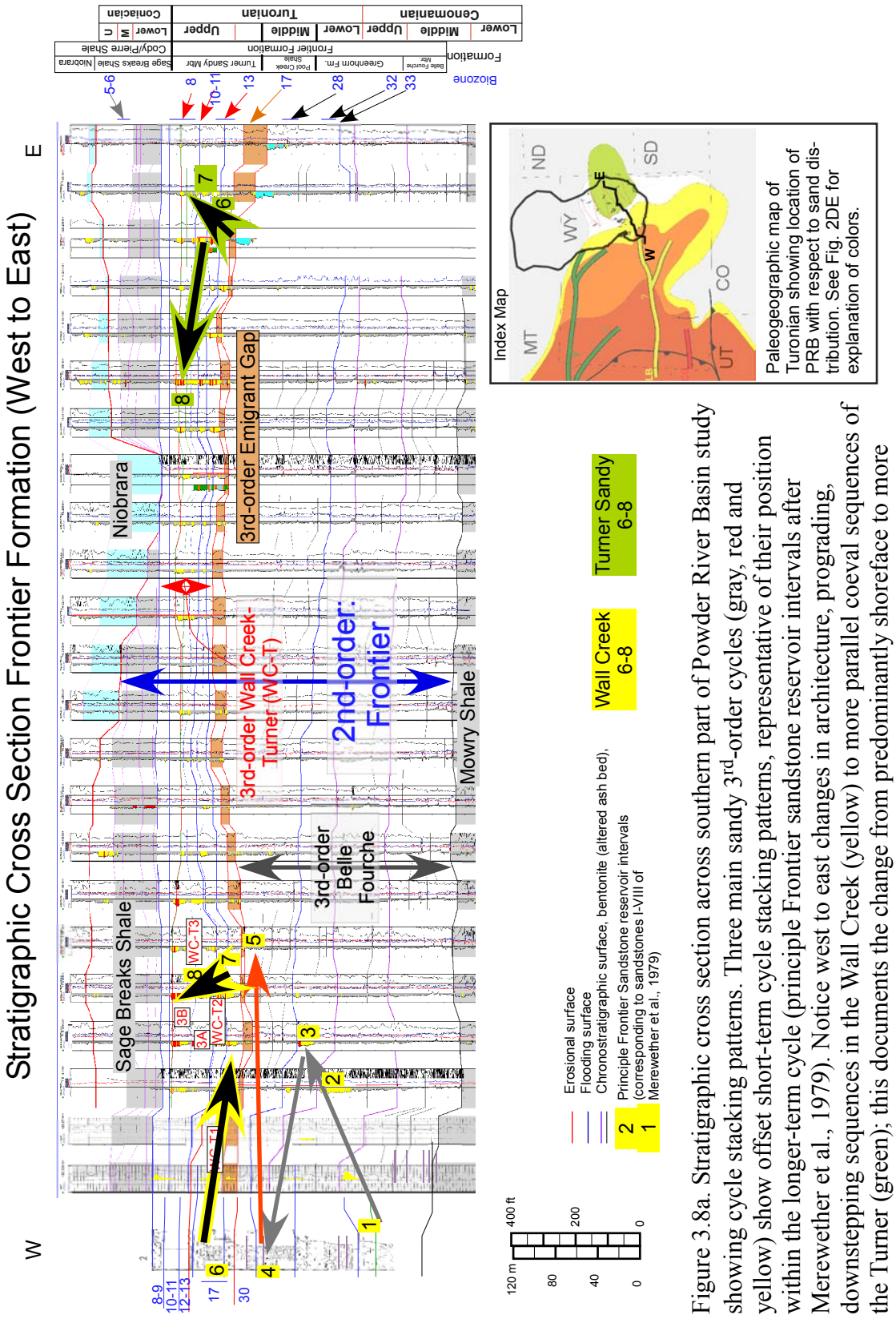

Figure 3.8a. Stratigraphic cross section across southern part of Powder River Basin study showing cycle stacking patterns. Three main sandy 3rd-order cycles (gray, red and yellow) show offset short-term cycle stacking patterns, representative of their position within the longer-term cycle (principle Frontier sandstone reservoir intervals after Merewether et al., 1979). Notice west to east changes in architecture, prograding, downstepping sequences in the Wall Creek (yellow) to more parallel coeval sequences of the Turner (green); this documents the change from predominantly shoreface to more sheetlike architecture of turbidites, respectively. Biozones from Merewether et. al., 2007.

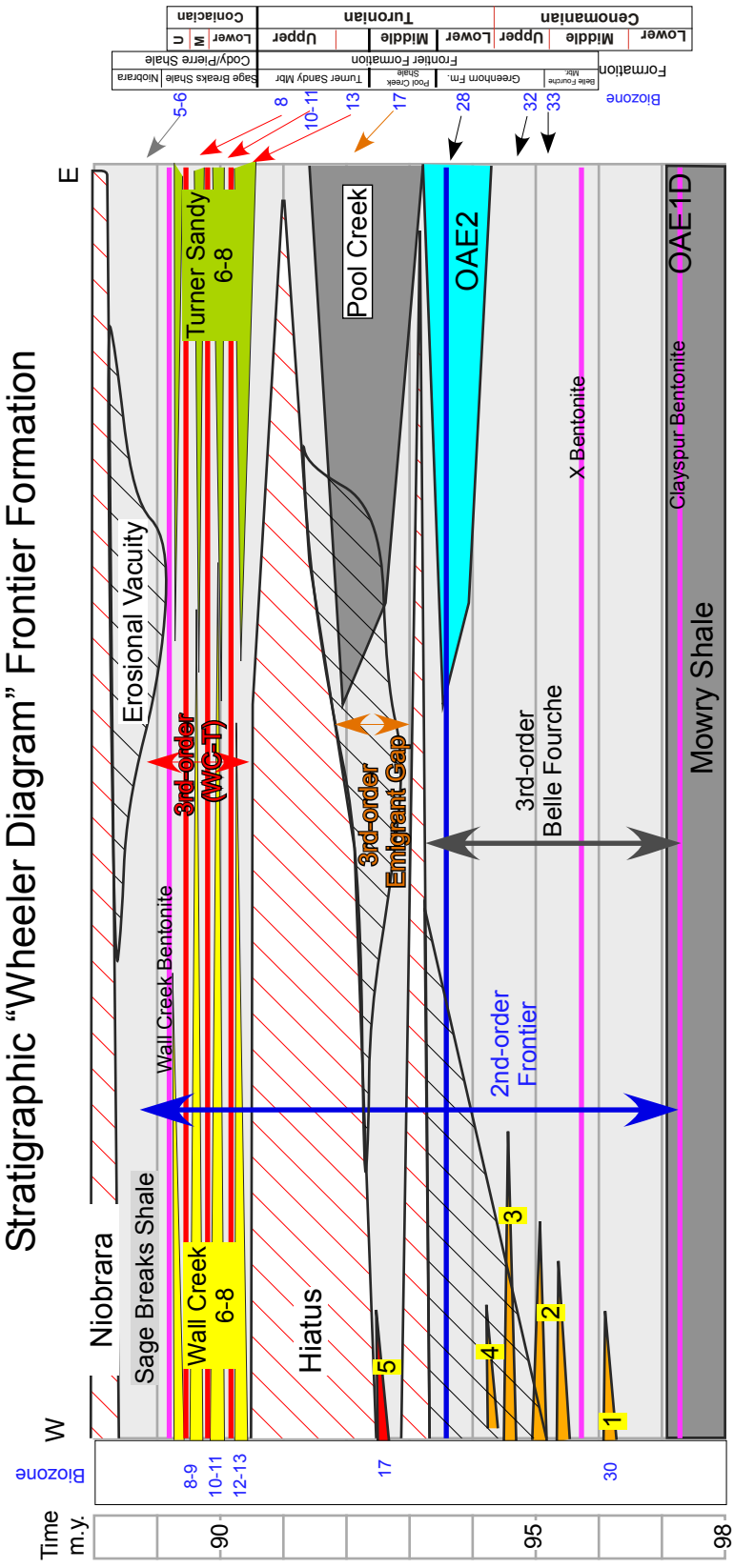

Figure 3.8B. Time (m.y. - million years) stratigraphic section (Wheeler diagram, after Wheeler, 1964) across southern part of Powder River Basin study aligned with depth stratigraphic section of Figure 8a. Major hiatuses (red hatchered), minor transgressive surfaces of erosion (red lines) and erosional vacuities (black hatcherd) are related to low subsidence, interpreted as main control on Wall Creek-Turner sandstone architecture. Orange shoreface sandstones of Belle Fourche, red valley-fill sandstones of Emigrant Gap and coeval yellow shoreface sandstones of Wall Creek and green turbiditic sandstones of the Turner. See explanation as Figure 8a; biozones are from Merewether et. al., 2007.

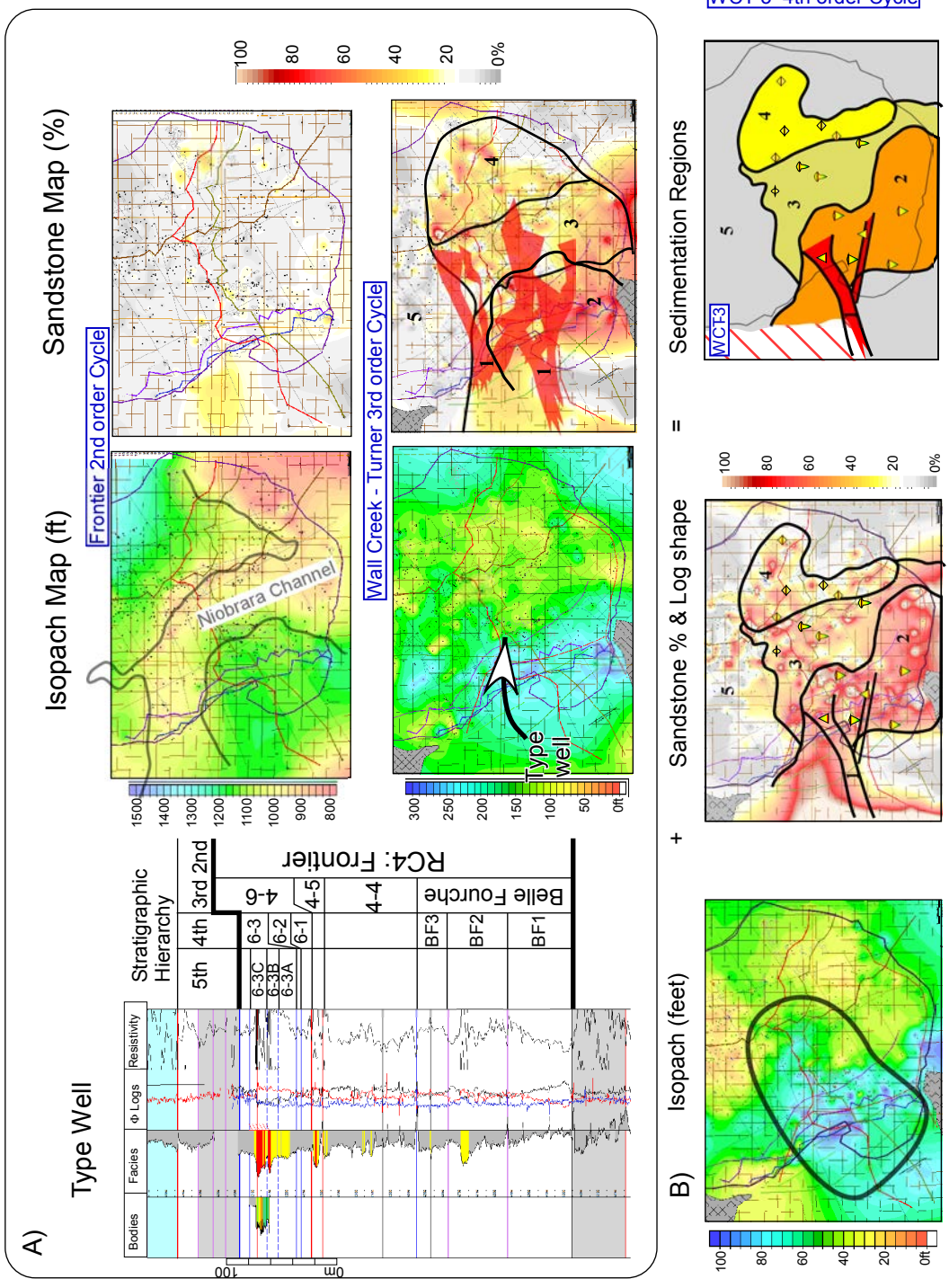

Figure 3.9. Sedimentation regions are best defined at the highest resolution possible, typically at the 4th or 5th-order. Thickness maps and facies and lithology maps are evaluated in conjunction with log shape to determine predominant architectural style in a mapping domain. This provides boundaries for constraining rock property distribution with sedimentation regions (see Fig. 3.7 for explanation).

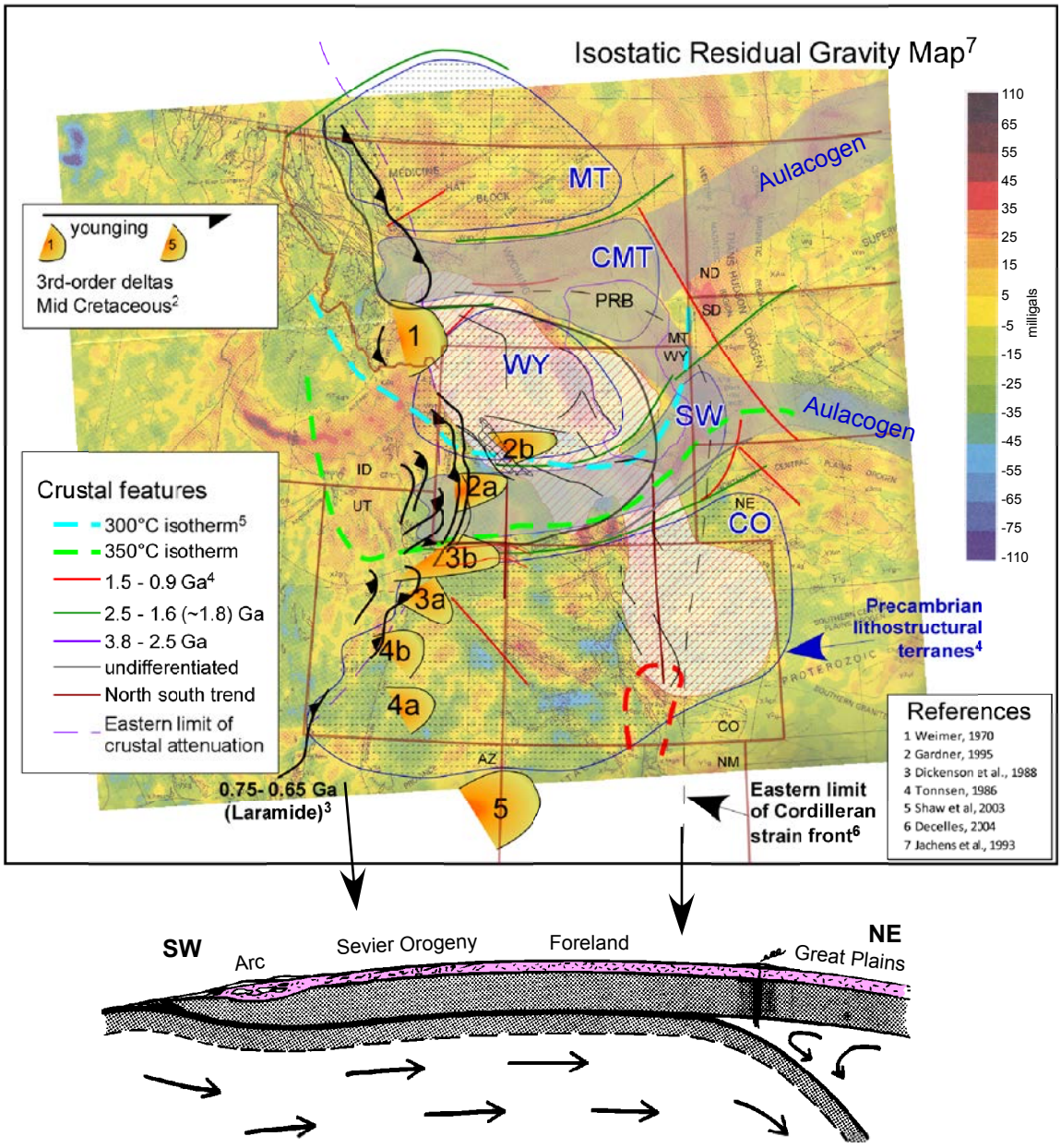

Figure 3.10. Regional tectonic setting showing multiple orders of structural control on sediment supply and accommodation patterns. Aulacogens are highlighted (gray) on residual gravity map and provide 1st order control on crustal heterogeneity. The Wyoming Craton is therefore sitting on positive tectonic elements between aulacogen and control distribution of Mid-Cretaceous lacunas (red hatchered is Turonian). The cross section highlights the position of the eastern edge of the Wyoming shelf coinciding with the transition from flat slab to steep slab crustal arrangement (Bird, 1998). Continental crust is stippled, oceanic is black and the lithosphere is shaded. Tectonic terranes: CO-Colorado, SW-Southern Wyoming, WY-Wyoming, CMT-Central Montana Trough, and MT-Montana (after Tonnsen, 1996).

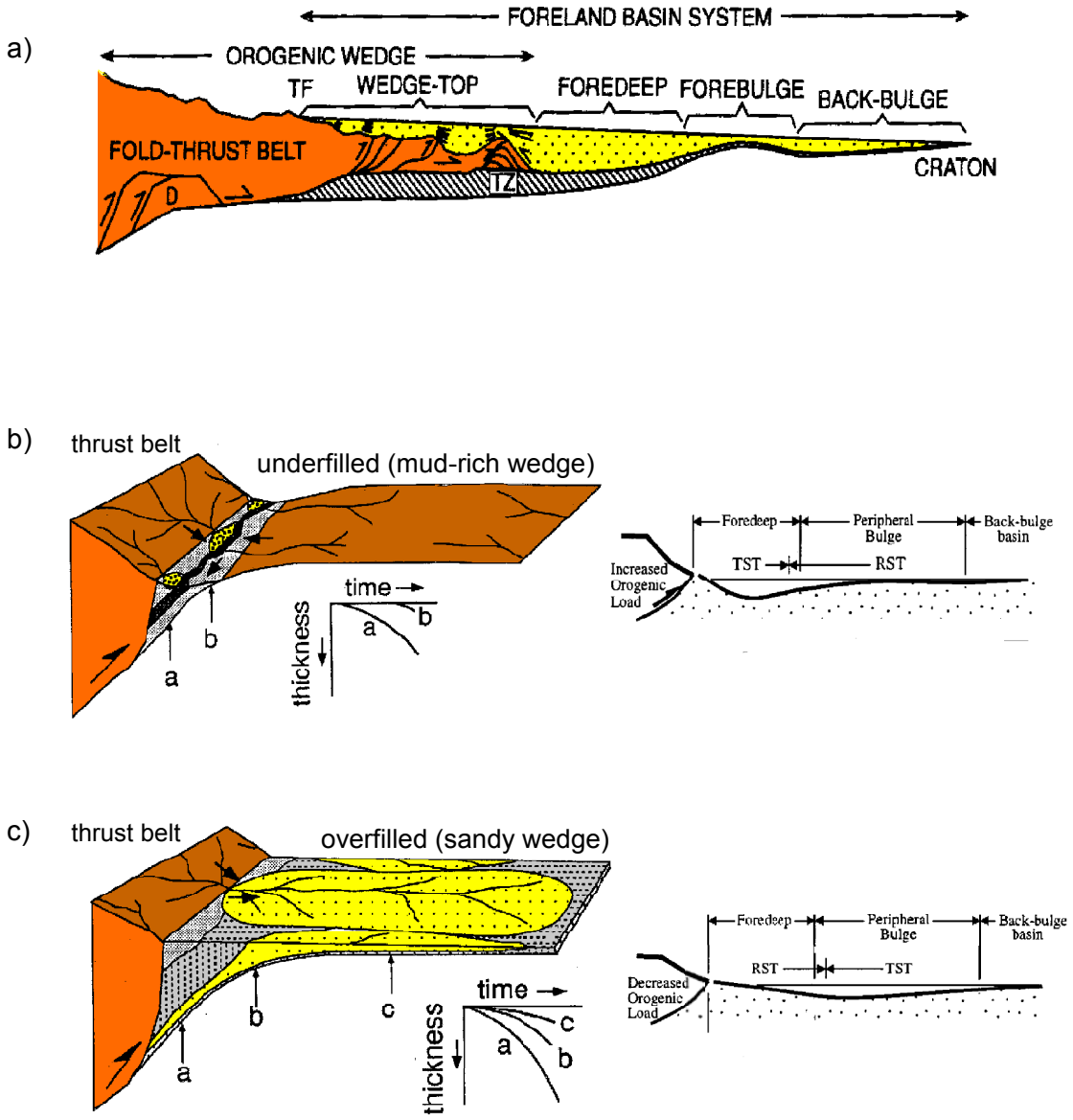

Figure 3.11. Foreland basin model (a) used in this study (after Horton and DeCelles 1995). Overfilled and underfilled foreland basins; b) underfilled condition record periods of active thrusting and increased subsidence in the foredeep, c) overfilled conditions occur from periods of tectonic quiescence, foredeep expansion and deposition of a prograding, basinward-thickening clastic wedge (modified from Flemings and Jordan, 1990; Jordan, 1981; Catuneanu et al., 1997).

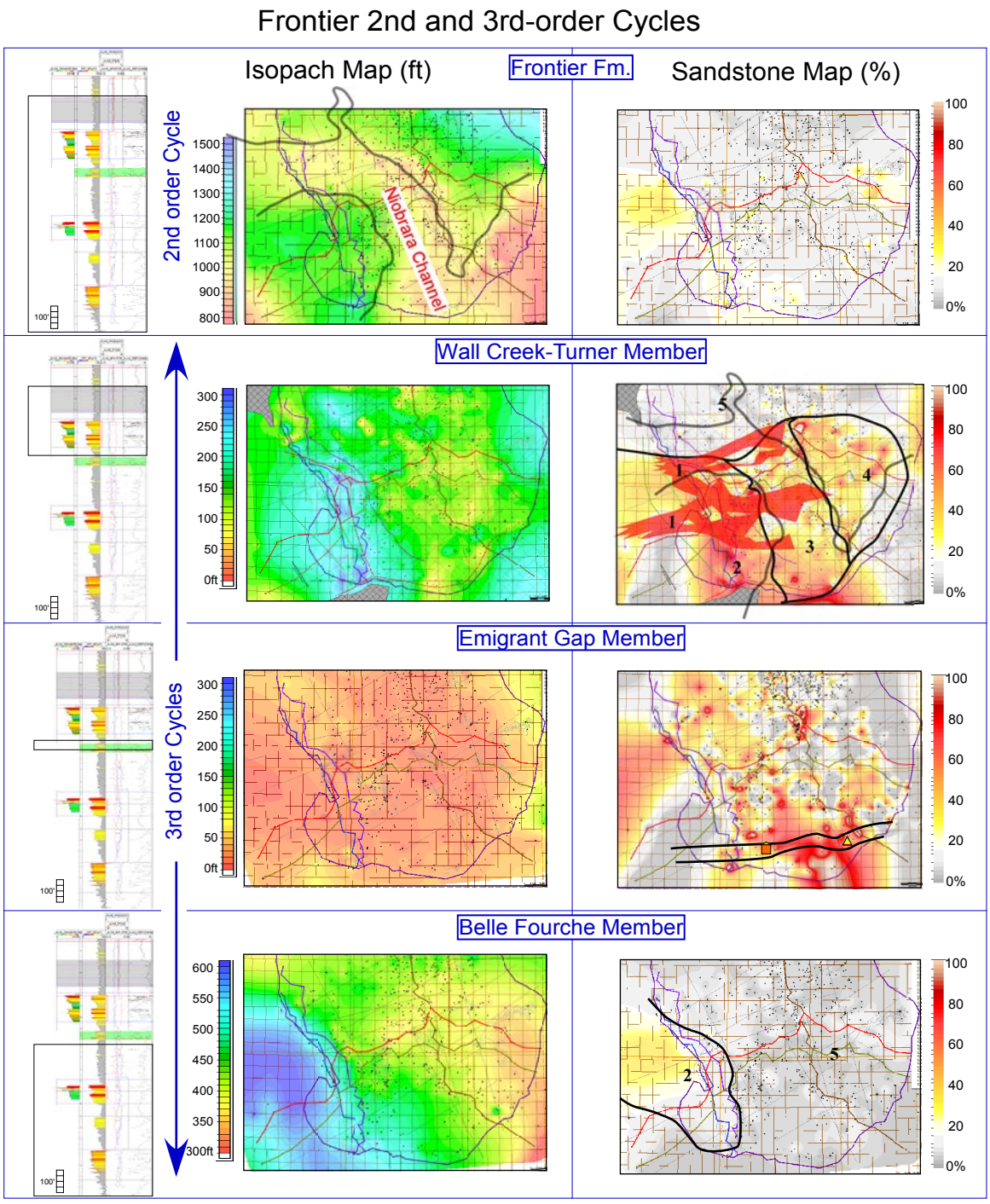

Figure 3.12. Maps showing thickness and facies distributions for 2nd-order Frontier top, and its three 3rd-order sequences below. Notice variability in thickness trends; truncation in the Frontier map by the Niobrara channel and thicks in the southwest for Belle Fourche and Wall Creek. preservation appears to be dominant control. The sandstone percent maps highlight the sandy sequences and its lateral distribution. Cross sections in Appendix C are indicated in colored lines across this southern PRB focus area.

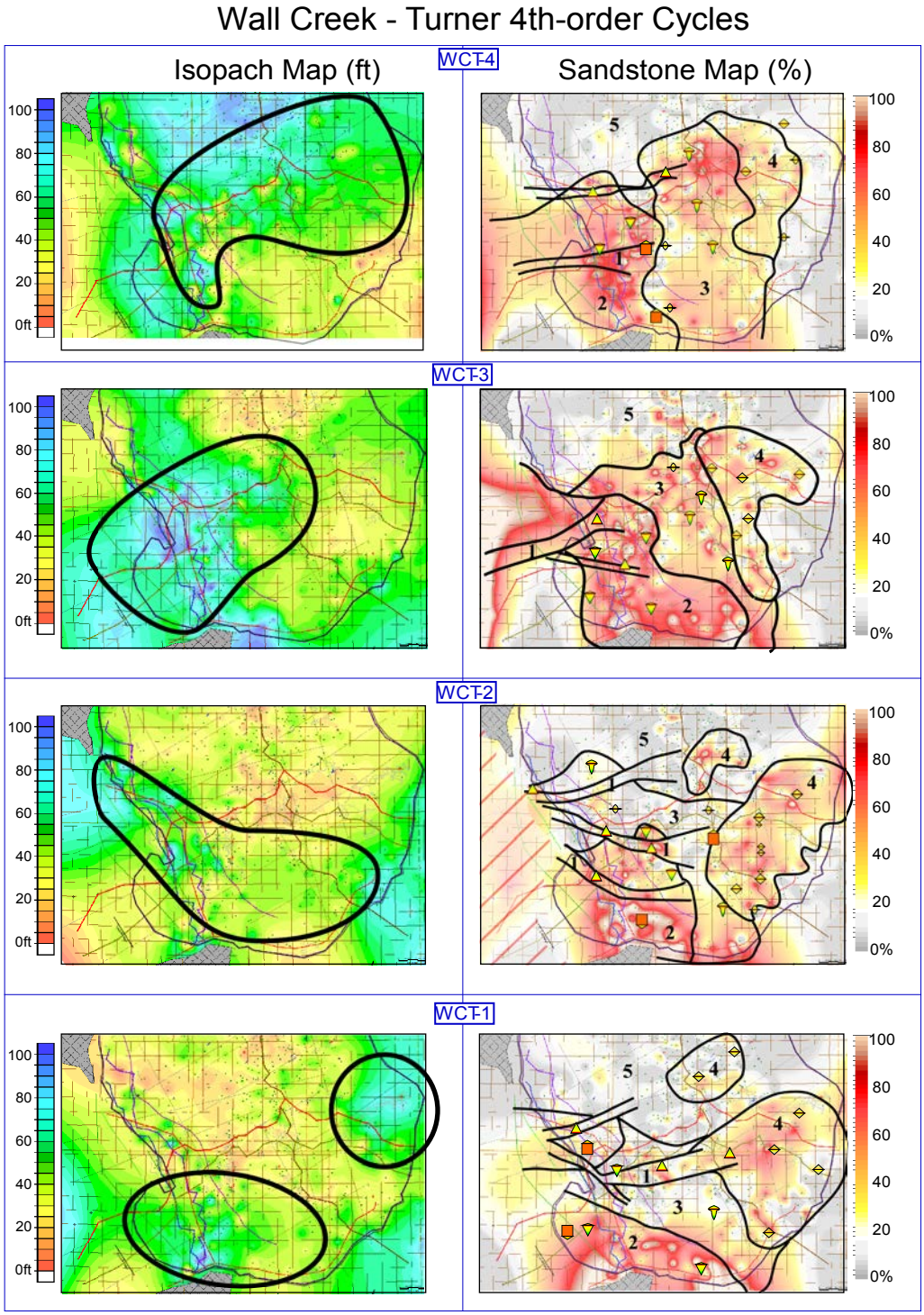

Figure 3.13. Maps showing thickness (ft - feet; 20ft = 7 meters) and sandstone facies distributions for the four Wall Creek-Turner (WCT) 4th-order cycles. Depocenters (black polygons on the isopach maps) shift at this high-resolution, as do sedimentation regions outlined in the sandstone percent maps. See Figure 3.7 for key log shapes. See Figure 3.14 for summary of sedimentation regions (1-5, E= eroded).

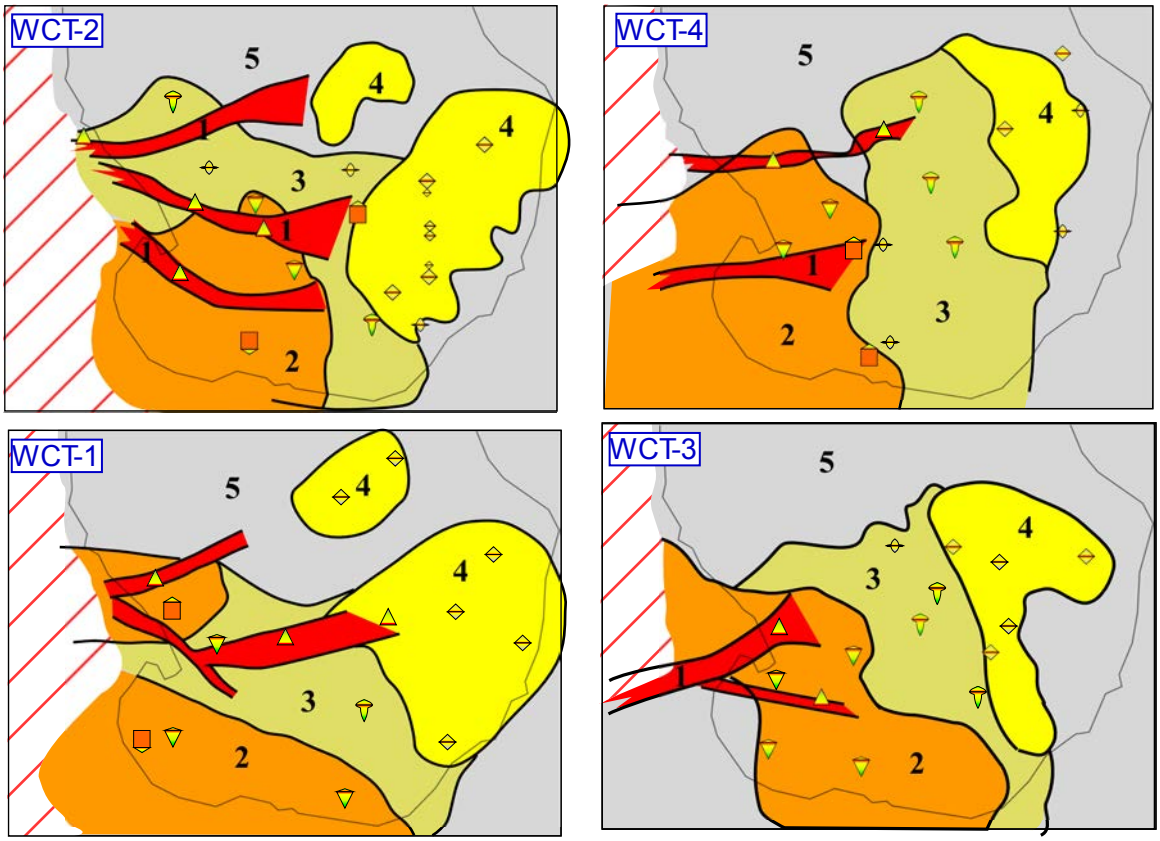

Figure 3.14. Wall Creek-Turner 4th-order cycles (WCT1-4) show distribution of channelized regions (1), shoreface (2), proximal shelf (3) distal shelf (4) and (5) muddy offshore. See Figure 3.7 for explanation of sedimentation regions. These sedimentation patterns document the interplay between submarine channel and lobe (regions 1 and 4, respectively), shoreface (region 2) and combined wave agitation / geostrophic currents (region 3).

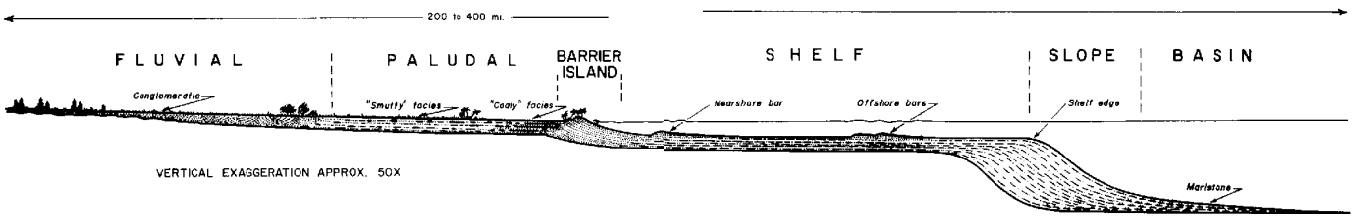

A) Wide-shelf sedimentary model, showing configuration of facies and rock types for lower and upper Cretaceous of Wyoming (Asquith, 1970).

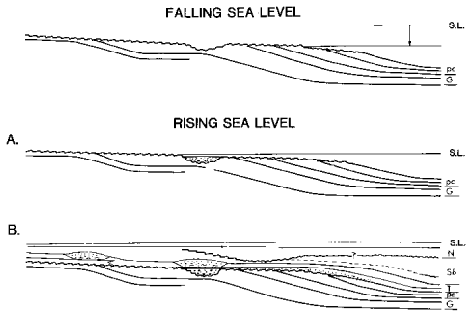

B) Cross sections explaining the origin of the distal shelf "Turner" sandstone, in incised valleys during low stands of sea level (Weimer and Flexer, 1985).

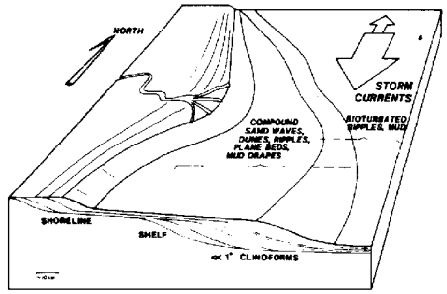

C) Schematic diagram of environments including delta-strandplain deposits, which must have been removed during transgression. This model emphasizes delta progradation and storm currents, as principle agent for redistributing sandstone bodies (Winn, 1991).

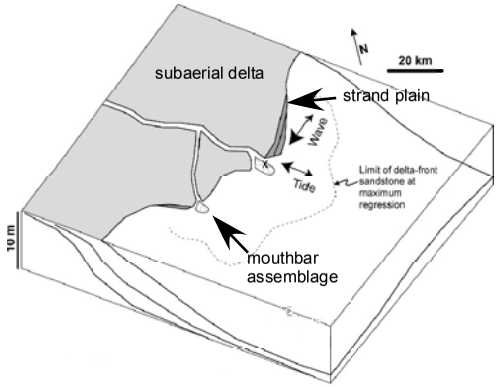

D) Delta morphology based on mapping sandstone isolith, facies and paleocurrents in outcrop marked with "x" emphasizes tide and wave processes as principle agents of sediment transport (Gani and Bhattacharya, 2007).

Figure 3.15A-D. Alternative models for the Wall Creek - Turner cycle.

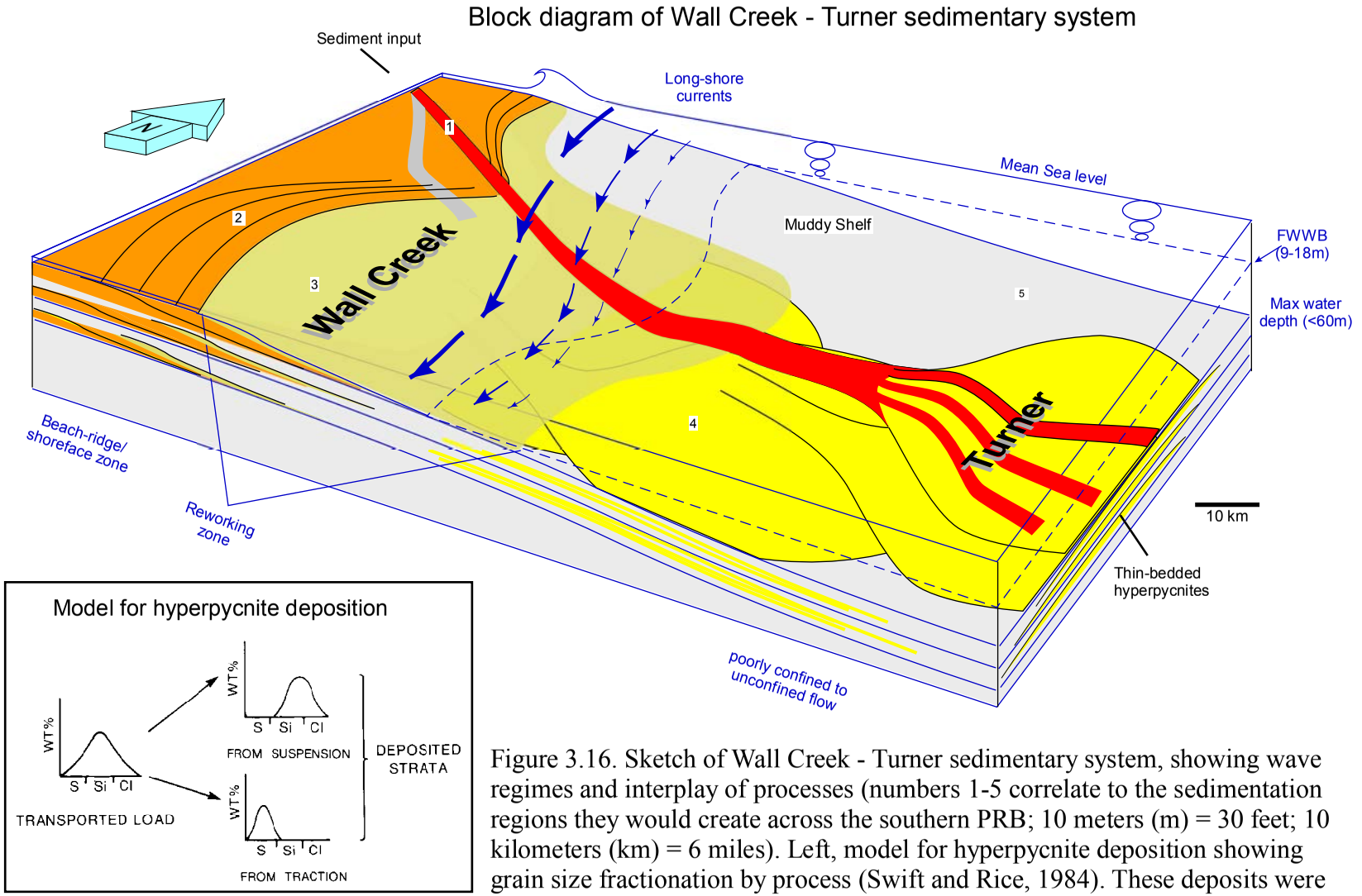

Figure 3.16. Sketch of Wall Creek - Turner sedimentary system, showing wave regimes and interplay of processes (numbers 1-5 correlate to the sedimentation regions they would create across the southern PRB; 10 meters (m) = 30 feet; 10 kilometers (km) = 6 miles). Left, model for hyperpycnite deposition showing grain size fractionation by process (Swift and Rice, 1984). These deposits were then resuspended by storm waves and remobilized by southerly geostrophic currents (Slingerland, 1996).

References Cited

Anna, L.O., 1986, Structural influence on Cretaceous sedimentation, northern Great Plains, in Peterson, J.A., ed., Paleotectonics and sedimentation in the Rocky Mountain region: Tulsa, AAPG Memoir 41: 173–192.

Asquith, D.O., 1970, Depositional topography and major marine environments, Late Cretaceous, Wyoming, AAPG Bulletin, 54/7: 1184-1224.

Asquith, D.O., 1974, Sedimentary models, cycles, and deltas, Upper Cretaceous, Wyoming: AAPG Bull., 58/11: 2274-2283.

Barrell, J., 1912, Criteria for the recognition of ancient delta deposits, Bulletin of the Geological Society of America 23: 377-446.

Barrell, J., 1917, Rhythms and the measurements of geologic time, Bulletin of the Geological Society of America 28: 745-904.

Barlow, J.A., Jr., and J.D. Haun, 1966, Regional stratigraphy of Frontier Formation and relation to Salt Creek field, Wyoming: AAPG Bull., 50/10: 2185–2196.

Bekker, A. and Eriksson K.A., 2003, A Paleoproterozoic drowned carbonate platform on the southeastern margin of the Wyoming Craton: a record of the Kenorland breakup, Precambrian Research, 120/3-4: 327-364. Berg, R.R., 1962, Mountain flank thrusting in Rocky Mountain foreland, Wyoming and Colorado, AAPG Bull., 46/11: 2019-2032.

Berg, R.R., 1962, Mountain flank thrusting in Rocky Mountain foreland, Wyoming and Colorado, *AAPG Bull*., 46/11: 2019-2032.

Bhattacharya, J.P., and B.J. Willis, 2001, Lowstand deltas in the Frontier Formation, Powder River Basin, Wyoming—Implications for sequence stratigraphic models: AAPG Bull, 85: 261–294.

Bird, P., 1995, Lithosphere dynamics and continental deformation, Reviews of Geophysics, Supplement, Pages 379-383, July 1995 U.S. National Report To International Union Of Geodesy And Geophysics 1991-1994.

Bird, P., 1998, Kinematic history of the Laramide orogeny in latitudes 35°–49°N, western United States, Tectonics, 17/5: 780-801.

Blackstone, D. L., Jr., 1983, Laramide compressional tectonics, southeastern Wyoming: Contributions to Geology, University of Wyoming, Rocky Mountain Geology 22: 1–38.

Catuneanu, O., Beaumont, C., and Waschbusch, P., 1997, Interplay of static loads and subduction dynamics in foreland basins: Reciprocal stratigraphies and the "missing" peripheral bulge, Geology, 25: 1087-1090.

Cavanaugh, E.T., 1976, Stratigraphy of the Frontier Formation, Emigrant Gap Anticline, Natrona County, Wyoming, unpublished MS thesis, Colorado School of Mines, 173 p.

Chamberlain, K.R. 1998. Medicine Bow orogeny: Timing of deformation and model of crustal structure produced during continent-arc collision, ca. 1.78 Ga, southeastern Wyoming. Rocky Mountain Geology, 33: 259-277.

Cobban, W.A., and J.B. Reeside Jr., 1952, Correlation of the Cretaceous formations of the Western Interior of the United States: Geological Society of America Bulletin, 63: 1011–1044.

Cobban, W.A., 1958, Late Cretaceous fossil zones of the Powder River Basin, Wyoming and Montana, In Wyoming Geological Association Guidebook, 13th Annual Field Conference, Powder River Basin: 114-119.

Cobban, W.A., 1990, Ammonites and some characteristic bivalves from the Upper Cretaceous Frontier Formation, Natrona County, Wyoming, in, Evolution of Sedimentary Basins; Powder River Basin: U.S. Geological Survey Bulletin, 1917-B, p. B1-B13.

Cobban, W.A., Obradovich, J.D., Walaszcyk, I., and McKinney, K.C., 2006, A USGS Zonal Table for the Upper Cretaceous Middle Cenomanian−Maastrichtian of the Western Interior of the United States Based on Ammonites, Inoceramids, and Radiometric Ages, USGS Open-File Report 2006-1250, 47 p.

Coleman, J.M., and L.D. Wright, 1975, Modern river deltas—Variability of processes and sand bodies, in Broussard, M.L., ed., Deltas, models for exploration: Houston Geological Society, p. 99–149.

Cox, D.M., Frost, C.D. and Chamberlin, K.R., 2000, 2.01-Ga Kennedy dike swarm, southeastern Wyoming Record of a rifted margin along the southern Wyoming province, Rocky Mountain Geology, 35/1: 7-30.

Cross, T.A., 1986, Tectonic controls of foreland basin subsidence and Laramide style deformation, western United States. In: Foreland Basins (Ed. by P. A. Allen & P. Homewood), Special Publication - International Association of Sedimentologists 8, 15–40.

Cross, T.A., 1988, Controls on coal distribution in transgressive-regressive cycles, Upper Cretaceous, Western Interior, U.S.A. in: C.K. Wilgus, B.S. Hasting, C.G. Kendall, H.W. Posamentier, C.A. Ross and J.C. Van Wagoner eds., Sea-level Changes: An Integrated Approach. Society of Economic Paleontologists and Mineralogists Special Publication 42, Tulsa, OK: 371-380.

Cross, T.A., Lessenger, M.A., 1998, Sediment volume partitioning: rationale for stratigraphic model evaluation and high-resolution stratigraphic correlation, *in*: Gradstein, F.M., Sandvik, K.O., Milton, N.J. (Eds.), Sequence Stratigraphy — Concepts and Applications, Special Publication 8, Norwegian Petroleum Society (NPF): 171–195.

Curry, W.H., III, 1986, Clinoform slope geometry of a Wall Creek sandstone, Salt Creek oil field, Wyoming, IN: Noll, J.H., ed., Rocky Mountain Oil and Gas Fields: Wyoming Geological Association Symposium: 189-197.

Dahl, P.S., Hamilton, M.A., Wooden, J.L., Foland, K.A., Frei, R., McCombs, J.A., and Holm, D.K., 2006, 2480 Ma mafic magmatism in the northern Black Hills, South Dakota: a new link connecting the Wyoming and Superior cratons, Canadian Journal of Earth Sciences, 43/10: 1579-1600.

DeChadenedes, J.F., 1975, Frontier Deltas fo the Western Green River Basin, Wyoming, Rocky Mountain Association of Geologists, 1975 Symposium: 149-157.

DeCelles, P.G., 2004, Late Jurassic to Eocene evolution of the Cordilleran Thrust Belt and Foreland Basin System, Western U.S.A., American Journal of Science, 304: 105–168

DeCelles, P.G. and Giles, K.A., 1996, Foreland basin systems, Basin Research 8: 105-123.

Dickinson, W.R., 1976, Sedimentary basins developed during evolution of Mesozoic-Cenozoic arc-trench system in western North America: Canadian Journal of Earth Sciences, 13: 1268-1287.

Dickinson, W. R., M. A. Klute, M. J. Hayes, S. U. Janecke, E. R. Lundin, M. A. McKittrick, and M. D. Olivares, 1988, Paleogeographic and paleotectonic setting of Laramide sedimentary basins in the central Rocky Mountain region, Geological Society of America Bulletin 100/7: 1023-1039.

Dutton, S. P., and Willis, B. J., 1998, Comparison of outcrop and subsurface sandstone permeability distribution, Lower Cretaceous Fall River Formation, South Dakota and Wyoming: *Journal of Sedimentary Petrology, v. 68, no. 5, p. 890–900.*

Dyman, T. S.; Tysdal, R. G.; Perry, Jr. , W. J.; Nichols, D. J.; Obradovich, J. D., 2008, Stratigraphy and structural setting of Upper Cretaceous Frontier Formation, western Centennial Mountains, southwestern Montana and southeastern Idaho, Cretaceous Research, 29: 237 – 248.

Eicher, D.L., and R. Diner, 1985, Foraminifera as indicators of water mass in the Cretaceous Greenhorn sea, Western Interior, in Pratt, L.M., E.G. Kauffman, and F.B. Zelt, eds., Fine-grained deposits and biofacies of the Cretaceous Western Interior Seaway—Evidence of cyclic sedimentary processes: Society of Economic Paleontologists and Mineralogists Midyear Meeting, Golden, Colorado, Field Trip Guidebook 4: 60–71.

Erbacher, J., Thurrow, J. and Littke, R., 1996, Evolution patterns of radiolaria and organic matter variations: a new approach to identify sea-level changes in mid-Cretaceous pelagic environments, Geology, 24: 499–502.

Fisk, H.N. and McFarlan, Jr., E, 1955, Late Quaternary deltaic deposits of the Mississippi river, GSA Special Paper 62: 279-302.

Fitzsimmons, R. and S. Johnson, 2000, Forced regressions; recognition, architecture and genesis in the Campanian of the Bighorn Basin, Wyoming, IN: Hunt, D. and R.L. Gawthorpe (eds) Sedimentary Responses to Forced Regressions. Geological Society Special Publications 172: 113-139.

Flemings. P.B., and Jordan, T.E., 1990, Stratigraphic modeling of foreland basins: interpreting thrust deformation and lithosphere rheology. Geology 18: 430-434.

Galloway, W.E., 1975, Process framework for describing the morphologic and stratigraphic evolution of deltaic depositional systems, in Broussard, M.L., ed., Deltas, models for exploration: Houston Geological Society, p. 87-98.

Gani, M.R., and J.P. Bhattacharya, 2007, Basic Building Blocks and Process Variability of a Cretaceous Delta: Internal Facies Architecture Reveals a More Dynamic Interaction of River, Wave and Tidal Processes Than Is Indicated By External Shape, Journal of Sedimentary Research, 77/4: 284-302.

Gardner, M.H., 1995, Tectonic and Eustatic Controls on the Stratal Architecture of Mid-Cretaceous Stratigraphic Sequences, Central Western Interior Foreland Basin of North America, in S. Dorobek, and J. Ross (eds.), Stratigraphic Evolution of Foreland Basins, Society of Sedimentary Geology (SEPM) Special Publication 52, p. 283-303.

Gardner, M.H., Borer, J.M., Romans, B.W., Baptista, N., Kling, E.K., Hanggoro, D., Melick, J.J., Wagerle, R.N., Dechesne, M., Carr, M.M., Amerman, R., and Atan, S., 2008, Stratigraphic models for deepwater sedimentary systems. GCSSEPM Special Publication, Answering the Challenges of Production from Deepwater Reservoirs: Analogues and Case Histories to Aid a New Generation, p. 77-175.

Gardner, M. H., T. A. Cross, and M. Leverson, 2004, Stacking Patterns, Sediment Volume Partitioning and Facies Differentiation in Shallow-Marine and Coastal-Plain Strata: in Chidsey, T.C., R.D. Adams, and T.H. Morris, eds., Regional to Wellbore Analog for Fluvial-Deltaic Reservoir Modeling: The Ferron Sandstone of Utah, American Association of Petroleum Geologists, Studies in Geology, No. 50, p. 95-125.

Gilbert, G.K., 1885, The topographic features of lake shores: U.S. Geological Survey, 5th Annual Report, p. 104-108.

Grabau, A.W., 1960, Principles of stratigraphy, Dover Publications, New York.

Gradstein, F., J. Ogg and A. Smith, eds., 2004, A Geologic Time Scale, Cambridge, London.

Hamlin, H.S., 1996, Frontier Formation stratigraphy on the Moxa Arch, Green River Basin, Wyoming, Then Mountain Geologist 33/2: 35-44.

Harms, J.C., Southard, J.B., Spearing, D.R., and Walker, R.G., 1975, Depositional environments as interpreted from primary sedimentary structures and stratification sequences, SEPM Short Course, no.2, 161pp.

Haq, B.U., J. Hardenbol, and P. R. Vail, 1987, The new chronostratigraphic basis of Cenozoic and Mesozoic sea level cycles, in: Timing and depositional history of eustatic sequences; constraints on seismic stratigraphy Special Publications - Cushman Foundation for Foraminiferal Research 24: 7-13.

Harlan, S.S., Geissman, J.W., and Premo, W.R. 2003. Paleomagnetism and geochronology of an Early Proterozoic quartz diorite in the southern Wind River Range, Wyoming, USA. Tectonophysics, 362: 105-122.

Hills, F.A. and Armstrong, R.L., 1974, Geochronology of Precambrian rocks in the Laramie Range and implications for the tectonic framework of Precambrian southern Wyoming, Precambrian Research, 1/3: 213-225. Hu, G., 1992, Tectonic analysis of the southern and southeastern margins of the Powder River Basin and the adjoining uplifts: Newcastle to Casper, Wyoming, Ph.D. dissertation, South Dakota School of Mines: 187p.

Horton, B.K. and DeCelles, P.G., 1997, The Modern foreland basin system adjacent to the Central Andes, Geology 25/10: 895-898.

Hu, G., 1992, Tectonic analysis of the southern and southeastern margins of the Powder River Basin and the adjoining uplifts: Newcastle to Casper, Wyoming, Ph.D. dissertation, South Dakota School of Mines: 187p.

Jachens, R.C., Simpson, R.W., Blakey, R.J. and Saltus, R.W., 1993, Isostatic residual gravity map of the Precambrian, IN: Precambrian: Conterminous U.S., DNAG Vol C2, Boulder 1993.

Jenkins, C., 1985, A preliminary tectonic analysis of the northeastern margin of the Bighorn Uplift: Buffalo to Dayton, Wyoming, M.S. thesis, South Dakota school of Mines: 135p.

Jenkyns, H.C., 2010, Geochemistry of oceanic anoxic events, Geochemistry, Geopphysics, Geosystems, 11/3, Q03004.

Jordan, T.E., 1981, Thrust loads and foreland basin evolution, Cretaceous, Western United States. America Association of Petroleum Geologists Bulletin, 65/12: 2506-2520.

Kaufmann, E.G., 1985, Cretaceous evolution of the Western interior basin of the United States, in, L.M. Pratt, E.G. Kaufmann, and F.B. Zelt, eds., SEPM 2nd Annual Midyear Meeting, Golden, Colorado: Field Trip Guidebook, P. IV-XIII.

King, D., 1990, Tectonic analysis of the southwestern margin of the Powder River Basin: Kaycee to Casper, Wyoming, M.S. thesis, South Dakota School of Mines: 55 p.

Knechtel, M.M. and Patterson, S.H., 1962, Bentonite deposits of the northern Black Hills district, Wyoming, Montana, and South Dakota, USGS Bulletin: 1082-M, 137 p.

Krystinik, L. F., and DeJarnett, B., 1995, Lateral variability of sequence stratigraphic framework in the Campanian and early Maastrichtian of the Western Interior Seaway, *in* Van Wagoner, J. C., and Bertram, G. T., eds., Sequence stratigraphy of foreland basin deposits: outcrop and subsurface examples from the Cretaceous of North America: American Association of Petroleum Geologists Memoir No. 64, p. 11–26.

Larue, D.K., 1995, Structurally aligned, sediment-starved fluvial valleys encased in marine deposits; sequence boundaries between the Carlile Shale and Niobrara Formation, central Powder River basin, U.S.A., IN: Van Wagoner, J.C. and G.T. Bertram (eds.) Sequence stratigraphy of foreland basin deposits; outcrop and subsurface examples from the Cretaceous of North America, AAPG Memoir, 64: 371-394.

Lindquist, T.W., 1986, A provenance study of the Wall Creek Member of the Frontier Formation and the Turner Sandy Member of the Carlile Shale in the Powder River Basin, Wyoming, unpublished MS thesis, Texas Christian University, 76 p.

Lisenbee, A L. 1978, Laramide structure of the Black Hills Uplift, South Dakota-Wyoming-Montana, Memoir - Geological Society of America, 151: 165-196.

Lisenbee, A.L., 1988, Tectonic history of the Black Hills uplift, Guidebook - Wyoming Geological Association, 39: 45-52.

Lisenbee, A.L., 1993, Laramide evolution of the Black Hills Uplift, Memoir - Geological Survey of Wyoming, 5: 374-412.

Mancarci, M., 1989, Tectonic analysis of the southeastern margin of the Bighorn Uplift, Buffalo to Kaycee, M.S. thesis: South Dakota School of Mines, 89 p.

Marrs, R. W., and G. L. *Raines*, 1984, Tectonic framework of *Powder River basin*, Wyoming and Montana, interpreted from Landsat imagery: AAPG Bulletin 68: 1718-1731.

Martinsen, R. S., 2003A, Depositional remnants; Part 1, Common components of the stratigraphic record with important implications for hydrocarbon exploration and production, AAPG Bulletin. 87/12: 1869-1882.

Martinsen, R. S., 2003B, Depositional remnants; Part 2, Examples from the Western Interior Cretaceous basin of North America, AAPG Bulletin. 87/12: 1883-1909.

McGookey, D.P., J.D. Haun, L.A. Hale, H.G. Goodell, D.G. McCubbin, R.J. Weimer, and G.R. Wulf, 1972, Cretaceous system, in Mallory, W.W., ed., Geologic atlas of the Rocky Mountain Region: Denver, Rocky Mountain Association of Geologists, p. 189–228.

Merewether, E.A., 1980, Stratigraphy of mid-Cretaceous formations at drilling sites in Weston and Johnson Counties, northeastern Wyoming: U.S. Geological Survey Professional Paper 1186–A, 25 p.

Merewether, E.A., 1983, The Frontier Formation and Mid-Cretaceous orogeny in the foreland of southwestern Wyoming, The Mountain Geologist, 20/4: 121-138.

Merewether, E.A., 1996, Stratigraphy and tectonic implications of Upper Cretaceous rocks in the Powder River Basin, northeastern Wyoming and southeastern Montana: U.S. Geological Survey Bulletin 1917–T, 92 p.

Merewether, E.A., W.A. Cobban, and E.T. Cavanaugh, 1979, Frontier Formation and equivalent rocks in eastern Wyoming: The Mountain Geologist, v. 6, no. 3, p. 67–102.

Merewether, E.A., W.A. Cobban, and CW. Spencer, 1976, The Upper Cretaceous Frontier Formation in the Kaycee-Tisdale Mountain area, Johnson County, Wyoming, in Laudon, R.B., Curry, W.H. III, and Runge, J.S., eds., Geology and energy resources of the Powder River: Wyoming Geological Association 28th Annual Field Conference Guidebook, p. 33–44.

Merewether, E.A. and W.A. Cobban, 1972, Unconformities within the Frontier Formation, northwestern Carbon County, Wyoming, In Geological Survey Research 1972: U.S. Geological Survey Professional Paper 800-D: D57-D66.

Merewether, E.A. and W.A. Cobban, 1986, Biostratigraphic units and tectonism in the mid-Cretaceous foreland of Wyoming, Colorado, and adjoining areas, in Peterson, J.A., ed., Paleotectonics and Sedimentation in the Rocky Mountain region, United States, part III, middle Rocky Mountains: Tulsa, American Association of Petroleum Geologists Memoir 41: 443-468.

Merewether, E A., W. A. Cobban;, J. D. Obradovich, 2007, Regional disconformities in Turonian and Coniacian (Upper Cretaceous) strata in Colorado, Wyoming, and adjoining states; biochronological evidence, Rocky Mountain Geology, 42/ 2: 95-122.

Merewether, E.A., Blackmon, P.D. and Webb, J.C., 1984, The Mid-Cretaceous Frontier Formation near the Moxa Arch, Southwestern Wyoming, USGS Professional Paper 1290, 29 p.

Middleton, G. W., 1973, Johannes Walther's Law of the Correlation of Facies: Geological Society of America Bulletin, v. 84, p. 979-988.

Myers, R.C., 1977, Stratigraphy of the Frontier Formation (Upper Cretaceous), Kemmerer area, Lincoln County Wyoming, Twenty-Ninth Annual Field conference – 1977 Wyoming Geological Association Guidebook: 271- 311.

Myrow, P.M., and Southard, J.B., 1991, Combined-flow model for vertical stratification sequences in shallow marine storm-deposited beds: Journal of Sedimentary Petrology, 61: 202–210.

Naus, M., 2000, A tectonic investigation of the Northern Bighorn / Pryor Uplift and surrounding areas, south-central Montana, unpublished M.S. thesis, South Dakota School of Mines: 147 p.

Plint, A.G., 1988, Sharp-based shoreface sequences and "offshore bars" in the Cardium Formation of Alberta—Their relationship to relative changes in sea level, in Wilgus, C.K., B.S. Hastings, Kendall, H.W. Posamentier, C.A. Ross, and J. Van Wagoner, eds., Sea-level changes—An integrated approach: SEPM Special Publication 42: 357–370.

Plint, A.G. and M.A. Kreitner, 2007, Extensive thin sequences spanning Cretaceous foredeep suggest high-frequency eustatic control: Late Cenomanian, Western Canada foreland basin, Geology, 35/8: 735–738.

Plint, A.G., A. Tyagi, M.J. Hay, B.L. Varban, H. Zhang, X. Roca, 2009, Clinoforms, Paleobathymetry, and Mud Dispersal Across the Western Canada Cretaceous Foreland Basin: Evidence from the Cenomanian Dunvegan Formation and Contiguous Strata, Journal of Sedimentary Research 79: 144-161.

Rice, D.D., and C.W. Keighin, 1989, Configuration of shelf sandstone oil reservoirs, Upper Cretaceous (Turonian) Turner Sandy Member of Carlile Shale, Powder River basin, Wyoming: AAPG abs, 73/3: 405.

Roberts, L.N.R., and M.A. Kirschbaum, 1995, Paleogeography of the Late Cretaceous of the Western Interior of Middle North America – Coal distribution and sediment accumulation, USGS Professional Paper 1591, 63 p. & plates.

Robinson, C.S., Mapel, W.J., and Bergendahl, M.H., 1964, Stratigraphy and structure of the northern and western flanks of the Black Hills uplift, Wyoming, Montana, and South Dakota: U.S. Geological Survey Professional Paper, 404, 134 p.

Roscoe, S.M., and Card, K.D. 1993. The reappearance of the Huronian in Wyoming: rifting and drifting of ancient continents. Canadian Journal of Earth Sciences, 30: 2475-2480.

Rubey, W.W., 1930, Lithologic studies of fine-grained Upper Cretaceous sedimentary rocks of the Black Hills region, IN Shorter contributions to general geology, 1930: U.S. Geological Survey Professional Paper, 165-A, p. A1-A54.

Ryer, T.A., and J.R. Lovekin, 1986, The Upper Cretaceous Vernal Delta of Utah; depositional or paleotectonic feature? AAPG Memoir 41: 497-510.

Sadeque, J., 2006, Regional Reservoir Compartmentalization within Offlapping, Top-Truncated, Mixed-Influenced Deltas, Wall Creek Member, Frontier Formation, Powder River Basin, Wyoming, unpublished Ph.D. thesis, University of Texas at Dallas, 156p.

Sageman, B. R., and Arthur, M. A., 1994, Early Turonian paleogeographic/paleobathymetric map, Western Interior, US, in Caputo, M. V., Peterson, A., and Franczyk, K. J., eds., Mesozoic systems of the Rocky Mountain Region, USA: Rocky Mountain Section, Society for Sedimentary Geology (SEPM), p. 457–469.

Sageman, B. R., Meyers, S.R., and Arthur, M. A., 2006, Orbital time scale and new C-isotope record for Cenomanian-Turonian boundary stratotype, Geology 34/2: 125-128.

Sears, J.W., and Price, R.A., 1978, The Siberian connection: A case for the Precambrian separation of the North American and Siberian cratons, Geology, 6, 267-270.

Shaw, C.A.**,** Karlstrom, K.E., Williams, M.L., Jercinovic, M.J., McCoy, A.M., and Dueker, K., 2003. Proterozoic Shear Zones of the Colorado Rocky Mountains: From continental assembly to intracontinental reactivation. *in* Lageson, D.R., Erslev, E., and Magloughlin, J., Southern Rocky Mountains: Geological Society of America Field Guide, p. 102–117.

Slack, P.B., 1981, Paleotectonics and hydrocarbon accumulation, Powder River Basin, Wyoming: AAPG, v. 65, no. 4, p. 730–743.

Sloss, L.L., 1963, Sequences in the cratonic interior of North America: GSA Bulletin, 74: 93-114.

Slingerland, R., Kump, L.R., Arthur, M.A., Fawcett, P.J., Sageman, B.B., and Barron, E.J., 1996, Estuarine circulation in the Turonian Western Interior seaway of North America, GSA Bulletin; August 1996; v. 108; no. 7; p. 941–952

Stewart, J.H., 1976 Late Precambrian evolution of North America: plate tectonics implication: Geology, v. 4, p. 11–15.

Stone, D.S., 1993, Basement-involved thrust-generated folds as seismically imaged in the subsurface of the central Rocky Mountain foreland, Special Paper - Geological Society of America, 280: 271-318.

Stone, D.S., 2002, Morphology of the Casper Mountain uplift and related, subsidiary structures, central Wyoming—Implications for Laramide kinematics, dynamics, and crustal inheritance: AAPG Bull. 86/8: 1417–1439.

Stone, D.S., 2003, New Interpretations of the Piney Creek thrust and associated Granite Ridge tear fault, northeastern Bighorn Mountains, Wyoming, Rocky Mountain Geology, 38/2: 205-235.

Swift, D.J.P, and Rice, D.D., 1984, Sand bodies on muddy shelves: a model for sedimentation in the Western Interior Cretaceous Seaway, North America, IN: Tillman, R.W., and Siemers, C.T., eds., Siliciclastic Shelf Sediments: SEPM Special Publication 34: 43-62

Tillman, R.W., and W.R. Almond, 1979, Diagenesis of Frontier Formation offshore bar sandstones, Spearhead Ranch Field, Wyoming, in Scholle, P.A., and P.R. Schluger, eds., Aspects of diagenesis: SEPM Special Publication 26: 337–378.

Tonnsen, J.J., 1986, Influence of tectonic terranes adjacent to the Precambrian Wyoming Province on Phanerozoic stratigraphy in the Rocky Mountain Region, AAPG Memoir 41: 21-39.

Vakarelov, B., and J.P. Bhattacharya, 2009, Local tectonic control on parasequence architecture: Second Frontier sandstone, Powder River Basin, Wyoming, AAPG Bulletin, 93/3: 295–327.

Van Wagoner, J.C., R.M. Mitchum, K.M. Campion, and V.D. Rahmanian, 1990, Siliciclastic sequence stratigraphy in well logs, cores, and outcrops: AAPG Methods in Exploration Series, no. 7, 55 p.

Weimer, R.J, 1970, Rates of deltaic sedimentation and intrabasin deformation, Upper Cretaceous of Rocky Mountain region, in JP Morgan, ed., Deltaic sedimentation, modern and ancient: SEPM Special Publication 15: 270-292.

Weimer, R.J., 1984, Relation of unconformities, tectonics, and sea-level changes, Cretaceous of Western Interior, U.S.A., in Schlee, J.S., ed., Interregional unconformities and hydrocarbon accumulation: AAPG Memoir 36, p. 7–35.

Weimer, R.J., and A. Flexer, 1985, Depositional patterns and unconformities, Upper Cretaceous, eastern Powder River Basin, Wyoming, in Nelson, G.E., ed., The Cretaceous geology of Wyoming: Wyoming Geological Association 36th Annual Field Conference Guidebook: 131–147.

Wheeler, H.E., 1964, Base level, lithosphere surface, and time-stratigraphy: Geological Society of America Bulletin 75: 599–609.

Williams, H., Hoffman, P.F., Lewry, J.F., Monger, J.W.F., and Rivers, T. 1991. Anatomy of North America: thematic portrayals of the continent. Tectonophysics, 187: 117-134.

Winn, R.D., Jr., 1991, Storm deposition in marine sand sheets: Wall Creek Member, Frontier Formation, Powder River Basin, Wyoming: Journal of Sedimentary Petrology, 61: 86–101.

Winn, R.D., Stonecipher, S.A., and Bishop, M.G., 1983, Depositional environments and diagenesis of offshore sand ridges, Frontier Fm, Spearhead Ranch field, Wyoming, The Mountain Geologist, 20/2: 41-58.

Wright, L.D. and Coleman, J.M., 1975, Variations in morphology of major river deltas as functions of ocean wave and river discharge regimes, AAPG Bulletin, 57/2: 370-398.

CHAPTER 4

GENERAL CONCLUSIONS

The two manuscripts presented in this thesis demonstrate the importance of multiscale characterization of continental stratigraphic sequences, especially considering the sedimentary basin and crust upon which the stratigraphy was deposited. The sedimentary response to crustal subsidence and therefore accommodation patterns is shown over a range of temporal and spatial scales, from short-term site-specific sedimentary process facies to Precambrian craton assemblages. The interaction of these overprinted responses must be considered in order to generate effective and predictive basin-scale models to be used to assess geologic storage of supercritical carbon dioxide. Results from the two studies presented herein are summarized below.

This study provides three main contributions: 1) Emphasis on multiple scales of stratigraphic cyclicity correlated to dominant formative processes; 2) illustration of a detailed geologic characterization workflow for one reservoir class; 3) implication of technique used to calculate gross pore volume in five reservoir classes representative of GCS in onshore structural basins worldwide.

This thesis emphasizes multi-scalar reservoir characterization recognizing that scale-dependent processes produce a remnant stratigraphic record. Although many datasets may have sparse detailed geologic analysis, full description of core and outcrop analog data can improve subsurface characterization and modeling. Furthermore, when application of a depositional model becomes difficult to establish, as in the case with the

Frontier Fm. of Wyoming, it may be likely that the scale of investigation should be expanded and consider the role of preservation. Remnant patterns amplify tectonic subsidence and obscuring a clear link with shorter-term site-specific processes.

Capturing multiple scales of geologic detail is fundamental to increasing the heterogeneity in 3-D basin-scale static reservoir models as well as their upscaled fluid simulation models. The workflow presented here outlines novel techniques at multiple scales whereby fine-scale geologic information can be retained in each stage of upscaling during the model-building process. Capturing spatial trends of attribute variation is well established in the petroleum industry but is typically at the reservoir scale. Representative prediction of CO_2 storage at the basin scale will benefit significantly by modeling using the workflow presented in this thesis.

Future Work

1) Test hypothesis that tectonic control on the stratigraphy of the Frontier Formation by characterizing Wyoming Cratonic movement during Middle Cretaceous.
2) Finish building the static model of the PRB using the preliminary stratigraphic framework in this thesis, including: (1) characterization of remaining four RCs at level of detail of RC4; (2) basinwide structural analysis and fracture characterization incorporated into geomodel; and (3) regional hydrological and production analysis of the PRB using published and well log data (e.g., water chemistry, temperature, pressure, water saturation, oil production data).

3) Perform up-scaling to fluid-flow simulation and test a wide range of GCS scenarios (e.g., target evaluation, well planning, pipeline routing, volume of supercritical CO_2 injected to each target). Providing this predictive tool to the CCS community can enable better informed decisions and may predict key opportunities and limitations to this resource-intensive task

REFERENCES

Ambrose, W.A., Lakshminarasimhan, S., Holtz, M.H., Nunez-Lopez, V., Hovorka, S.D. and Duncan, I., 2008, Geologic factors controlling CO_2 storage capacity and permanence: case studies based on experience with heterogeneity in oil and gas reservoirs applied to CO_2 storage, Environmental Geology 54:1619–1633.

Anna, L.O., 1986, Structural influence on Cretaceous sedimentation, northern Great Plains, in Peterson, J.A., ed., Paleotectonics and sedimentation in the Rocky Mountain region: Tulsa, AAPG Memoir 41: 173–192.

Asquith, D.O., 1970, Depositional topography and major marine environments, Late Cretaceous, Wyoming, AAPG Bulletin, 54/7: 1184-1224.

Asquith, D.O., 1974, Sedimentary models, cycles, and deltas, Upper Cretaceous, Wyoming: AAPG Bull., 58/11: 2274-2283.

Atan, S., Gardner, M.H., Borer, J.M., and Wagerle, R.N., 2001, Implications of Upscaling Submarine Channel Reservoir Models, American Association of Petroleum Geologists National Convention, Abstracts with Program, Denver.

Bailie, A., Strait, R., Roe, S., Jamison, A. and Lindquist, H., 2007, Wyoming Greenhouse Gas Inventory and Reference Case Projections 1990-2020, downloaded from The Center for Climate Strategies, www.climatestrategies.us/library/library/download/411.

Barlow, J.A., Jr., and J.D. Haun, 1966, Regional stratigraphy of Frontier Formation and relation to Salt Creek field, Wyoming: AAPG Bull., 50/10: 2185–2196.

Barrell, J., 1912, Criteria for the recognition of ancient delta deposits, Bulletin of the Geological Society of America 23: 377-446.

Barrell, J., 1917, Rhythms and the measurements of geologic time, Bulletin of the Geological Society of America 28: 745-904.

Bekker, A. and Eriksson K.A., 2003, A Paleoproterozoic drowned carbonate platform on the southeastern margin of the Wyoming Craton: a record of the Kenorland breakup, Precambrian Research, 120/3-4: 327-364. Berg, R.R., 1962, Mountain flank thrusting in Rocky Mountain foreland, Wyoming and Colorado, AAPG Bull., 46/11: 2019-2032.

Berg, R.R., 1962, Mountain flank thrusting in Rocky Mountain foreland, Wyoming and Colorado, *AAPG Bull*., 46/11: 2019-2032.

Bhattacharya, J.P., and B.J. Willis, 2001, Lowstand deltas in the Frontier Formation, Powder River Basin, Wyoming—Implications for sequence stratigraphic models: AAPG Bull, 85: 261–294.

Bird, P., 1995, Lithosphere dynamics and continental deformation, Reviews of Geophysics, Supplement, Pages 379-383, July 1995 U.S. National Report To International Union Of Geodesy And Geophysics 1991-1994.

Bird, P., 1998, Kinematic history of the Laramide orogeny in latitudes 35°–49°N, western United States, Tectonics, 17/5: 780-801.

Blackstone, D. L., Jr., 1983, Laramide compressional tectonics, southeastern Wyoming: Contributions to Geology, University of Wyoming, Rocky Mountain Geology, v. 22, p. 1–38.

Borer, J. M., 2005, Outcrop Analysis and Geologic Modeling of Submarine Channel and Related Strata, Permian Middle Brushy Canyon Formation, West Texas, USA: unpublished Ph.D. thesis, Colorado School of Mines, Golden, Co, 269p.

Burruss, R.C., and 13 others, 2009, Development of a probabilistic assessment methodology for evaluation of carbon dioxide storage, U.S.G.S. Open-file report 2009-1035: 81p.

Carneiro, J. F., 2009, Numerical simulations on the influence of matrix diffusion to carbon sequestration in double porosity fissured aquifers, *International Journal of Greenhouse Gas Control* 3: 431-443.

Catuneanu, O., Beaumont, C., and Waschbusch, P., 1997, Interplay of static loads and subduction dynamics in foreland basins: Reciprocal stratigraphies and the "missing" peripheral bulge, Geology, 25: 1087-1090.

Cavanaugh, E.T., 1976, Stratigraphy of the Frontier Formation, Emigrant Gap Anticline, Natrona County, Wyoming, unpublished MS thesis, Colorado School of Mines, 173 p.

Celia, M.A., 2008, Geological storage as a carbon mitigation option, The 2008 Darcy Lecture (Final Version), http://www.princeton.edu/cee/people/data/c/celia/profile/the-darcy-lecture-outline/the-darcy-lecture/Darcy-Lecture-NGWA-3Dec08.pdf Accessed July 2, 2010.

Chamberlain, K.R. 1998. Medicine Bow orogeny: Timing of deformation and model of crustal structure produced during continent-arc collision, ca. 1.78 Ga, southeastern Wyoming. Rocky Mountain Geology, 33: 259-277.

Cobban, W.A., 1958, Late Cretaceous fossil zones of the Powder River Basin, Wyoming and Montana, In Wyoming Geological Association Guidebook, 13th Annual Field Conference, Powder River Basin: 114-119.

Cobban, W.A., 1990, Ammonites and some characteristic bivalves from the Upper Cretaceous Frontier Formation, Natrona County, Wyoming, in, Evolution of Sedimentary Basins; Powder River Basin: U.S. Geological Survey Bulletin, 1917-B, p. B1-B13.

Cobban, W.A., and J.B. Reeside Jr., 1952, Correlation of the Cretaceous formations of the Western Interior of the United States: Geological Society of America Bulletin, 63: 1011–1044.

Cobban, W.A., Obradovich, J.D., Walaszcyk, I., and McKinney, K.C., 2006, A USGS Zonal Table for the Upper Cretaceous Middle Cenomanian−Maastrichtian of the Western Interior of the United States Based on Ammonites, Inoceramids, and Radiometric Ages, USGS Open-File Report 2006-1250, 47 p.

Coleman, J.M., and L.D. Wright, 1975, Modern river deltas—Variability of processes and sand bodies, in Broussard, M.L., ed., Deltas, models for exploration: Houston Geological Society, p. 99–149.

Cox, D.M., Frost, C.D. and Chamberlin, K.R., 2000, 2.01-Ga Kennedy dike swarm, southeastern Wyoming Record of a rifted margin along the southern Wyoming province, Rocky Mountain Geology, 35/1: 7-30.

Cross, T.A., 1986, Tectonic controls of foreland basin subsidence and Laramide style deformation, western United States. In: Foreland Basins (Ed. by P. A. Allen & P. Homewood), Special Publication - International Association of Sedimentologists 8, 15–40.

Cross, T.A., 1988, Controls on coal distribution in transgressive-regressive cycles, Upper Cretaceous, Western Interior, U.S.A. in: C.K. Wilgus, B.S. Hasting, C.G. Kendall, H.W. Posamentier, C.A. Ross and J.C. Van Wagoner eds., Sea-level Changes: An Integrated Approach. Society of Economic Paleontologists and Mineralogists Special Publication 42, Tulsa, OK: 371-380.

Cross, T.A., Lessenger, M.A., 1998, Sediment volume partitioning: rationale for stratigraphic model evaluation and high-resolution stratigraphic correlation, *in*: Gradstein, F.M., Sandvik, K.O., Milton, N.J. (Eds.), Sequence Stratigraphy — Concepts and Applications, Special Publication 8, Norwegian Petroleum Society (NPF): 171–195.

Curry, W.H., III, 1986, Clinoform slope geometry of a Wall Creek sandstone, Salt Creek oil field, Wyoming, IN: Noll, J.H., ed., Rocky Mountain Oil and Gas Fields: Wyoming Geological Association Symposium: 189-197.

Dahl, P.S., Hamilton, M.A., Wooden, J.L., Foland, K.A., Frei, R., McCombs, J.A., and Holm, D.K., 2006, 2480 Ma mafic magmatism in the northern Black Hills, South Dakota: a new link connecting the Wyoming and Superior cratons, Canadian Journal of Earth Sciences, 43/10: 1579-1600.

De Chadenedes, J.F., 1975, Frontier Deltas fo the Western Green River Basin, Wyoming, Rocky Mountain Association of Geologists, 1975 Symposium: 149-157.

DeCelles, P.G. and Giles, K.A., 1996, Foreland basin systems, Basin Research 8: 105-123.

DeCelles, P.G., 2004, Late Jurassic to Eocene evolution of the Cordilleran Thrust Belt and Foreland Basin System, Western U.S.A., American Journal of Science, 304: 105–168

Desmond, R.J, Steidtmann, J.R. and Cardinal D.F., 1984, Stratigraphy and depositional environments of the middle member of the Minnelusa Formation, Central Powder River Basin, Wyoming, 35th Annual Field Conference, Wyoming Geological Association Guidebook: 213-239.

Dickinson, W. R., M. A. Klute, M. J. Hayes, S. U. Janecke, E. R. Lundin, M. A. McKittrick, and M. D. Olivares, 1988, Paleogeographic and paleotectonic setting of Laramide sedimentary basins in the central Rocky Mountain region, Geological Society of America Bulletin 100/7: 1023-1039.

Dickinson, W.R., 1976, Sedimentary basins developed during evolution of Mesozoic-Cenozoic arc-trench system in western North America: Canadian Journal of Earth Sciences, 13: 1268-1287.

DOE/NETL-401/090808, 2010, Site Screening, Selection, and Initial Characterization for Storage of CO2 in Deep Geologic Formations, http://www.netl.doe.gov/technologies/carbon_seq/refshelf/project%20portfolio/2010/BP-Manuals/BPM-SiteScreening.pdf.

Dolson, J., Muller, D., Evetts, MlJ., and Stein, J.A., 1991, Regional Paleotopographic Trends and Production, Muddy Sandstone (Lower Cretaceous), Central and Northern Rocky Mountains, *American Association of Petroleum Geologists Bulletin* 75/3: 409-435.

Doughty, C., B.M. Freifeld, and R.C. Trautz. 2008. Site characterization for CO_2 geologic storage and vice versa: The Frio brine pilot, Texas, USA as a case study. *Environmental Geology* 54, no. 8: 1635–1656.

Dutton, S.P. and Willis, B.J., 1998, Comparison of outcrop and subsurface sandstone permeability distribution, Lower Cretaceous Fall River Formation, South Dakota and Wyoming, *Journal of Sedimentary Research*, 68/5: 890-900.

Dyman, T. S.; Tysdal, R. G.; Perry, Jr. , W. J.; Nichols, D. J.; Obradovich, J. D., 2008, Stratigraphy and structural setting of Upper Cretaceous Frontier Formation, western Centennial Mountains, southwestern Montana and southeastern Idaho, Cretaceous Research, 29: 237 – 248.

Eicher, D.L., and R. Diner, 1985, Foraminifera as indicators of water mass in the Cretaceous Greenhorn sea, Western Interior, in Pratt, L.M., E.G. Kauffman, and F.B. Zelt, eds., Fine-grained deposits and biofacies of the Cretaceous Western Interior Seaway—Evidence of cyclic sedimentary processes: Society of Economic Paleontologists and Mineralogists Midyear Meeting, Golden, Colorado, Field Trip Guidebook 4: 60–71.

Elrick, M., 1990, Development of cyclic ramp-to-basin carbonate deposits, Lower Mississippian, Wyoming and Montana: [unpublished Ph.D., dissertation]: Virginia Polytechnic Institute, 170 p.

Erbacher, J., Thurrow, J. and Littke, R., 1996, Evolution patterns of radiolaria and organic matter variations: a new approach to identify sea-level changes in mid-Cretaceous pelagic environments, Geology, 24: 499–502.

Fischer, D.W., Smith, S.A., Peck, W.D., LeFever, J.A., LeFever, R.D., Helms, L.D., Sorensen, J.A., Steadman, E.N., and Harju, J.A., 2005, Sequestration Potential of the Madison of the Northern Great Plains Aquifer System (Madison Geological Sequestration Unit), Plains CO2 Reduction (PCOR) Partnership Report: 19 pp.

Fisk, H.N. and McFarlan, Jr., E, 1955, Late Quaternary deltaic deposits of the Mississippi river, GSA Special Paper 62: 279-302.

Fitzsimmons, R. and S. Johnson, 2000, Forced regressions; recognition, architecture and genesis in the Campanian of the Bighorn Basin, Wyoming, IN: Hunt, D. and R.L. Gawthorpe (eds) Sedimentary Responses to Forced Regressions. Geological Society Special Publications 172: 113-139.

Flemings. P.B., and Jordan, T.E., 1990, Stratigraphic modeling of foreland basins: interpreting thrust deformation and lithosphere rheology. Geology 18: 430-434.

Frederick, J.B., Dean, K.T., Fryberger, S.G., and Wilcox, T.D., 1995, Donkey Creek North Minnelusa 3-D: Challenging conventional wisdom, in: Ray, R.R. ed., High-definition seismic guidebook, Rocky Mountain Association of Geologists: 135-141.

Friedmann, S.J., 2007, Geological Carbon Dioxide Sequestration, Elements, 3/3: 179-184.

Galloway, W.E., 1975, Process framework for describing the morphologic and stratigraphic evolution of deltaic depositional systems, in Broussard, M.L., ed., Deltas, models for exploration: Houston Geological Society, p. 87-98.

Gani, M.R., and J.P. Bhattacharya, 2007, Basic Building Blocks and Process Variability of a Cretaceous Delta: Internal Facies Architecture Reveals a More Dynamic Interaction of River, Wave and Tidal Processes Than Is Indicated By External Shape, Journal of Sedimentary Research, 77/4: 284-302.

Gardner, M. H., Borer, J. M., Romans, B. W., Baptista, N., Kling, E., K., Melick, J. J., Wagerle, R., and Carr, M. M., 2008, Stratigraphic Models for Deepwater Sedimentary Systems, 28th Annual GCSSEPM, December 7-9, 2008, Houston, Texas.

Gardner, M. H., T. A. Cross, and M. Leverson, 2004, Stacking Patterns, Sediment Volume Partitioning and Facies Differentiation in Shallow-Marine and Coastal-Plain Strata: in Chidsey, T.C., R.D. Adams, and T.H. Morris, eds., Regional to Wellbore Analog for Fluvial-Deltaic Reservoir Modeling: The Ferron Sandstone of Utah, American Association of Petroleum Geologists, Studies in Geology, No. 50, p. 95-125.

Gardner, M.H., 1995, Tectonic and Eustatic Controls on the Stratal Architecture of Mid-Cretaceous Stratigraphic Sequences, Central Western Interior Foreland Basin of North America, in S. Dorobek, and J. Ross (eds.), Stratigraphic Evolution of Foreland Basins, Society of Sedimentary Geology (SEPM) Special Publication 52, p. 283-303.

Gardner, M.H., Barton, M.D., Tyler, N., and Fisher, R.S., 1992, Architecture and permeability structure of fluvial-deltaic sandstones, Ferron Sandstone, east-central Utah, in Flores, R.M., ed., Mesozoic of the Western Interior: Society of Economic Paleontologists and Mineralogists, Theme Meeting Field Guidebook, p. 5-21.

Gardner, M.H., Borer, J.M., Romans, B.W., Baptista, N., Kling, E.K., Hanggoro, D., Melick, J.J., Wagerle, R.N., Dechesne, M., Carr, M.M., Amerman, R., and Atan, S., 2008, Stratigraphic models for deepwater sedimentary systems. GCSSEPM Special Publication, Answering the Challenges of Production from Deepwater Reservoirs: Analogues and Case Histories to Aid a New Generation, p. 77-175.

Gardner, M.H., Willis, B.J., and Dharmasamadhi, I.N.W., 1995, Outcrop-based reservoir characterization of low accommodation/sediment supply fluvial deltaic sandbodies, *in* Japan National Oil Company, Technology Research Center, Special Publication 5, Reservoir Characterization: Integration of Geology, Geophysics, and Reservoir Engineering, p. 17–54.

Geoscience Institute for Oil and Gas Recovery Research, 1990, *Reservoir Heterogeneity Classification System for Characterization and Analysis of Oil Resource Base in Known Reservoirs,* prepared for U.S. Department of Energy, Office of Fossil Energy, Bartlesville Project Office.

Gilbert, G.K., 1885, The topographic features of lake shores: U.S. Geological Survey, 5th Annual Report, p. 104-108.

Grabau, A.W., 1960, Principles of stratigraphy, Dover Publications, New York.

Gradstein, F., J. Ogg and A. Smith, eds., 2004, A Geologic Time Scale, Cambridge, London.

Hamlin, H.S., 1996, Frontier Formation stratigraphy on the Moxa Arch, Green River Basin, Wyoming, Then Mountain Geologist 33/2: 35-44.

Haq, B.U., J. Hardenbol, and P. R. Vail, 1987, The new chronostratigraphic basis of Cenozoic and Mesozoic sea level cycles, in: Timing and depositional history of eustatic sequences; constraints on seismic stratigraphy Special Publications - Cushman Foundation for Foraminiferal Research 24: 7-13.

Harlan, S.S., Geissman, J.W., and Premo, W.R. 2003. Paleomagnetism and geochronology of an Early Proterozoic quartz diorite in the southern Wind River Range, Wyoming, USA. Tectonophysics, 362: 105-122.

Harms, J.C., Southard, J.B., Spearing, D.R., and Walker, R.G., 1975, Depositional environments as interpreted from primary sedimentary structures and stratification sequences, SEPM Short Course, no.2, 161pp.

Heyek, M., Mouche, E. and Mugler, C., 2009. Modeling vertical stratification of CO2 injected into a deep layered aquifer. *Advances in Water Resources* 32: 450–462.

Hills, F.A. and Armstrong, R.L., 1974, Geochronology of Precambrian rocks in the Laramie Range and implications for the tectonic framework of Precambrian southern Wyoming, Precambrian Research, 1/3: 213-225. Hu, G., 1992, Tectonic analysis of the southern and southeastern margins of the Powder River Basin and the adjoining uplifts: Newcastle to Casper, Wyoming, Ph.D. dissertation, South Dakota School of Mines: 187p.

Hobson, J.P., Fowler, M.L., and Beaumont, E.A., 1982, Depositional and statistical exploration models, Upper Cretaceous off shore sandstone complex, Sussex Member, House Creek Field, Wyoming, *AAPG*, 66/6: 689-707.

Horton, B.K. and DeCelles, P.G., 1997, The Modern foreland basin system adjacent to the Central Andes, Geology 25/10: 895-898.

Hovorka, S.D., Doughty, C., Benson, S.M., Puress, K. and Knox, P.R., 2004, The impact of geological heterogeneity on CO2 storage in brine formations: a case study from the Texas Gulf Coast, IN: Baines, S.J. and Worden, R.H. (eds) Geological Storage of Carbon Dioxide. Geological Society, London, Special Publications, 233: 147-163.

Hu, G., 1992, Tectonic analysis of the southern and southeastern margins of the Powder River Basin and the adjoining uplifts: Newcastle to Casper, Wyoming, Ph.D. dissertation, South Dakota School of Mines: 187p.

Huntoon, P.W., 1976, Permeability and ground water circulation in the Madison Aquifer along the eastern flank of the Bighorn Mountains of Wyoming, 28th annual Field Conference, Wyoming Geological Association Guidebook: 283-290.

Jachens, R.C., Simpson, R.W., Blakey, R.J. and Saltus, R.W., 1993, Isostatic residual gravity map of the Precambrian, IN: Precambrian: Conterminous U.S., DNAG Vol C2, Boulder 1993.

Jenkins, C., 1985, A preliminary tectonic analysis of the northeastern margin of the Bighorn Uplift: Buffalo to Dayton, Wyoming, M.S. thesis, South Dakota school of Mines: 135p.

Jenkyns, H.C., 2010, Geochemistry of oceanic anoxic events, Geochemistry, Geopphysics, Geosystems, 11/3, Q03004.

Jordan, T.E., 1981, Thrust loads and foreland basin evolution, Cretaceous, Western United States. America Association of Petroleum Geologists Bulletin, 65/12: 2506-2520.

Kaufmann, E.G., 1985, Cretaceous evolution of the Western interior basin of the United States, in, L.M. Pratt, E.G. Kaufmann, and F.B. Zelt, eds., SEPM 2nd Annual Midyear Meeting, Golden, Colorado: Field Trip Guidebook, P. IV-XIII.

Kerr, D.R., Wheeler, D.M., Rittersbacher, D.J. and Horne, J.C., 1986, Stratigraphy and sedimentology of the Tensleep Sandstone (Pennsylvanian and Permian), Bighorn Mountains, Wyoming, *Earth Science Bull*., 19/1-2: 61-78.

King, D., 1990, Tectonic analysis of the southwestern margin of the Powder River Basin: Kaycee to Casper, Wyoming, M.S. thesis, South Dakota School of Mines: 55 p.

Knechtel, M.M. and Patterson, S.H., 1962, Bentonite deposits of the northern Black Hills district, Wyoming, Montana, and South Dakota, USGS Bulletin: 1082-M, 137 p.

Kneller, B.C. and Branney, M.J., 1995, Sustained high density turbidity currents and the deposition of thick massive sands. *Sedimentology*, 42: 607-616.

Krystinik, L. F., and DeJarnett, B., 1995, Lateral variability of sequence stratigraphic framework in the Campanian and early Maastrichtian of the Western Interior Seaway, *in* Van Wagoner, J. C., and Bertram, G. T., eds., Sequence stratigraphy of foreland basin deposits: outcrop and subsurface examples from the Cretaceous of North America: American Association of Petroleum Geologists Memoir No. 64, p. 11–26.

Larue, D.K. and Yue, Y., 2003, How stratigraphy influences oil recovery: a comparative reservoir database study concentrating on deepwater reservoirs, *The Leading Edge*, April: 332-339.

Larue, D.K., 1995, Structurally aligned, sediment-starved fluvial valleys encased in marine deposits; sequence boundaries between the Carlile Shale and Niobrara Formation, central Powder River basin, U.S.A., IN: Van Wagoner, J.C. and G.T. Bertram (eds.) Sequence stratigraphy of foreland basin deposits; outcrop and subsurface examples from the Cretaceous of North America, AAPG Memoir, 64: 371-394.

Lindquist, T.W., 1986, A provenance study of the Wall Creek Member of the Frontier Formation and the Turner Sandy Member of the Carlile Shale in the Powder River Basin, Wyoming, unpublished MS thesis, Texas Christian University, 76 p.

Lisenbee, A L. 1978, Laramide structure of the Black Hills Uplift, South Dakota-Wyoming-Montana, Memoir - Geological Society of America, 151: 165-196.

Lisenbee, A.L., 1988, Tectonic history of the Black Hills uplift, Guidebook - Wyoming Geological Association, vol. 39: 45-52.

Lisenbee, A.L., 1993, Laramide evolution of the Black Hills Uplift, Memoir - Geological Survey of Wyoming, volume 5: 374-412.

Lorenz, J.C., Rizer, W.D., Farrell, H.E., Sonnenfeld, M.D., and Hanks, C.L., 1997, Characteristics of natural fractures in carbonate strata, Carbonate Seismology, Geophysical Development Series 6: 179-201.

Luppens, J.A., Scott, D.C., Haacke, J.E., Osmonson, L.M., Rohrbacher, T.J., and Ellis, M.S., 2008, Assessment of coal geology, resources, and reserves in in the Gillette Coalfield, Powder River Basin, Wyoming, U.S. Geological Survey Open-File Report 2008-1202.

Mancarci, M., 1989, Tectonic analysis of the southeastern margin of the Bighorn Uplift, Buffalo to Kaycee, M.S. thesis: South Dakota School of Mines, 89 p.

Marrs, R. W., and G. L. Raines, 1984, Tectonic framework of *Powder River basin*, Wyoming and Montana, interpreted from Landsat imagery: AAPG Bulletin 68: 1718-1731.

Martinsen, R. S., 2003A, Depositional remnants; Part 1, Common components of the stratigraphic record with important implications for hydrocarbon exploration and production, AAPG Bulletin. 87/12: 1869-1882.

Martinsen, R. S., 2003B, Depositional remnants; Part 2, Examples from the Western Interior Cretaceous basin of North America, AAPG Bulletin. 87/12: 1883-1909.

McGookey, D.P., J.D. Haun, L.A. Hale, H.G. Goodell, D.G. McCubbin, R.J. Weimer, and G.R. Wulf, 1972, Cretaceous system, in Mallory, W.W., ed., Geologic atlas of the Rocky Mountain Region: Denver, Rocky Mountain Association of Geologists, p. 189–228.

Merewether, E A., W. A. Cobban;, J. D. Obradovich, 2007, Regional disconformities in Turonian and Coniacian (Upper Cretaceous) strata in Colorado, Wyoming, and adjoining states; biochronological evidence, Rocky Mountain Geology, 42/ 2: 95-122.

Merewether, E.A. and W.A. Cobban, 1972, Unconformities within the Frontier Formation, northwestern Carbon County, Wyoming, In Geological Survey Research 1972: U.S. Geological Survey Professional Paper 800-D: D57-D66.

Merewether, E.A. and W.A. Cobban, 1986, Biostratigraphic units and tectonism in the mid-Cretaceous foreland of Wyoming, Colorado, and adjoining areas, in Peterson, J.A., ed., Paleotectonics and Sedimentation in the Rocky Mountain region, United States, part III, middle Rocky Mountains: Tulsa, American Association of Petroleum Geologists Memoir 41: 443-468.

Merewether, E.A., 1980, Stratigraphy of mid-Cretaceous formations at drilling sites in Weston and Johnson Counties, northeastern Wyoming: U.S. Geological Survey Professional Paper 1186–A, 25 p.

Merewether, E.A., 1983, The Frontier Formation and Mid-Cretaceous orogeny in the foreland of southwestern Wyoming, The Mountain Geologist, 20/4: 121-138.

Merewether, E.A., 1996, Stratigraphy and tectonic implications of Upper Cretaceous rocks in the Powder River Basin, northeastern Wyoming and southeastern Montana: U.S. Geological Survey Bulletin 1917–T, 92 p.

Merewether, E.A., Blackmon, P.D. and Webb, J.C., 1984, The Mid-Cretaceous Frontier Formation near the Moxa Arch, Southwestern Wyooming, USGS Professional Paper 1290, 29 p.

Merewether, E.A., Cobban, W.A., and Cavanaugh, E.T., 1979, Frontier Formation and equivalent rocks in Eastern Wyoming, *The Mountain Geologist*, 16/3: 67-101.

Merewether, E.A., W.A. Cobban, and CW. Spencer, 1976, The Upper Cretaceous Frontier Formation in the Kaycee-Tisdale Mountain area, Johnson County, Wyoming, in Laudon, R.B., Curry, W.H. III, and Runge, J.S., eds., Geology and energy resources of the Powder River: Wyoming Geological Association 28th Annual Field Conference Guidebook, p. 33–44.

Merewether, E.A., W.A. Cobban, and E.T. Cavanaugh, 1979, Frontier Formation and equivalent rocks in eastern Wyoming: The Mountain Geologist, v. 6, no. 3, p. 67–102.w

Middleton, G. W., 1973, Johannes Walther's Law of the Correlation of Facies: *Geological Society of America Bulletin*, 84: 979-988.

Myers, R.C., 1977, Stratigraphy of the Frontier Formation (Upper Cretaceous), Kemmerer area, Lincoln County Wyoming, Twenty-Ninth Annual Field conference – 1977 Wyoming Geological Association Guidebook: 271- 311.

Myrow, P.M., and Southard, J.B., 1991, Combined-flow model for vertical stratification sequences in shallow marine storm-deposited beds: Journal of Sedimentary Petrology, 61: 202–210.

N.E.T.L., 2010, Best practices for: Site screening, site selection, and initial characterization for storage of CO2 in deep geologic formations, http://www.netl.doe.gov/technologies/carbon_seq/refshelf/BPM_PublicOutreach.pdf .

Naus, M., 2000, A tectonic investigation of the Northern Bighorn / Pryor Uplift and surrounding areas, south-central Montana, unpublished M.S. thesis, South Dakota School of Mines: 147 p.

Nicot, J.P. 2008. Evaluation of large-scale CO_2 storage on freshwater sections of aquifers: An example from the Texas Gulf Coast Basin. *International Journal of Greenhouse Gas Control* 2, no. 4: 582–593.

Pacala, S., and Socolow, R., 2004, Stabilization wedges: Solving the climate problem for the next 50 years with current technologies: *Science*, v. 305, p. 968–972.

Peterson, C., 2009, The Beaver Creek Field, Madison CO2 Project – Spring 2009 update, Wyoming EORI, 3rd Annual Wyoming CO2 Conference.

Plint, A.G. and M.A. Kreitner, 2007, Extensive thin sequences spanning Cretaceous foredeep suggest high-frequency eustatic control: Late Cenomanian, Western Canada foreland basin, Geology, 35/8: 735–738.

Plint, A.G., 1988, Sharp-based shoreface sequences and "offshore bars" in the Cardium Formation of Alberta—Their relationship to relative changes in sea level, in Wilgus, C.K., B.S. Hastings, Kendall, H.W. Posamentier, C.A. Ross, and J. Van Wagoner, eds., Sea-level changes—An integrated approach: SEPM Special Publication 42: 357–370.

Plint, A.G., A. Tyagi, M.J. Hay, B.L. Varban, H. Zhang, X. Roca, 2009, Clinoforms, Paleobathymetry, and Mud Dispersal Across the Western Canada Cretaceous Foreland Basin: Evidence from the Cenomanian Dunvegan Formation and Contiguous Strata, Journal of Sedimentary Research 79: 144-161.

Ray, M.R., J.P. Brashear, and J. Biglarbigi, 1991, Classification system targets unrecovered U.S. oil reserves, *Oil and Gas Journal,* 89/39, p. 89.

Regional Carbon Sequestration Partnerships, 2003, http://www.netl.doe.gov/technologies/carbon_seq/infrastructure/rcsp.html.

Rice, D.D., and C.W. Keighin, 1989, Configuration of shelf sandstone oil reservoirs, Upper Cretaceous (Turonian) Turner Sandy Member of Carlile Shale, Powder River basin, Wyoming: AAPG abs, 73/3: 405.

Roberts, L.N.R., and M.A. Kirschbaum, 1995, Paleogeography of the Late Cretaceous of the Western Interior of Middle North America – Coal distribution and sediment accumulation, USGS Professional Paper 1591, 63 p. & plates.

Robinson, C.S., Mapel, W.J., and Bergendahl, M.H., 1964, Stratigraphy and structure of the northern and western flanks of the Black Hills uplift, Wyoming, Montana, and South Dakota: U.S. Geological Survey Professional Paper, 404, 134 p.

Roscoe, S.M., and Card, K.D. 1993. The reappearance of the Huronian in Wyoming: rifting and drifting of ancient continents. Canadian Journal of Earth Sciences, 30: 2475-2480.

Rubey, W.W., 1930, Lithologic studies of fine-grained Upper Cretaceous sedimentary rocks of the Black Hills region, IN Shorter contributions to general geology, 1930: U.S. Geological Survey Professional Paper, 165-A, p. A1-A54.

Ryer, T.A., and J.R. Lovekin, 1986, The Upper Cretaceous Vernal Delta of Utah; depositional or paleotectonic feature? AAPG Memoir 41: 497-510**.**

Sadeque, J., 2006, Regional Reservoir Compartmentalization within Offlapping, Top-Truncated, Mixed-Influenced Deltas, Wall Creek Member, Frontier Formation, Powder River Basin, Wyoming, unpublished Ph.D. thesis, University of Texas at Dallas, 156p.

Sageman, B. R., and Arthur, M. A., 1994, Early Turonian paleogeographic/paleobathymetric map, Western Interior, US, in Caputo, M. V., Peterson, A., and Franczyk, K. J., eds., Mesozoic systems of the Rocky Mountain Region, USA: Rocky Mountain Section, Society for Sedimentary Geology (SEPM), p. 457–469.

Sageman, B. R., Meyers, S.R., and Arthur, M. A., 2006, Orbital time scale and new C-isotope record for Cenomanian-Turonian boundary stratotype, Geology 34/2: 125-128.

Sears, J.W., and Price, R.A., 1978, The Siberian connection: A case for the Precambrian separation of the North American and Siberian cratons, Geology, 6, 267-270.

Shaw, C.A.**,** Karlstrom, K.E., Williams, M.L., Jercinovic, M.J., McCoy, A.M., and Dueker, K., 2003. Proterozoic Shear Zones of the Colorado Rocky Mountains: From continental assembly to intracontinental reactivation. *in* Lageson, D.R., Erslev, E., and Magloughlin, J., Southern Rocky Mountains: Geological Society of America Field Guide, p. 102–117.

Slack, P.B., 1981, Paleotectonics and hydrocarbon accumulation, Powder River Basin, Wyoming, *AAPG*, 65/6: 730-743.

Slingerland, R., Kump, L.R., Arthur, M.A., Fawcett, P.J., Sageman, B.B., and Barron, E.J., 1996, Estuarine circulation in the Turonian Western Interior seaway of North America, GSA Bulletin; August 1996; v. 108; no. 7; p. 941–952

Sloss, L.L., 1963, Sequences in the cratonic interior of North America: GSA Bulletin, 74: 93-114.

Smith, L. B. Jr., G. P. Eberli, and M. D. Sonnenfeld, 2004, Sequence-stratigraphic and paleogeographic distribution of reservoir-quality dolomite, Madison Formation, Wyoming and Montana, in G. M. Grammer, G. P. Eberli, and P. M. Harris, eds., Integration of outcrop and modern analogs in reservoir modeling: AAPG Memoir 80, p. 94–118.

Sneider, R.; Young, T., 2009, Facing major challenges in carbon capture and sequestration, *GSA Today*, 19/11: 36-37.

Sonnenfeld, M.D., 1996, An integrated sequence stratigraphic approach to reservoir characterization of the Lower Mississippian Madison Limestone, emphasizing Elk Basin field, Bighorn Basin, Wyoming: Unpublished Ph.D. dissertation, Colorado School of Mines, Golden Colorado 437 p.

Stewart, J.H., 1976 Late Precambrian evolution of North America: plate tectonics implication: Geology, v. 4, p. 11–15.

Stone, D.S., 1993, Basement-involved thrust-generated folds as seismically imaged in the subsurface of the central Rocky Mountain foreland, Special Paper - *Geological Society of America*, vol. 280: 271-318,

Stone, D.S., 2002, Morphology of the Casper Mountain uplift and related, subsidiary structures, central Wyoming; implications for Laramide kinematics, dynamics, and crustal inheritance, *AAPG Bulletin*, 86/8: 1417-1440.

Stone, D.S., 2003, New Interpretations of the Piney Creek thrust and associated Granite Ridge tear fault, northeastern Bighorn Mountains, Wyoming, *Rocky Mountain Geology*, 38/2: 205-235.

Swift, D.J.P, and Rice, D.D., 1984, Sand bodies on muddy shelves: a model for sedimentation in the Western Interior Cretaceous Seaway, North America, IN: Tillman, R.W., and Siemers, C.T., eds., Siliciclastic Shelf Sediments: SEPM Special Publication 34: 43-62

Tillman, R.W., 1997, Shannon Sandstone, Salt Creek Area, Wyoming, Prospect to Pipeline, 48th Annual WGA Field Conference, Guidebook: 29-68.

Tillman, R.W., and Martinsen, R.S., 1987, Sedimentological model and production characteristics of Hartzog Draw field, Wyoming, A Shannon shelf-ridge sandstone, IN: Tillman, R.W., and Weber, K.J., eds., Reservoir sedimentology, Society of Economic Paleontologists and Mineralogists Special Publication No. 40: 15-67.

Tillman, R.W., and W.R. Almond, 1979, Diagenesis of Frontier Formation offshore bar sandstones, Spearhead Ranch Field, Wyoming, in Scholle, P.A., and P.R. Schluger, eds., Aspects of diagenesis: SEPM Special Publication 26: 337–378.

Tonnsen, J.J., 1986, Influence of tectonic terranes adjacent to the Precambrian Wyoming Province on Phanerozoic stratigraphy in the Rocky Mountain Region, AAPG Memoir 41: 21-39.

Trotter, J.F., 1963, The Minnelusa play of the Northern Powder River, Wyoming and adjacent areas, 18th Annual WGA Field Conference, Guidebook: 117-122.

U.S. Department of Energy, National Energy Technology Laboratory, 2008, Carbon sequestration atlas of the United States and Canada (2nd ed.; Atlas II): 142 p.

Vakarelov, B., and J.P. Bhattacharya, 2009, Local tectonic control on parasequence architecture: Second Frontier sandstone, Powder River Basin, Wyoming, AAPG Bulletin, 93/3: 295–327.

Van Wagoner, J.C., 1985, Reservoir facies distribution as controlled by sea-level change, abstract: Society of Economic Paleontologists and Mineralogists Mid-year Meeting, Golden, Colorado, August 11-14, p. 91-92.

Van Wagoner, J.C., R.M. Mitchum, K.M. Campion, and V.D. Rahmanian, 1990, Siliciclastic sequence stratigraphy in well logs, cores, and outcrops: AAPG Methods in Exploration Series, no. 7, 55 p.

Weimer, 1960, Upper Cretaceous stratigraphy, Rocky Mountain area, AAPG Bull. 44/1: 1-20.

Weimer, R.J, 1970, Rates of deltaic sedimentation and intrabasin deformation, Upper Cretaceous of Rocky Mountain region, in JP Morgan, ed., Deltaic sedimentation, modern and ancient: SEPM Special Publication 15: 270-292.

Weimer, R.J., 1984, Relation of unconformities, tectonics, and sea-level changes, Cretaceous of Western Interior, U.S.A., in Schlee, J.S., ed., Interregional unconformities and hydrocarbon accumulation: AAPG Memoir 36, p. 7–35.

Weimer, R.J., and Flexer, A., 1985, Depositional patterns and unconformities, Upper Cretaceous, Eastern Powder River Basin, Wyoming, IN: The Cretaceous Geology of Wyoming, 36th Annual WGA Field Conference Guidebook, 131-147.

Westphal, H., Eberli, G.P., Smith, L.B., Grammer, M. and Kislak, J., 2004, Reservoir characterization of the Mississippian Madison Formation, wind River basin, Wyoming, AAPG Bull., 88/4: 405-432.

Wheeler, D., 1986, Stratigraphy and sedimentology of the Tensleep Sandstone, Southeast Bighorn Basin, Wyoming, Unpublished Masters Thesis, Colorado School of Mines, 169 p.

Wheeler, H.E., 1964, Base level, lithosphere surface, and time-stratigraphy: Geological Society of America Bulletin 75: 599–609.

Williams, H., Hoffman, P.F., Lewry, J.F., Monger, J.W.F., and Rivers, T. 1991. Anatomy of North America: thematic portrayals of the continent. Tectonophysics, 187: 117-134.

Winn, R.D., Jr., 1991, Storm deposition in marine sand sheets: Wall Creek Member, Frontier Formation, Powder River Basin, Wyoming: Journal of Sedimentary Petrology, 61: 86–101.

Winn, R.D., Stonecipher, S.A., and Bishop, M.G., 1983, Depositional environments and diagenesis of offshore sand ridges, Frontier Fm, Spearhead Ranch field, Wyoming, The Mountain Geologist, 20/2: 41-58.

Woodward, L. A., 1988, Tectonic map of the Rocky Mountain region of the United States, in Sloss, L. L., ed., Sedimentary cover — North American craton: U.S.: Boulder, Colorado, Geological Society of America, Geology of North America, v. D-2, Plate 2.

Wright, L.D. and Coleman, J.M., 1975, Variations in morphology of major river deltas as functions of ocean wave and river discharge regimes, AAPG Bulletin, 57/2: 370-398.

Wyoming Geological Association, 2000, Wyoming oil and gas fields symposium, Powder River Basin, 2 volume set, Mountain States Lithographing Company, Casper, Wyoming: 565 pp.

Wyoming Oil and Gas Conservation Commission (WOGCC) website, http://wogcc.state.wy.us/ , accessed between 2006 and 2011.

Yamamoto, H., K. Zhang, K. Karasaki, A. Marui, H. Uehara, and N. Nishikawa. 2009. Numerical investigation concerning the impact of CO2 geologic storage on regional groundwater flow. *International Journal of Greenhouse Gas Control* 3, no. 5: 586–599.

Zaitlin, B.A., Dalrymple, R.W. and Boyd, R., 1994, The stratigraphic organisation of incised-valley systems associated with relative sea-level changes. In: Incised-valley systems: Origin and sedimentary sequences, Ed. by R. W. Dalrymple, R. Boyd and B. A. Zaitlin, Spec. Publication Society of Economic Paleontologists and Mineralogists, 51, 45–62.

Zhou, Q., Birkholzer, J.T., Mehnert, E., Lin, Y. and Zhang, K., 2010, Modeling basin- and plume-scale processes of CO_2 storage for full-scale deployment, *Ground Water* 48/4: 494–514.

APPENDICES

APPENDIX A:

CORE DESCRIPTIONS OF THE FRONTIER FORMATION

Appendix A.

Core descriptions. 22 process sedimentology facies were grouped into 12 core facies representing similar process and therefore characterizing specific porosity/ permeability relationships.

Frontier Facies Explanation

core facies	process facies	
1	1a	Coarse lag, med SS - granule
	1b	Clast-rich to conglom Med - coarse SS
2 a b c	2a	Amalgamated cross-bedded UF - coarse SS
	2b	PT Cross bedded UF - coarse SS
	2c	Muddy cross bedded UF - coarse SS
3	3a	Soft sed deformed F-Med SS
	3b	Structureless F-Med SS
4	4	Plane parallel Uf - med SS A
5 a b c	5a	Swaley Uf - med SS
	5b	Hummocky Fine SS
	5c	Plane parallel Fine SS B
6 a c	6a	Faintly stratified amalgamated VF SS
	6b	Interbedded deformed/ BT F SS
6 b 7	6c	Amalgamated bioturbated VF - Fine SS
	7	Ripple laminated VF - Fine SS
8 a b	8a	Interbedded thinly laminated VF - Fine SS with mud drapes
	8b	Bioturbated VF - Fine SS and mud
9	9a	Interlaminated mud, and Silt - VF SS
	9b	Bioturbated shale and SS
10	10	Shale with thin SS beds
	11	Dark marine shale
	12	Claystone

Core porosity and permeability is plotted in upper left, color-coded by core facies with porosity, permeability and grain size logs.

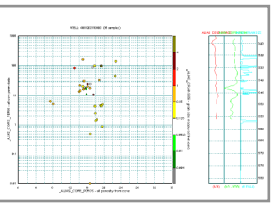

Well name, location & unique well ID (UWI)

FEDERAL AQUITAINE WELL NO-2

T42N R79W S29

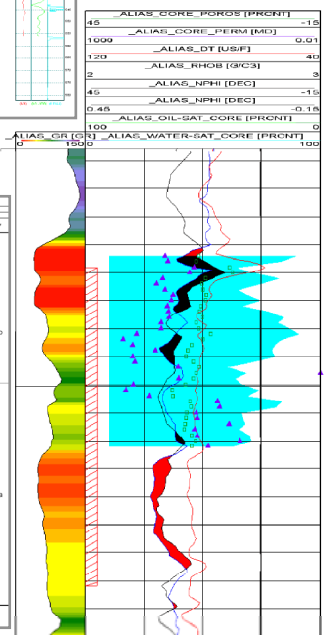

Facies are placed within sedimentary bodies and stratigraphic cycle, placed in columns to right of notes. Photograph depths are indicated at far left.

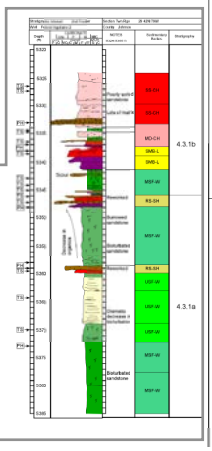

The cored interval is at the same scale as the well logs (red hatchered)

Sedimentary Body Explanation

	Code	Lithology	Body type	Interpretation
1	SS-CH	sandy	channelform	distributary (submarine) channel fill
2	MD-CH	muddy/heterolithic	channelform	underfilled (submarine) channel - tidal?
3	SMB-L	sandy mouthbar	lobe	proximal mouthbar
4	MMB-L	muddy-sandy mouthbar	lobe	distal/lateral/inter mouthbar
5	FS-L	sand and shale	lobe	frontal splay / turbidite lobe
6	RS-SH	reworked sandstone	sheet	transgressive lag
7	SS-SH	sand	sheet	storm deposit - turbidite
8	USF-W	sandy-silt	wedge	upper shoreface
9	MSF-W	silty-sand	wedge	middle shoreface
10	LSF-W	shaly-silt	wedge	lower shoreface
11	CF-W	sand and shale	wedge	submarine channel levee
12	SH-DR	shale	drape	suspension deposits, sediment starved

Sedimentary Structures Explanation

- Climbing ripple laminations
- Asymmetric ripple laminations
- Asymmetric ripple lamination (ARL)
- Truncated foresets of ARL
- Floating intraclasts (cm-sized)
- Intraclasts (cm-sized)
- Floating intraclasts (mm-sized)
- Intraclasts (mm-sized)
- Plant fragments
- ? Low confidence
- Missing core
- Recumbant fold
- Soft-sediment deformation (SSD)
- Microfault (MF)
- Calcite cement
- Pyrite nodule
- Undifferentiated shell
- Spriete
- Sand-filled burrow
- Undifferentiated horizontal burrow
- Undifferentiated vertical burrow
- Bioturbation

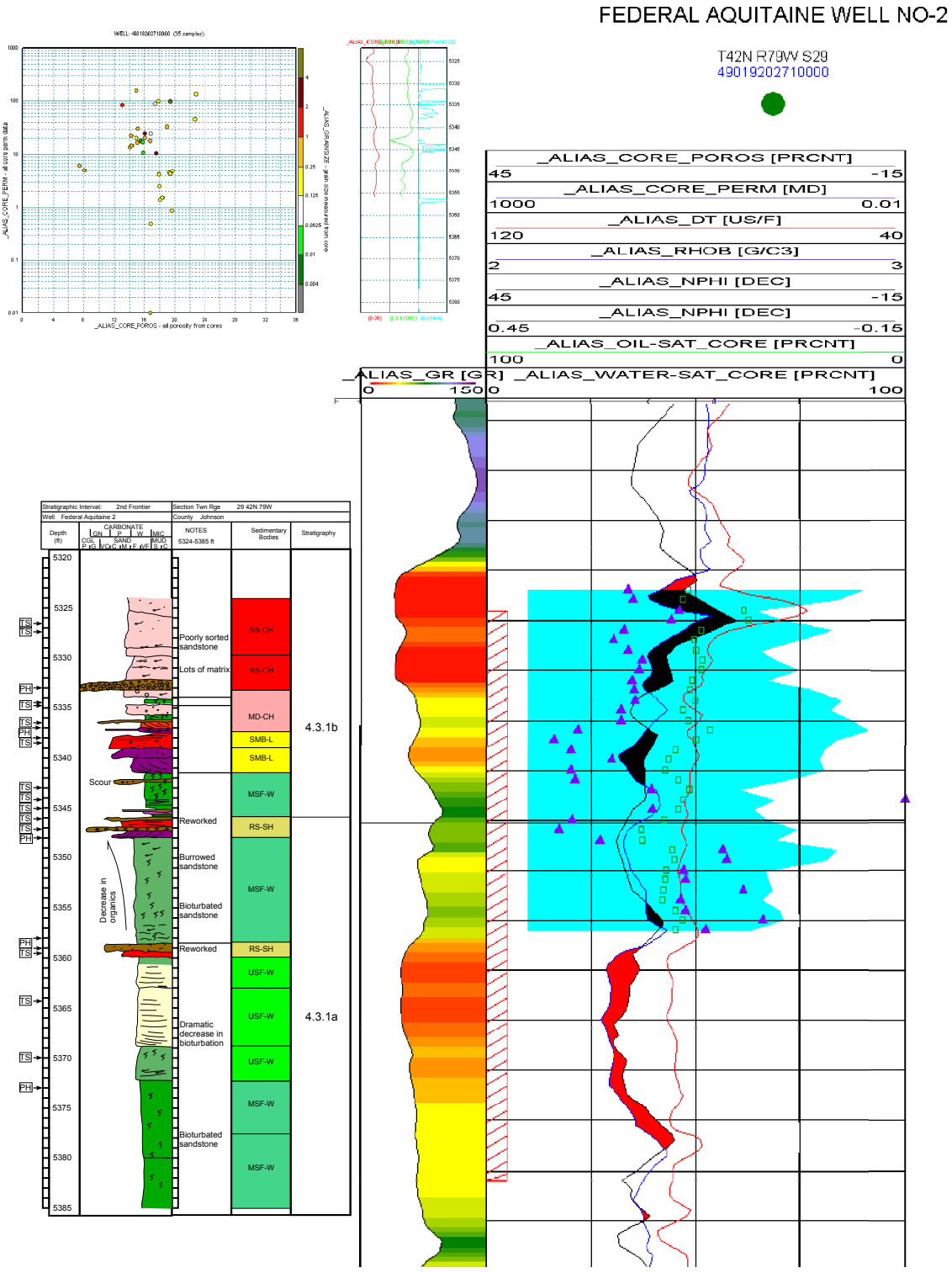
FEDERAL AQUITAINE WELL NO-2
T42N R79W S29
49019202710000
_ALIAS_CORE_POROS [PRCNT]
45 -15
_ALIAS_CORE_PERM [MD]
1000 0.01
_ALIAS_DT [US/F]
120 40
_ALIAS_RHOB [G/C3]
2 3
_ALIAS_NPHI [DEC]
45 -15
_ALIAS_NPHI [DEC]
0.45 -0.15
_ALIAS_OIL-SAT_CORE [PRCNT]
100 0
_ALIAS_GR [GR]
0 150
_ALIAS_WATER-SAT_CORE [PRCNT]
0 100
Stratigraphic Interval: 2nd Frontier
Well Federal Aquitaine 2
Section Twn Rge 29 42N 79W
County Johnson
Depth (ft)
CARBONATE
SAND
NOTES
5324-5385 ft
Sedimentary Bodies
Stratigraphy
Poorly sorted sandstone
Lots of matrix
Scour
Reworked
Burrowed sandstone
Bioturbated sandstone
Decrease in organics
Reworked
Dramatic decrease in bioturbation
Bioturbated sandstone
SS-CH
SS-CH
MD-CH
SMB-L
SMB-L
MSF-W
RS-SH
MSF-W
RS-SH
USF-W
USF-W
USF-W
MSF-W
MSF-W
4.3.1b
4.3.1a

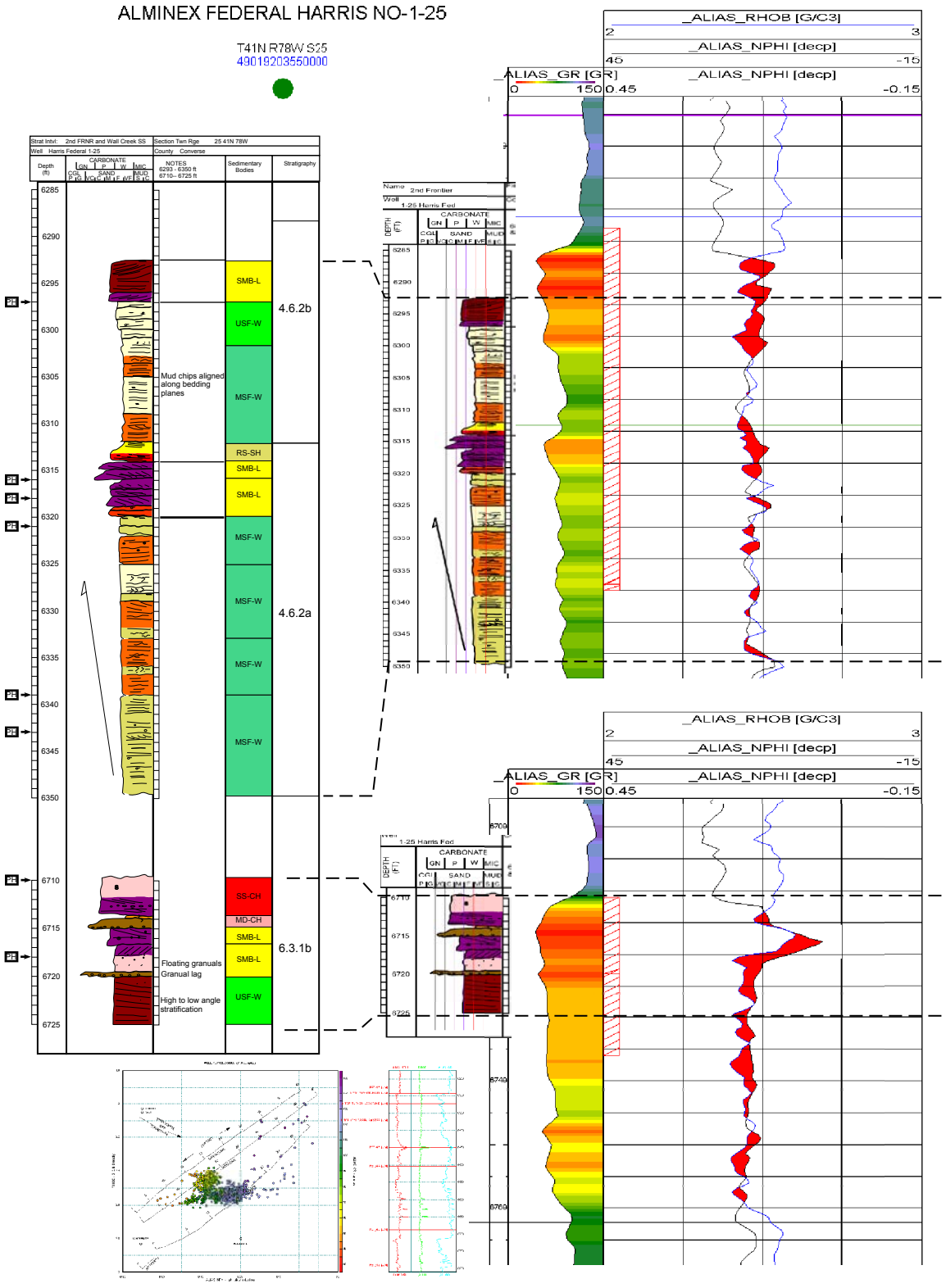
ALMINEX FEDERAL HARRIS NO-1-25
T41N R78W S25
49019203550000
_ALIAS_RHOB [G/C3]
_ALIAS_NPHI [decp]
_ALIAS_GR [GR]
Mud chips aligned along bedding planes
Floating granuals
Granual lag
High to low angle stratification
SMB-L
USF-W
MSF-W
RS-SH
SS-CH
MD-CH
4.6.2b
4.6.2a
6.3.1b

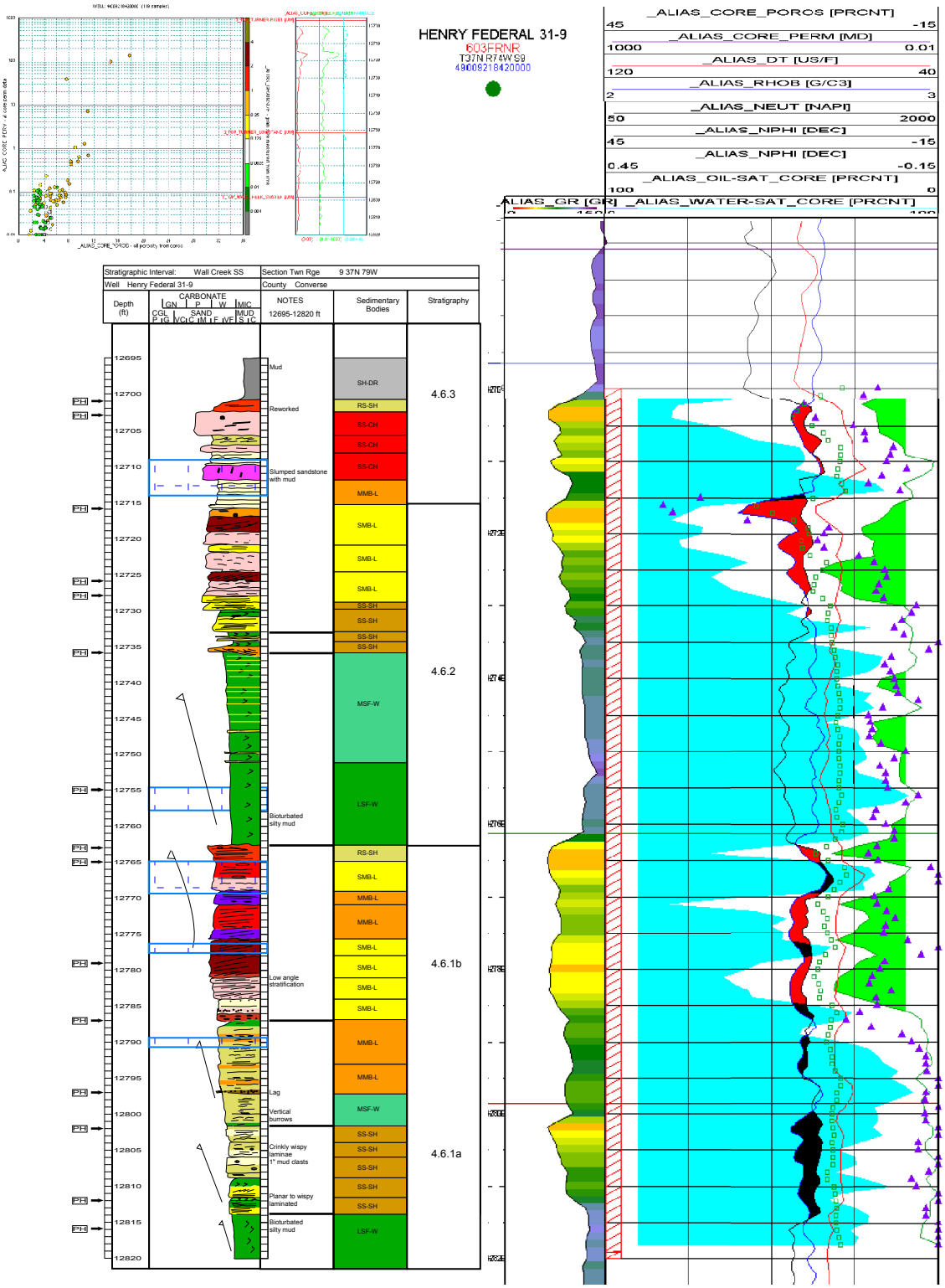
HENRY FEDERAL 31-9
603FRNR
T37N R74W S9
49009218420000
_ALIAS_CORE_POROS [PRCNT]
45
-15
_ALIAS_CORE_PERM [MD]
1000
0.01
_ALIAS_DT [US/F]
120
40
_ALIAS_RHOB [G/C3]
2
3
_ALIAS_NEUT [NAPI]
50
2000
_ALIAS_NPHI [DEC]
45
-15
_ALIAS_NPHI [DEC]
0.45
-0.15
_ALIAS_OIL-SAT_CORE [PRCNT]
100
0
_ALIAS_GR [GR]
_ALIAS_WATER-SAT_CORE [PRCNT]
Stratigraphic Interval: Wall Creek SS
Section Twn Rge 9 37N 79W
Well Henry Federal 31-9
County Converse
Depth (ft)
CARBONATE
GN P W MIC
CGL I SAND MUD
P LG VCLC LM LF VFS LC
NOTES
12695-12820 ft
Sedimentary Bodies
Stratigraphy
12695
12700
12705
12710
12715
12720
12725
12730
12735
12740
12745
12750
12755
12760
12765
12770
12775
12780
12785
12790
12795
12800
12805
12810
12815
12820
Mud
Reworked
Slumped sandstone with mud
Bioturbated silty mud
Low angle stratification
Lag
Vertical burrows
Crinkly wispy laminae 1" mud clasts
Planar to wispy laminated
Bioturbated silty mud
SH-DR
RS-SH
SS-CH
SS-CH
SS-CH
MMB-L
SMB-L
SMB-L
SMB-L
SS-SH
SS-SH
SS-SH
SS-SH
MSF-W
LSF-W
RS-SH
SMB-L
MMB-L
MMB-L
SMB-L
SMB-L
SMB-L
SMB-L
MMB-L
MMB-L
MSF-W
SS-SH
SS-SH
SS-SH
SS-SH
SS-SH
LSF-W
4.6.3
4.6.2
4.6.1b
4.6.1a

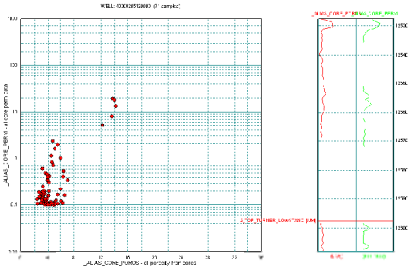

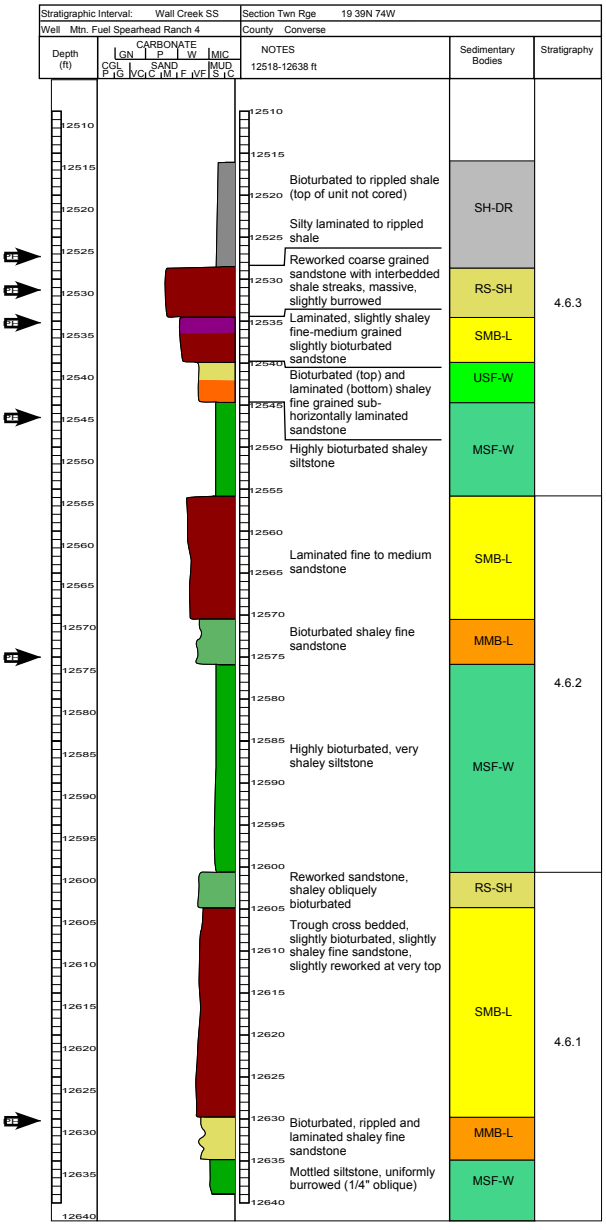
Stratigraphic Interval: Wall Creek SS
Section Twn Rge 19 39N 74W
Well Mtn. Fuel Spearhead Ranch 4
County Converse
Depth (ft)
CARBONATE
GN P W MIC
CGL P IG SAND VC C M F VF MUD S IC
NOTES
12518-12638 ft
Sedimentary Bodies
Stratigraphy
Bioturbated to rippled shale (top of unit not cored)
Silty laminated to rippled shale
Reworked coarse grained sandstone with interbedded shale streaks, massive, slightly burrowed
Laminated, slightly shaley fine-medium grained slightly bioturbated sandstone
Bioturbated (top) and laminated (bottom) shaley fine grained sub-horizontally laminated sandstone
Highly bioturbated shaley siltstone
Laminated fine to medium sandstone
Bioturbated shaley fine sandstone
Highly bioturbated, very shaley siltstone
Reworked sandstone, shaley obliquely bioturbated
Trough cross bedded, slightly bioturbated, slightly shaley fine sandstone, slightly reworked at very top
Bioturbated, rippled and laminated shaley fine sandstone
Mottled siltstone, uniformly burrowed (1/4" oblique)
SH-DR
RS-SH
SMB-L
USF-W
MSF-W
SMB-L
MMB-L
MSF-W
RS-SH
SMB-L
MMB-L
MSF-W
4.6.3
4.6.2
4.6.1

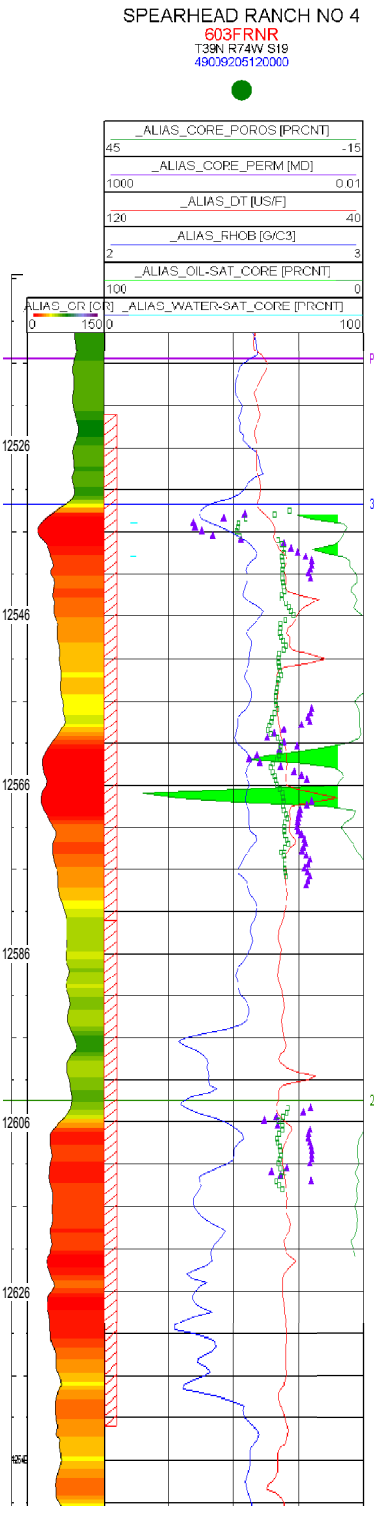
SPEARHEAD RANCH NO 4
603FRNR
T39N R74W S19
49009205120000
_ALIAS_CORE_POROS [PRCNT]
45 -15
_ALIAS_CORE_PERM [MD]
1000 0.01
_ALIAS_DT [US/F]
120 40
_ALIAS_RHOB [G/C3]
2 3
_ALIAS_OIL-SAT_CORE [PRCNT]
100 0
_ALIAS_OR [CR] _ALIAS_WATER-SAT_CORE [PRCNT]
0 150 0 100
12526
12546
12566
12586
12606
12626

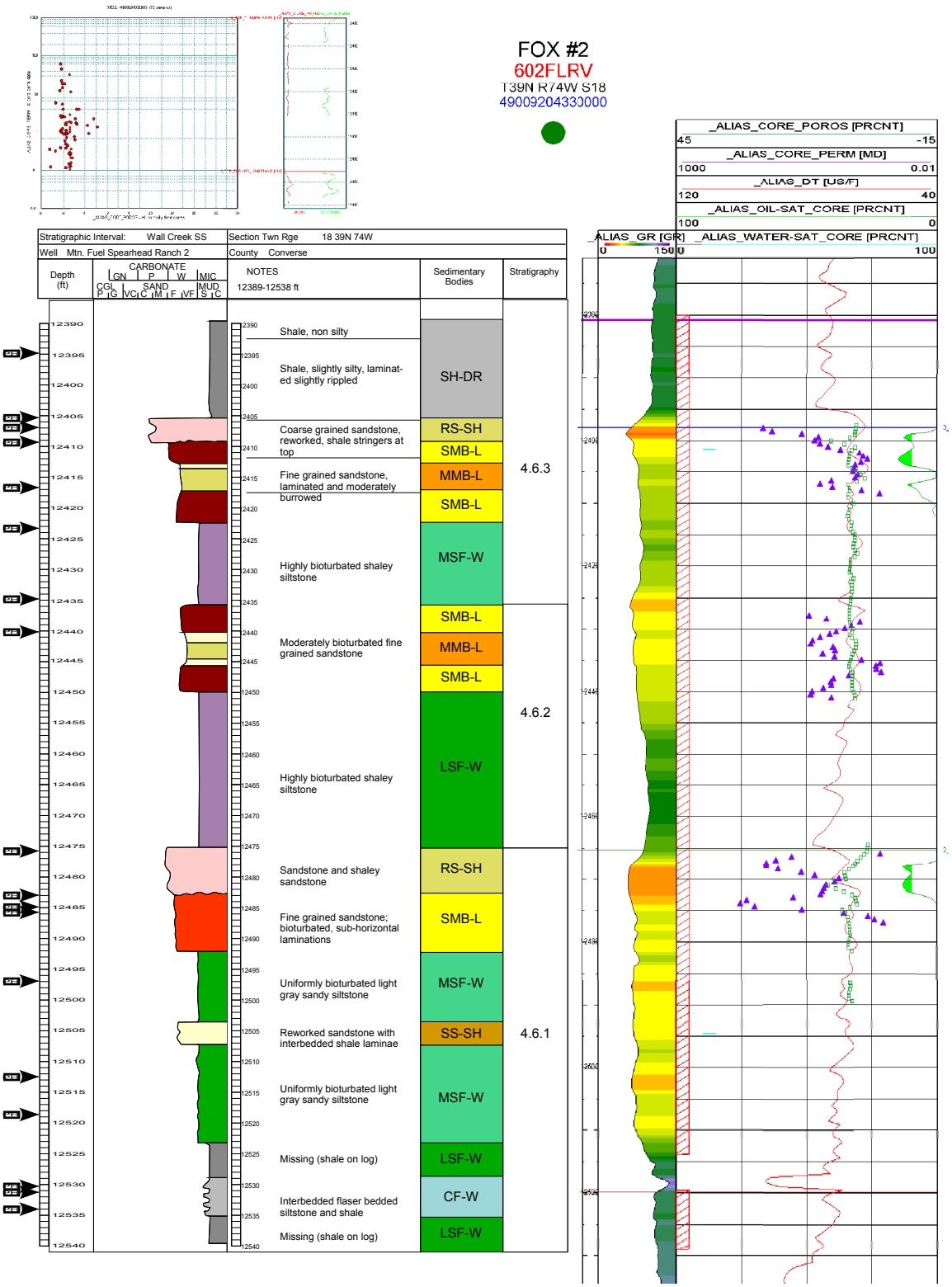
FOX #2
602FLRV
T39N R74W S18
49009204330000
_ALIAS_CORE_POROS [PRCNT]
45
-15
_ALIAS_CORE_PERM [MD]
1000
0.01
_ALIAS_DT [US/F]
120
40
_ALIAS_OIL-SAT_CORE [PRCNT]
100
0
_ALIAS_GR [GR]
0
150
_ALIAS_WATER-SAT_CORE [PRCNT]
0
100
Stratigraphic Interval: Wall Creek SS
Section Twn Rge 18 39N 74W
Well Mtn. Fuel Spearhead Ranch 2
County Converse
Depth (ft)
CARBONATE
GN P W MIC
CGL P G SAND VC C M F VF MUD S C
NOTES
12389-12538 ft
Sedimentary Bodies
Stratigraphy
Shale, non silty
Shale, slightly silty, laminated slightly rippled
Coarse grained sandstone, reworked, shale stringers at top
Fine grained sandstone, laminated and moderately burrowed
Highly bioturbated shaley siltstone
Moderately bioturbated fine grained sandstone
Highly bioturbated shaley siltstone
Sandstone and shaley sandstone
Fine grained sandstone; bioturbated, sub-horizontal laminations
Uniformly bioturbated light gray sandy siltstone
Reworked sandstone with interbedded shale laminae
Uniformly bioturbated light gray sandy siltstone
Missing (shale on log)
Interbedded flaser bedded siltstone and shale
Missing (shale on log)
SH-DR
RS-SH
SMB-L
MMB-L
SMB-L
MSF-W
SMB-L
MMB-L
SMB-L
LSF-W
RS-SH
SMB-L
MSF-W
SS-SH
MSF-W
LSF-W
CF-W
LSF-W
4.6.3
4.6.2
4.6.1

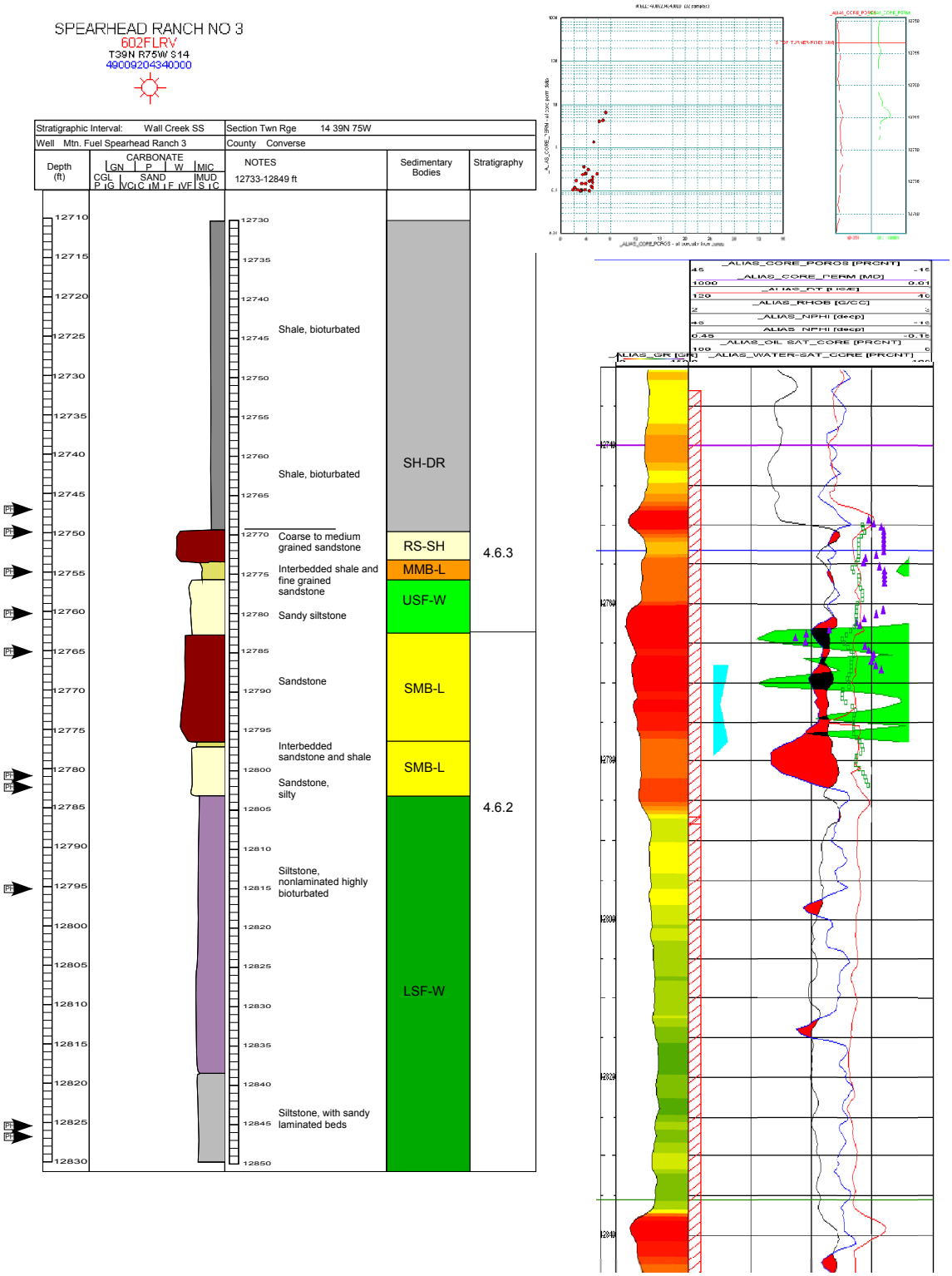
SPEARHEAD RANCH NO 3
602FLRV
T39N R75W S14
49009204340000
Stratigraphic Interval: Wall Creek SS
Section Twn Rge 14 39N 75W
Well Mtn. Fuel Spearhead Ranch 3
County Converse
Depth (ft)
CARBONATE
SAND
MUD
NOTES
12733-12849 ft
Sedimentary Bodies
Stratigraphy
Shale, bioturbated
Shale, bioturbated
Coarse to medium grained sandstone
Interbedded shale and fine grained sandstone
Sandy siltstone
Sandstone
Interbedded sandstone and shale
Sandstone, silty
Siltstone, nonlaminated highly bioturbated
Siltstone, with sandy laminated beds
SH-DR
RS-SH
MMB-L
USF-W
SMB-L
SMB-L
LSF-W
4.6.3
4.6.2
_ALIAS_CORE_POROS [PRCNT]
_ALIAS_CORE_PERM [MD]
_ALIAS_RHOB [G/CC]
_ALIAS_NPHI [decp]
_ALIAS_OIL SAT_CORE [PRCNT]
_ALIAS_WATER-SAT_CORE [PRCNT]
ALIAS_GR [GAPI]

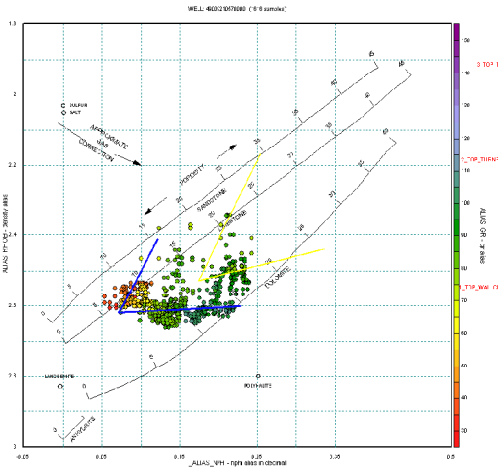

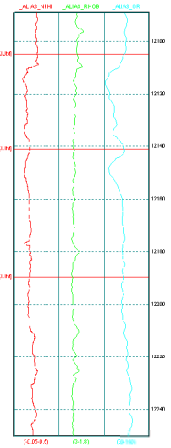

MOORE FEDERAL NO 1-1
603FRNR
T40N R75W S1
49009210570000

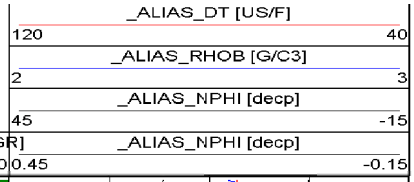

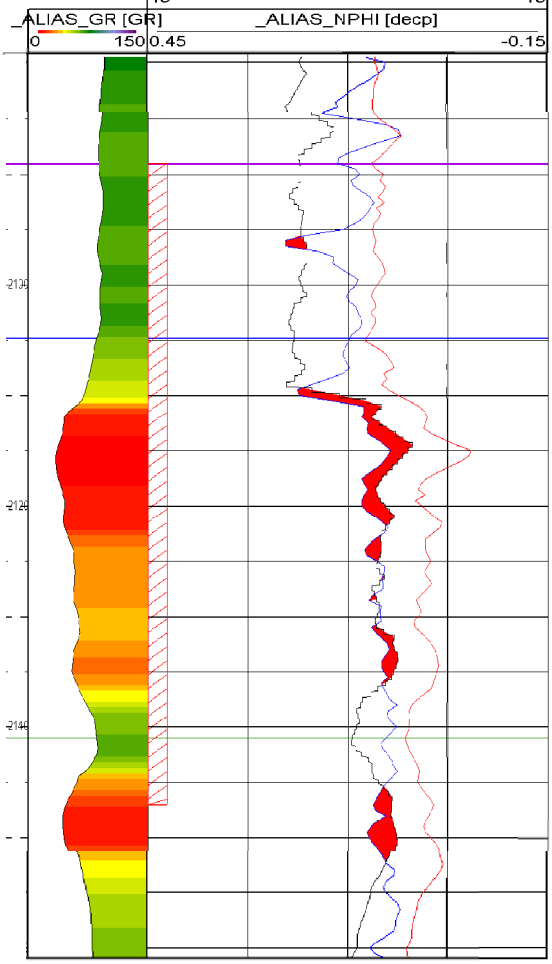

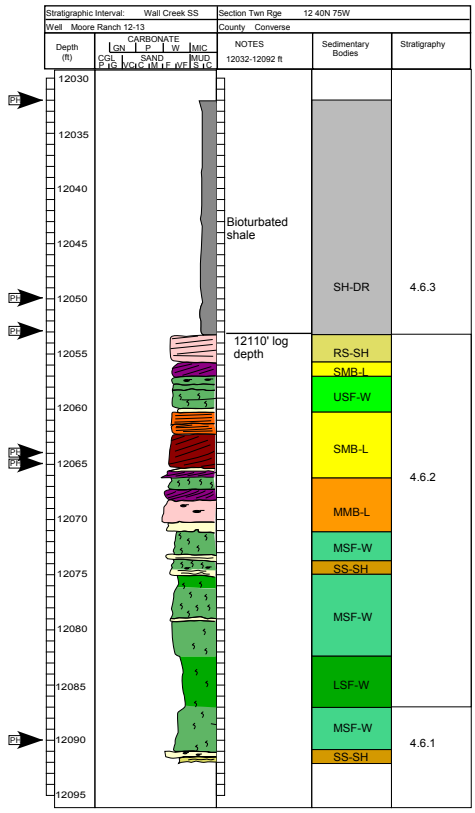

DILTS FEDERAL NO 1 30

T40N R71W S30
49009224980000

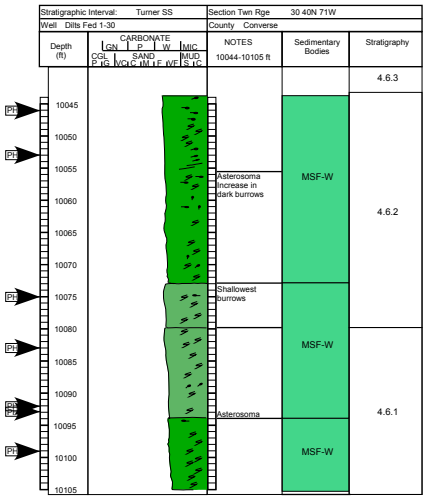

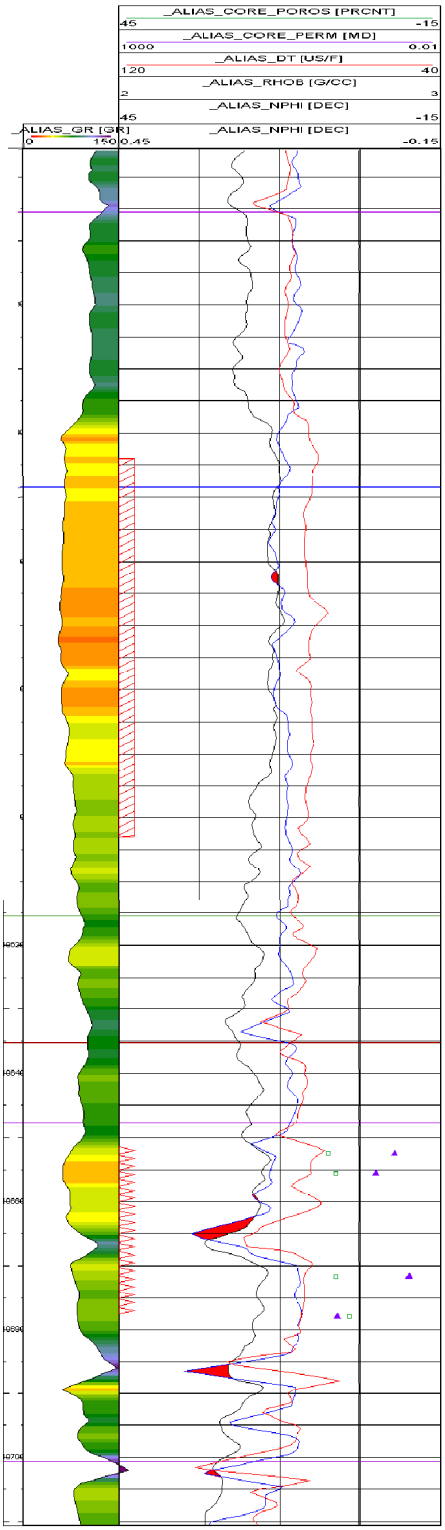

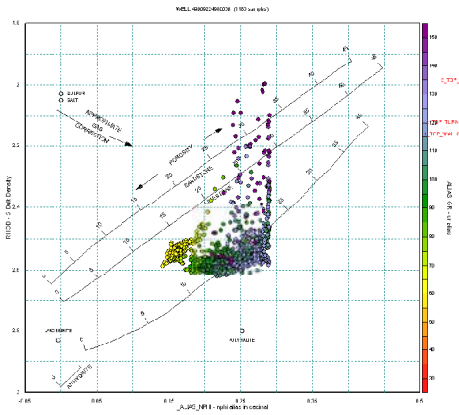

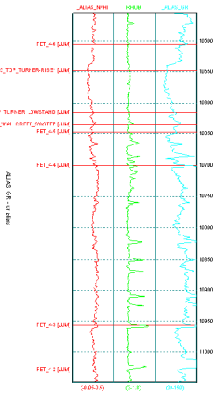

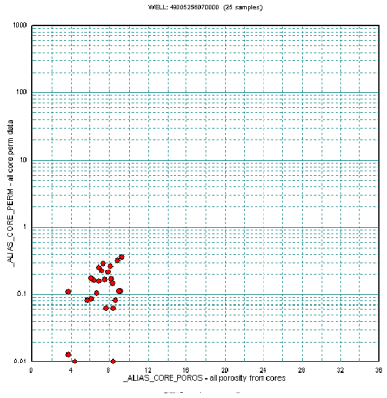

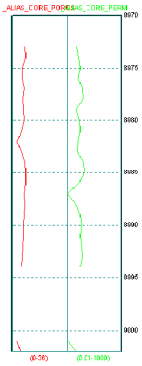

CONNELLY FEDERAL 1

T41N R69W S30

49005256070000

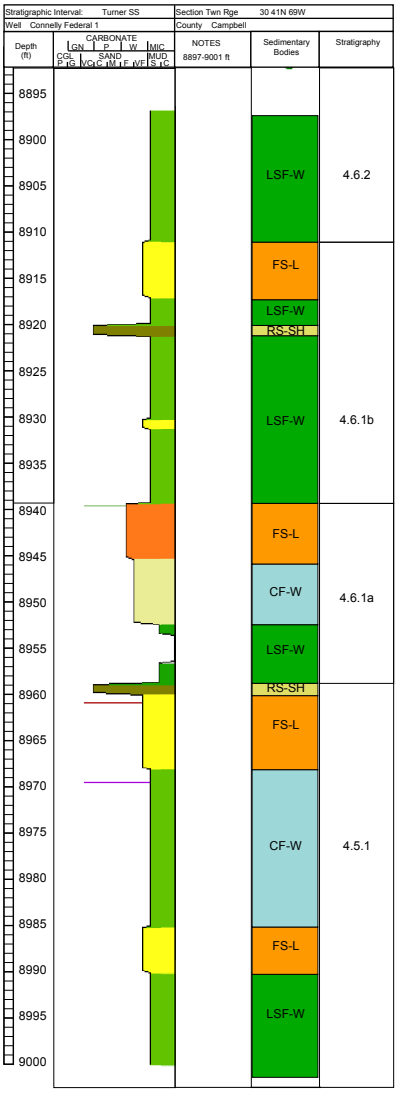

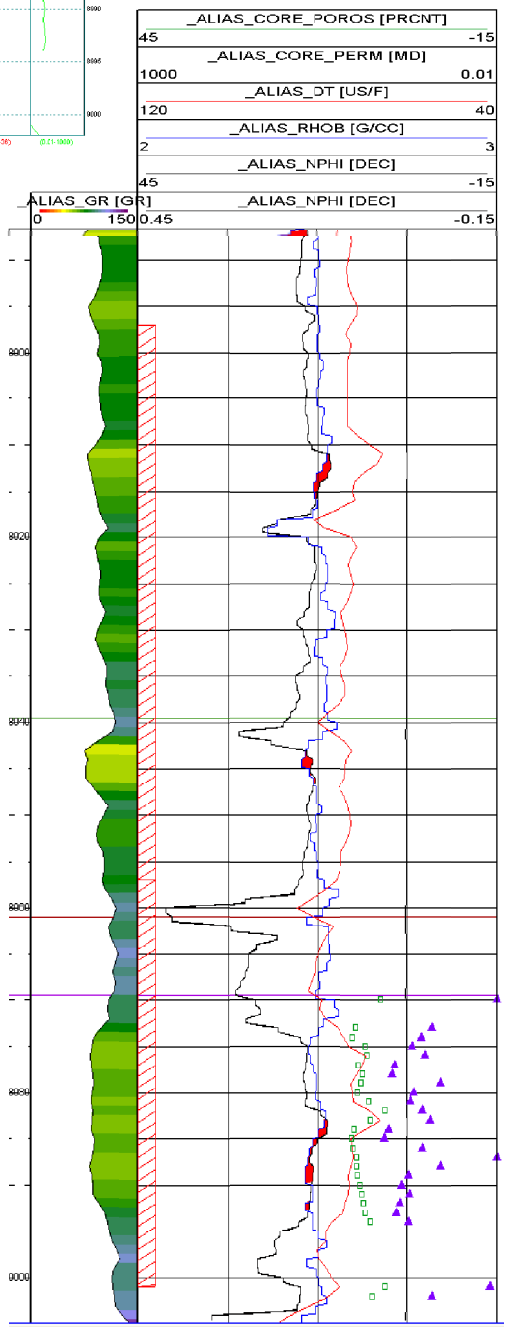

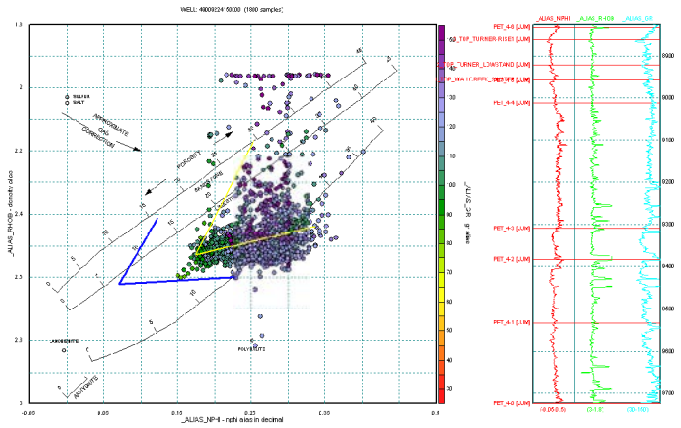

FLEMING FEDERAL 24 1

T37N R68W S1

49009224150000

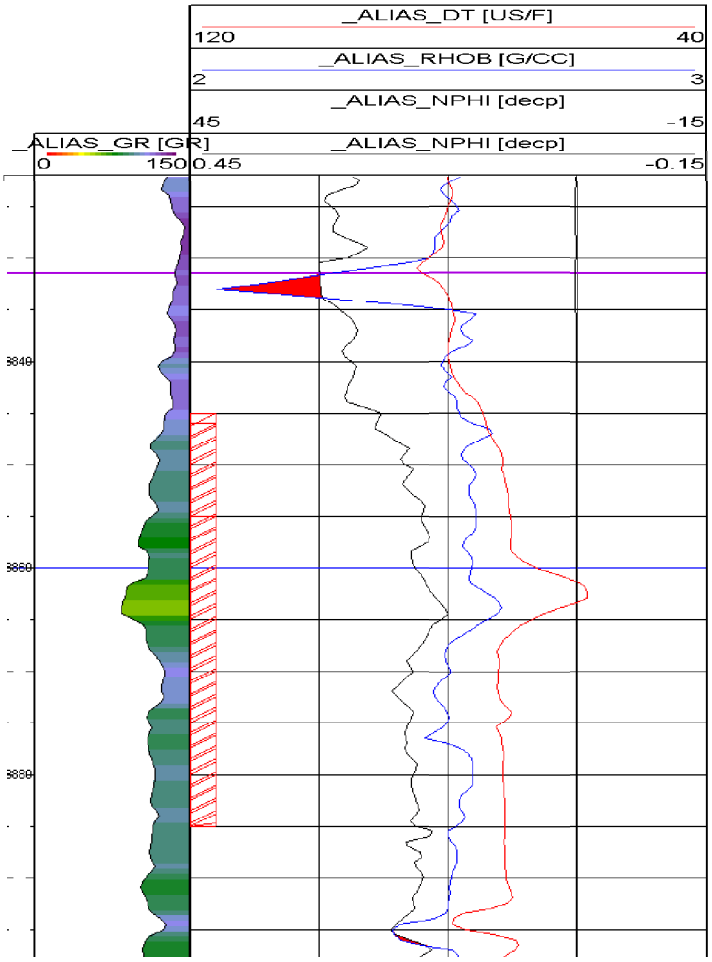

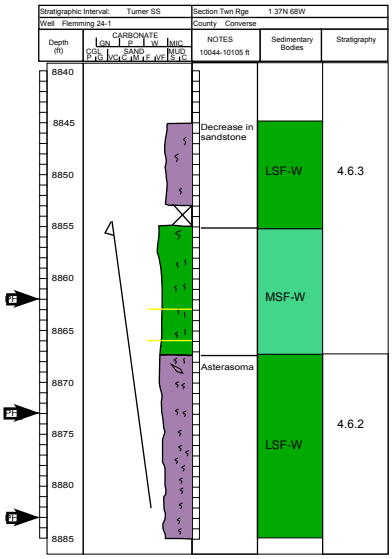

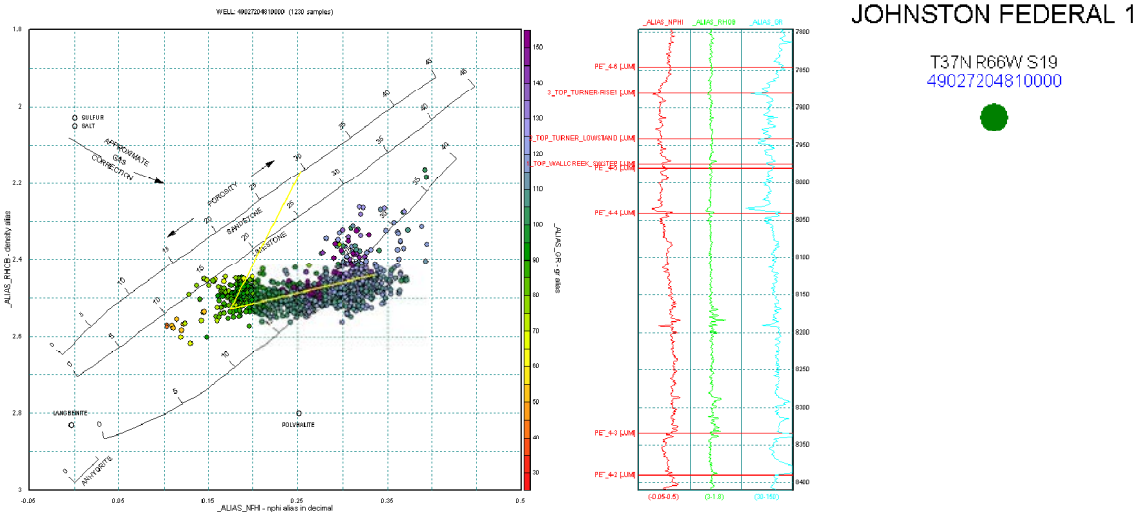
JOHNSTON FEDERAL 1
T37N R66W S19
49027204810000

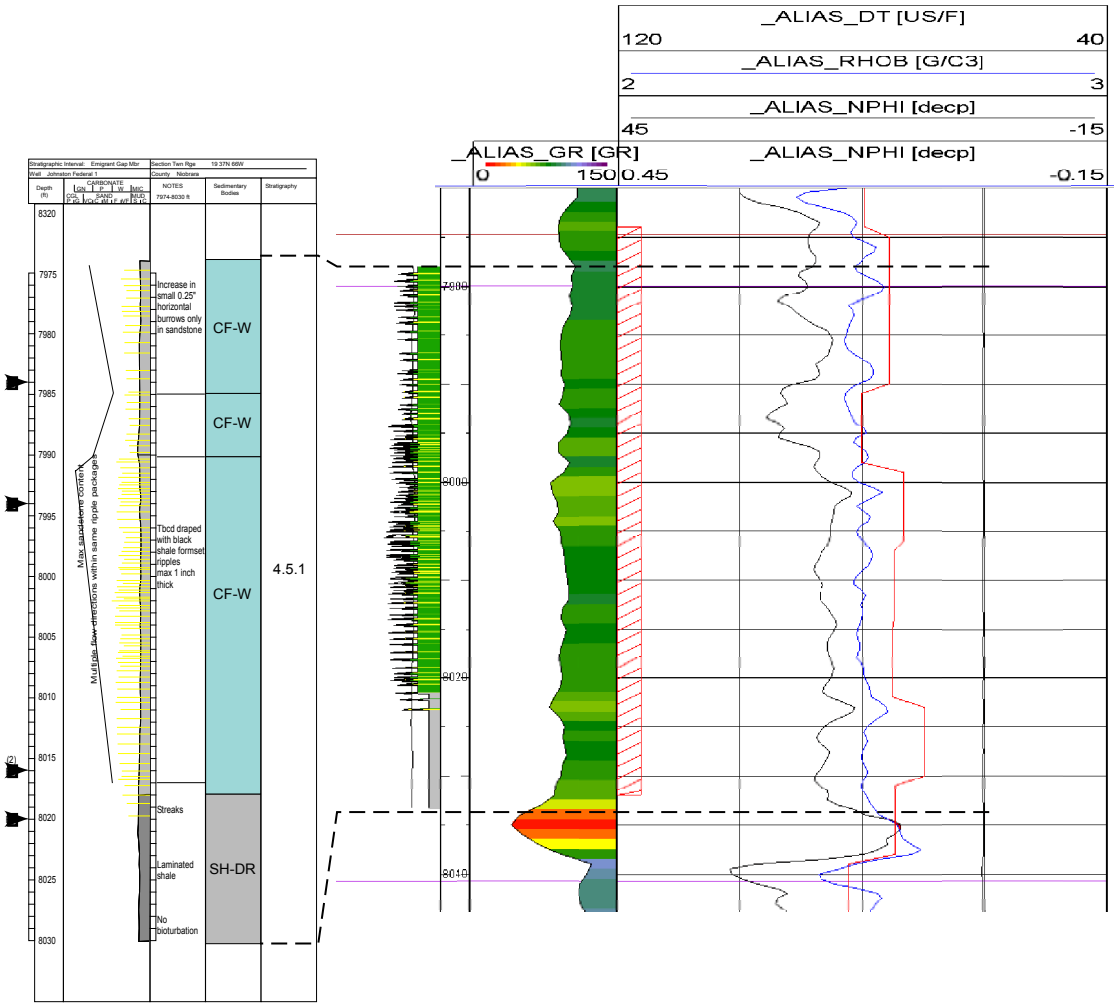
_ALIAS_DT [US/F]
120
40
_ALIAS_RHOB [G/C3]
2
3
_ALIAS_NPHI [decp]
45
-15
_ALIAS_GR [GR]
_ALIAS_NPHI [decp]
0
150
0.45
-0.15
Increase in small 0.25" horizontal burrows only in sandstone
CF-W
CF-W
Tbcd draped with black shale formset ripples max 1 inch thick
CF-W
4.5.1
Streaks
Laminated shale
No bioturbation
SH-DR

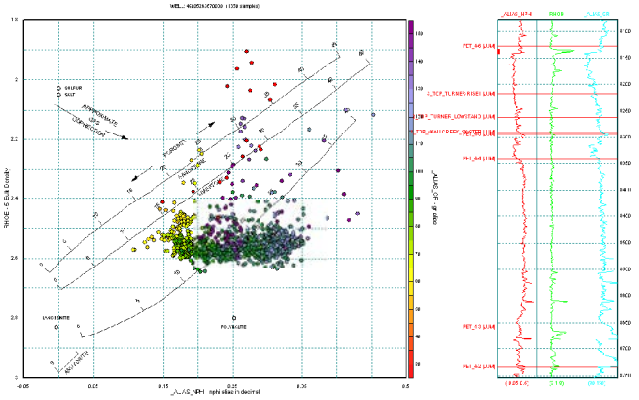

KELLY NO-1-3

T44N R70W S3

49005263670000

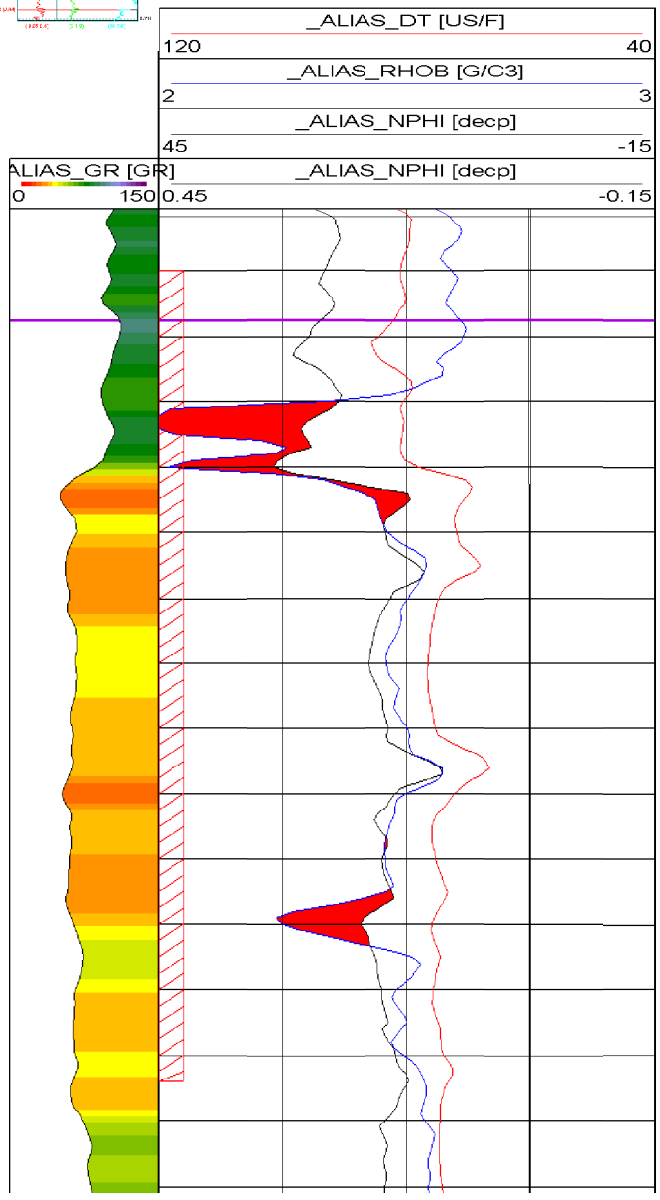

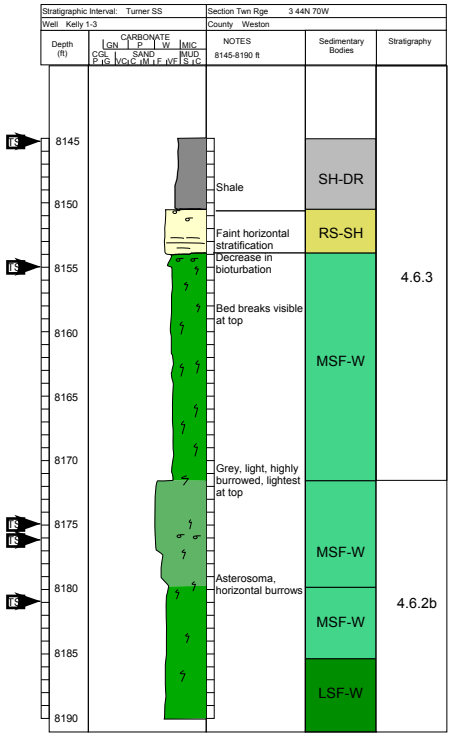

CITIES FEDERAL NO-1-8
603TRNR
T44N R68W S8
49045215420000

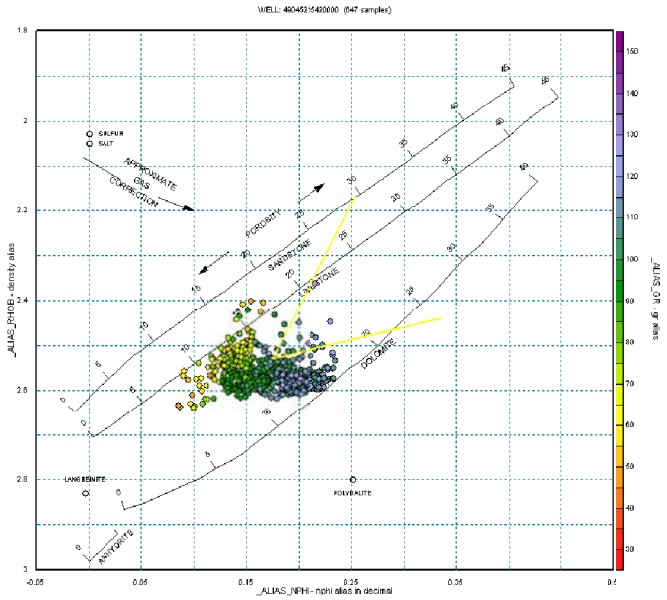

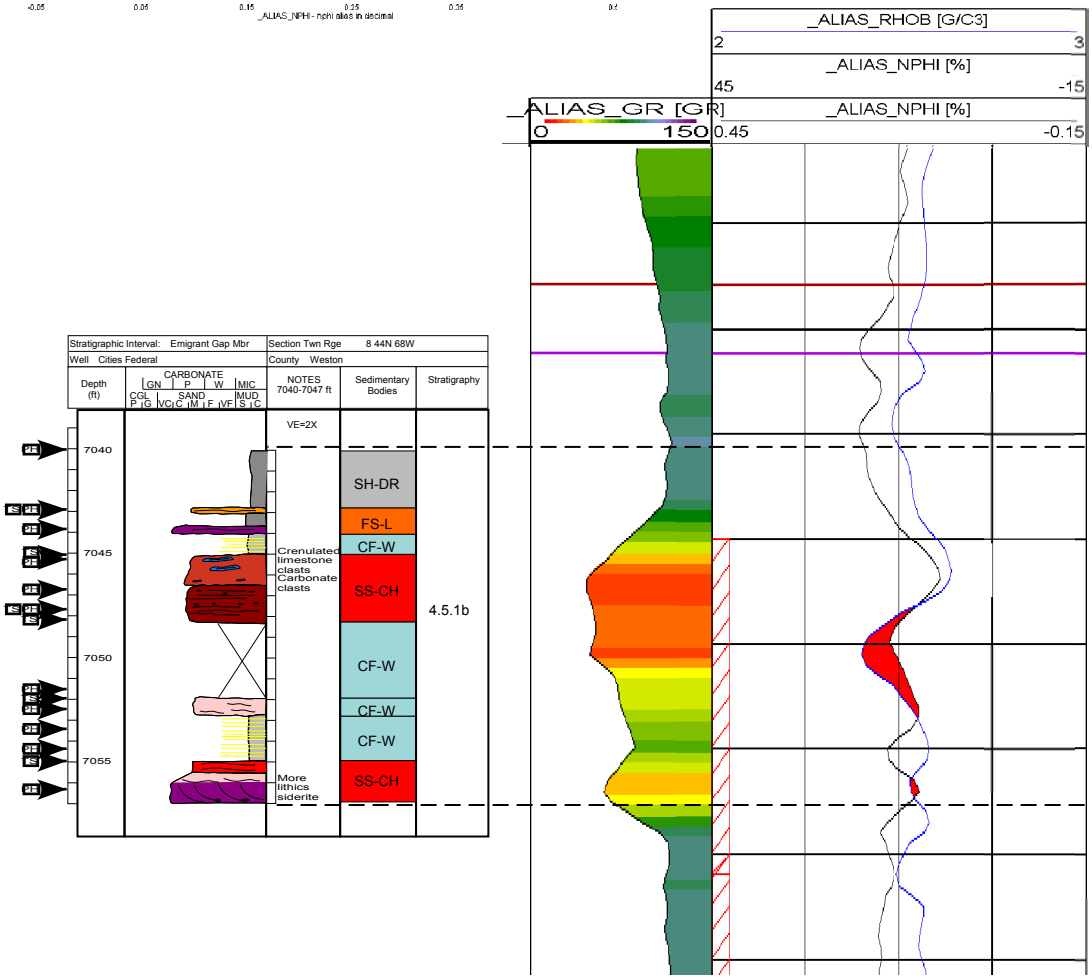

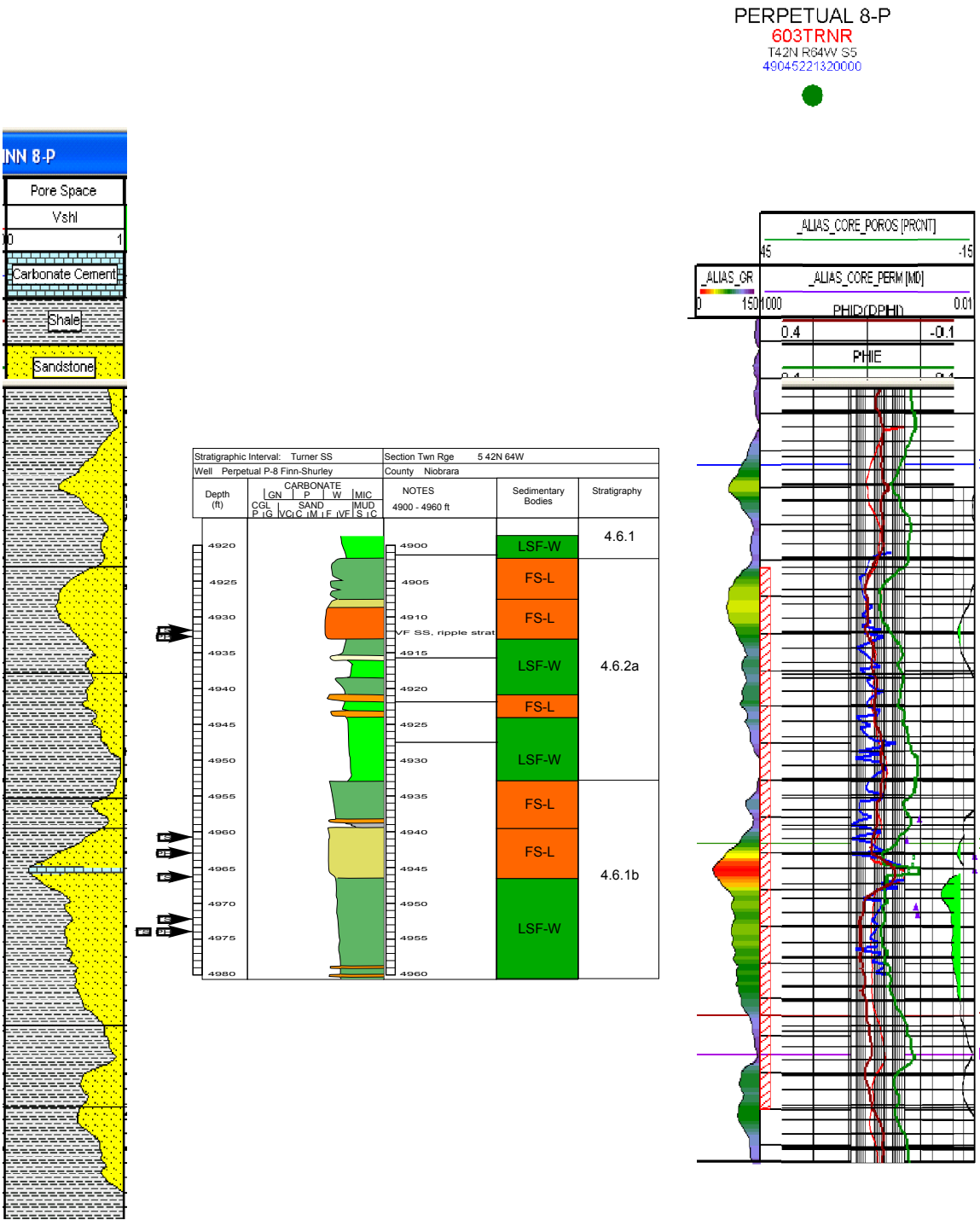
PERPETUAL 8-P
603TRNR
T42N R64W S5
49045221320000
NN 8-P
Pore Space
Vshl
0
1
Carbonate Cement
Shale
Sandstone
Stratigraphic Interval: Turner SS
Section Twn Rge 5 42N 64W
Well Perpetual P-8 Finn-Shurley
County Niobrara
Depth (ft)
CARBONATE
GN P W MIC
CGL SAND MUD
P G VC C M F VF S C
NOTES
4900 - 4960 ft
Sedimentary Bodies
Stratigraphy
4920
4925
4930
4935
4940
4945
4950
4955
4960
4965
4970
4975
4980
4900
4905
4910
VF SS, ripple strat
4915
4920
4925
4930
4935
4940
4945
4950
4955
4960
LSF-W
FS-L
FS-L
LSF-W
FS-L
LSF-W
FS-L
FS-L
LSF-W
4.6.1
4.6.2a
4.6.1b
_ALIAS_CORE_POROS [PRONT]
45
-15
_ALIAS_GR
0
150
_ALIAS_CORE_PERM [MD]
1000
0.01
PHID (DPHID)
0.4
-0.1
PHIE

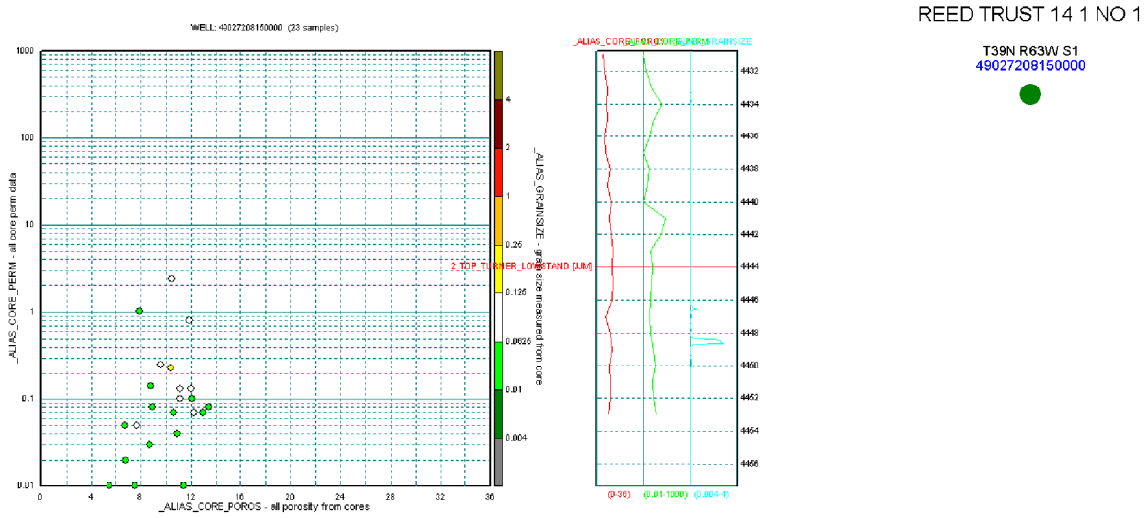
REED TRUST 14 1 NO 1
T39N R63W S1
49027208150000
WELL: 49027208150000 (33 samples)
_ALIAS_CORE_PERM - all core perm data
_ALIAS_CORE_POROS - all porosity from cores
_ALIAS_GRAINSIZE - grain size measured from core
_ALIAS_CORE_POROS _ALIAS_CORE_PERM _ALIAS_GRAINSIZE

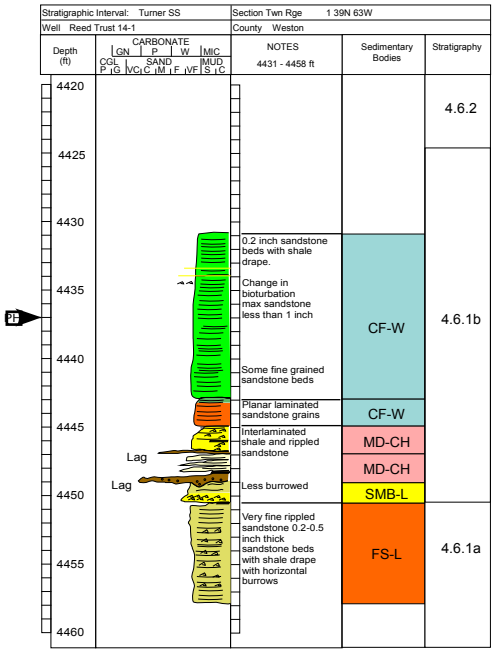
Stratigraphic Interval: Turner SS
Section Twn Rge 1 39N 63W
Well Reed Trust 14-1
County Weston
Depth (ft)
CARBONATE
SAND
NOTES
4431 - 4458 ft
Sedimentary Bodies
Stratigraphy
0.2 inch sandstone beds with shale drape.
Change in bioturbation max sandstone less than 1 inch
Some fine grained sandstone beds
Planar laminated sandstone grains
Interlaminated shale and rippled sandstone
Lag
Lag
Less burrowed
Very fine rippled sandstone 0.2-0.5 inch thick sandstone beds with shale drape with horizontal burrows
CF-W
CF-W
MD-CH
MD-CH
SMB-L
FS-L
4.6.2
4.6.1b
4.6.1a

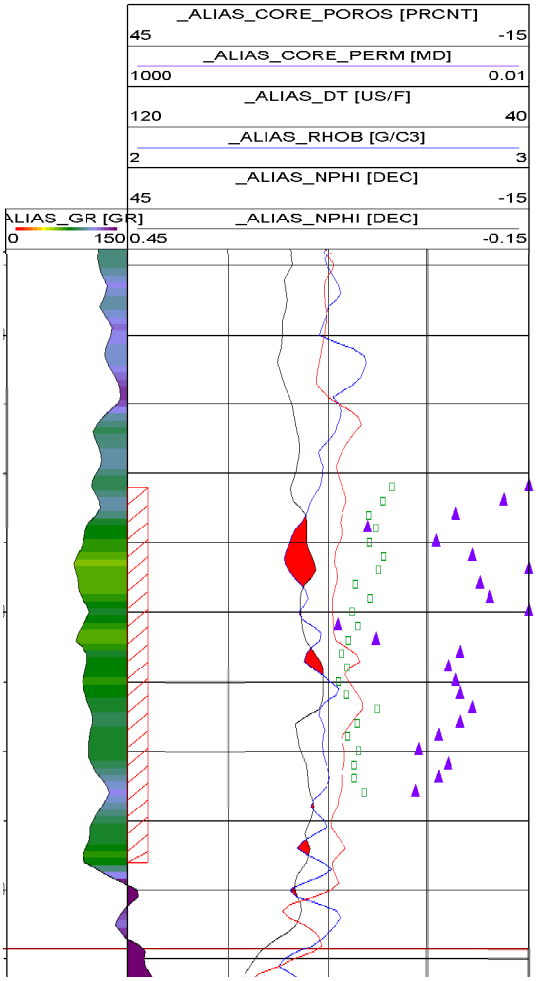
_ALIAS_CORE_POROS [PRCNT]
45 -15
_ALIAS_CORE_PERM [MD]
1000 0.01
_ALIAS_DT [US/F]
120 40
_ALIAS_RHOB [G/C3]
2 3
_ALIAS_NPHI [DEC]
45 -15
ALIAS_GR [GR]
0 150
_ALIAS_NPHI [DEC]
0.45 -0.15

APPENDIX B:

SEDIMENTARY BODIES DESCRIPTIONS OF THE FRONTIER FORMATION

Appendix B.

Sedimentary body descriptions.

Sedimentary Body Explanation

	Code	Lithology	Body type	Interpretation
1	SS-CH	sandy	channelform	distributary (submarine) channel fill
2	MD-CH	muddy/heterolithic	channelform	underfilled (submarine) channel - tidal?
3	SMB-L	sandy mouthbar	lobe	proximal mouthbar
4	MMB-L	muddy-sandy mouthbar	lobe	distal/lateral/inter mouthbar
5	FS-L	sand and shale	lobe	frontal splay / turbidite lobe
6	RS-SH	reworked sandstone	sheet	transgressive lag
7	SS-SH	sand	sheet	storm deposit - turbidite
8	USF-W	sandy-silt	wedge	upper shoreface
9	MSF-W	silty-sand	wedge	middle shoreface
10	LSF-W	shaly-silt	wedge	lower shoreface
11	CF-W	sand and shale	wedge	submarine channel levee
12	SH-DR	shale	drape	suspension deposits, sediment starved

Frontier Facies Explanation

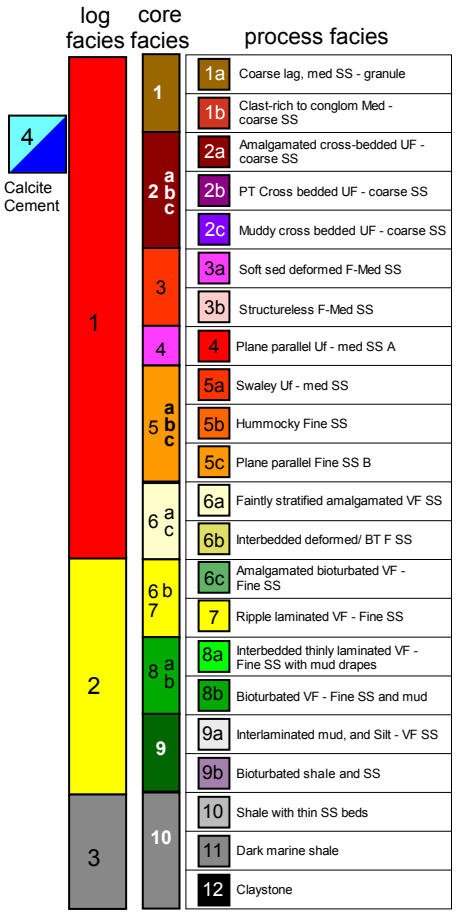

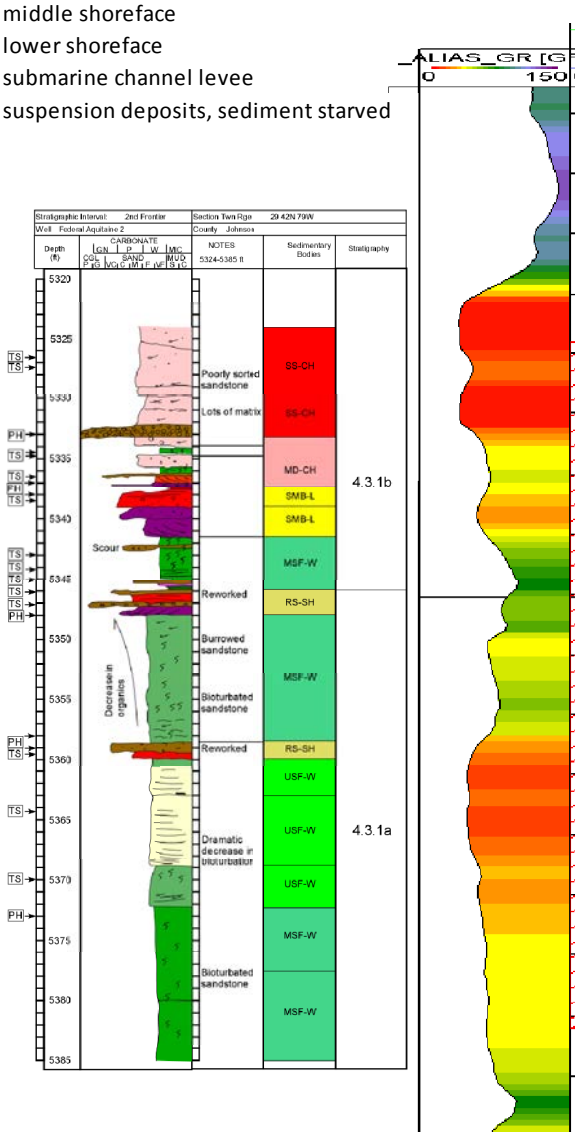

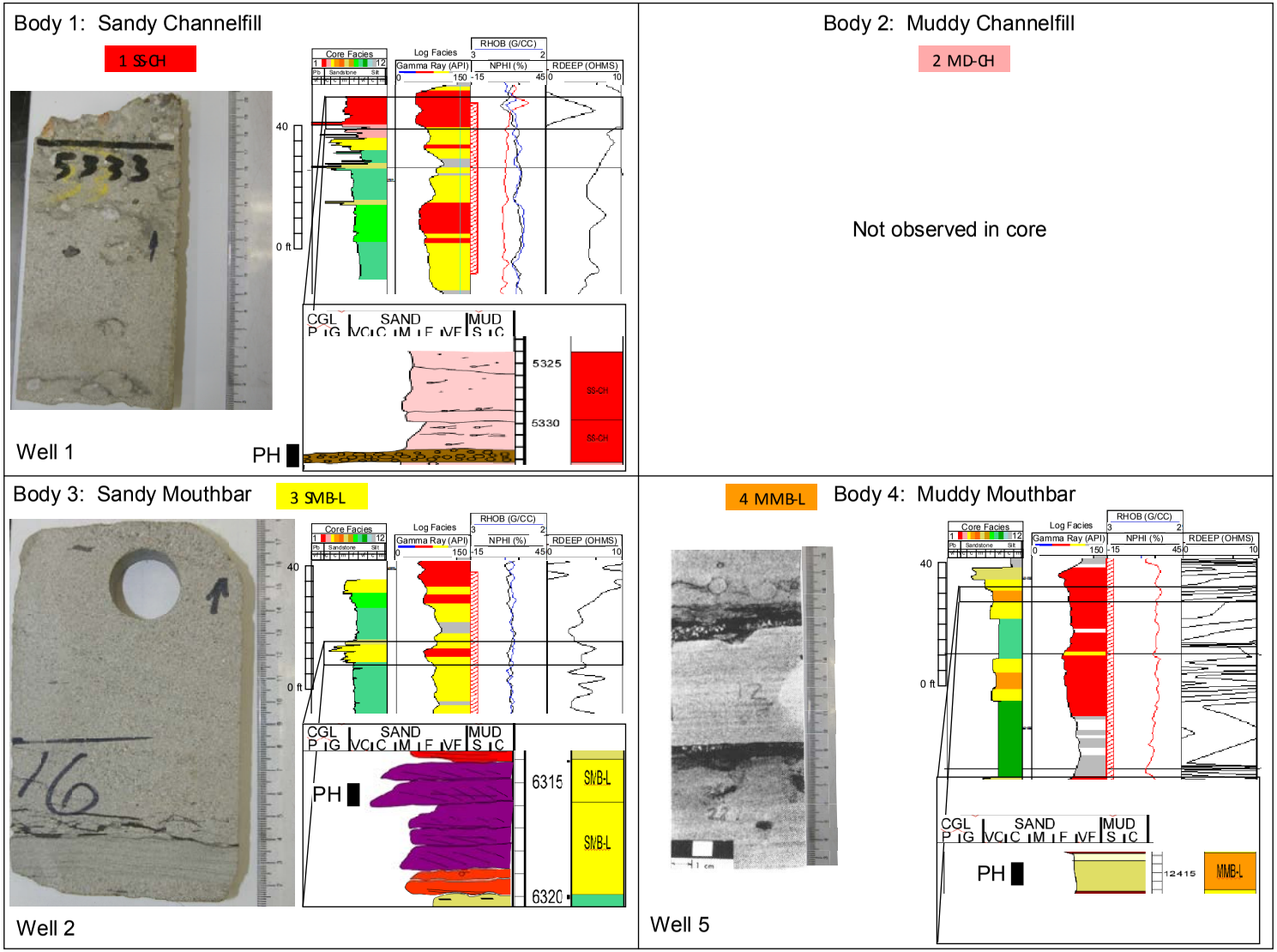

Appendix B. Sedimentary bodies identified in the Frontier Fm. Frontier sedimentary bodies. PH indicates core photo location; all units in feet, except 4 inch wide core photos, where depth is in centimeters.

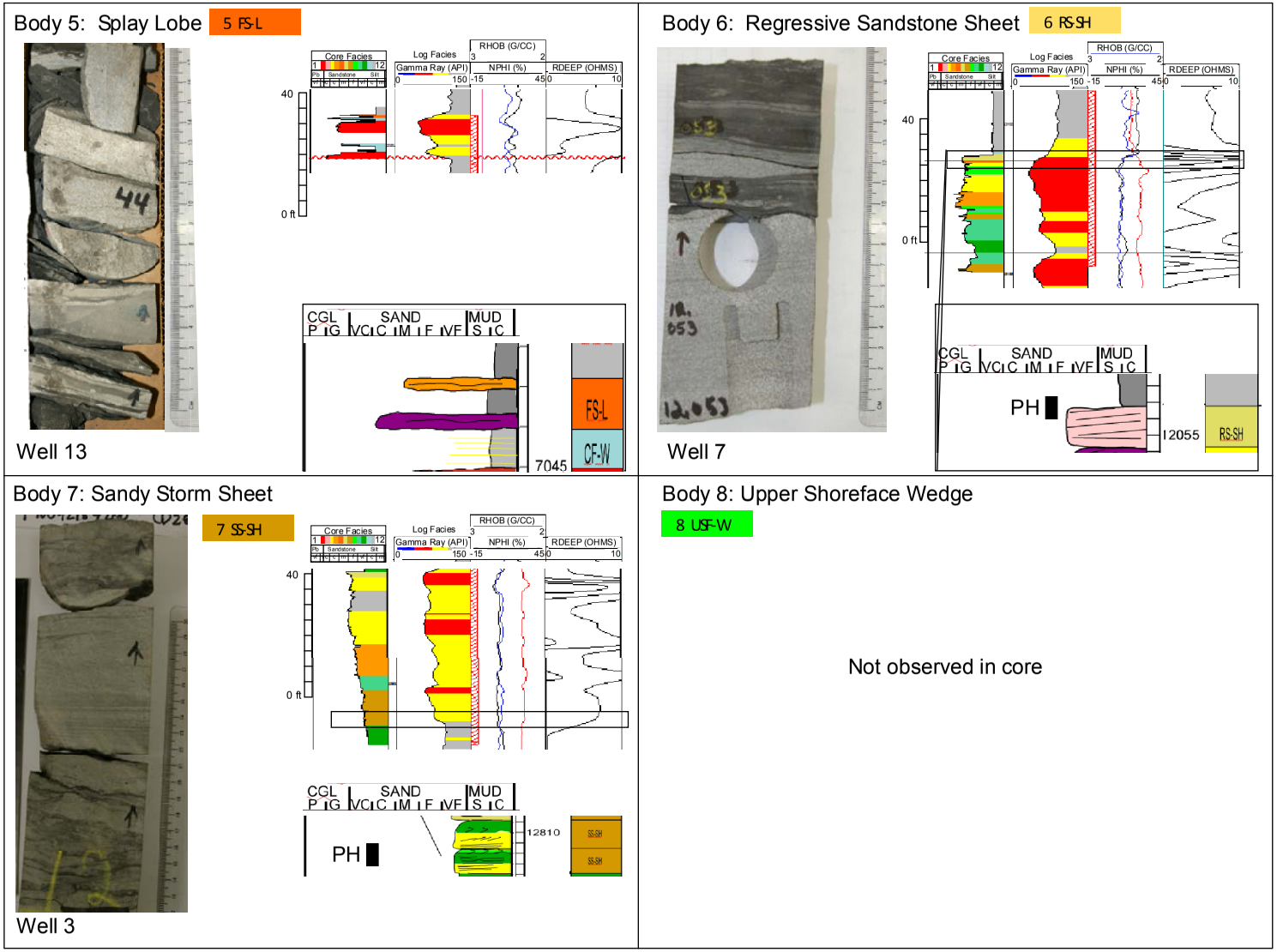

Appendix B continued. Sedimentary bodies identified in the Frontier Fm. Frontier sedimentary bodies. PH indicates core photo location; all units in feet, except 4 inch wide core photos, where depth is in centimeters.

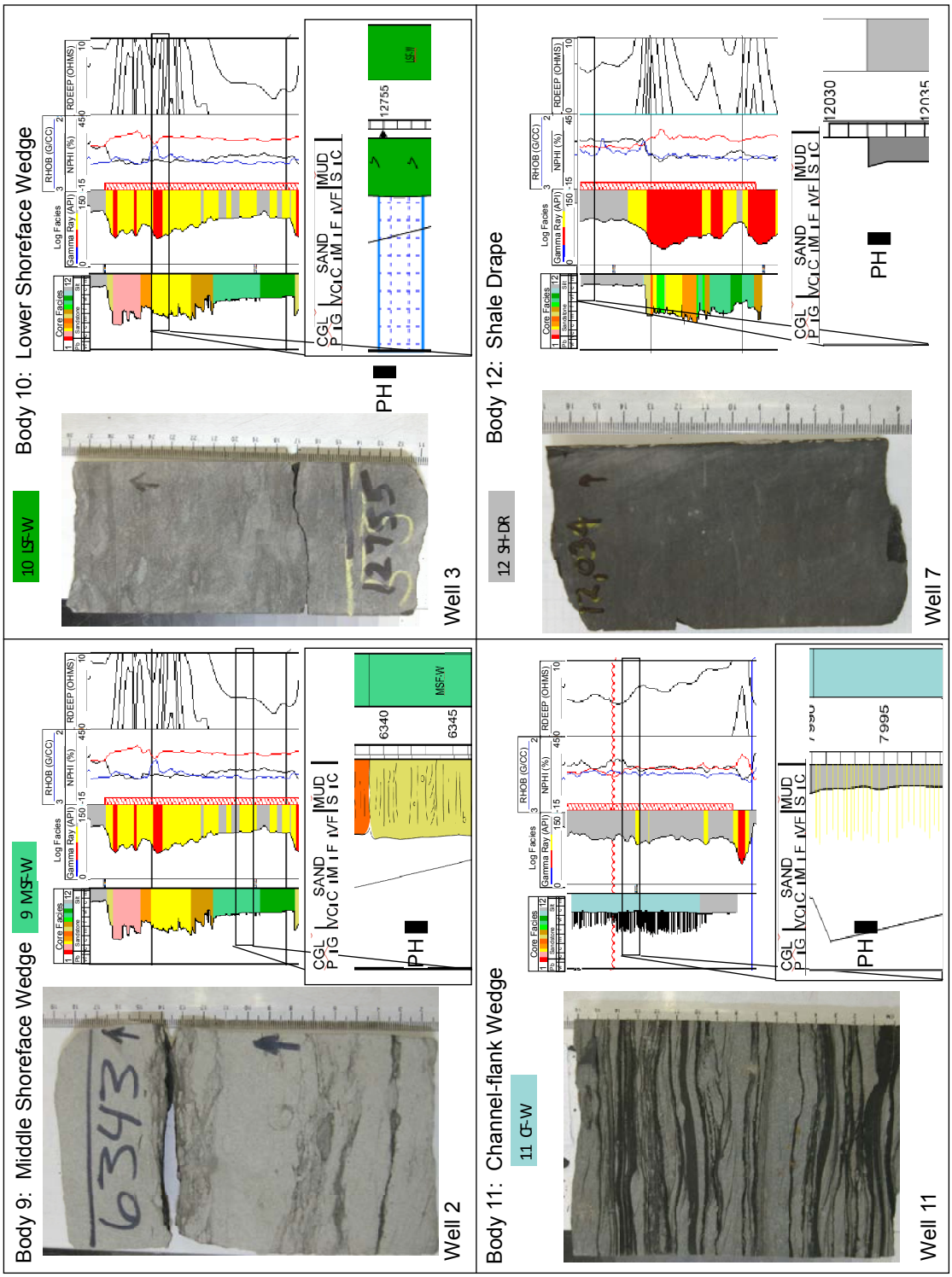

Appendix B continued. Frontier sedimentary bodies. PH indicates core photo location; all units in feet, except 4 inch wide core photos, where depth is in centimeters.

APPENDIX C:

CROSS SECTIONS OF THE FRONTIER FORMATION

Appendix C.
Frontier Cross Sections. Exported from Petra database. Common wells in sections marked. Basemap is from Figure 3.13 and shows distribution of sandstone in Frontier cycle. See Appendix A for core descriptions and explanation of facies. See Figure 3.8 for stratigraphic framework (thick gray cross section line) and explanation of lines used in cross sections.

Well Header Explanation

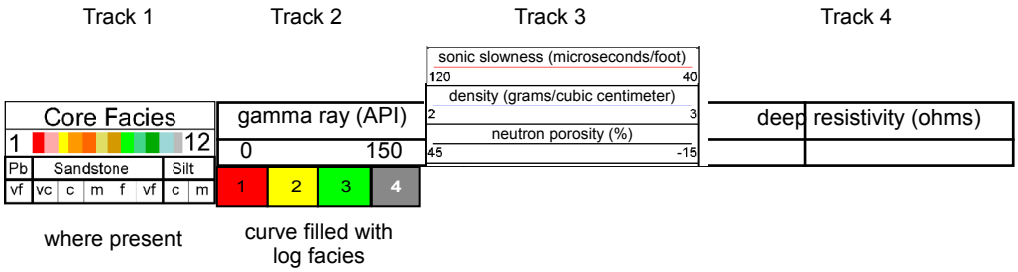

Basemap of Cross Sections

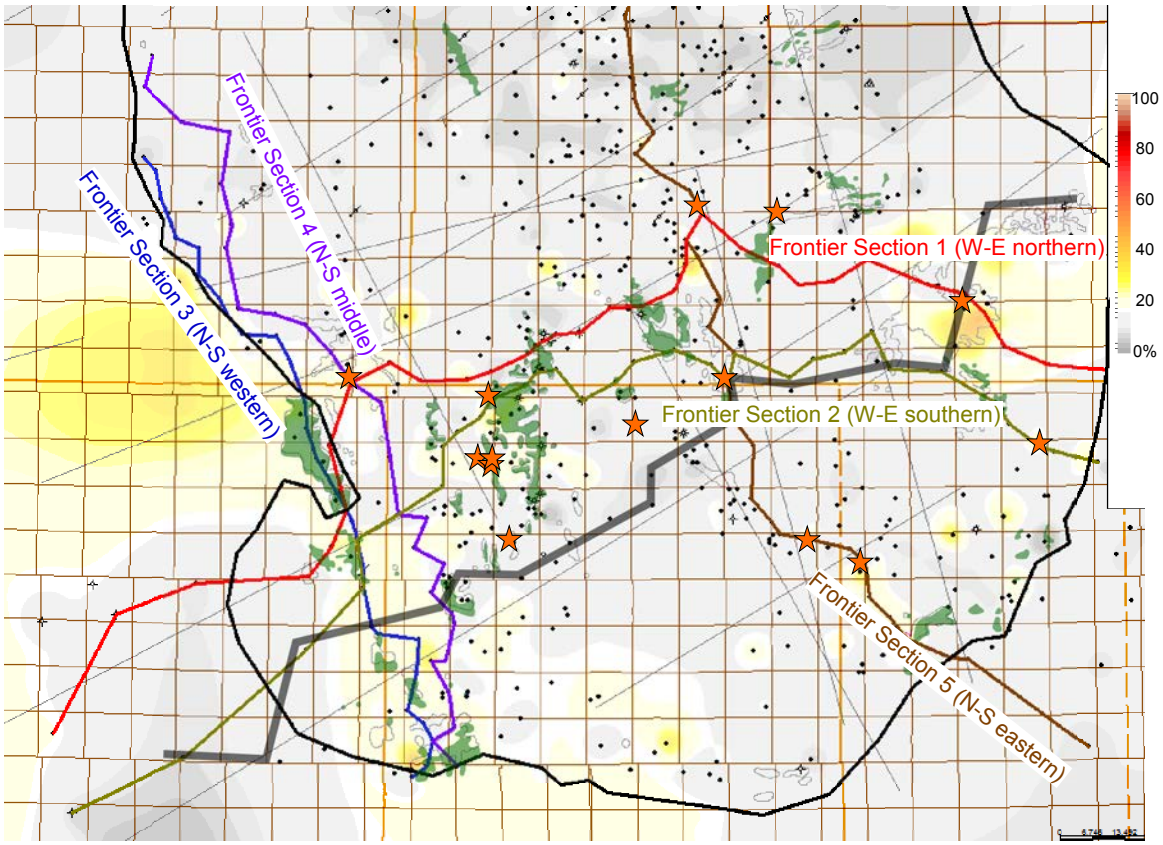

Frontier Section 1 (W-E northern)

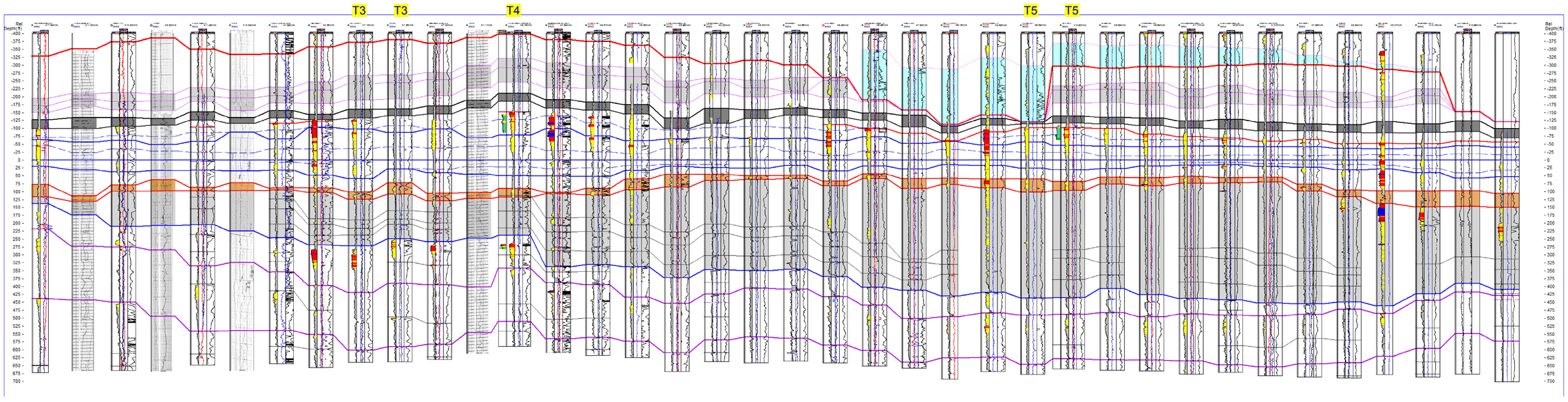

Frontier Section 2 (W-E southern)

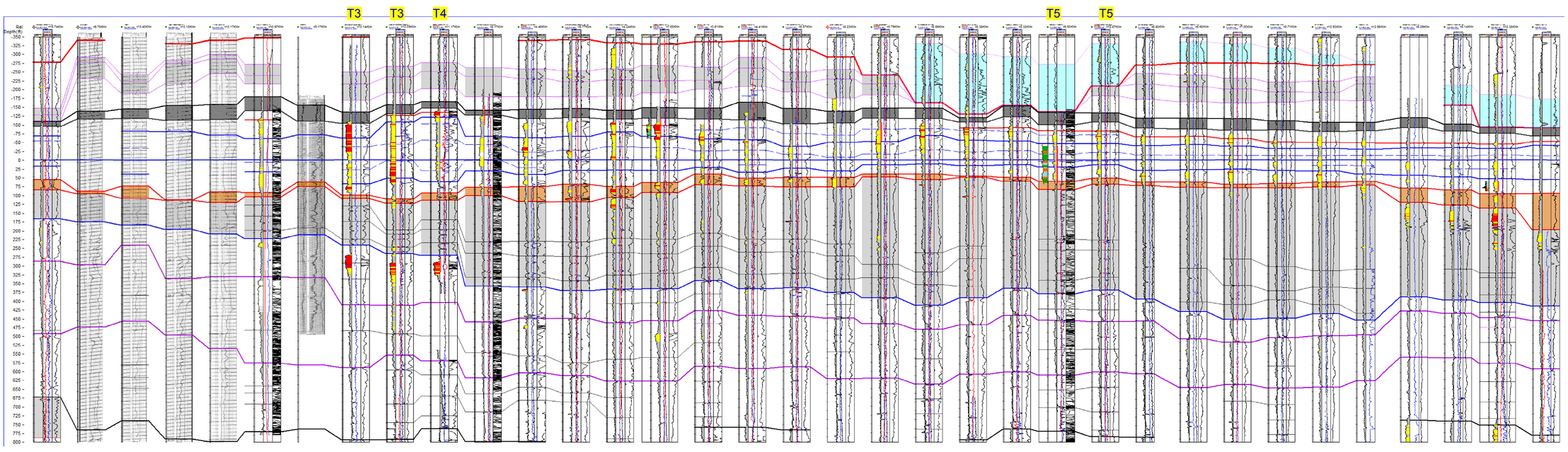

Frontier Section 3 (N-S western)

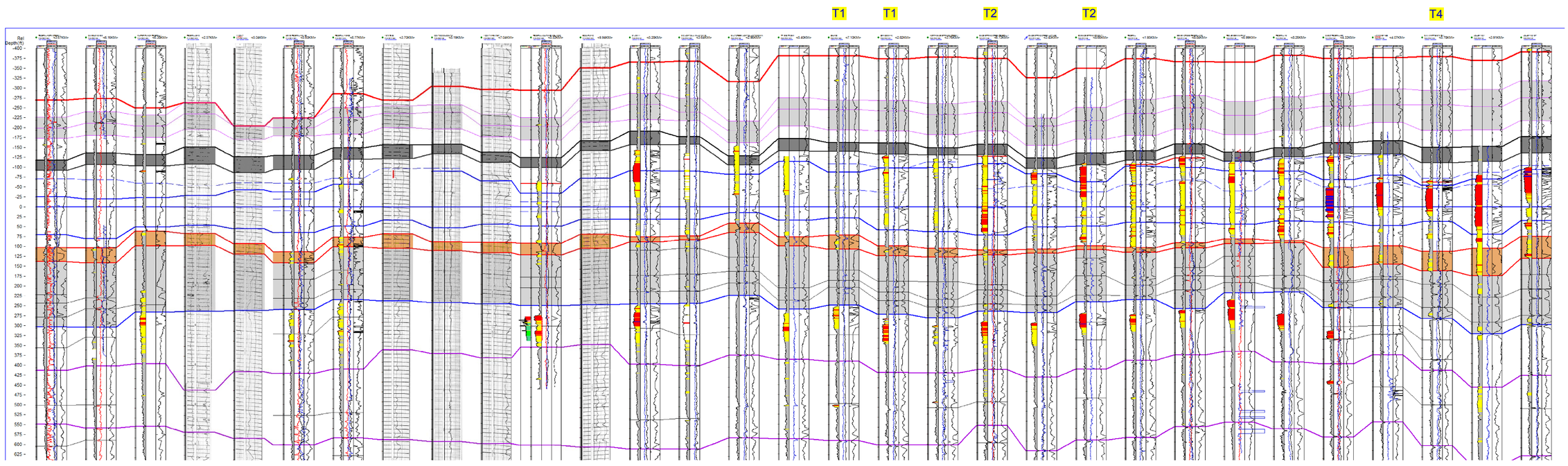

Frontier Section 4 (N-S middle)

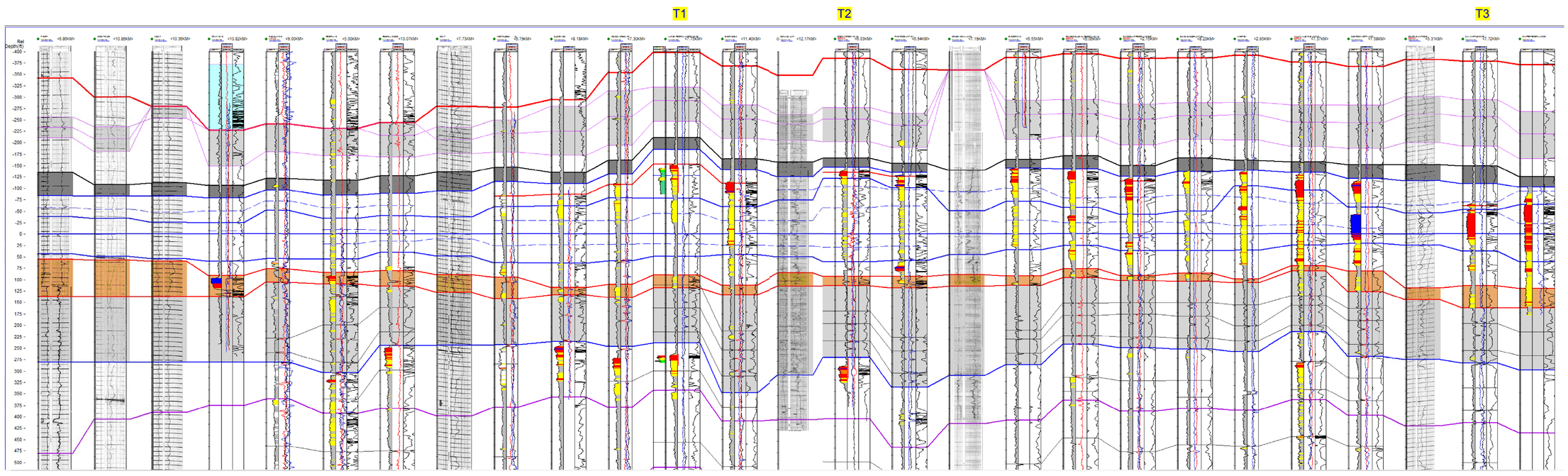

Frontier Section 5 (N-S eastern)

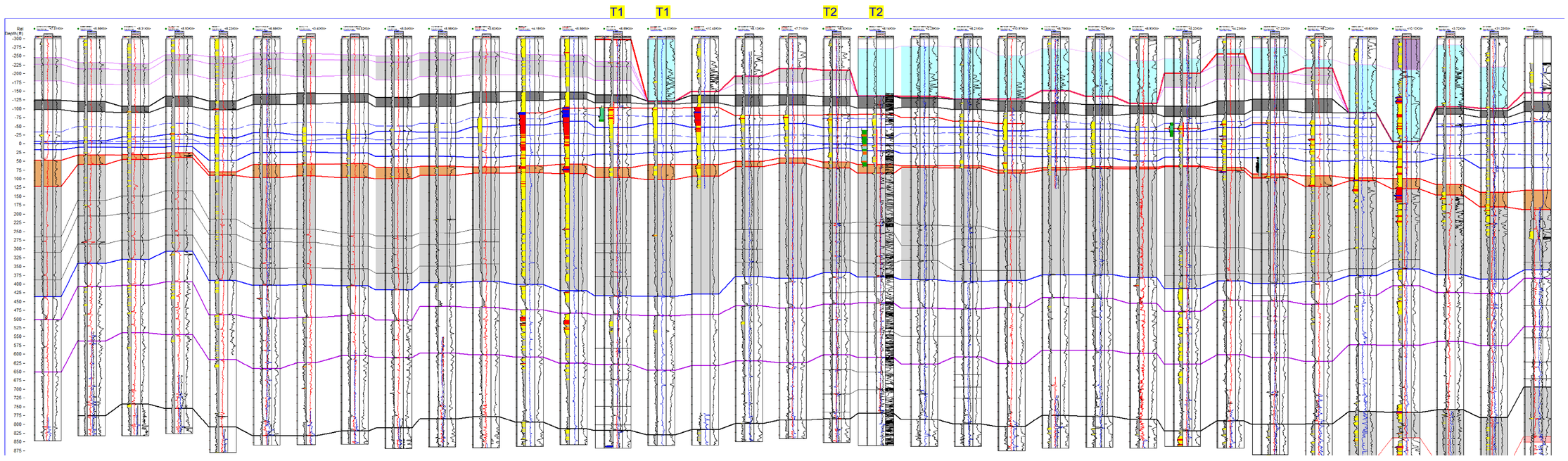

APPENDIX D:

MAPS OF THE FRONTIER FORMATION

Appendix D.
Frontier maps. See Figure 14 for explanation of colors. All thickness is in feet. See Figure 3.8 for explanation of hierarchy (erected along type cross section - gray line). Cores in orange stars below.

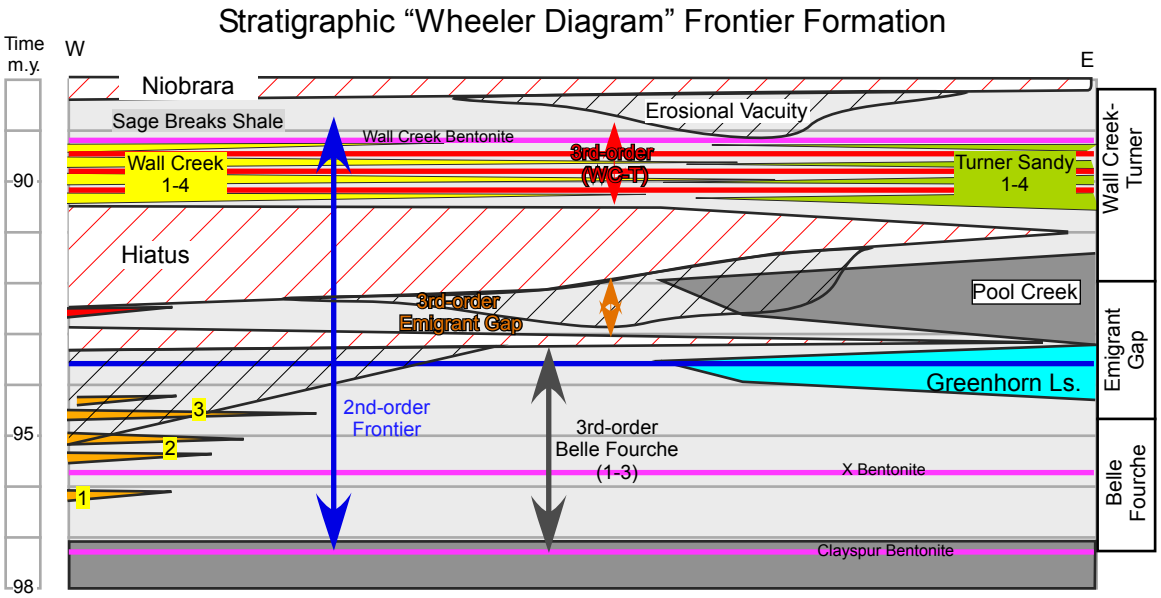

Key to Cross Sections in Appendix 2

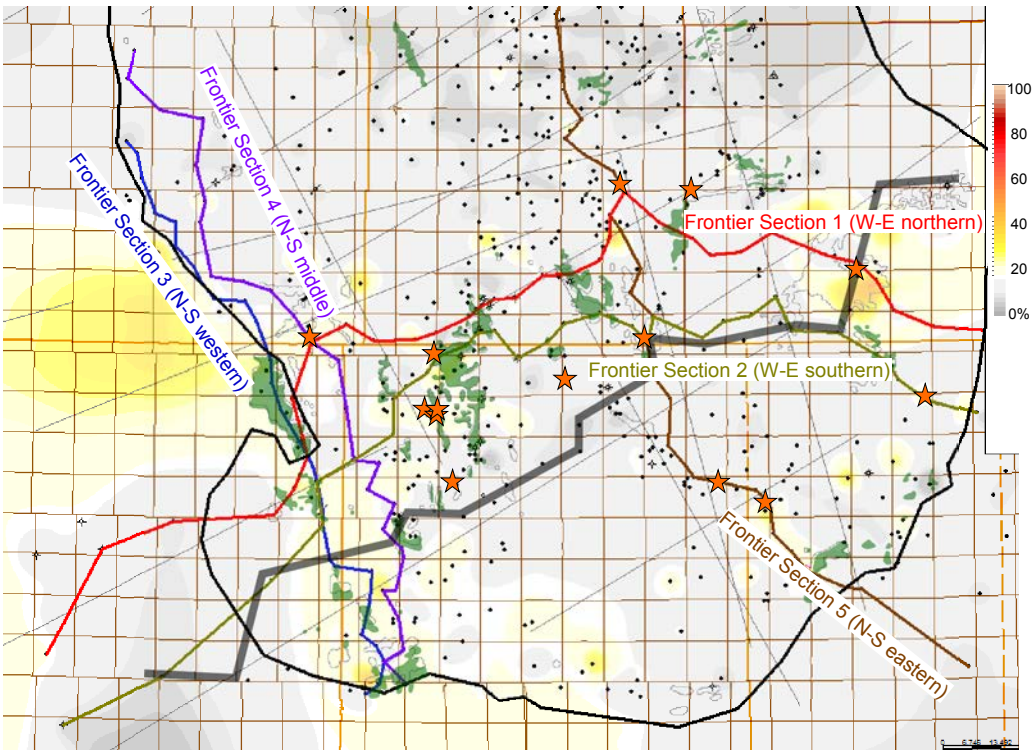

Frontier 3rd-order Cycles

Wall Creek - Turner (WC-T) 4th-order Cycles

Belle Fourche 3rd-order

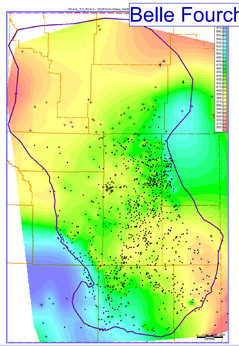

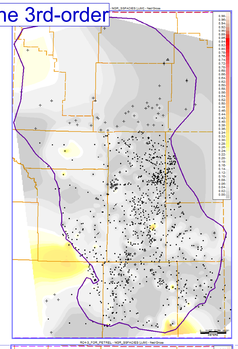

Sage Breaks (upper part of Wall Creek-Turner

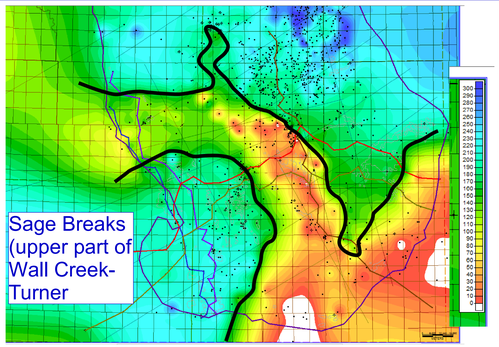

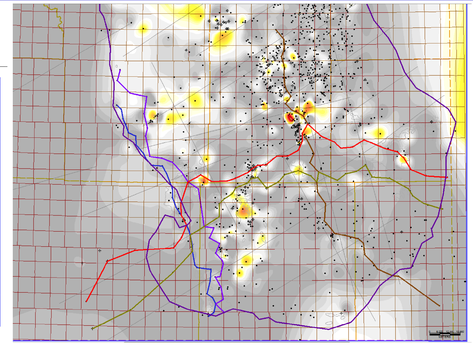

WCT4

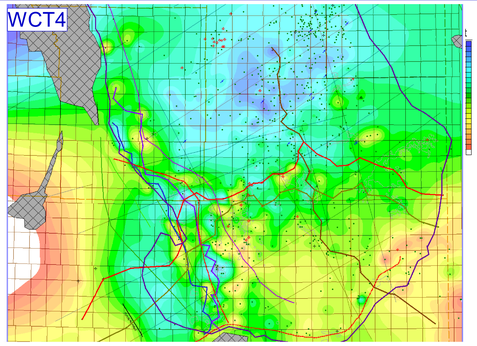

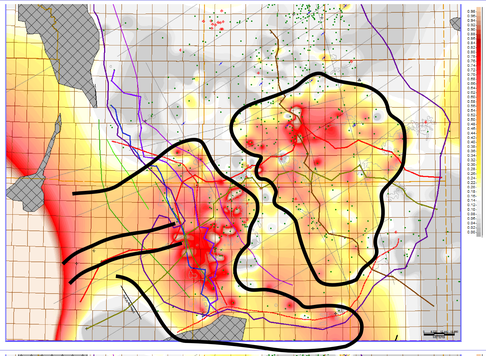

Belle Fourche-3

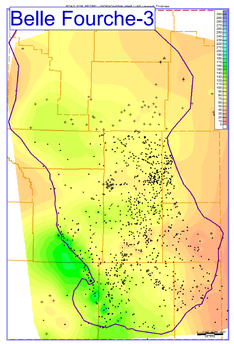

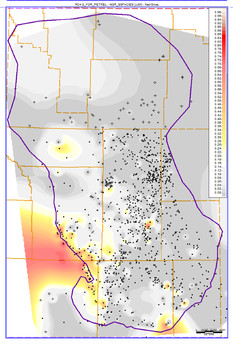

Wall Creek-Turner 3rd-order

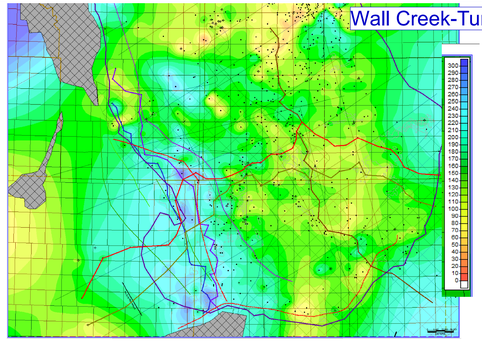

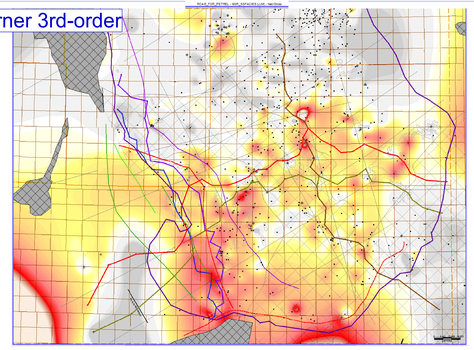

WCT3

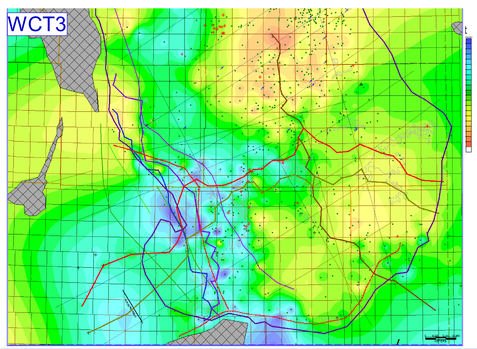

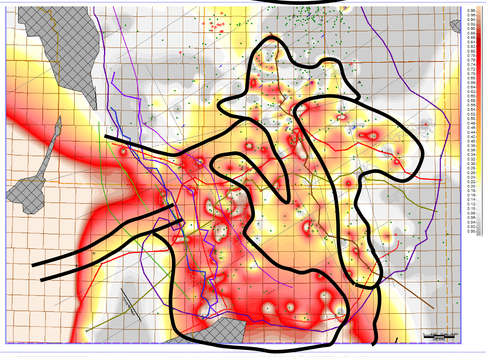

Belle Fourche-2

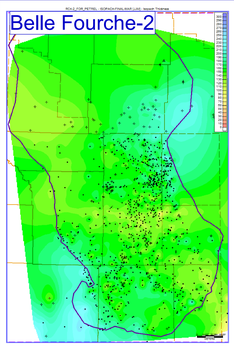

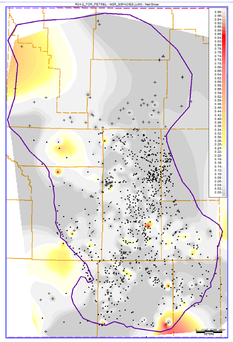

Emigrant Gap 3rd-order

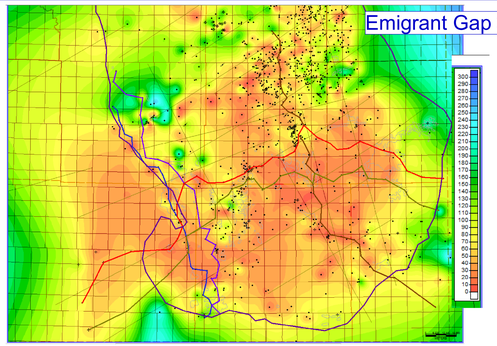

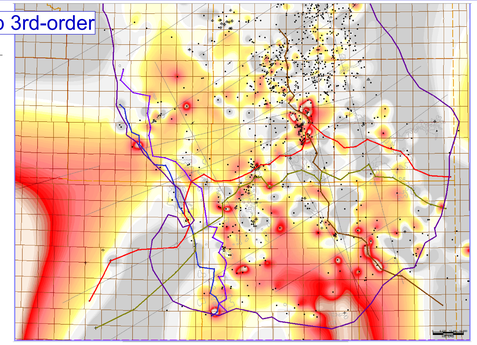

WCT2

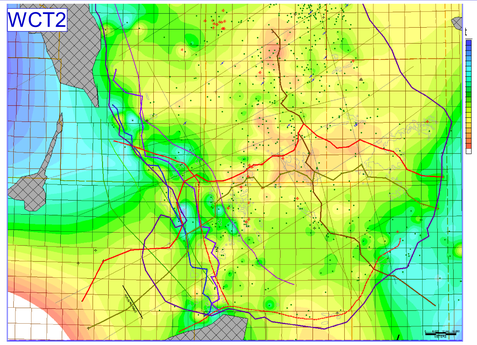

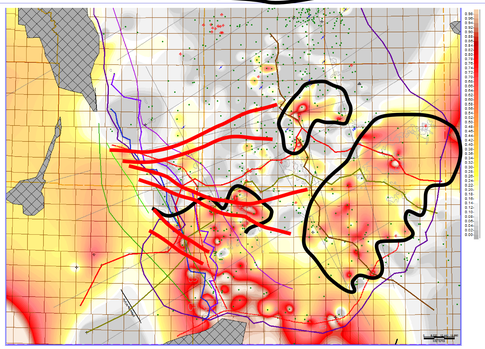

Belle Fourche-1

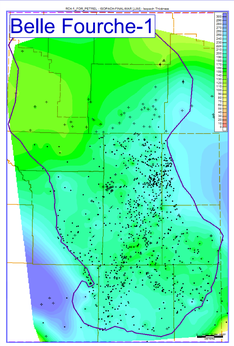

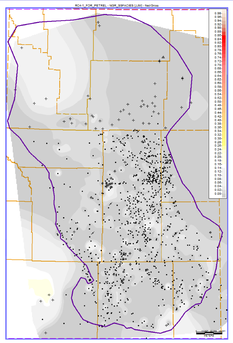

GreenHorn (upper part of Belle Fourche)

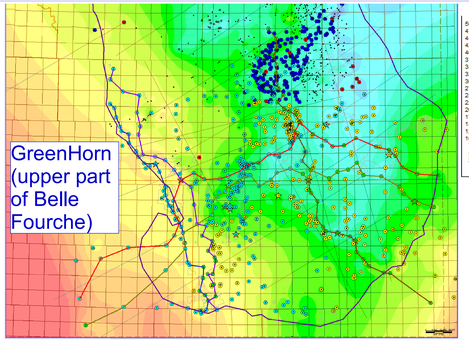

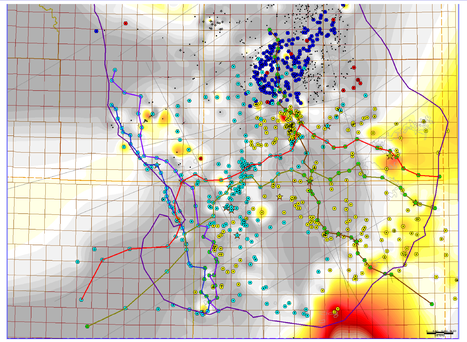

WCT1

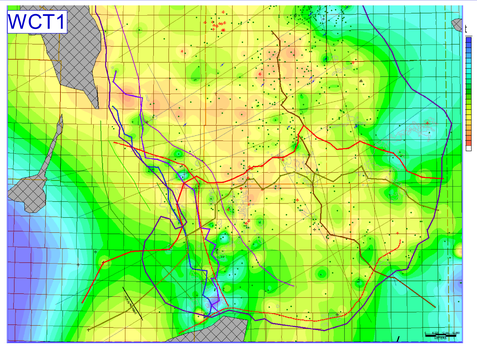

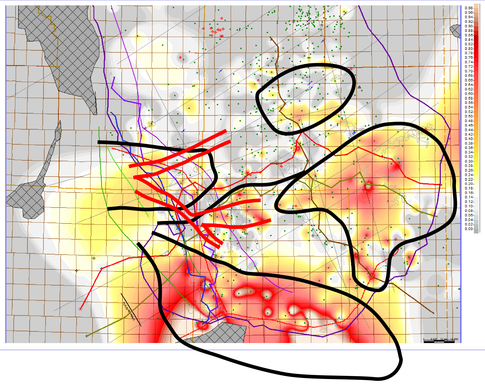

APPENDIX E:

TABLE OF LOG FACIES VALUES

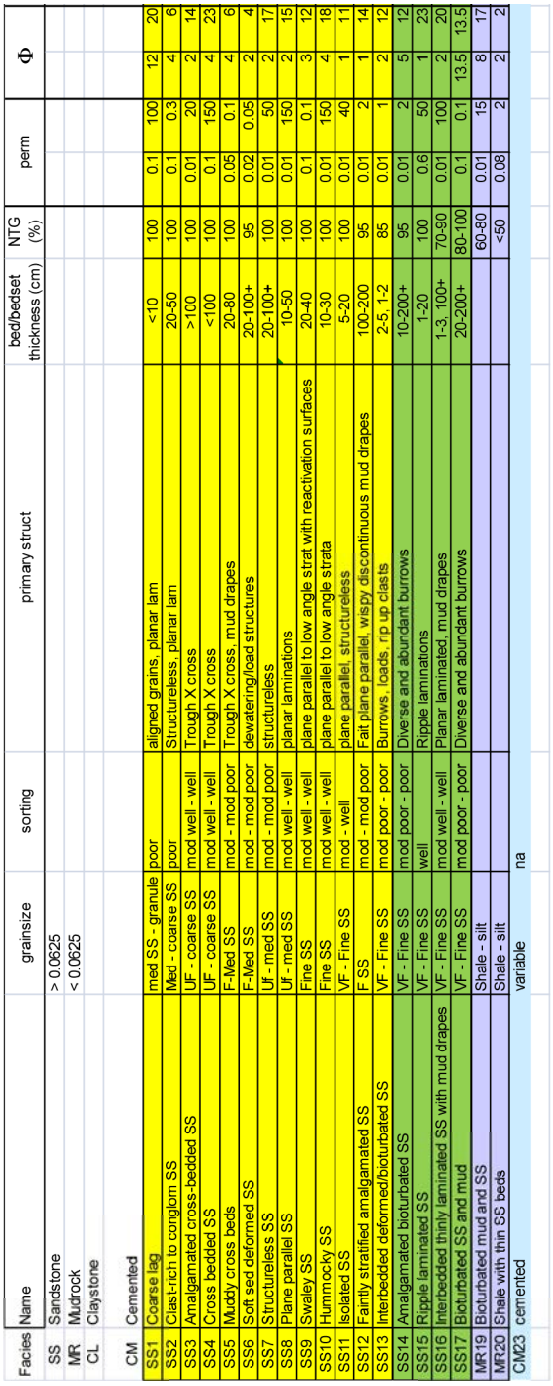

Facies	Name	grainsize	sorting	primary struct	bed/bedset thickness (cm)	NTG (%)	perm	Φ
SS	Sandstone	> 0.0625						
MR	Mudrock	< 0.0625						
CL	Claystone							
CM	Cemented							
SS1	Coarse lag	med SS - granule	poor	aligned grains, planar lam	<10	100	0.1 100 12	20
SS2	Clast-rich to conglom SS	Med - coarse SS	poor	Structureless, planar lam	20-50	100	0.1 0.3 4	6
SS3	Amalgamated cross-bedded SS	UF - coarse SS	mod well - well	Trough X cross	>100	100	0.01 20 2	14
SS4	Cross bedded SS	UF - coarse SS	mod well - well	Trough X cross	<100	100	0.1 150 4	23
SS5	Muddy cross beds	F-Med SS	mod - mod poor	Trough X cross, mud drapes	20-80	100	0.05 0.1 4	6
SS6	Soft sed deformed SS	F-Med SS	mod - mod poor	dewatering/load structures	20-100+	95	0.02 0.05 2	4
SS7	Structureless SS	Uf - med SS	mod - mod poor	structureless	20-100+	100	0.01 50 2	17
SS8	Plane parallel SS	Uf - med SS	mod well - well	planar laminations	10-50	100	0.01 150 2	15
SS9	Swaley SS	Fine SS	mod well - well	plane parallel to low angle strat with reactivation surfaces	20-40	100	0.1 0.1 3	12
SS10	Hummocky SS	Fine SS	mod well - well	plane parallel to low angle strata	10-30	100	0.01 150 4	18
SS11	Isolated SS	VF - Fine SS	mod - well	plane parallel, structureless	5-20	100	0.01 40 1	11
SS12	Faintly stratified amalgamated SS	F SS	mod - mod poor	Fait plane parallel, wispy discontinuous mud drapes	100-200	95	0.01 2 1	14
SS13	Interbedded deformed/bioturbated SS	VF - Fine SS	mod poor - poor	Burrows, loads, rip up clasts	2-5, 1-2	85	0.01 1 2	12
SS14	Amalgamated bioturbated SS	VF - Fine SS	mod poor - poor	Diverse and aburdant burrows	10-200+	95	0.01 2 5	12
SS15	Ripple laminated SS	VF - Fine SS	well	Ripple laminations	1-20	100	0.6 50 1	23
SS16	Interbedded thinly laminated SS with mud drapes	VF - Fine SS	mod well - well	Planar laminated, mud drapes	1-3, 100+	70-90	0.01 100 2	20
SS17	Bioturbated SS and mud	VF - Fine SS	mod poor - poor	Diverse and aburdant burrows	20-200+	80-100	0.1 0.1 13.5	13.5
MR19	Bioturbated mud and SS	Shale - silt				60-80	0.01 15 8	17
MR20	Shale with thin SS beds	Shale - silt				<50	0.08 2 2	2
CM23	cemented	variable	na					

Facies	GR-low	GR-hi	RHOB-lo	RHOB-hi	NPHI-lo	NPHI-hi	DT-lo	DT-hi			GR-low	GR-hi	RHOB-lo	RHOB-hi	NPHI-lo	NPHI-hi	DT-lo	DT-hi	REST-lo	REST-hi
SS	30	80	2.3	2.5	0.10	0.17	60	74												
MR	80	150	2.5	2.7	0.17	0.30	74	95												
CL	150	400	2	2.3	0.30	0.50	95	150												
CM	0	60	2.7	3	0.00	0.10	0	60												
SS1	40	80	2.35	2.42	***11.5***	***15.5***	***66***	***74***												
SS2	35	55	***2.55***	***2.60***	***8.5***	***12.5***	***60***	***65***												
SS3	30	80	***2.43***	***2.54***	***10.5***	***16.5***	***60***	***70***												
SS4	40	85	***2.46***	***2.53***	***10.5***	***15***	***69***	***75***												
SS5	45	55	2.55	2.65	5	10	60	65												
SS6	35	45	2.63	2.65	5	7	55	60												
SS7	30	85	***2.45***	***2.58***	***7***	***15***	***66.5***	***78***	2	Stratified or thick bedded SS	30	85	2.4	2.7	0.1	0.165	60	75	3	200
SS8	30	85	***2.46***	***2.57***	***10.5***	***18***	***71.5***	***77.5***		Higher energy facies										
SS9	40	85	***2.48***	***2.55***	***13.5***	***16.5***	***67.5***	***72***												
SS10	40	85	2.40	2.63	***12***	***15***	62	70												
SS11	35	85	***2.47***	***2.56***	***9.5***	***16.5***	***71***	***81***												
SS12	35	95	***2.49***	***2.58***	***9.5***	***15.5***	***67.5***	***74***												
SS13	40	85	***2.48***	***2.62***	***10.5***	***16***	***68.5***	***74***												
SS14	65	100	2.39	2.47	***11.5***	***14.5***	75	80	3	Interbedded or bioturbated SS/mud Lower energy facies	60	100	2.4	2.7	0.12	0.18	70	120	1	100
SS15	53	100	***2.39***	***2.56***	***12***	***21***	***65***	***80***												
SS16	53	90	***2.43***	***2.63***	***12.5***	***21***	***72.5***	***81***												
SS17	80	105	***2.54***	***2.61***	***14.5***	***18.5***	***65***	***80***												
MR19	85	110	2.46	2.56	18	26	70	85	4	Interbedded or bioturbated mud/SS	85	400	0	2.625	0.16	1	70	120	0	50
MR20	85	115	***2.43***	***2.61***	***18***	***26***	70	87												
CM23	30	60	2.45	2.70	5	11	40	70	1	Cemented SS	0	60	2.45	3	0	0.11	0	70	1	299

Appendix E. Table showing statistics generated from Petra database and resulting log facies values from running IF-THEN script.

APPENDIX F:

CONTACT INFORMATION FOR OBTAINING

POWDER RIVER BASIN PETREL MODEL

Structural model in Petrel version 2009 can be copied onto a user supplied disk (multi-gig) without the private log ascii (LAS logs) for academic use.

Please contact Jesse Melick (jessemelick@gmail.com) or Mike Uland at

Mike Uland
Technology Director
iReservoir.com Inc.
1490 West Cannel Court, Suite 2000
Littleton CO 80120
Phone: (303) 713-1112
uland@ireservoir.com